PROCEEDINGS BOOK OF THE 6th

ADVANCED ENGINEERING DAYS

5 March 2023 / MERSIN, TURKIYE

International Engineering Symposium

Congress Chairman

PROF. DR. MURAT YAKAR

http://aed.mersin.edu.tr/

6th Advanced Engineering Symposium

I would like to thank all of the contributing authors and reviewers to the 6th Advanced Engineering Days (AED) Symposium, on 5 March 2023. In this international symposium there are 59 papers. 29 of them are from Türkiye and the rest are from 9 different countries. We would like to see you in the 7th AED which will be held on 2 July 2023.

Best regards

Prof. Dr. Murat YAKAR

The proceedings of the
6th Advanced Engineering Days

Editor-in-Chief

Prof. Dr. Murat YAKAR

Editors

Prof. Dr. Fatmir BASHOLLI

Prof. Dr. Şükrü DURSUN

Lec. Lale KARATAŞ

Res. Asst. Aydın ALPTEKİN

Session 1	
10:00-10.10	**Investigation of the historical process of the Mardin Castle** Lale Karataş, Aydın Alptekin, Murat Yakar, Murat Dal
10.10-10.20	**Mardin Castle building material and construction technique analysis** Lale Karataş, Aydın Alptekin, Murat Yakar, Murat Dal
10.20-10.30	**Assessment of structural problems in Mardin Castle** Lale Karataş, Aydın Alptekin, Murat Yakar, Murat Dal
10.30-10.40	**Evaluation of conservation and restoration works in protected areas: A case study of Mardin Castle** Lale Karataş, Aydın Alptekin, Murat Yakar, Murat Dal
10.40-10.50	**Mardin Castle landscaping and landscape interventions proposal** Lale Karataş, Aydın Alptekin, Murat Yakar, Murat Dal

Session 2	
11:00-11.10	**The role of Notch and Wnt signaling pathways in neurodevelopment** Ece Tümkaya, Furkan Ayaz
11.10-11.20	**The role of soil microbiome in plant growth and development under stress conditions** Ceren Küçümen Aslan, Furkan Ayaz
11.20-11.30	**BRCA1 and BRCA2 genes in breast cancer** Hülya Servi, Furkan Ayaz
11.30-11.40	**Cancer and Wnt Pathway** Simay Ayden, Furkan Ayaz
11.40-11.50	**Diagnosis of ovarian cancer and biomarkers** Helin Aytar, Furkan Ayaz
11.50-12.00	**General properties and production technologies of liposomes** Ebru Öner Usta, Furkan Ayaz

Session 3	
12.10-12.20	**The role of uterine natural killer (uNK) cells in the endometrium of infertile women** Tiinçe Aksak
12.20-12.30	**Lifesaving open areas after earthquake and land management** Nurhan Koçan
12.30-12.40	**Increase die life in hot forging process by using coating processes** Sait Gül, Adil Yağmur, Esat Erdinç Önel
12.40-12.50	**Flood modeling with FLO-2D: Mersin / Lamas River** Vahdettin Demir, Abdulkadir Özcan
12.50-13.00	**Internet of Things (IoT) in GIS** Çetin Önder İncekara
13.00-13.10	**Synthesis of cobalt-doped bead type catalyst for hydrogen production via hydrolysis reaction of $NaBH_4$** Filiz Akti

Session 4	
13.20-13.30	**Precise point positioning technique with single frequency raw GNSS observations using different products on android smartphones** Barış Karadeniz, Hüseyin Pehlivan, Barışcan Arı
13.30-13.40	**Deep learning based poplar tree detection and counting using multispectral UAV images** Ismail Colkesen, Taskin Kavzoglu, Umut Gunes Sefercik, Osman Yavuz Altuntas, Mertcan Nazar, Muhammed Yusuf Ozturk, Mustafacan Saygı
13.40-13.50	**Analyzing of court decisions cancelling zoning applications in implementation boundary** Hüseyin Pehlivan, Seyfullah Aybal
13.50-14.00	**Improving GNSS data accuracy using DBSCAN, moving averages, and Hampel identifier** Hüseyin Pehlivan
14.00-14.10	**Explainable artificial intelligence empowered landslide susceptibility mapping using Extreme Gradient Boosting (XGBoost)** Alihan Teke, Taskin Kavzoglu
14.10-14.20	**GIS-based real estate legislation information system design: The case of İzmir, Foça** Mert Kayalık, Zeynel Abidin Polat

Session 5	
14.30-14.40	**A brief evaluation regarding the use of street view images for urban studies** Mehmet İşiler, M. Oğuz Selbesoğlu
14.40-14.50	**Sentinel-2 derivatives are rewriting land-cover history** Arif Oguz Altunel, Durmus Ali Celik
14.50-15.00	**3D modeling of Mersin Akyar Cliffs with wearable mobile LIDAR** Atilla Karabacak, Murat Yakar
15.00-15.10	**3D modeling of Mersin Sarisih Caravanserai with wearable mobile LIDAR** Atilla Karabacak, Murat Yakar
15.10-15.20	**Production of road maps in highway projects by unmanned aerial vehicle (UAV)** Fatih Tükenmez, Murat Yakar
15.20-15.30	**Modeling of the historical monument with mobile phone-based photogrammetry method** Abdurahman Yasin Yiğit, Murat Yakar

Session 6	
15.40-15.50	**An overview of organic pollutants concentrations in the port of Durres, Adriatic Sea** Esmeralda Halo, Aurel Nuro, Bledar Myrtaj, Jonida Tahiraj, Sonila Kane
15.50-16.00	**Determination of volatile organic pollutants in water samples of White Drin River, Kosovo** Aferdita Camaj, Arben Haziri, Aurel Nuro, Arieta Camaj Ibrahimi
16.00-16.10	**Study of chemical profile for essential oil of *Salvia officinalis* L. plants by using CO_2 supercritical extraction** Miranda Misini, Arben Haziri, Fatmir Faiku, Aurel Nuro
16.10-16.20	**Influence of the instability form on the traffic safety of freight rolling stock** Angela Shvets
16.20-16.30	**How hospitals response to disasters; a conceptual deep reinforcement learning approach** Ardeshir Mirbakhsh

Session 7	
16.40-16.50	**The impact of hybrid cars on reducing urban pollution and global warming** Ledia Bozo, Asllan Hajderi, Fatmir Basholli
16.50-17.00	**Health Care Cyber Security, Albania Case Study** Dolantina Hyka, Fatmir Basholli
17.00-17.10	**Complex network approach to detect faults in photovoltaic plants: Albanian case study** Xhilda Dhamo, Eglantina Kalluçi, Eva Noka, Darjon Dhamo
17.10-17.20	**Hand gesture and voice-controlled mouse for physically challenged using computer vision** Aarti Morajkar, Atheena Mariyam James, Minoli Bagwe, Aleena Sara James, Aruna Pavate
17.20-17.30	**Machine learning algorithms for predicting life expectancy** Miranda Harizaj, Olgerta Idrizi, Alfons Harizaj

Session 8	
17.40-17.50	**Finding the closest and lowest price pharmacy over a given location** Julian Imami
17.50-18.00	**Detection and prevention of intrusions into computer systems** Fatmir Basholli, Adisa Daberdini, Armand Basholli
18.00-18.10	**Improvement of e-education systems in Albania** Alfons Harızaj, Olgerta Idrizi
18.10-18.20	**Assessing bio-diverse foods in dietary intake surveys-a case study considering random selected samples** Samanda Gjoni, Flavia Gjata, Florida Hajderaj, Emirjana Hasanaj, Klodjana Lamaj, Aurora Manaj, Manjola Sala, Megisa Sulenji, Nertila Mucollari, Spase Shumka
18.20-18.30	**Practical QoS measurement and analyzes on a 5G non-standalone architecture** Olimpjon Shurdi, Alban Rakipi, Arjola Biti

Session 9	
18.40-18.50	**IOT integration of electric vehicle charging infrastructure** Miranda Harizaj, Igli Bisha, Fatmir Basholli
18.50-19.00	**Neural networks for bitcoin price forecasting** Katerina Zela, Lorena Saliaj
19.00-19.10	**Functional substances in grape seed and seed processing research** Farmonov Jasur Boykharayevich, Sobirova Mohichehra Shamsiddin Qizi, Kalonova Moxinur Muzaffar Qizi
19.10-19.20	**BattSim-GDC Simulator: How much battery your green datacenter needs?** Enida Sheme Igli Tafa, Fatmir Basholli
19.20-19.30	**The trend of use of ICT among households and individuals in Albania** Berina Metanj

Session 10	
19.40-19.50	**On the formulation of the Cauchy problem for matrix factorizations of the Helmholtz equation** Davron Aslonqulovich Juraev, Mahir Jalal oglu Jalalov, Vagif Rza oglu Ibrahimov
19.50-20.00	**Hospital capacity management through simulation** Farzaneh Sarbandi Farahani
20.00-20.10	**Steady state error and equivalent noise bandwidth analysis of the null-seeker architecture for GPS receivers** Alban Rakipi, Olimpjon Shurdi, Aleksander Biberaj
20.10-20.20	**Fundamental solution for the Helmholtz equation in the plane** Davron Aslonqulovich Juraev
20.20-20.30	**Speed control of three phase induction motor using Field Oriented Control technique** Darjon Dhamo, Denis Panxhi, Aida Spahiu, Jonadri Bundo

Session 11	
20.40-20.50	**Application of the ratio of satellite image channels for mineral mapping using the example of Kokpatas-Okjetpes from the direction of the trend (Bukantau Mountains)** Goipov Akrom, Khaydarova Arofat, Jurabekov Navruzbek
20.50-21.00	**Remote piloting UAS in extreme environments with challanging climatic conditions - An overview of modern UAS capabilities in the field of volcanology, geosciences, atmospheric chemistry and interplanetary exploration** Ian Godfrey, José Pablo Sibaja Brenes, Emanuel Montealegre Viales
21.00-21.10	**Research of ore-controlling factors and significant sign of mineralization of Kokpatas and Cenral Bukantau Regions (Uzbekistan)** Goipov Akrom, Jurabekov Navruzbek, Khaydarova Arofat
21.10-21.20	**Prospects of the mafic-ultramafic belt of the Nuratau Mountains for platinoids (Uzbekistan)** Jurabekov Navruzbek, Khaydarova Arofat, Kholikov Azimjon
21.20-21.30	**Geobotanical and comparative data on vegetation in selected areas of central Albania, Elbasan region** Selma Myslihaka

Content	Page

Advanced Engineering Days

aed.mersin.edu.tr

Investigation of the historical process of the Mardin Castle

Lale Karataş *[1] ⓘ, **Aydın Alptekin** [2] ⓘ, **Murat Yakar** [3] ⓘ, **Murat Dal**[4] ⓘ

[1]Mardin Artuklu University, Department of Architecture and Urban Planning, Türkiye, lalekaratas@artuklu.edu.tr
[2]Mersin University, Faculty of Engineering, Department of Geological Engineering, Türkiye, aydinalptekin@mersin.edu.tr
[3]Mersin University, Faculty of Engineering, Department of Geomatics Engineering, Türkiye, myakar@mersin.edu.tr
[4]Munzur University, Department of Architecture, Türkiye, muratdal@munzur.edu.tr

Keywords
Mardin Castle
Restitution
Period Analysis
Restoration
Sustainability

Abstract
Mardin Castle is a historical landmark for the city. The aim of the study is to make a situation analysis about the present and original state of the building and to present the historical change process in a systematic way. For this purpose, the survey/restoration projects and photo albums in the archives of the Regional Conservation Board and local institutions of the castle were examined. In order to reveal the historical change process of the building in a systematic way, the building was divided into six sections and the periodic analyzes of the sections were mapped. As a result of the study, the castle; It has been determined that the period of Hamdani (10th century), Artuqid period (12th-15th century), Akkoyunlu period (15th century), Ottoman Period (16th century) and 20th century.

Introduction

The ancient history of the castle is not clear. In the records of Ammianus Marcellinus, one of the Roman historians of the 4th century AD, which is among the earliest written information about the castle, it is claimed that Maride, which is mentioned among the castles on the Diyarbakır-Nusaybin road, is Mardin [1].

Material and Method

The survey/restoration projects and photo albums in the archives of the Regional Conservation Board and local institutions were examined. The present situation of the castle and its original state have been analyzed comparatively. The castle structure is a huge structure that is difficult to examine. For this reason, the structure is divided into six parts so that the historical change process can be put forward in a systematic way. Periodic analyzes of the departments are presented by mapping. The periodic mapping legend is given in the Figure 1.

1 — 10th century Hamdani Period
2 — 12th century -15th century Ottoman Period
3 — 15th century -16th century first quarter Ottoman Period
4 — 16th century Ottoman Period
5 — 20th Century Ottoman Period
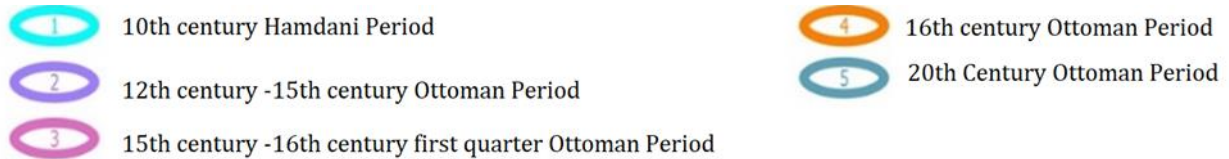
Figure 1. Periodic mapping legend

Results

Although the walls that fortified the castle along the western wing, as a natural continuation of the bedrock floor and by making right-angle or semi-circular breaks in accordance with the topography, have been largely destroyed over time, it still seems possible to determine the line of the rampart. Accordingly, the wall at the western end of the wall and extending in the south-north direction is in a relatively solid condition, with a bossage at the bottom and a coarse stone masonry that has remained in five rows on the top. In terms of material and technique, it has stonework of two different periods. The next part of the wall line, which makes various breaks in accordance with the rocky topography, proceeds in the north direction with the coarse wall masonry consisting of large rows of stones at the bottom and smaller stones at the top, as the characteristics of two separate periods. There is no doubt that the semi-circular ashlar remnant located approximately in the middle of the wall is the remains of a small tower located at this point, which can easily be understood as having a different period addition [2-6] (Figure 2).
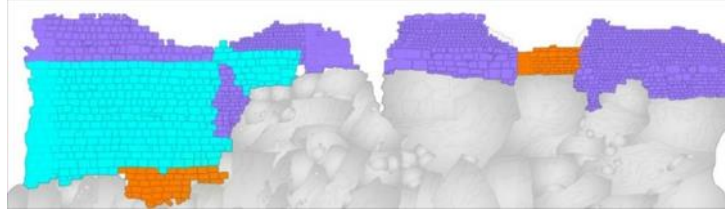
Figure 2. Drawing Showing Period Analysis

The part of the wall, starting from the northern corner and extending to the east with a right-angle break, has survived to the present day with some details that give information about its original condition, although it was destroyed over time. According to this, it can be easily understood that the semi-circular ashlar remnant, which is located in the north corner of the wall where the wall breaks diagonally, and which was later added to the wall extending in the south-north direction, belonged to a tower that was once located in this corner. The circular slot that remained in-situ on one of the ashlar blocks forming the opening on the upper edge of the remains, which gives the impression of a window, explains that it also served as a ball bed in the past [2-6] (Figure 3).
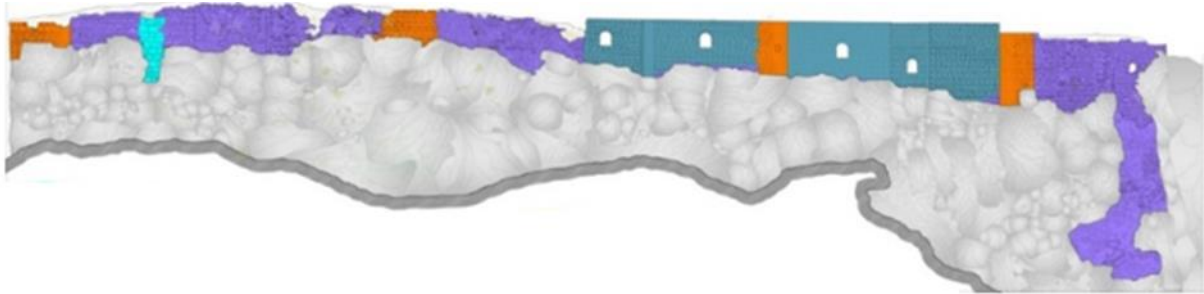
Figure 3. Drawing Showing the Period Analysis

The part that makes up the third section; the wall line, the original part of which can be seen again on the east wing, where the repairs were finalized, at this point, following the border line of the rock that extends to the south by making a nose, it turns to the north direction. The rotating part forms a conical line. Looking at the current state of the ruins here, it is understood that the building in question functioned as a bastion protecting the gate number 2 (Nizamiye), which was the starting point of the road route that provides access to İçkale. However, the original plan features have largely disappeared as a result of recent repairs [2-6] (Figure 4).
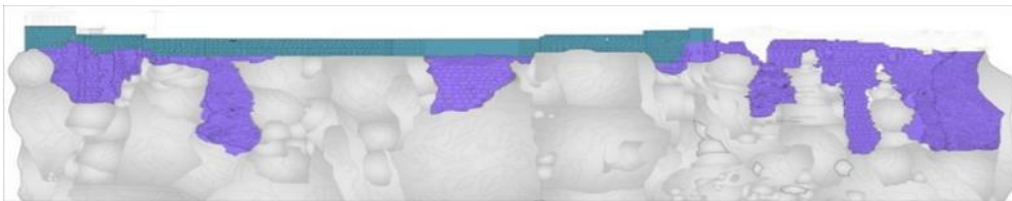
Figure 4. Drawing Showing the Period Analysis

The fourth section is oriented towards the İçkale settlement in the north direction and extends along the north-east and east directions by making various breaks in the form of a sloping wall whose elevation gradually decreases. The wall in question has masonry from two different periods in terms of material and technique, with

its coarse and cut stone weaves. It seems that in the part of the cliff where the cliff made a narrow strait and was most suitable for defense, the wall in question was essentially rising above the main gate no. 1, which was included in İçkale. In this context, there is a cut stone braided remnant that can be detected in the middle of the wall line and between the rock formations at the lower level. There is no doubt that these remnants originally belonged to a square bastion that fortified the İçkale gate in the south-west direction and bounded the gate in the north direction [2-6] (Figure 5).
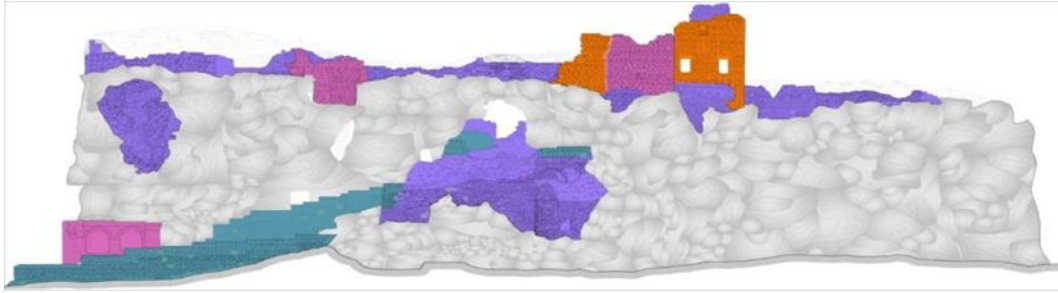
Figure 5. Drawing Showing Period Analysis

Following the qibla wall of the Kale Mosque, the wall breaking to the north and forming the façade of the mosque in this direction turns to the east again on the rock formations in this section and extends in various breaks. It is clear that the wall remains, which can be seen as coarse stone masonry, are the product of a single construction period in this most damaged part of the city wall; it is clear that, at least, no physical interventions were made on the current wall remains. Although it is understood that the vertical rectangular window openings with hewn stone frames, which can be seen in the middle parts of the wall in question, are related to the structures that are understood to be articulated from the inside of the wall, it is not possible to determine their functions today because they are completely underground. On the other hand, it has been understood that the remains of a building, which can be described as the Vaulted Gallery, were able to remain in the aforementioned section, that Gabriel succeeded in making his survey in the 1930s and that it was largely standing in the aforementioned dates. It can be pointed out that Konak-Saray, which A. Altun states that it disappeared completely in the second half of the 1960s and dates back to the 15th century, has survived as an annex [2-6] (Figure 6).
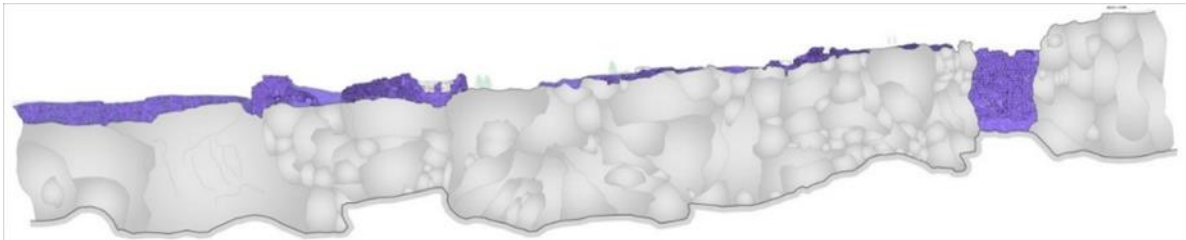
Figure 6. Drawing Showing the Period Analysis

The five-sided south façade of the wall extending to the east and forming the border of the radar base, and the walls in the last part of the wall ending in a rectangular prismatic bastion rising on the rock formation, have almost completely disappeared and can only be partially traced as foundation walls on the west wing. A reinforced concrete wall and concrete bollards imitating dendan were built on the wall line, on which the disappearing wall continued in the past. Historically, five different periods have been identified on the part constituting this part of the gigantic fortification structure. The drawing explaining the period analysis of this section, which constitutes the sixth section of the wall, is presented in Figure 7.
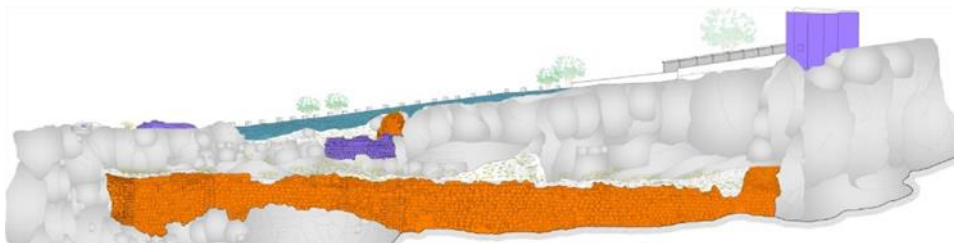
Figure 7. Drawing Showing Period Analysis

Discussion

The historical analysis studies to be carried out are of great importance in terms of providing documents for the applications to be made in the restitution process of the building [10-15]. In this context, this study is valuable in terms of revealing the historical change processes of the castle structure in a systematic way. In addition, it is seen that historical castles in many cities have been damaged or even destroyed as a result of the earthquake-induced events in our country recently [16]. In this context, in future studies, seismic risk and loss estimation studies of the castle are important for the process of deciding on the hazard calculation [17-24].

Conclusion

As a result of the study, the castle structure has been determined that the period of Hamdani (10th century), Artuqid period (12th-15th century), Akkoyunlu period (15th century), Ottoman Period (16th century) and 20th century. In this study, we aim to make a situation analysis about the present and original state of the building and to present the historical change process in a systematic way.

References

1. Altun, A. (1971). Mardin'de Türk Devri Mimarisi. İstanbul.
2. Gabrıel, A. (1940). Voyages Archeologique Dans La Turquie Orientale, Paris.
3. Altun, A. (1978). Anadolu'da Artuklu Devri Türk Mimarisinin Gelişmesi. İstanbul
4. Dolapönü, M. H. (1972). Tarihte Mardin (Itr-El-Nardin Fi Tarih Merdin). İstanbul.
5. Dolapönü, M. H. (1988). Yaşayan Tarih Mardin. İstanbul.
6. Göyünç, N. (1991). XVI. Yüzyılda Mardin Sancağı, TTK, Ankara.
7. Karataş, L. (2022). Mardin'de Kültürel Miras Yapılarında Restorasyon Sırasında Yapılan Hatalı Onarımlar, Restorasyon Sonrası Süreçte Karşılaşılan Sorunlar ve Çözüm Önerileri. *Kültürel Miras Araştırmaları*, *3*(2), 78-86.
8. Karataş, L. (2022). Conservation status of intangible cultural heritage after restoration: Case study of Mardin Spice Bazaar. *Cultural Heritage and Science*, *3*(2), 30-36.
9. Karataş, L., Alptekin, A., & Yakar, M. (2022). Elimination of unqualified additions that distort the silhouette of the historical places: Artuklu example. *Advanced Land Management*, *2*(2), 89-98.
10. Aktekin, S. (2010). The place and importance of local history in the secondary history education. *Journal of theory and practice in Education*, *6*(1), 86-105.
11. Özcoşar, İ., Güneş, H. H., & Gümüş, E. (2007). *238 nolu Mardin şer'iye sicili belge özetleri ve Mardin* (Vol. 6). Mardin Valiliği İl Özel İdaresi.
12. Karataş, L., Alptekin, A., & Yakar, M. (2022). Mardin Tarihî 1. Cadde Yayalaştırma ve Sokak Sağlıklaştırma Projesinin Mekânsal ve Sosyokültürel Etkileri. *Türkiye Arazi Yönetimi Dergisi*, *4*(2), 82-89.
13. Karataş, L., Alptekin, A., & Yakar, M. (2022). Restitution suggestion for Mardin TatlıDede Mansion. *Advanced Engineering Days (AED)*, *4*, 61-63.
14. Karataş, L., Alptekin, A., & Yakar, M. (2022). Mardin historical Kuyumcular (Jewelers) Bazaar restoration evaluation. *Advanced Engineering Days (AED)*, *5*, 15-17.
15. Karataş, L., Ateş, T., Alptekin, A., Dal, M., & Yakar, M. (2023). A systematic method for post-earthquake damage assessment: Case study of the Antep Castle, Türkiye. *Advanced Engineering Science*, *3*, 62-71.
16. Ay, B. Ö. (2018). The Effects of Implementing Different Ground-motionLogic-tree Frameworks on Seismic Risk Assessment. 16th European Conference on Earthquake Engineering.
17. Ay, B. Ö., Erberik, M. A., & Eroğlu Azak, T. (2016). Deprem Tehlikesine Maruz Bina Envanterinin İstatistiki Yöntemler ile İncelenmesi.
18. Bayhan, B., & Gülkan, P. (2011). Buildings subjected to recurring earthquakes: A tale of three cities. *Earthquake spectra*, *27*(3), 635-659.
19. Çağlar, N., Sert, S., & Serdar, A. H. (2021). Basement-Storey Effect on the Seismic Response of RC Buildings on Soft Surface Soil. *Arabian Journal for Science and Engineering*, *46*(11), 11291-11302.
20. Çağlar, N. (2001). Yapay sinir ağları ile binaların dinamik analizi. Doctoral Dissertation, Sakarya University.
21. Ilgın, H. E. (2022). Use of aerodynamically favorable tapered form in contemporary supertall buildings. *Journal of Design for Resilience in Architecture and Planning*, *3*(2), 183-196.
22. Türkeri, İ. (2018). Cami tasariminda planimetrik kurgunun yeniden tartişilmasi: İskele Cami tasarimi. *Atlas Journal*, *4*(11), 841-850.
23. Akincitürk, N. (2003). Yapi tasariminda mimarin deprem bilinci. *Uludag Üniversitesi, Mühendislik-Mimarlık Fak. Yayini*, *8*, 189-201.
24. Akıncıtürk, N. (2003). *Ülkemizdeki deprem etkileri ve yapısal tasarımda alınması gereken önlemler*. Uludağ Üniversitesi Mühendislik Mimarlık Fakültesi.

Mardin Castle building material and construction technique analysis

Lale Karataş *1 , **Aydın Alptekin** 2 , **Murat Yakar** 3 , **Murat Dal**4

1Mardin Artuklu University, Department of Architecture and Urban Planning, Türkiye, lalekaratas@artuklu.edu.tr
2Mersin University, Faculty of Engineering, Department of Geological Engineering, Türkiye, aydinalptekin@mersin.edu.tr
3Mersin University, Faculty of Engineering, Department of Geomatics Engineering, Türkiye, myakar@mersin.edu.tr
4Munzur University, Department of Architecture, Türkiye, muratdal@munzur.edu.tr

Keywords
Mardin Castle
Stone Material
Material analysis
Construction Technique
Conservation

Abstract
Mardin Castle, also known as the "Eagle's Nest"; It is a very important castle that lived the periods of Subari, Sumerian, Babylonian, Mitanid, Assyrian, Persian, Roman, Byzantine, Umayyad, Abbasid, Hamdanid, Seljuk, Artuklu, Karakoyunlu, Akkoyunlu, Safaviler and Ottomans. Its height from the Harran plain is about a thousand meters. The aim of the study is to reveal the building materials and construction technique of the Mardin castle, which is a symbol for the region and a great value in terms of its historical importance. For documentation purposes, the building was examined on site and photographed. As a result of the study, it was determined that stone, brick, mortar and plaster materials were used in the construction of the castle structure and it was built using the masonry construction technique.

Introduction

When looking at the general view of the city of Mardin, the majority of these calcareous local stone structures are seen. Straw-yellow cut stone material attracts attention in almost all of the buildings [1-6]. Mardin Castle is also mostly made of stone material and contains different kinds of materials [7]. In addition, the building was built with the construction technique that reflects the architectural characteristics of the period. In this context, it is aimed to investigate the material properties and construction technique of Mardin Castle, which is a historical symbol for the city.

Material and Method

Archival research and field research method were used in the study. First of all, a literature review was made for Mardin Castle. Later, the castle was examined on site and the building materials were documented by the photography method. Canon Digital IXUS 82 IS (8 MegaPixel) digital cameras were used for sampling and Canon Digital IXUS 870 IS (10 MegaPixel) digital cameras were used for documenting the samples.

Results

Stone

It is understood that the limestone type peculiar to the region was used in the castle both in the original weave and in the restored weaves (Figure 1a). When the stone material is examined in terms of workmanship, it is seen that the masonry on the main walls is covered with smooth cut / rough cut inside and outside, coarse rubble stone

with smoothed outer face and rubble filled with irregular joints between the coatings (Figure 1b,1c). On the walls near the western end of the southern rim, masonry stones with a smooth cut around the joint, the outer facing surface of which was smoothed and left with a kind of bossage, coarse-cut blocks and completely cut stone masonry can be seen together (Figure 1d-1ı). In the building remains, the vaults made of brick or rubble stone, the arch of rubble stone-rough cut stone and brickwork, the pillars, the wall sections, are the workmanship features in the traceable sections (Figure 1k,1l). The masonry using neatly cut-worked stones in the building has contiguous joints, and the gaps between the stones are filled with a thin layer of lime-bonded joint mortar (Figure 1a,1d,1m). The rough cut-rubble stones have irregular edges. However, it can be observed that the stones were chosen in the same order, with close height measurements, and that large and irregular joint gaps in rubble masonry were placed in the masonry by using small rubble stone fillings next to the mortar material (Figure 1e-1ı). It is understood that the rubble filling between the cut stone-rough-hewn wall coverings in the destroyed sections was filled with rubble stone/mortar of various sizes, and the rubble filling was made with irregular joints [1] (Figure 1b,1c).
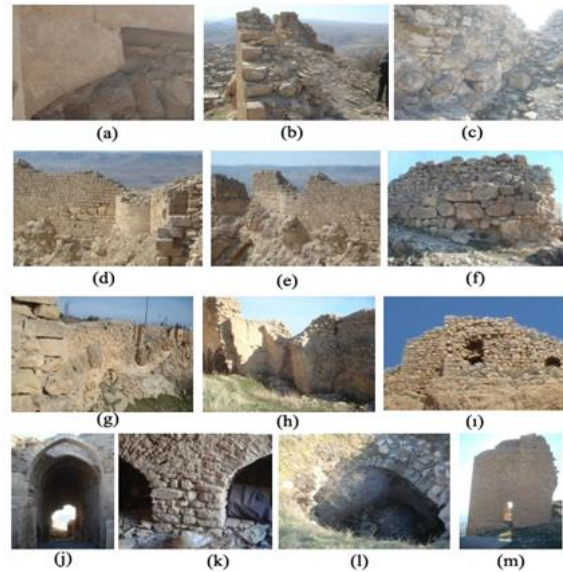
Figure 1. The use of stones in various parts of the building [8]

Brick

The use of brick material in the castle is limited compared to stone. The use of brick in the construction is seen in the vaulted cover in front of the castle gate (inside) in the south of the castle and in the weave of the building elements such as arches and vaults of the building remains in the castle, close to the entrance. The use of brick is also seen in the mosque transition elements (Figure 2). The brick material used is red colored paste and tightly porous. Brick material was evaluated in the lattice in order to form regular rows with mortar joint fillers with lime binder kept slightly thinner than the brick thickness.
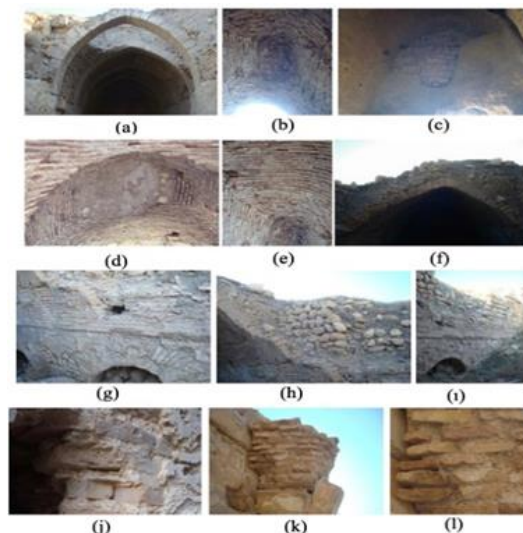
Figure 2. Examples of brick materials used in various parts of the building [8]

Mortar

Mortar was used as joint filling material. Its material is a mixture of lime, stone dust and stone fragments, cream-white in color and tightly porous. The joint mortars are in the form of a thin layer, generally less than ∼1 cm thick, between the stones in cut stone-rough cut stone masonry. The rubble weaves are of irregular size. The thickness of the joint filling mortar between the brickwork gives regular measurements. According to the weave samples examined, it is a requirement of the rubble weave to keep the joint mortars, which perform their binding duties between the rubble stones, unevenly. In the same way, keeping the joint fillings thin in the cut stone mesh is only to provide a smooth transition between the stones and to fulfill a functional task. The cementitious mortars used in all the masonry where recent repairs were made differ markedly from the lime-binding mortars used in the original masonry, with a gray color (white due to white cement in the eastern polygonal tower).

Plaster

Plaster can be seen on the interior wall, transition and dome surfaces of the mosque adjoining the city wall, and on the interior wall surfaces of the building remains, some parts of which can be seen inside the castle. When the plaster-wall relationship is examined, it is seen that the plasters are on the smooth cut stone coated walls and dome surfaces in the mosque, on the smooth cut stone and brick masonry transitions; Covering material was applied on the partially visible brick and rubble stone vault, brick and stone arch and rubble masonry wall surfaces inside the castle. The plasters, of which only the remains of the masonry can be seen on the walls, vaults and transition systems, are a mixture of lime and stone powder, fine-grained, cream-colored and tightly porous.

Discussion

The aim of the study is to reveal the building materials and construction technique of the Mardin castle, which is a symbol for the region and a great value in terms of its historical importance. For documentation purposes, the building was examined on site and photographed. As a result of the study, it was determined that stone, brick, mortar and plaster materials were used in the construction of the castle structure and it was built using the masonry construction technique. It has been observed that historical buildings and castles in many cities have been damaged or even demolished as a result of earthquake-induced events in our country recently [9-17]. In this context, against such dangers that may occur in the Mardin Castle, it is thought that the material deterioration and structural deterioration of the castle will be determined in 3D with today's technologies. Today, material problems and structural problems of such gigantic structures can be easily detected by methods such as UAV and terrestrial lidar scanning [18-23].

Conclusion

When the fortification walls and other building remains are examined in terms of construction technique, the vertical carriers were built with the technique also called chest wall. On the outer parts of the wall, a row of outer stones with faceted stones (sheath-surface coating) is observed, and inside, a rubble core made of a mixture consisting of small stone pieces and lime-binding mortar is observed. Although this masonry technique is a technique that is frequently encountered in stone-masonry structures, there are also applications made with the same technique but consisting of stones of different quality. In addition, there are wall and muhdes building additions that were added to the building at different times, mostly in recent times, especially due to military use. The walls built in the new period were mostly made of cut stone and cement-containing mortars.

References

1. Gabriel, A. (1940). Voyagés Archéologique Dans la Turquie Orientale. Paris.
2. Karataş, L. (2022). Mardin'de Kültürel Miras Yapılarında Restorasyon Sırasında Yapılan Hatalı Onarımlar, Restorasyon Sonrası Süreçte Karşılaşılan Sorunlar ve Çözüm Önerileri. *Kültürel Miras Araştırmaları*, *3*(2), 78-86.
3. Karataş, L., Alptekin, A., & Yakar, M. (2022). Elimination of unqualified additions that distort the silhouette of the historical places: Artuklu example. *Advanced Land Management*, *2*(2), 89-98.
4. Karataş, L., Alptekin, A., & Yakar, M. (2022). Mardin Tarihî 1. Cadde Yayalaştırma ve Sokak Sağlıklaştırma Projesinin Mekânsal ve Sosyokültürel Etkileri. *Türkiye Arazi Yönetimi Dergisi*, *4*(2), 82-89.

5. Özcoşar, İ., Ateş, T., & Güneş, H. (2006). Tarihi Mardin evlerinde kemerler. *I. Uluslararası Mardin Tarihi Sempozyumu Bildirileri), İmak Ofset*, 843-866.

6. Karataş, L., Alptekin, A., & Yakar, M. (2022). Contribution of architectural design of ancient city Dara's water cisterns to the water efficiency of the city. *Advanced Engineering Days (AED)*, *4*, 52-54.

7. Karataş, L. (2023). Investigating the historical building materials with spectroscopic and geophysical methods: A case study of Mardin Castle. *Turkish Journal of Engineering*, *7*(3), 266-278.

8. Mardin Büyükşehir Belediyesi (2023). KUDEB arşivi, Mardin.

9. Karataş, L., Ateş, T., Alptekin, A., Dal, M., & Yakar, M. (2023). A systematic method for post-earthquake damage assessment: Case study of the Antep Castle, Türkiye. *Advanced Engineering Science*, *3*, 62-71.

10. Ay, B. Ö. (2018). The Effects of Implementing Different Ground-motionLogic-tree Frameworks on Seismic Risk Assessment. 16th European Conference on Earthquake Engineering.

11. Ay, B. Ö., Erberik, M. A., & Eroğlu Azak, T. (2016). Deprem Tehlikesine Maruz Bina Envanterinin İstatistiki Yöntemler ile İncelenmesi.

12. Bayhan, B., & Gülkan, P. (2011). Buildings subjected to recurring earthquakes: A tale of three cities. *Earthquake spectra*, *27*(3), 635-659.

13. Ilgın, H. E. (2022). Use of aerodynamically favorable tapered form in contemporary supertall buildings. *Journal of Design for Resilience in Architecture and Planning*, *3*(2), 183-196.

14. Çağlar, N., Sert, S., & Serdar, A. H. (2021). Basement-Storey Effect on the Seismic Response of RC Buildings on Soft Surface Soil. *Arabian Journal for Science and Engineering*, *46*(11), 11291-11302.

15. Çağlar, N. (2001). Yapay sinir ağları ile binaların dinamik analizi. Doctoral Dissertation, Sakarya University.

16. Akincitürk, N. (2003). Yapi tasariminda mimarin deprem bilinci. Uludag Üniversitesi, Mühendislik-Mimarlik Fakültesi Yayini, 8, 189-201.

17. Akıncıtürk, N. (2003). Ülkemizdeki deprem etkileri ve yapısal tasarımda alınması gereken önlemler. Uludağ Üniversitesi Mühendislik Mimarlık Fakültesi.

18. Karataş, L., Alptekin, A., & Yakar, M. (2022). Creating Architectural Surveys of Traditional Buildings with the Help of Terrestrial Laser Scanning Method (TLS) and Orthophotos: Historical Diyarbakır Sur Mansion. *Advanced LiDAR*, *2*(2), 54-63.

19. Karataş, L., Alptekin, A., & Yakar, M. (2022). Determination of Stone Material Deteriorations on the Facades with the Combination of Terrestrial Laser Scanning and Photogrammetric Methods: Case Study of Historical Burdur Station Premises. *Advanced Geomatics*, *2*(2), 65-72.

20. Karataş, L., & Alptekin, A. (2022). Kagir Yapılardaki Taş Malzeme Bozulmalarının Lidar Tarama Yöntemi ile Belgelenmesi: Geleneksel Silvan Konağı Vaka Çalışması. *Türkiye Lidar Dergisi*, *4*(2), 71-84.

21. Karataş, L. (2023). Yersel lazer tarama yöntemi ve ortofotoların kullanımı ile kültür varlıklarının cephelerindeki malzeme bozulmalarının dokümantasyonu: Mardin Mungan Konağı örneği. *Geomatik*, *8*(2), 152-162.

22. Karataş, L., Alptekin, A., Kanun, E., & Yakar, M. (2022). Tarihi kârgir yapılarda taş malzeme bozulmalarının İHA fotogrametrisi kullanarak tespiti ve belgelenmesi: Mersin Kanlıdivane ören yeri vaka çalışması. *İçel Dergisi*, *2*(2), 41-49.

23. Kanun, E., Alptekin, A., Karataş, L., & Yakar, M. (2022). The use of UAV photogrammetry in modeling ancient structures: A case study of "Kanytellis". *Advanced UAV*, *2*(2), 41-50.

Advanced Engineering Days

aed.mersin.edu.tr

Assessment of structural problems in Mardin Castle

Lale Karataş *1 , Aydın Alptekin 2 , Murat Yakar 3 , Murat Dal4

1Mardin Artuklu University, Department of Architecture and Urban Planning, Türkiye, lalekaratas@artuklu.edu.tr
2Mersin University, Faculty of Engineering, Department of Geological Engineering, Türkiye, aydinalptekin@mersin.edu.tr
3Mersin University, Faculty of Engineering, Department of Geomatics Engineering, Türkiye, myakar@mersin.edu.tr
4Munzur University, Department of Architecture, Türkiye, muratdal@munzur.edu.tr

Keywords
Mardin Castle
Structural damages
Stone material
Restoration

Abstract
The hill on which Mardin Castle is built consists of cliffs in the form of a cliff. Large-scale displacements and separations in the rocky formation cause serious structural and static problems on the huge structure, and smaller-scale erosion and deterioration in the castle structure. In the castle structure, which is a symbol for the region; In its current form, it needs maintenance, repair and protection interventions. Our study aims to determine the structural problems of Mardin Castle in response to this need. Observational detection and photographing documentation methods were used in the study. As a result of the study, the biggest structural problems in the castle; It has been determined that there are deteriorations in the form of cracks, separations and losses in the natural rock that forms a carrier for the fortification walls. Losses in natural rock leads to the collapse of parts of the main walls; cracking, splitting and splits caused joint openings, lattice load balance changes and partial lattice losses. Our study is valuable in terms of revealing the structural problems that carry risks at the point of ensuring the sustainability of the building and offering intervention proposals to prevent new problems.

Introduction

The hill on which Mardin Castle is built consists of cliffs in the form of a cliff. The plain on the top of the hill naturally forms a castle. Existing remains of the castle include the fortification and bastion walls, starting from the western edge and extending along the southern edge, and ending with a polygonal structure in the east. Both the city walls and bastions and the remains of the buildings in the castle have undergone changes with the deteriorations that occurred over time due to debris and earth filling, repairs and other interventions; It has reached the present day by losing its architectural integrity to a large extent. Problems in the natural rock on which the main walls sit, precipitation, water absorption-salt outflows from the ground and physical stresses due to plant growth, joint mortar/filler discharges (losses) in the wall and other carrier elements, unit material and mesh section losses in the mesh, joint in the mesh These are the problems that threaten the building elements and materials such as openings, plant (tree roots and stems) development, openings in the top cover and increased moisture as a result of soil filling. Structural problems in the castle include deteriorations that weaken the weave and thus accelerate the process that threatens the weave and its material. These problems, which accelerate the destruction, also show themselves as an important factor in material deterioration. The building in its current form needs maintenance, repair and protection interventions [1]. This study aims to determine the structural problems of Mardin Castle in response to this need.

Material and Method

In order to determine the structural problems of the castle, the structure was examined on site. The problems observed in the structure were photographed and documented. The data obtained from the field has been

classified under various sub-headings and an ontological approach has been adopted in the representation of structural problems.

Results

Ground Damages

The castle is perched on a high rocky hill with steep slopes. The fortification walls sit on the natural limestone rock, which is partially processed and used as a foundation. This natural rock on which the fortification walls are located is subject to a great deal of erosion (mechanical) due to environmental effects, natural causes and the soil filling accumulated in the castle (with mechanical effects such as water, moisture and salt outflows, frost and tectonic movements and/or softening of the clayey texture within the stone by water absorption). abrasion=erosion and chemical dissolution=corrosion); In addition to mechanical stress (water and frost, water and salt outflow) effects, large and small blocks, mono-blocks have been separated into pieces. With the erosion and separation of the natural rocks (growing cracks and crevices, formation of deep crevices, fragmentation, ruptures and losses) reaching an advanced level, the movements and losses in the carrier foundation also affected the fortification walls resting on the rock. part of it has survived to the present day. Joint enlargement-opening, deterioration in the masonry, masonry stone losses, edge and corner fractures have occurred in most of the existing walls that have survived to the present day (Figure 1).

Figure 1. Erosion of the natural rocks on which the walls sit [2]

Structural Crack

It is the situation where the masonry unit stones are separated from their joints in a horizontal, vertical or diagonal manner and emerge as a structural problem throughout the building. These cracks and splits show themselves in the form of splits between the masonry stones on the body walls and cracks / crevices in the weave. Under this title, cases where cracks, crevices and separations are continuous along a part of the masonry are examined. These cracks and disintegration also cause breakage and fragmentation in unit stone elements (Figure 2).
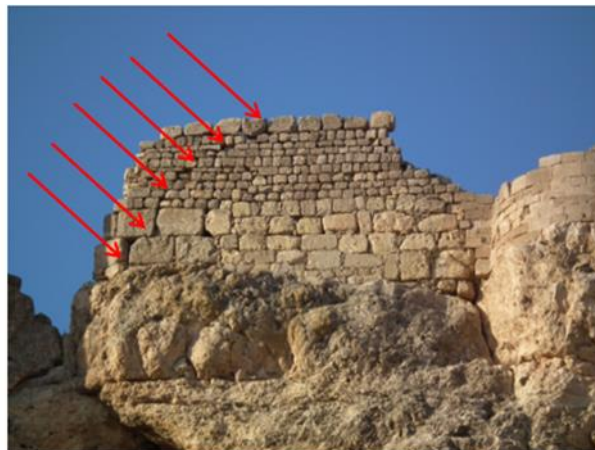
Figure 2. Structural crack [2]

Joint mortar losses in the mesh

In the upper sections of the wall, the gap between the mesh material, the water inlets to the mesh, the salt outflows from the repair mortars and the vegetative growth are the sources of deterioration. Precipitation, which is one of the important sources of deterioration, and salt outflow caused by humidity and frost events cause

crumbling and fragmentation in the weaker mortar materials as well as in the stone materials with the mechanical pressures they create. It can be observed that the deterioration starts with crumbling from the surface of the mortar that provides the connection, and in the areas of advanced deterioration, it also causes the joint filling consisting of small rubble stones in the rubble mesh to spill, gradually leading to losses up to the shedding of all the joint material. It is understood that the deterioration also caused the masonry unit material stones and lattice sections on the walls to fall due to the ongoing problems. Openings on the walls, precipitation and plant growth, joint openings and losses caused by problems in the rocks on which the wall sits are other factors that have a chain effect on the occurrence of such problems. The source of the deterioration is mostly due to the changes in the load balance (balance transferred from top to bottom in load bearing) due to ruptures/separations in the natural rock bearing the wall, new load pressures in the lattice and unit material losses. Joint openings in the mesh pose a static protection risk for the wall where the problem is seen, as well as a source for new deteriorations that will increase in the material and mesh in the formation zone (Figure 3).

Figure 3. Joint mortar discharges/losses in the lattice [2]

Losses in knitting unit material and knitting sections

These are the dissolutions and dispersions that are observed between one or more of the unit stone elements, where the weathering and cracks in the masonry texture do not follow a linear line and are not continuous. In such damages, a few unit elements constituting the lattice were locally weathered and the masonry stones were dissolved and dispersed. In the occurrence of damage; The changes in the load balance, the displacement and static problems in the rock formation on which the structure is located, and the effects of unit element losses in the masonry can be counted as triggering the discharge of the bonding joints and mortars between the unit elements. (Figure 4).

Figure 4. Losses in knit unit material and knit sections [2]

Dissolution / Dispersion in Tissue

These are the dissolutions and dispersions that are observed mostly between one or more of the unit stone elements, where the weathering and cracks in the masonry texture do not follow a linear line and are not continuous. In such damages, a few unit elements constituting the lattice were locally weathered and the masonry stones were dissolved and dispersed. In the occurrence of damage; The changes in the load balance, displacement and static problems in the rock formation on which the structure is located, and the effects of unit element losses

in the masonry can be counted as triggering the discharge of the joint and mortar between the unit elements (Figure 5).

Figure 5. Example Photo of Dissolution / Dispersion Problem in Tissue [2]

Damages caused by landfill

The earth fill, which covers the ruins of buildings with different functions, which accumulates in the intermediate part between the inner and outer walls within the fortification translation in the castle, and is even partially seen in the castle, can dissolve in the water accumulated by the rains. It is a source of deterioration that dissolves salt and causes it to reach building materials and building elements, and to damage it with frost events and salt outflows. It is known that soil filling facilitates the access of water to the building materials, and the movement of water brings with it problems such as salt formation, thus crumbling, cracks and losses in the mortar and stone materials, and the change of the load balance. The earth fill, which covers the building remains under the ground and accumulates around the fortification walls, ensures the continuous contact of the building parts with the ground water (moisture) and threatens the durability of the building materials with the formation of salt and frost (Figure 6).

Figure 6. Soil, Debris, etc. in the Masonry. Architectural Gaps Closed with Fillers [2]

Discussion

The biggest risk for the castle walls and the structures in the upper part of the castle is the erosion and displacement problems of the rocky structure on which the castle structure is built. Pieces that broke off and fell from the rocky structure in the past have emerged as an important threat to the settlements on the southern slope of the Castle. The natural rock formation forms the natural basis of both the city walls and the structures on the Kale. Therefore, it has been determined that if the problems in this rocky formation cannot be solved, the problems of the castle wall structure and the structures above it cannot be solved. In addition, it is seen that castles in many cities have been damaged or even demolished as a result of earthquake-induced events in our country recently [3]. In this context, in future studies, seismic risk and loss estimation studies of the castle are important for the process of deciding on the hazard calculation [4-12]. In addition, storing all these historical and seismic data on HBIM platforms in order to ensure a sustainable preservation of the historical building will be of great benefit in ensuring the conservation management of the building. In many studies in the literature, it is emphasized as a necessity to transfer the data of historical buildings to the HBIM environment [13-18]. At the point of preserving our local history, such civil initiatives made by scientists in academia as well as state institutions are of great importance [19].

Conclusion

One of the biggest problems in the castle is the deterioration seen in the form of cracks, separations and losses in the natural rock that forms a carrier for the fortification walls. Losses in natural rock leads to the collapse of parts of the main walls; cracking, splitting and splits caused joint openings, lattice load balance changes and partial lattice losses. There are problems, it is necessary to intervene in the natural rock in order to take precautions and prevent new problems. It is possible to examine the necessary interventions in natural rock sections with cracking, splitting and separation under the following headings.

• Natural rock sections/areas deemed appropriate to remain in place should be determined by static calculations and measurements made by subject experts.

• As was done in the construction of the castle, the problematic natural timber section should be strengthened with support structures. However, solutions should be produced by considering the strength, adequacy and compatibility of the systems such as walls and buttresses with the original.

References

1. Karataş, L. (2023). Investigating the historical building materials with spectroscopic and geophysical methods: A case study of Mardin Castle. *Turkish Journal of Engineering*, *7*(3), 266-278.
2. Mardin Büyükşehir Belediyesi (2023). KUDEB arşivi, Mardin.
3. Karataş, L., Ateş, T., Alptekin, A., Dal, M., & Yakar, M. (2023). A systematic method for post-earthquake damage assessment: Case study of the Antep Castle, Türkiye. Advanced Engineering Science, 3, 62-71.
4. Akincitürk, N. (2003). Yapi tasariminda mimarin deprem bilinci. Uludag Üniversitesi, Mühendislik-Mimarlik Fakültesi Yayini, 8, 189-201.
5. Akıncıtürk, N. (2003). Ülkemizdeki deprem etkileri ve yapısal tasarımda alınması gereken önlemler. Uludağ Üniversitesi Mühendislik Mimarlık Fakültesi.
6. Ay, B. Ö. (2018). The Effects of Implementing Different Ground-motionLogic-tree Frameworks on Seismic Risk Assessment. 16th European Conference on Earthquake Engineering.
7. Ay, B. Ö., Erberik, M. A., & Eroğlu Azak, T. (2016). Deprem Tehlikesine Maruz Bina Envanterinin İstatistiki Yöntemler ile İncelenmesi.
8. Ilgın, H. E. (2022). Use of aerodynamically favorable tapered form in contemporary supertall buildings. Journal of Design for Resilience in Architecture and Planning, 3(2), 183-196.
9. Bayhan, B., & Gülkan, P. (2011). Buildings subjected to recurring earthquakes: A tale of three cities. Earthquake spectra, 27(3), 635-659.
10. Çağlar, N., Sert, S., & Serdar, A. H. (2021). Basement-Storey Effect on the Seismic Response of RC Buildings on Soft Surface Soil. Arabian Journal for Science and Engineering, 46(11), 11291-11302.
11. Çağlar, N. (2001). Yapay sinir ağları ile binaların dinamik analizi. Doctoral Dissertation, Sakarya University.
12. Türkeri, İ. (2018). Cami tasariminda planimetrik kurgunun yeniden tartişilmasi: İskele Cami tasarimi. *Atlas Journal*, *4*(11), 841-850.
13. Karataş, L., Alptekin, A., & Yakar, M. (2022). Creating Architectural Surveys of Traditional Buildings with the Help of Terrestrial Laser Scanning Method (TLS) and Orthophotos: Historical Diyarbakır Sur Mansion. *Advanced LiDAR*, *2*(2), 54-63.
14. Karataş, L., Alptekin, A., Karabacak, A., & Yakar, M. (2022). Detection and documentation of stone material deterioration in historical masonry buildings using UAV photogrammetry: A case study of Mersin Sarisih Inn. *Mersin Photogrammetry Journal*, *4*(2), 53-61.
15. Karataş, L., & Menteşe, D. H. (2022). Dara Antik Kenti (Anastasiopolis) Nekropol Alanının Malzeme Sorunlarının Yersel Lazer Tarama Yönteminden Elde Edilen Ortofotolar Yardımıyla Belgelenmesi. *Türkiye Fotogrametri Dergisi*, *4*(2), 41-50.
16. Karataş, L., Alptekin, A., & Yakar, M. (2022). Detection and documentation of stone material deterioration in historical masonry structures using UAV photogrammetry: A case study of Mersin Aba Mausoleum. *Advanced UAV*, *2*(2), 51-64.
17. Karataş, L., Alptekin, A., Kanun, E., & Yakar, M. (2022). Tarihi kârgir yapılarda taş malzeme bozulmalarının İHA fotogrametrisi kullanarak tespiti ve belgelenmesi: Mersin Kanlıdivane ören yeri vaka çalışması. *İçel Dergisi*, *2*(2), 41-49.
18. Karataş, L. (2022). Integration of 2D mapping, photogrammetry and virtual reality in documentation of material deterioration of stone buildings: Case of Mardin Şeyh Çabuk Mosque. *Advanced Engineering Science*, *2*, 135-146.
19. Aktekin, S. (2001). Yerel Tarihçilik, Kent, Sivil Girişim Yerel Tarih Grupları Deneyimi.

Advanced Engineering Days

aed.mersin.edu.tr

Evaluation of conservation and restoration works in protected areas: A case study of Mardin Castle

Lale Karataş *1 , **Aydın Alptekin** 2 , **Murat Yakar** 3 , **Murat Dal**4

¹Mardin Artuklu University, Department of Architecture and Urban Planning, Türkiye, lalekaratas@artuklu.edu.tr
²Mersin University, Faculty of Engineering, Department of Geological Engineering, Türkiye, aydinalptekin@mersin.edu.tr
³Mersin University, Faculty of Engineering, Department of Geomatics Engineering, Türkiye, myakar@mersin.edu.tr
⁴Munzur University, Department of Architecture, Türkiye, muratdal@munzur.edu.tr

Keywords
Mardin Castle
Conservation
Restoration
Archaeological Site

Abstract
The city of Mardin, which developed at the foot of the castle, is among the rare Anatolian cities that could preserve its traditional urban texture. Today, the entire area of the castle and the old quarters where the traditional urban texture is preserved remains within the urban protected area. The most important factor in the preservation of the traditional urban fabric is undoubtedly the ethnic structure features of the neighborhoods that have been preserved in the historical process. In this context, the aim of the study is to evaluate the Mardin castle protection and restoration works, which are still being carried out by the Mardin Metropolitan Municipality, in terms of the protection of the urban and archaeological sites of Mardin.

Introduction

Mardin settlement, which is a monumental city today, consists of two elements. These are the Mardin Castle and the main settlement that developed on the skirt of the castle. The castle is located on a thin-long plain on a hill with a height of 1200 meters. This plain is 800 m in east-west direction. 150 m at the widest point in the north-south direction. 30m at the narrowest point. in size. The castle gives the impression of a natural formation since it was built to include the existing rocks with its walls and towers [1]. Access to the main entrance gate of the castle from the historical settlement located on the southern slope of the Mardin Castle is made from a middle point allowed by the topography. Mardin Castle, which has gained a reputation as a difficult place to capture throughout history, was first built by İ.S. IV. century historian Ammianus Marcellinus mentions it. After a long time, the Mardin Castle began to be mentioned in historical records by Arab scientists only from the 10th century. During this period, Mardin Castle is known as Şahin Castle or Karga Castle. In the memories of the merchant Barbaro, who came to Mardin in 1471, the castle is 12 m. It is stated that there are about 300 houses in the inner castle, which are reached by stairs and have walls exceeding [2-4].

Material and Method

In terms of urban and archaeological protection, the evaluation of Mardin Castle and its defense walls was made under three headings.

i) The effects of the measures to be taken against the problems of instability in the cliffs and slopes located on the southern skirts of the Castle, on the Mardin urban site and urban-archaeological landscape, within the scope of Mardin Castle conservation and restoration works;

ii) drainage of surface waters in the plain of Mardin Castle;

iii) It can be summarized as the effects of the current uses of Mardin Castle on the protected areas.

Results

Measures to be taken against the problems of instability in the cliffs and slopes

Various measures have been developed by the Mardin Metropolitan Municipality against possible rockfalls and instability problems on the southern slopes of Mardin Castle, which pose a great risk for the Mardin urban site and monumental structures such as Zinciriye (Sultan Isa) Madrasa. Within the scope of these measures, in order to prevent or reduce possible risks such as rockfalls on the urban site of the cliff on the southern slope of the Mardin Castle, especially the consolidation of the rock blocks was emphasized as measures to support and rehabilitate the cliff geological structure, and alternative solutions were produced against the risks of those with possible control. It has been stated that the construction and improvement of terraces and benches is an important factor in reducing the negative effects of the cliff on the urban protected area. Considering that the blocks have a higher risk of slipping in the cliff section of Mardin Castle, since the sliding and overturning heights are limited, especially in the 1st and 2nd regions, the natural terrace can be made lower inclined by cellular filling method and arranging the natural terrace by laying soil, as suggested in the current landscaping project. introduced is specified. On the other hand, more expensive solutions such as barriers will only be required in the 1st, 2nd and 3rd zones of the cliff; In the other regions from the 4th to the 12th region, it is suggested that there is no need for a barrier, that improvement and support measures will be sufficient, and that only the methods of laying soil or creating beds will be sufficient for safety. He states that if the existing terraces are raised and new terraces are built, as suggested by the experts, they should be built at a level (scale, wall technique, material, etc.) that will not change the integrity of the urban-archaeological landscape between the Mardin urban site and the Castle. In this context; The measures developed according to the engineering criteria, taking into account the characteristics of the Mardin Castle ground structure, should meet the lowest possible risk level on the Mardin urban site and monumental structures. At the same time, since it was built to include the walls and towers of the Mardin castle and the existing rocks, this natural formation effect should not be disturbed. In other words, since the visual relationship between the Mardin Castle and the urban protected area constitutes a whole with the natural structure, these engineering measures should not stand out in the urban-archaeological landscape [5-6].

Drainage problem of surface waters in the plain of Mardin Castle

The prevention of surface waters, which is the most important cause of instability problems in Mardin Castle and the southern slopes, is considered as an important factor. Rain, snow, etc. falling directly on the castle plain. The drainage of the sourced surface waters should be collected in certain places or places within the castle by making small diameter channels, and then evacuated outside the castle by an appropriate method. Leveling the inclined planes together with the channels to provide the flow on the castle plain for the drainage system to be built to collect the surface waters in certain places must have been made by the users of the Castle for centuries. The cisterns and water tanks in the Mardin Castle mentioned in historical sources and other storage systems such as grain must have been built within this scope. The defense walls and other structures in the castle IV. It can be thought that their use since the century has been possible with the correct drainage and use of surface waters. In this respect, it is certain that the possible results of archaeo-geophysical and archaeological surveys planned to identify old cisterns, warehouses, surface water drainage and other structures on the Kale plain will also provide a solution for the current surface water drainage problem. In this context, it should be expected that future archaeological research will bring suggestions for the reorganization of the Kale plain, as well as for the drainage of surface waters. Filling is recommended by the relevant experts in order to prevent surface waters for the cracks in the ground structure of the castle in the upper elevations. Filling the cracks in the lower elevations, especially in the cliffs, is inconvenient as it will prevent the drainage of the water that seeps from the surface, and it is recommended not to be applied. In this context, covering the known cisterns and new cisterns to be determined by archaeological surveys and large volumes that can hold water with a cover that will not collect rain and snow water after excavation (in accordance with the original characteristics of the archaeological remains in terms of scale, material and construction technique), where the Mardin Castle sits. It will greatly reduce the accumulation of groundwater that can go into small cracks in the ground structure.

The effects of current uses on the sites in Mardin Castle

It is known that Mardin Castle was used by the elite with its mansion structure even in the 1930s. However, it was used as a military area until recently. Therefore, the continuity of a building culture in which the surface water drainage was successfully solved by the users and the walls were integrated with the ground structure for centuries on the Kale plain has been lost. When the western part of the castle plain was arranged as a place open to visitors for tourism purposes, the ruins and archaeological traces seen by Gabriel were covered and road, parking lot and pedestrian path planes were created today. As mentioned above, with this arrangement, the regime of the surface waters, which had been drained for centuries on the Kale plain, changed, causing stability problems in the settlement structure of the Castle, as well as adversely affecting the context of the archaeological remains. On the plain of Mardin Castle, the main gate and magnificent entrance of the Castle, which can be reached by the shortest pedestrian path from the Mardin urban site due to intense visitor interest, the Kale Mosque, the ruins known as the Akkoyunlu Palace in the north are integrated with the castle defense walls in this region. constitutes the structure. This archaeological monumental building complex should be considered within the scope of the ongoing works for the castle walls and should be determined as the first priority area for the conservation and consolidation works. In the process of conservation and consolidation works here, a separate option should be sought for visitor entry to the Castle.

As a second priority work, the existing vehicular traffic, parking lots and pedestrian roads should be temporarily removed, especially in the western part of the Kale plain, which is open to visitors. As a result of the archaeological researches to be done, an archaeological landscape arrangement should be made to ensure the drainage of the surface waters. In this arrangement, the areas to be excavated should be limited to areas at risk (such as the complex at the entrance of the Castle), and reserve archaeological areas should be defined according to their importance. Visitor circulation (vehicle and pedestrian traffic) should be provided with minimal interference to the archaeological structures to be excavated and documented and the reserve archeological fillings. In the region, which is still used as a military area, archaeological landscaping should be handled with the same principles as the last stage of work. Accordingly, considering the sensitive archaeological features of the region where structures such as the magnificent main entrance gate complex, Kale Mosque, Akkoyunlu Palace complex, which can be reached from the Mardin Urban Site, are located, it should be considered as a first priority archaeological site integrated with the walls of Mardin Castle. This area is also determined as the 3rd area defined for the instability problems on the southern skirts of the Castle, so it also constitutes the first priority archaeological landscaping issue. Against the instability problems caused by the modern constructions on the Mardin Castle plain, archaeological research should be carried out in stages according to the priority order of the intervened areas, the old cistern systems should be examined, and the possibilities of restoring the old drainage system should be investigated. The area located in the hinterland of the walls of Mardin Castle, defined as the first region, was the area where the least modern constructions intervened, so this area should be defined as an archaeological reserve area and the use of an archaeological park should be suggested.

Discussion

These uses indirectly have negative effects on the Mardin Urban Protected Area. In the archaeological park arrangement to be made on the plain of Mardin Castle, the necessary intervention and arrangement for the archaeological sites of different importance to be determined according to the results of the archaeological survey will also determine the visitor plan of the area in question. In principle, the protection of archaeological cultural assets should be ensured as a priority; exhibiting and bringing it to tourism should be the second priority. Since it was built to include the walls and towers of Mardin Castle and the existing rocks, it should be preserved to give the impression of a natural formation. In addition, it is seen that historical castles in many cities have been damaged or even destroyed as a result of the earthquake-induced events in our country recently [7]. In this context, in future studies, seismic risk and loss estimation studies of the castle are important for the process of deciding on the hazard calculation [8-16]. In addition, if problems arise in the castle structure, which is a masonry structure, as in all historical masonry structures, it is an obligatory requirement to control the deterioration process of the structure by using a manageable platform for later restoration interventions and to ensure that it is repaired at regular intervals [17-21].

Conclusion

As a result, the measures to be taken within the scope of Mardin Castle conservation and restoration works in terms of the protection of Mardin Castle and Mardin Urban Site can be summarized as follows in terms of stages and regions:

i) Measures to be taken against instability problems in the cliffs and slopes located on the southern skirts of the Castle should be phased according to their importance, taking into account the Mardin urban site and its urban-archaeological landscape;

ii) The drainage of surface waters in the plain of Mardin Castle should be considered and staged as an important element, integrated with the archaeological researches and the repair of the castle walls;

iii) Existing uses in Mardin Castle have negative effects on the archaeological cultural assets on the Kale plain.

References

1. Altun,A.(1971). Mardin'de Türk Devri Mimarisi, İstanbul.
2. Alioğlu, E. F. (2000). Mardin Şehir Dokusu ve Evler, İstanbul.
3. Mardin Valiliği(1988). Yaşayan Tarih Mardin. İstanbul.
4. Gabrıel, A. (1940). Voyages Archeologique Dans La Turquie Orientale, Paris.
5. Mardin Büyükşehir Belediyesi (2023). KUDEB arşivi, Mardin.
6. Mardin Büyükşehir Belediyesi (2012). Mardin Kalesi Kaya Düşmeleri Analizi Ve Alınabilecek Önlemler Raporu.
7. Karataş, L., Ateş, T., Alptekin, A., Dal, M., & Yakar, M. (2023). A systematic method for post-earthquake damage assessment: Case study of the Antep Castle, Türkiye. Advanced Engineering Science, 3, 62-71.
8. Ay, B. Ö. (2018). The Effects of Implementing Different Ground-motionLogic-tree Frameworks on Seismic Risk Assessment. 16th European Conference on Earthquake Engineering.
9. Ay, B. Ö., Erberik, M. A., & Eroğlu Azak, T. (2016). Deprem Tehlikesine Maruz Bina Envanterinin İstatistiki Yöntemler ile İncelenmesi.
10. Ilgın, H. E. (2022). Use of aerodynamically favorable tapered form in contemporary supertall buildings. Journal of Design for Resilience in Architecture and Planning, 3(2), 183-196.
11. Bayhan, B., & Gülkan, P. (2011). Buildings subjected to recurring earthquakes: A tale of three cities. Earthquake spectra, 27(3), 635-659.
12. Çağlar, N., Sert, S., & Serdar, A. H. (2021). Basement-Storey Effect on the Seismic Response of RC Buildings on Soft Surface Soil. Arabian Journal for Science and Engineering, 46(11), 11291-11302.
13. Çağlar, N. (2001). Yapay sinir ağları ile binaların dinamik analizi. Doctoral Dissertation, Sakarya University.
14. Akincitürk, N. (2003). Yapi tasariminda mimarin deprem bilinci. Uludag Üniversitesi, Mühendislik-Mimarlik Fakültesi Yayini, 8, 189-201.
15. Akıncıtürk, N. (2003). Ülkemizdeki deprem etkileri ve yapısal tasarımda alınması gereken önlemler. Uludağ Üniversitesi Mühendislik Mimarlık Fakültesi.
16. Türkeri, İ. (2018). Cami tasariminda planimetrik kurgunun yeniden tartişilmasi: İskele Cami tasarimi. Atlas Journal, 4(11), 841-850.
17. Karataş, L., Alptekin, A., & Yakar, M. (2022). Analytical Documentation of Stone Material Deteriorations on Facades with Terrestrial Laser Scanning and Photogrammetric Methods: Case Study of Şanlıurfa Kışla Mosque. *Advanced LiDAR*, *2*(2), 36-47.
18. Karataş, L., Alptekin, A., Karabacak, A., & Yakar, M. (2022). Detection and documentation of stone material deterioration in historical masonry buildings using UAV photogrammetry: A case study of Mersin Sarisih Inn. *Mersin Photogrammetry Journal*, *4*(2), 53-61.
19. Karataş, L., & Menteşe, D. H. (2022). Dara Antik Kenti (Anastasiopolis) Nekropol Alanının Malzeme Sorunlarının Yersel Lazer Tarama Yönteminden Elde Edilen Ortofotolar Yardımıyla Belgelenmesi. *Türkiye Fotogrametri Dergisi*, *4*(2), 41-50.
20. Karataş, L., Alptekin, A., & Yakar, M. (2022). Detection and documentation of stone material deterioration in historical masonry structures using UAV photogrammetry: A case study of Mersin Aba Mausoleum. *Advanced UAV*, *2*(2), 51-64.
21. Karataş, L. (2022). Integration of 2D mapping, photogrammetry and virtual reality in documentation of material deterioration of stone buildings: Case of Mardin Şeyh Çabuk Mosque. *Advanced Engineering Science*, *2*, 135-146.

Mardin Castle landscaping and landscape interventions proposal

Lale Karataş *1 , **Aydın Alptekin** 2 , **Murat Yakar** 3 , **Murat Dal**4

1Mardin Artuklu University, Department of Architecture and Urban Planning, Türkiye, lalekaratas@artuklu.edu.tr
2Mersin University, Faculty of Engineering, Department of Geological Engineering, Türkiye, aydinalptekin@mersin.edu.tr
3Mersin University, Faculty of Engineering, Department of Geomatics Engineering, Türkiye, myakar@mersin.edu.tr
4Munzur University, Department of Architecture, Türkiye, muratdal@munzur.edu.tr

Keywords
Mardin Castle
Landscaping
landscape intervention
Conservation

Abstract
Mardin Castle is a historically important castle that has lived through the periods of many civilizations and is a symbol for the city. However, this magnificent structure also brings with it problems. The abrasive conditions that have emerged over time cause the rocks to decompose from the main structure and pose a threat to the historical urban fabric. The threat that the rocks will create for the city of Mardin is in the first place as a problem that needs to be solved as soon as possible from today to tomorrow. The main determinant of the study was the prevention of bouncing and rolling of falling and rolling rocks by hitting the hard structure on the ground. Within the scope of the study, Suggestions for landscaping and landscape interventions were made for the Mardin Castle.

Introduction

Mardin Castle is a very important castle that lived the periods of Subari, Sumerian, Babylonian, Mitanids, Assyrian, Persian, Roman, Byzantine, Umayyad, Abbasid, Hamdanids, Seljuks, Artuklu, Karakoyunlu, Akkoyunlu, Safavids and Ottomans. Its height from the Harran plain is about a thousand meters. Part of the castle sits on steep rocks [1]. However, this magnificent structure also brings with it problems. The abrasive conditions that have emerged over time cause the rocks to decompose from the main structure and pose a threat to the historical urban fabric. The threat that the rocks will create for the city of Mardin is in the first place as a problem that needs to be solved as soon as possible from today to tomorrow. The main determinant of the study was the prevention of bouncing and rolling of falling and rolling rocks by hitting the hard structure on the ground [2]. The fact that there was no change in the usual appearance of the Mardin castle while this structure was being built, and that it did not damage the archaeological structure, is one of the most important problems to be solved.

Material and Method

The study was carried out in two parts as office and field research. Within the scope of the study, firstly, the castle structure was examined in situ. Observational problems have been identified in the building and its surroundings. In the second stage, the office stage, some suggestions to prevent these problems have been determined by making use of the literature.

Results

When you look at the direction of the castle from the city, it is aimed to create a 60 cm soft soil layer with the 5-layer application of cellular filling elements with a thickness of 12 cm in the left section (Q.6.1), which has a steep structure. Peat (Lithuanian peat) is recommended in order to increase the soil permeability and create a spongy structure inside the cells in 50% of the talus, 20% of the sand and 30% of the existing in the area. This structure will reduce the threat of the barriers to be created by breaking the energy of the falling and rolling rocks. Cellular filling systems; It enables the compaction of simple filling materials to provide the most difficult load bearing and erosion control. It allows the use of natural filling material in the application area instead of expensive filling material. Increases load carrying capacity, reduces collapses. It creates a flexible structural bridge by distributing the concentrated loads over a wide area. The durable polyethylene partitions used in the cellular filling (Geoweb) system are folded to facilitate transportation. It maintains its flexibility, making it easier to carry during application. Provides mechanical filling and compression. It demonstrates an indisputable performance in the most difficult load support and erosion control applications [3] (Figure 1). Looking at the direction of the castle, it is aimed to bring a solution together with the Gabion walls and the geoarme cover system that will serve as a retaining wall by friction, in the middle section where the threat of rockfall is the highest. As stated in the details of the gabion wall system deployed in the front, it is aimed to develop a structure without deteriorating the natural appearance by filling the front surfaces with soil [3] (Figure 2).
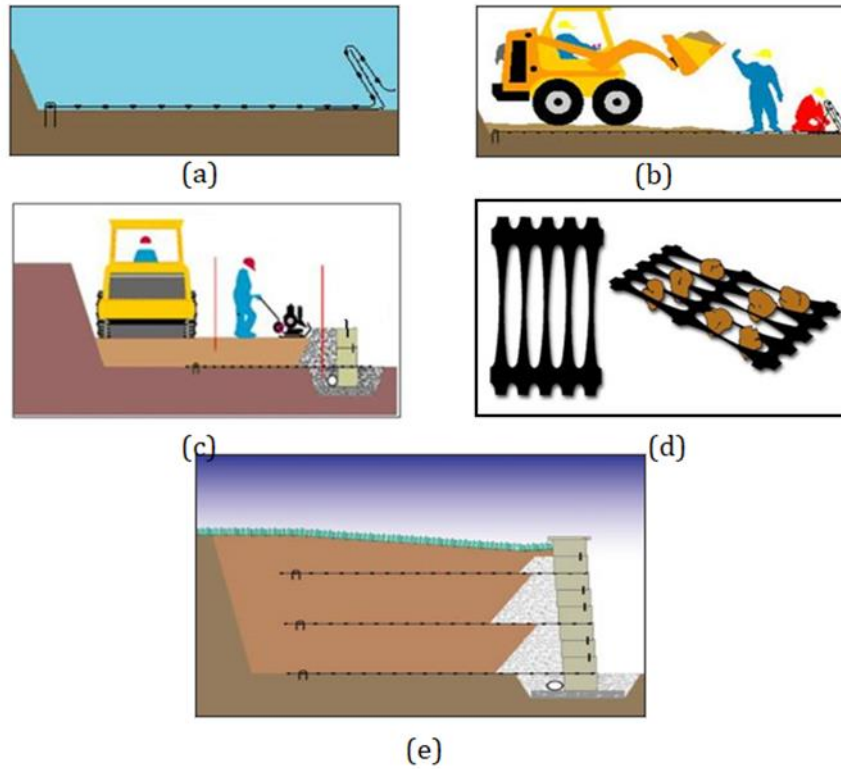
Figure 2. Workflow of Landscaping Proposal [(a)Laying the geogrid cover; (b) Making the filling (c) Gabion joint and soil compaction(d) Geogrid cover (d) Formation of the pillow layer

It is aimed to provide a structure that will prevent the rocks in the Mardin castle from rolling and maintain the natural slope view without damaging the existing plant tissue. In this section, a single-row cellular filling system is proposed. The main road that reaches the castle inside the castle is 3.5 m wide. It is not recommended to widen this road and speed up access to the tin. However, repairing the slope elevator that provides access to the radar facilities and providing access to the castle should be the first priority in transportation. A transportation arrangement to be made in this way will reduce the load of the existing road. 10x10x10 cm granite parquet is recommended for this road to create a more natural structure without creating any change on the existing road. For the roads that will provide circulation in the castle;

a. It is recommended to lay a plastic block that will provide a comfortable circulation without damaging the existing structure made of recycled plastic material (grass block). It is suggested that the pores of the cover be filled with 5-7 mm beige mosaic material. A Geotextile cover to be laid on the bottom of the cover will prevent grazing that may develop over time.

b. Galvanized steel grating is recommended as another option for these roads, considering that there may be wear over time. These gratings will be connected to the ground with steel studs and will form a stable ground. The grid cells will be filled with the same material and compacted.

Protection will be provided with mini sprinkler heads within the first 2 m of the area protected by a fence against the risk of fire. The effective wetting diameter of these heads is 2 m. As soon as the fire starts, the system will be activated and will end the burning process. Gabion has been determined as the main purpose of regaining the natural appearance in areas where cellular filling is applied. For this reason, in hydroseeding applications, mulch (wood fiber) and plant seed mixture supplemented with slow-melting fertilizers will be sprayed onto the areas. In the plant seed mixture to be applied as 80 gr per m^2;

• Capparis spinosa
• Festuca ovine
• Peganum harmala
• Melissa oficinalis
• Cynedon sp.
 • Astragalus mardinensis
• Bunium microcarpum

Discussion

As a result of the earthquake-induced events in our country recently, it is seen that the castles in many cities have been damaged or even demolished [4]. In this context, it is an inevitable fact that the dangers described in my writing in Mardin Castle will continue to increase as long as earthquakes continue. In this context, against the seismic damages that may occur, the damages that may occur in the castle due to seismic effects should be evaluated in advance in the future works. In this context, in future studies, seismic risk and loss estimation studies for the castle are important for the process of deciding on the hazard calculation [5-13].

It is very important that various disciplinary disciplines decide together within the scope of the preservation of historical buildings and the historical silhouette around them. In this context, the data of various disciplines on historical buildings brought together on HBIM platforms provide great convenience for experts from various disciplines to work together. Many studies in the literature emphasize that historical buildings should be inspected in a controlled manner on HBIM platforms and undergo regular repair interventions during the conservation process [14-20].

Conclusion

Mardin Castle is a historically important castle that has lived through the periods of many civilizations and is a symbol for the city. However, this magnificent structure also brings with it problems. The abrasive conditions that have emerged over time cause the rocks to decompose from the main structure and pose a threat to the historical urban fabric. The threat that the rocks will create for the city of Mardin is in the first place as a problem that needs to be solved as soon as possible from today to tomorrow. Preventing the falling and rolling rocks from splashing and rolling by hitting the hard structure on the ground was the main determinant of the study. Within the scope of the study, landscaping and landscape interventions were suggested for the Mardin Castle.

References

1. Altun, A. (1971). Mardin'de Türk Devri Mimarisi, İstanbul.
2. Karataş, L. (2023). Investigating the historical building materials with spectroscopic and geophysical methods: A case study of Mardin Castle. *Turkish Journal of Engineering*, *7*(3), 266-278.
3. Yünkül, K., & Gürbüz A. (2018), Hücresel Dolguların Kullanım Alanları ve Çalışma Mekanizması, ISAS 2018, Antalya, Türkiye.
4. Karataş, L., Ateş, T., Alptekin, A., Dal, M., & Yakar, M. (2023). A systematic method for post-earthquake damage assessment: Case study of the Antep Castle, Türkiye. *Advanced Engineering Science*, *3*, 62-71.
5. Akincitürk, N. (2003). Yapi tasariminda mimarin deprem bilinci. Uludag Üniversitesi, Mühendislik-Mimarlik Fakültesi Yayini, 8, 189-201.
6. Akıncıtürk, N. (2003). Ülkemizdeki deprem etkileri ve yapısal tasarımda alınması gereken önlemler. Uludağ Üniversitesi Mühendislik Mimarlık Fakültesi.

7. Ay, B. Ö. (2018). The Effects of Implementing Different Ground-motionLogic-tree Frameworks on Seismic Risk Assessment. 16th European Conference on Earthquake Engineering.
8. Ay, B. Ö., Erberik, M. A., & Eroğlu Azak, T. (2016). Deprem Tehlikesine Maruz Bina Envanterinin İstatistiki Yöntemler ile İncelenmesi.
9. Ilgın, H. E. (2022). Use of aerodynamically favorable tapered form in contemporary supertall buildings. Journal of Design for Resilience in Architecture and Planning, 3(2), 183-196
10. Bayhan, B., & Gülkan, P. (2011). Buildings subjected to recurring earthquakes: A tale of three cities. Earthquake spectra, 27(3), 635-659.
11. Çağlar, N., Sert, S., & Serdar, A. H. (2021). Basement-Storey Effect on the Seismic Response of RC Buildings on Soft Surface Soil. Arabian Journal for Science and Engineering, 46(11), 11291-11302.
12. Çağlar, N. (2001). Yapay sinir ağları ile binaların dinamik analizi. Doctoral Dissertation, Sakarya University.
13. Türkeri, İ. (2018). Cami tasariminda planimetrik kurgunun yeniden tartişilmasi: İskele Cami tasarimi. Atlas Journal, 4(11), 841-850.
14. Karataş, L., Alptekin, A., Karabacak, A., & Yakar, M. (2022). Detection and documentation of stone material deterioration in historical masonry buildings using UAV photogrammetry: A case study of Mersin Sarisih Inn. Mersin Photogrammetry Journal, 4(2), 53-61.
15. Karataş, L., & Menteşe, D. H. (2022). Dara Antik Kenti (Anastasiopolis) Nekropol Alanının Malzeme Sorunlarının Yersel Lazer Tarama Yönteminden Elde Edilen Ortofotolar Yardımıyla Belgelenmesi. Türkiye Fotogrametri Dergisi, 4(2), 41-50.
16. Karataş, L. (2023). Yersel lazer tarama yöntemi ve ortofotoların kullanımı ile kültür varlıklarının cephelerindeki malzeme bozulmalarının dokümantasyonu: Mardin Mungan Konağı örneği. *Geomatik*, *8*(2), 152-162.
17. Karataş, L., Alptekin, A., & Yakar, M. (2022). Detection and documentation of stone material deterioration in historical masonry structures using UAV photogrammetry: A case study of Mersin Aba Mausoleum. Advanced UAV, 2(2), 51-64.
18. Karataş, L. (2022). Integration of 2D mapping, photogrammetry and virtual reality in documentation of material deterioration of stone buildings: Case of Mardin Şeyh Çabuk Mosque. Advanced Engineering Science, 2, 135-146.
19. Karataş, L., Alptekin, A., & Yakar, M. (2022). Creating Architectural Surveys of Traditional Buildings with the Help of Terrestrial Laser Scanning Method (TLS) and Orthophotos: Historical Diyarbakır Sur Mansion. *Advanced LiDAR*, *2*(2), 54-63.
20. Karataş, L., Alptekin, A., & Yakar, M. (2022). Determination of Stone Material Deteriorations on the Facades with the Combination of Terrestrial Laser Scanning and Photogrammetric Methods: Case Study of Historical Burdur Station Premises. *Advanced Geomatics*, *2*(2), 65-72.

The role of Notch and Wnt signaling pathways in neurodevelopment

Ece Tümkaya *[1] , **Furkan Ayaz** [2]

[1]Mersin Univercity, Biotechnology Department, Türkiye, ece_tumkaya@hotmail.com
[2]Mersin Univercity, Research and Application Center, Türkiye, furkanayaz@mersin.edu.tr

Keywords
Signaling pathway
Neuron
Neurodevelopment
Diseases
Cancer

Abstract
Notch is a protein that decides the path that cells should take by interacting with its ligands. The Notch signaling pathway is involved in performing functions that ensure cell survival.Notch activity mediates the formation of new structures from certain cells with its effect on differentiation, proliferation and apoptosis of cell. Similarly, Wnt signaling pathway sare involved in versatile signal transduction pathways that start with proteins that transmit signals to a cell via cell surface receptors and have many functions, including the control of neurogenesis. In this review proceeding, we will address the role of Notch and Wnt signaling pathways on neuronal development.

Introduction

John S. Dexter noticed that a notch appeared on the wings of the fruit fly Drosophila melanogaster in 1914. The alleles of this gene were described by Thomas Hunt Morgan in 1917, and in this way the notch signaling pathway was discovered [1]. The Notch pathway controls the continuity of stem cells, which undertake numerous tasks in our body, and is also a human cancer pathway known to have great activity in cancer. WNT, on the other hand, has two members that made it possible to get its name. The name Wnt was created by combining the first discovered Int-1 and later the Wingless gene, which was found to be homologous to this gene and discovered in Drosophila [2]. 19 proteins in the Wnt family are stimulants that contribute to the stimulation of the signaling pathway. These signaling pathways control neural stem cell activation, cell division and migration. Among its most important functions are being the main regulator of neurogenesis in the CNS and controlling brain plasticity. The brain sometimes undergoes changes due to different reasons. These can be structural or physiological. Some of these changes are the result of the neuron production mechanism. This production is of vital importance in the whole body as well as in the brain [3]. The control of a certain part of the changes and production mechanism in the brain is in the hands of the signaling pathways. With this explanation, we emphasize the importance of Notch and Wnt signaling pathways. Studies have revealed that Notch and Wnt signaling pathway sinteract in Drosophila and prevent early neuro-competence in ectodermal cells. In another study, it has been proven that a defect in these signaling pathways creates major deficits in learning and memory abilities [4]. Considering the effect of these signaling pathways on neurodevelopment, any dysregulation of the sepathways can be very serious, including T-cell leukemia, spondylocostal dysostosis, schizophrenia, Alzheimer's, Parkinson's, CADASIL syndrome and Alagille syndrome, ADHD, learning and communication disorder, and intellectual disabilities [1,5]. It is becoming clear that it can pave the way for a large number of neurodevelopmental and neurodegenerative diseases.

Results

The indicated signal transduction pathways enable many reactions required for cell survival. They are cancer pathways, however, due to their important roles in the body, they can cause various neurodevelopmental and neurodegenerative problems, developmental delay and many diseases such as cancer.

Discussion

Contrary to the general belief that nerve cells in the brain end with the moment of birth and that there is no new formation, scientists have revealed that new nerve cells can be produced thanks to their discovery. It is known that newly formed neurons increase memory capacity and improve learning power [4]. As mentioned above, it has been discovered that the role of Notch and Wnt signaling pathways is quite large in these developments.

Conclusion

While significant progress has been made in understanding the molecular mechanisms behind the neurodevelopment, there is still much to explore [5]. The hundreds of interconnected signaling pathways probably lie behind the simplest phenomena. Elucidation of these mechanisms will be through further analysis of animal models, biochemistry analysis, and human diseases. We should not be hopeless within the scope of the treatment of neurodevelopmental disorders, we should concentrate on where and how the treatment should be found. The ability of the brain to renew itself is much stronger than we think, and we can direct this ability with the right steps [6]. Extensive studies on the indicated signaling pathways will lead to the discovery of new and promising treatments.

References

1. Xiao, M. J., Han, Z., Shao, B., & Jin, K. (2009). Notch signaling and neurogenesis in normal and stroke brain. *International journal of physiology, pathophysiology and pharmacology*, *1*(2), 192-202
2. Altinok, B., & Sunguroğlu, A. (2016). Wnt sinyal yolağı ve kanser. *Ankara Sağlık Hizmetleri Dergisi*, *15*(2), 27-38.
3. https://bilimfili.com/beyin-plastisitesi-nedir-ve-neden-cok-onemlidir
4. Chen, M., & Do, H. (2012). Wnt signaling in neurogenesis during aging and physical activity. *Brain Sciences*, *2*(4), 745-768.
5. Lasky, J. L., & Wu, H. (2005). Notch signaling, brain development, and human disease. *Pediatric research*, *57*(7), 104-109.
6. https://abapsikoloji.com/norogelisimsel-bozukluklar-icin-tedavi-ve-terapi-yontemi/

Advanced Engineering Days

aed.mersin.edu.tr

The role of soil microbiome in plant growth and development under stress conditions

Ceren Küçümen Aslan*[1] , Furkan Ayaz[1, 2]

[1]Mersin University, Biotechnology Department, Türkiye, 21020190001@mersin.edu.tr
[2]Mersin University, Biotechnology Research and Application Center, Türkiye, furkanayaz@mersin.edu.tr

Keywords
Plant
Growth
Microbiome

Abstract
Stress-related factors have a negative influence on plant growth and yield. Numerous approaches are used to alleviate these disadvantageous effects on the plant growth. Using soil microbiome and plant growth-promoting bacteria (PGPB) is another method for eradicating the adverse effects that stress-induced conditions have on plants. Numerous studies have shown that plant growth-promoting bacteria (PGPB) increase plant yield under a range of different stress conditions. In this proceeding review we will briefly discuss these issues.

Introduction

Plants, unlike other living things, do not have the option of relocating under stress environments. Numerous different changes happen in plants under stress conditions, including such membrane permeability degradation, increased ROS production, and decreased yield. As a result, they have different approaches for staying alive under stress [1]. Soil microbiome mutualistic relationships are one of these strategies. Soil microbiomes, regardless of whether they are dependent on stress conditions, take a significant part in plant growth and development [2]. Additionally, there are bacterial species called plant growth-promoting bacteria that positively influences plant growth in the soil microbiome. These bacteria play a significant role in improving plants' capability to withstand stress [3]. Plant growth-promoting bacteria can always be inserted into the soil to enhance plant growth, sustain nutrient status, and keep improving hormonal balance [4,5].

Results

Numerous studies have been published in the literature that demonstrate the beneficial impact of soil microbiomes on plant growth.

Bacillus safensis and *Ochrobactrum pseudogregnonens*, which are known to be osmotic stress tolerant bacteria, were used in the studies conducted by Chakraborty et al. on six different varieties of wheat [6]. In their research, they observed that in six wheat varieties exposed to water stress, both bacterial groups enhanced biomass, plant height, chlorophyll content, and indirectly increased yield [6]. Kohler et al. [7] studied the responses to drought stress by inoculating lettuce with different combinations of mycorrhiza and bacteria, alone or in combination. Phosphatase activity in lettuce roots and proline accumulation in leaves were seen after P.mendocina was inoculated on lettuce plants that had been exposed to severe drought. While superoxide dismutase (SOD) activity was reported to decrease in the literature, an increase in peroxidase (POX) and catalase (CAT) activities was seen

as a response to drought stress. This implies that bacteria that encourage plant growth are extremely important, particularly in the response to drought stress [7].

Marulanda et al. examined the effects of plant growth-promoting bacteria (PGPB) on the plasma membrane of the plant under unstressed and salt stress conditions by inoculating Bacillus megaterium strain on maize plant [8]. In their study, they discovered that Bacillus megaterium-inoculated plants exhibited enhanced root hydraulic conductance (L) values both under stress and not. Nevertheless, it has been noted that roots of plants with higher L values which have been exposed to salt stress and bacterial inoculation have high concentrations of plasma membrane type two (PIP2) aquaporin. All of this data demonstrates that bacteria are essential to the growth of stress tolerance and that the response of maize plants inoculated with the Bacillus megaterium strain to salt stress changes [8].

Conclusion

In conclusion, it has been found that soil microbiomes have an influence on how well plants grow under stress conditions [9,10]. Additionally, research has shown that soil microbiomes, such as PGPB, have a positive impact on plant growth and development while they are not under stress [3,4,5,9,10]. This research suggests that soil microbiomes or bacteria that stimulate plant growth stimulated plant growth and yield. More studies are required to determine the beneficial bacteria that support the plant growth under stress conditions to utilize them in the field with changing climate conditions.

References

1. Taiz, L., Zeiger, E., Møller, I. M., & Murphy, A. (2015). *Plant Physiology and development*. Ankara: Palme Yayıncılık
2. Chen, C., Wang, M., Zhu, J., Tang, Y., Zhang, H., Zhao, Q., ... & Shen, Z. (2022). Long-term effect of epigenetic modification in plant–microbe interactions: modification of DNA methylation induced by plant growth-promoting bacteria mediates promotion process. *Microbiome*, *10*(1), 1-19.
3. Egamberdiyeva, D. (2007). The effect of plant growth promoting bacteria on growth and nutrient uptake of maize in two different soils. *applied soil ecology*, *36*(2-3), 184-189.
4. Abdelaal, K., AlKahtani, M., Attia, K., Hafez, Y., Király, L., & Künstler, A. (2021). The role of plant growth-promoting bacteria in alleviating the adverse effects of drought on plants. *Biology*, *10*(6), 520.
5. Souza, R. D., Ambrosini, A., & Passaglia, L. M. (2015). Plant growth-promoting bacteria as inoculants in agricultural soils. *Genetics and molecular biology*, *38*, 401-419.
6. Chakraborty, U., Chakraborty, B. N., Chakraborty, A. P., & Dey, P. L. (2013). Water stress amelioration and plant growth promotion in wheat plants by osmotic stress tolerant bacteria. *World Journal of Microbiology and Biotechnology*, *29*(5), 789-803.
7. Kohler, J., Hernández, J. A., Caravaca, F., & Roldán, A. (2008). Plant-growth-promoting rhizobacteria and arbuscular mycorrhizal fungi modify alleviation biochemical mechanisms in water-stressed plants. *Functional Plant Biology*, *35*(2), 141-151.
8. Marulanda, A., Azcón, R., Chaumont, F., Ruiz-Lozano, J. M., & Aroca, R. (2010). Regulation of plasma membrane aquaporins by inoculation with a Bacillus megaterium strain in maize (Zea mays L.) plants under unstressed and salt-stressed conditions. *Planta*, *232*(2), 533-543.
9. Vandana, U. K., Rajkumari, J., Singha, L. P., Satish, L., Alavilli, H., Sudheer, P. D., ... & Pandey, P. (2021). The endophytic microbiome as a hotspot of synergistic interactions, with prospects of plant growth promotion. *Biology*, *10*(2), 101.
10. Tiwari, M., Pati, D., Mohapatra, R., Sahu, B. B., & Singh, P. (2022). The Impact of Microbes in Plant Immunity and Priming Induced Inheritance: A Sustainable Approach for Crop protection. *Plant Stress*, 100072.

Advanced Engineering Days

aed.mersin.edu.tr

BRCA1 and BRCA2 genes in breast cancer

Hülya Servi *1 ⓘ, **Furkan Ayaz**1,2 ⓘ

1Mersin University, Biotechnology Department, Türkiye, hulyaservi582@gmail.com, 19133015@mersin.edu.tr
2Mersin University, Biotechnology Research and Application Center, Türkiye, furkanayaz@mersin.edu.tr

Keywords
Cancer
BRCA1
BRCA2
Mutation

Abstract
Cancer is a disease characterized by uncontrolled and abnormally growing cells that develop as a result of the uncontrolled proliferation of cells in the body. With the increasing incidence of cancer day by day, cancer diagnosis and treatment methods are gaining more and more importance. Mutations in BRCA1 and BRCA2 genes are predominantly detected in the breast cancer patients. An inherited mutation in the BRCA gene becomes carried by all cells in the body. The process of carcinogenesis can begin with a "second hit" somatic mutation in the intact allele. For this reason, the identification of variants in BRCA gene mutations is important in the prevention and estimation of cancer risk and in the early diagnosis of cancer. It is recommended that people with a family history of breast cancer undergo screening for genetic risk factors. With technological developments, additional programs are being used to the models used for cancer risk detection today. In this way, it is aimed to provide effective treatment, detect cancer at an early stage, reduce cancer risks as much as possible, and ensure a long and high-quality life. In this proceeding study, we are reviewing the BRCA gene mutations and their association with breast cancer.

Introduction

Carcinogenesis is characterized by cell survival and proliferation even after genetic mutations. This genetic damage, on the other hand, can occur in the genes of the cell, and cancer can occur as a result of this uncontrolled proliferation. Regulatory genes collected in three groups:

1-Genes that can control apoptosis
2-Proto oncogenes that can ensure growth
3-Tumor suppressing genes that can inhibit growth are called.

Carcinogenesis is multi-step and occurs as a result of the accumulation of mutations in many genes within the three genes we have listed [1]. Cancer usually occurs by metastasis. Early diagnosis of cancer is life-saving, but like other diseases, it can result in death when it is delayed [2].

Examples of modifiable risk factors for breast cancer include demographic changes, physical activity, environmental factors, hormone therapy, obesity, use of oral contraceptives, smoking and alcohol use; Family history, race, early age at menopause, late menopause, age and genetic mutations can be given as examples of non-modifiable risk factors [2]. It is thought that 85% of breast cancers are caused by genetic factors. The fact that women have more breast tissue than men increase the risk of breast cancer [3]. It has been determined that 50-60% of hereditary breast cancers occur as a result of a mutation affecting one of the Breast Cancer 1(BRCA1) and Breast Cancer 2(BRCA2) genes located on the 17th chromosome [2]. The location of the BRCA mutation in the gene and the type of mutation may affect the risk of developing breast cancer. This breast cancer risk may vary depending on the median age at the time of cancer diagnosis, the nucleotide position of the mutations in patients

with germline BRCA1 and BRCA2 mutations, the functional outcome of the mutations, and the type of mutations [4]. The BRCA gene is a tumor suppressor gene, which functions as a regulatory mechanism together with its companion proteins, and as a control mechanism and repair of DNA double strand damage by homologous recombination in the cell cycle [5].

The BRCA1 gene is located on the long arm of chromosome 17 (17q21), consists of 24 exons and encodes a protein of 1863 amino acids. The BRCA1 gene is expressed in endocrine tissues and is highest in the developing neuroepithelium of the nervous system, the lifetime risk of breast cancer with a BRCA1 gene mutation is 85%, the age-related risk is 20% after the age of 40, 51% after the age of 50 and 85% after the age of 70. Epithelial neoplasms (carcinomas) are the most commonly reported histological diagnosis in patients with BRCA1 mutations. The BRCA2 gene is located on the long arm of the 13th chromosome (13q12-13), consists of 27 exons and encodes a protein of 3418 amino acids. The BRCA2 gene is expressed in normal cells, particularly in the late G1/early S phase of the cell cycle. It plays a role in double strand breaks and DNA repair. The incidence is increasing in early stage breast cancer and male breast cancer cases [6].

More than 860 mutations in the BRCA1 gene and more than 880 mutations in the BRCA2 gene have been identified. 1. Frameshift: This mutation is seen in the stages of carcinogenesis. They cause premature termination of protein translation. 2. Non-sense mutations: It occurs when a single nucleotide in a codon is replaced, and the codon, which acts as a coding, turns into a stop codon. 3. Missense mutations: Substitution of a single nucleotide in the amino acid coding stage results in the formation of a functional codon encoding a different amino acid [6].

Approximately 80-85% of the mutations are non-sense mutations or frameshift mutations that are determined to be strictly associated with the disease. Missense mutations account for the remaining 15%. Variations occur in the BRCA gene as a result of mutations. While these variations have malignant properties, pathogenic variations predispose to cancer. There are also BRCA gene mutations that cannot be detected by standard screening methods and are detected in 10% of high-risk families. It has even been stated that these mutations comprise one-third of all BRCA1 mutations [6].

Breast cancer risk assessment is of great importance in early disease diagnosis and treatment. the Gail and Claus model is frequently used to determine breast cancer risk. Today, with the increase in testing of risk factors used in these models, different programs (MYRIAD II, Tyrer-Cuzick Model/IBIS, BOIDICEA, BRCA-PRO etc.) have been developed for risk detection. Using one of these models, the risk of developing cancer or the presence of a mutation in an individual can be calculated. Today, the BRCA-PRO model is frequently used. In this model, which is based on autosomal dominant inheritance, the risks of breast cancer susceptibility 1 and 2 (BRCA1 and BRCA2) gene mutations were calculated, a three-generation family tree was drawn, and the cancer risk of the whole family was evaluated. By adding breast cancer pathological features (progesterone and estrogen receptor status, stage) into this model, the probability of detecting BRCA gene mutations has been increased. The BRCA-PRO model can provide better efficiency than models (Claus and Gail, etc.) that evaluate risks according to their subgroups (familial/genetic factors, reproductive history, demographic characteristics, etc.) [7].

Results

One in four people in the world has a lifetime risk of developing cancer. Today, more than 14 million new cancer cases are diagnosed worldwide every year. For these reasons, early diagnosis and initiation of treatment for cancer are of great importance [8]. One of the risks that cannot be changed in catching breast cancer is genetic factors. People with a family history of breast cancer are 80% more likely to have BRCA1 and BRCA2 mutations than those without. Mutations in the BRCA1 and BRCA2 genes stop the activation of the proteins, and as a result, tumor formation begins in the cell. For these reasons, it would be beneficial for individuals with a family history of cancer to have genetic screening for early breast cancer diagnosis [2].

Conclusion

Breast cancer poses a great threat especially to women with its high incidence all over the world. Thanks to raising awareness of the society, which is seen as a solution to this issue, more women today have their check-ups done at certain intervals, even though they do not have any symptoms. Curative treatment becomes possible with the diagnosis of cancer in the early stages. In this way, proposing some protective treatment methods for women in the high-risk group has increased the importance of cancer screening and identifying the patients in this group [9].

References

1. Çandır, Ö., Karahan, N., Bülbül, M., Kılınç, F., & Başpınar, Ş. (2005). Ispartada Meme Kanserli h-Hastalarda BRCA1 ve BRCA2 Ekspresyonu. SDÜ Tıp Fakültesi Dergisi, 12(2), 50-54.
2. Olgun, Ş. (2021). Meme Kanserinde Genetik Risk Faktörleri: BRCA1 ve BRCA2 Genleri. ERÜ Sağlık Bilimleri Fakültesi Dergisi, 8(1), 23-25.

3. Karakaş, H. (2022). Meme Kanserli Kadınlara Uygulanan Gülme Terapisinin Algılanan Stres Düzeyi ve Yaşam Kalitesine Etkisi (Master's thesis, Bakırçay Üniversitesi Lisansüstü Eğitim Enstitüsü).
4. Otçu, S. M., Kamalak, Z., & Özdemi, İ. Over Kanserinde Güncel Yaklaşımlar ve Tedavi Yöntemlerinin Değerlendirilmesi.
5. Eyüpoğlu, M. (2022). BRCA Gen Mutasyonu Nedeniyle Profilaktik Jinekolojik Cerrahi Uygulanan Olguların Değerlendirilmesi.
6. Şengün, K. (2019). Meme Kanseri Genetik Taşıyıcılık Riski Olan Hastalarda BRCA Taramasının Kan ve Ağız İçi Yanak Sürüntüsü Örneklerinin Karşılaştırılması.
7. Akyolcu, N., Özhanli, Y., & Kandemir, D. (2019). Meme Kanserinde Güncel Gelişmeler. Sağlık Bilimleri ve Meslekleri Dergisi, 6(3), 583-594.
8. Babaç, M., Ekinci, M., & Derya, İ. Ö. Kanser Tanısı ve Tedavisinde Kullanılan Monoklonal Antikorlar. Ankara Üniversitesi Eczacılık Fakültesi Dergisi, 47 (1), 2-2.
9. Karakayali, F. Y., Ekici, Y., Sevmiş, Ş., Pehlivan, S., Arat, Z., & Moray, G. (2007). Meme Kanseri İçin Risk Belirlenmesinde Gail Modeli. Turkish Journal of Surgery, 23(4), 129-135.

Cancer and Wnt Pathway

Simay Ayden[*1] , **Furkan Ayaz** [1,2]

[1]Mersin University, Biotechnology Department, Türkiye, 21140940006@mersin.edu.tr
[2]Mersin University, Biotechnology Research and Application Center, Türkiye, furkanayaz@mersin.edu.tr

Keywords
Cancer
Wnt pathway
β –catenin

Abstract
Today, mutations in genes, diet and lifestyle play a major role in causing cancer. Genetic factors are much lower on the list. Stress in particular can affect all our bodily functions, causing cancer cells to form and multiply uncontrollably. Stress and other factors negatively affect our immune system, making it unable to fight cancer stem cells. The Wnt/β-catenin pathway, which is an important pathway in cancer development, constitutes a key point for cancer treatment. In this proceeding review study, we will briefly discuss Wnt pathway in cancer.

Introduction

In humans,19 proteins belonging to the Wnt gene family have been identified [1]. Wnt genes encode for a group of glycoproteins that are rich in cystein. The Wnt protein family consists of at least 19 glycoproteins that are highly conserved across species [2]. Activation of the Wnt pathway in the postnatal period causes cancer pathogenesis [1].

Wnt signaling pathway is divided into 3[1].

1. Wnt/ β-catenin Signaling
2. Wnt/ Ca^2 Signaling
3. Wnt/Planar Cell Polarity Signaling

Cancer development is caused by the canonical pathway Wnt/β-catenin pathway. Mutations in the Wnt pathway are linked to cancer formation [3].

Results

The β-catenin gene is evolutionarily conserved in living things. In the embryonic period, the Wnt/β-catenin pathway has a signifcant role in tissue and organ development; in adulthood, it is involved in cell renewal in organs [4]. The degradation complex phosphorylates β-catenin, which is normally in excess in the cell. However, in mutations, degradation is stopped by the Wnt pathway and β-catenin begins to accumulate in the cell. This leads to cancer formation [4]. In the absence of Wnt signaling pathway ligands, there is phosphorylation of the cytoplasmic β-catenin [5]. Cancer stem cells cause cancer initiation, metastasis and cancer recurrence. Cancer stem cells can self-renew and differentiate. Governed by the Wnt/β-catenin pathway [6].

Conclusion

Mutations in the Wnt pathway cause type 2 diabetes, leukemia, Alzheimer's, colon and breast cancer [6]. The Wnt pathway binds to the cysteine-rich receptor, disrupts the β-catenin degradation complex and triggers cytoplasmic accumulation [2]. If the function of this degradation complex is not disrupted, cancer stem cells cannot be formed to stimulate the cancer development. Since Wnt pathway is crucial for the stem cell maintenance, cell differentiation and organ development, having mutations or alterations in this pathway leads to tumor cell generation and eventually the development of the cancer [7]. More studies should be conducted to determine the role of Wnt pathway proteins specifically for each cancer case. This will enable the target determination for drug development and cancer stem cell targeting as therapeutic option to eradicate the tumor cells.

References

1. Wnt Yolağı – Ankara Üniversitesi Açık Ders Malzemeleri
2. Pai, S. G., Carneiro, B. A., Mota, J. M., Costa, R., Leite, C. A., Barroso-Sousa, R., ... & Giles, F. J. (2017). Wnt/beta-catenin pathway: modulating anticancer immune response. *Journal of hematology & oncology*, *10*, 1-12.
3. MacDonald, B. T., Tamai, K., & He, X. (2009). Wnt/β-catenin signaling: components, mechanisms, and diseases. *Developmental cell*, *17*(1), 9-26.
4. Valenta, T., Hausmann, G., & Basler, K. (2012). The many faces and functions of β-catenin. *The EMBO journal*, *31*(12), 2714-2736.
5. Moon, R. T. (2005). Wnt/β-catenin pathway. *Science's STKE*, *2005*(271), cm1-cm1.
6. Altınok, B. & Sunguroğlu, A. (2016). Wnt sinyal yolağı ve kanser . Ankara Sağlık Hizmetleri Dergisi , 15 (2) , 27-38 . https://doi.org/10.1501/Ashd_0000000118
7. Zhan, T., Rindtorff, N. & Boutros, M. Wnt signaling in cancer. *Oncogene,* 36, 1461–1473 (2017). https://doi.org/10.1038/onc.2016.304

Advanced Engineering Days

aed.mersin.edu.tr

Diagnosis of ovarian cancer and biomarkers

Helin Aytar*1 , Furkan Ayaz 2

¹Istanbul University, Student in Molecular Biology and Genetic Department, Türkiye, helinaytar1905@gmail.com
²Mersin University, Biotechnology Research and Application Center, Türkiye, furkanayaz@mersin.edu.tr

Keywords	Abstract
Ovarian Cancer Biomarkers CA-125 VEGF Diagnosis	Ovarian cancer; worldwide, ranks seventh among the types of cancer seen in women. Since the disease does not show symptoms at an early stage, it is usually detected at stage III and stage IV. In other words, early diagnosis of ovarian cancer is quite difficult. Although certain methods are used to detect ovarian cancer, there is no exact method that can give results at an early stage yet. Biomarkers are an important criterion for studies in this sense. CA-125 (cancer antigen 125 or carcinoma antigen 125), VEGF (Vascular Endothelial Growth Factor), Osteopontin and Kallikrein proteins are some biomarkers that are looked at from the blood and can be used for the diagnosis of ovarian cancer. When the VEGF levels in the blood of patients diagnosed with ovarian cancer were examined, it was found that they were high and caused the accumulation of peritoneal fluid. It has been found that patients with serous epithelial adenocarcinoma ovarian cancer with low VEGF levels survive more than those with high VEGF levels. This has shown that VEGF is an important biomarker for early diagnosis of ovarian cancer, and studies can focus on it.

Introduction

Occurring in the epithelium or embryonic cells, which form the main structure of the ovaries in women a condition of uncontrolled cell growth and proliferation is called ovarian cancer. About 95% of ovarian cancers occur in epithelial cells. The remaining cases occur as a result of tumor formation in other ovarian tissues or cells of embryonic origin [1]. Ovarian cancer is the seventh most common type of cancer in women worldwide [2]. in 2018, 300,000 new cases of ovarian cancer were detected worldwide [3]. The incidence of the disease in developed countries is 9.4/100,000, mortality is 5.1/100,000, while the incidence in developing countries is 5/100,000 and mortality is 3.1/100,000.[1] Symptoms of ovarian cancer present themselves in the late stages of the disease

shows. A diagnosis of ovarian cancer is usually detected at the third or fourth stage of the disease. The survival rate of patients with stage I and stage II ovarian cancer is 90% and 70%, respectively. The survival rate of patients with stage III and stage IV ovarian cancer is less than 20% [4]. The main methods used in the diagnosis of ovarian cancer are blood tests, pelvic examination, ultrasonography and CA-125(cancer antigen 125 or carcinoma antigen 125) measurement. Diagnosis of early-stage ovarian cancer by pelvic examination is very rare due to the location of the ovaries in the pelvic area. With these methods used, it is very difficult to diagnose ovarian cancer at an early stage. For this reason, studies have been directed to look at biomarkers in blood tests [4]. Some of the biomarkers used in the diagnosis of ovarian cancer are CA-125, ostepontin, kallikrein and VEGF (Vascular Endothelial Growth Factor) [3].

Results

CA-125 is a protein encoded by the MUC16(Mucin 16) gene. Clinically, it is used as a diagnostic test to measure the amount of the protein CA-125 in serum. The normal value for CA-125 is 0-35 IU/ML. CA-125 levels in the serums of about 80% of women diagnosed with advanced ovarian cancer have shown high results [3]. In the cases studied, only 50% of patients in stage I and stage II had a high CA-125 value. Therefore, CA-125 is not sufficient for early detection of ovarian cancer [3]. In addition, in pregnancy, endometriosis and some inflammatory diseases, the serum CA-125 level is high. This is one of the other reasons that CA-125 should not be used as a biomarker alone [3]. It has been determined that the HE4(Human Epididymis Protein 4) biomarker increases the serum level of patients diagnosed with ovarian cancer. The HE4 level does not increase as much as the CA-125 level. It has been found that VEGF levels increase in patients with ovarian cancer and cause peritoneal fluid accumulation. Another study looked at the VEGF levels in the preoperative sera of 314 patients with ovarian cancer and found that high VEGF levels shorten the survival time [3].

Conclusion

As a result of these studies, we understand that there are methods that are not sufficient in the early diagnosis of ovarian cancer. For this reason, many research and experimental studies have been directed to biomarkers for early diagnosis of this type of cancer that gives late symptoms. The results also show that biomarkers can be an important indicator for early diagnosis.

References

1. Güzel, D., Yildirim, N., Besler, A., Akman, L., Özdemir, N., Zekioğlu, O., ... & Özsaran, A. A. (2019). Over kanserinin epidemiyolojisi ve genel sağ kalım özellikleri. *Ege Tıp Dergisi*, 44-49.
2. Farinella, F., Merone, M., Bacco, L., Capirchio, A., Ciccozzi, M., & Caligiore, D. (2022). Machine Learning analysis of high-grade serous ovarian cancer proteomic dataset reveals novel candidate biomarkers. *Scientific Reports*, *12*(1), 3041.
3. Atallah, G. A., Abd. Aziz, N. H., Teik, C. K., Shafiee, M. N., & Kampan, N. C. (2021). New predictive biomarkers for ovarian cancer. *Diagnostics*, *11*(3), 465.
4. Çolak, A. (2013). Over Kanserinin Erken Tanı ve Takibinde Ca 125 ve He4 ün Sensitivitesi ve Spesifitesinin Karşılaştırılması.

Advanced Engineering Days

aed.mersin.edu.tr

General properties and production technologies of liposomes

Ebru Öner Usta *1 , **Furkan Ayaz** 1,2

1Mersin University, Biotechnology Department, Türkiye, oner_ebru@hotmail.com
2 Mersin University, Biotechnology Research and Application Center, Türkiye, furkanayaz@mersin.edu.tr

Keywords
Liposome
Liposome Production
Technology
Phospholipid
Proliposomes

Abstract
With its general definition, liposomes are lipid vesicles with a bilayer membrane structure consisting of two parts, hydrophilic and hydrophobic. Considering the similarity with the cell membrane of liposomes, which are mostly composed of phospholipids, it is seen that their biological compatibility is high. The liposome beads are capable of simultaneously encapsulating the hydrophobic and/or hydrophilic active. By delivering the active ingredients added to the liposome structure to the targeted area with high efficiency, they have widespread use in medical applications for therapeutic purposes. Liposomes can provide active and remote loading while protecting the active ingredients in their structure from the undesirable effects of external conditions. When the clinical usage areas of liposomes are examined, it is seen that they are one of the successful delivery systems and they are actively used by different disciplines. It has widespread usage areas especially in pharmaceutical applications due to its advantages such as not showing toxic tendencies and easy determination of chemical contents. Liposome production is commonly carried out by two different methods. The first method is carried out by forming a thin lipid layer in film hydration, and the second method is by adding lipids to the aqueous phase at transition temperature during appropriate hydration and mixing. This review article, it is aimed to examine the production technologies of liposomes and their common usage areas and potential usage areas. However, considering the general use of liposomes, physical and chemical stability problems limit their use and lay the groundwork for the development of new technologies.

Introduction

Liposomes have led to the emergence of Liposome Technology because they are water-filled vesicles with an amphipathic structure and their compatibility with the cell membrane. Phospholipid membranes, which are assigned as active substance carriers, are evaluated in the repair of the relevant cells when the process is completed. Thus, the liposome, which acts as both the targeted ethene and the carrier, remains in the body and becomes a part of the biological process [1]. The intravenous effect of oral use of liposome-based products has allowed the formation of irreplaceable product groups (Figure 1). The general structure of the liposome is shown. Figure 2 shows an example of a liposome used as a drug delivery system. Advantages of the pharmaceutical use of liposome technology; It can be summarized as the absorption of the active ingredient with high efficiency, high stability, low possibility of side effects, high biocompatibility, and low toxic effect. Liposome sizes vary between 20nm and 20 μm.
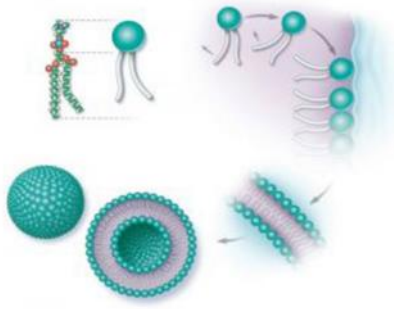
Figure 1. Lysosome hydrophilic-hydrophobic structure [1]
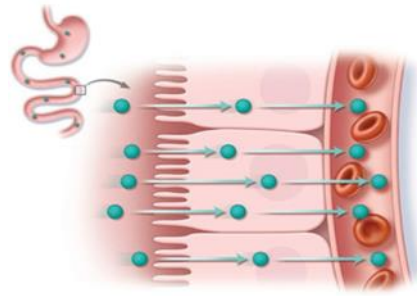
Figure 2. Drug delivery system [1]

While classifying liposomes, their size, lamellar structure and components are taken into account [2]:

Small unilamellar vesicles (SUV) ○

Large unilamellar vesicles (LUV) ◯

Multilamellar vesicles (MLV) ◎

Multivesicularvesicles(MVV)
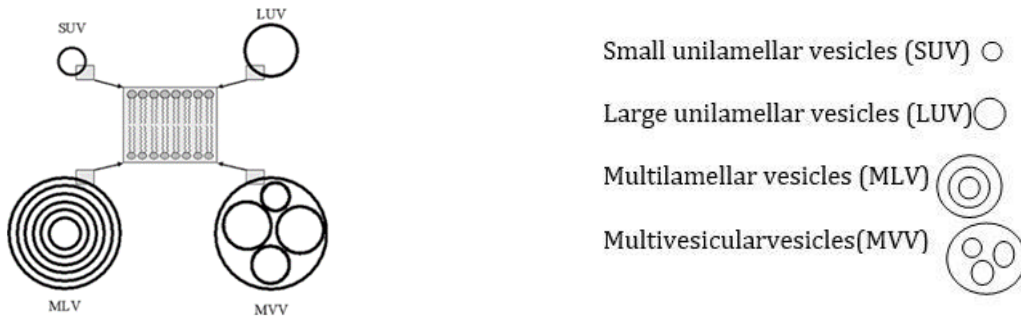
Figure 3. Classification of Liposomes [2,11]

According to their composition, liposomes are classified as follows [3,4];

• Conventional Liposomes
• Fusogenic Liposomes
• pH Sensitive Liposomes
• Cationic Liposomes
• Long Circulating Liposoms
• Immunoliposomes

The characteristics of the liposome, which is planned to be produced with liposome production technologies, are determined by the type of lipid used, the production technology used, the load, and the type of active substance used. At the same time, the size of the liposome is very important for the efficiency of its intended use. Particularly, it is observed that the biological benefits of active ingredient capsules produced orally with liposome technology are higher. The reason for this is both its structural similarity to the cell membrane and the fact that the active substance is protected from the liposome in the cell membrane and the components of the digestive system and maintains its stability until it is mixed with the blood [5,6,7,11].

Material and Method

The most commonly used type in liposomes, the main component of which is phospholipids, is lecithin. All phospholipids have specific gel liquid transition temperature (Tc) and surface charges, and before reaching this temperature, the fatty acid chains are in the crystalline phase. As this temperature increases, the chains pass into the liquid phase and expand their range of action [4]. The phospholipid types with the widest usage area and their transition temperatures (Tc) are given in Table 1.

When Table 1 of phospholipids is examined, it is seen that one of the most widely used phospholipids is DPPC. Its high Tc is considered to be important for stretching the working range and instability, which is known as its most important disadvantage [3,7,8,11].

Table 1. Phospholipid types used in encapsulation and liquid gel transition temperatures (Tc) [3]

LIPID TYPE	ABBREVIATION	Tc (˚C)
Egg Phosphatidylcholine	Egg PC	-15,-7
Dioleoylphosphatidylcholine	DOPC	-22
Dilaurylphosphatidylcholine	DLPC	0
Dimyristoylphosphatidylcholine	DMPC	23
dipalmitoylphosphatidylcholine	DPPC	41
Distearoylphosphatidylcholine	DSPC	58
Bovine Brain Sphingomyelin	Brain SM	32
Egg Phosphatidylethanolamine	Egg PE	-
Dimristoylphosphatidylethanolamine	DMPE	48
Dimyristoylphosphatidylglycerol	DMPG	23
Dimristoylphosphatidic Acid	DMPA	52
Bovine Brain Phosphatidylserine	Brain PS	5
Dycetylphosphate	DCP	
Stearylamine	SA	
Ps/Dspc/Dppc (1:4,5:4,5)		43

Liposome Production Methods

Liposome production can be carried out by many different methods. Traditional methods with the most common usage; It is known as Thin Film Hydration (TFH) Method (Bangham Method), Reverse Phase Evaporation Method, Detergent Dialysis Method, Electroformation, Solvent Injection Method (Ethanol, ether injection method). However, since these methods are based on bulk production, additional processes such as membrane extraction, sonication, and high-pressure homogenization are required to obtain homogeneous and small-sized particles after production is completed. By eliminating the shortcomings of these methods, microfluidization Methods were developed for the production of more homogeneous liposomes in fewer sample sizes, and as a result of the method, no additional processing was required to reduce the particle sizes.

The developed methods of liposome technology are grouped into two parts with the most basic stages;
- ➢ Drying of lipids dissolved in the organic solvent
- ➢ Formation of liposomes in aqueous medium

The process is completed by analyzing the resulting liposomes. Liposome production methods continue to be developed and their usage areas continue to be expanded.

MLV Preparation Method

The lipid film is formed by dissolving the lipids that will be included in the liposome structure in organic solvents such as chloroform and then evaporating this solvent with nitrogen gas. At room temperature, the formed lipid film is hydrated with a buffer solution. The hydrated lipid film is immersed in water at a temperature higher than its anaphase transition temperature (Tm) (Tm + 20°C) for one minute before being removed and shaken for one minute with the aid of a vortex. These steps are repeated for 15 minutes. Multilayered liposomes are produced as a result of these processes [9-11].

SUV and LUV Preparation Method

Various processes are applied to change the size or properties of the layers of multilayer liposomes formed by dry lipid film hydration. MLVs are large and heterogeneous. Therefore, MLVs can be converted into SUVs or LUVs using methods such as sonication, extrusion, and vortexing. The liposome extruder, which is one of the devices used during these processes, is used to separate liposomes according to the pore diameter it has. Liposomes with a smaller diameter than the pore dissociate by passing through the pore. With the sonication device, a high level of energy is applied to the MLVs to obtain an SUV.

LUV and SUV can also be made in a variety of ways. The detergent used as a solvent in this method ensures that proteins are separated from the lipid-protein mixture. In the use of detergent, colloidal solutions serve as buffer solutions. To remove the detergent, centrifuge, gel filtration, or accelerated controlled dialysis methods are used, yielding SUV or LUV [9-11].
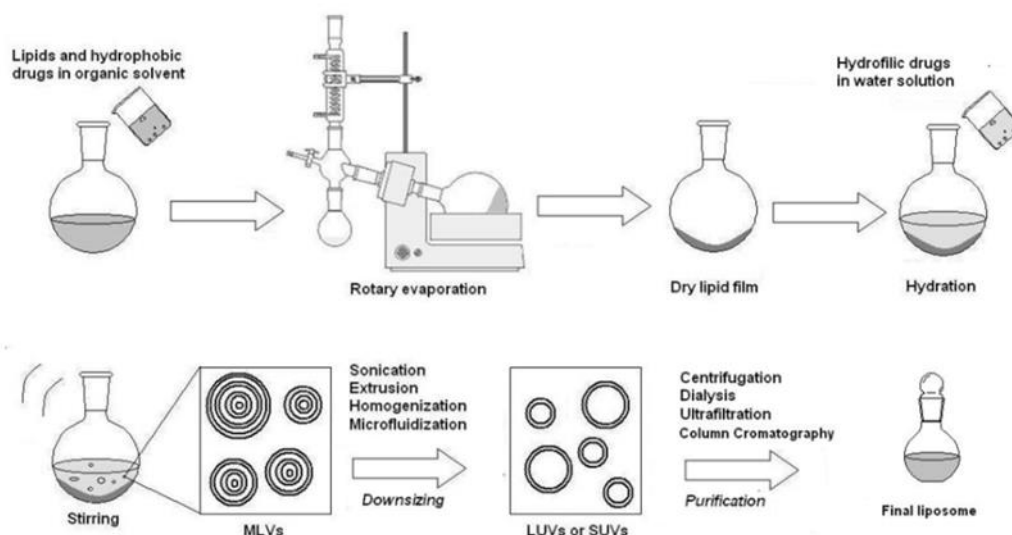
Figure 4. MLV Preparation Method [11]

Results

In the first method of liposome production, a thin lipid layer is formed in the hydration of the film, and the film is mixed above the transition temperature with the addition of water with a preprocessor providing high speed or high shear force. During appropriate hydration and mixing, lipids are added to the aqueous phase at the transition temperature in the other liposome production pathway. The stability problem is one of the issues that must be identified and resolved as a result of the production studies. To address the stability issue, new solution-oriented studies were conducted. Among these studies are lyophilization, appropriate particle size, layering, combined ratio, and so on.

Proliposomes were first developed in 1986; they are dry, granular products with good flow properties made up of active substance, phospholipids, and a water-soluble carrier material that transforms into a multilayered liposomal suspension when exposed to water [9].

In 1991, the concept of pro-liposome was expanded to include liquid phospholipid formulations capable of forming liposomes by adding an aqueous phase. Concentrated solutions of phospholipids in ethanol are the liquid formulations. As a result, pro-liposomes can be defined as a powder or liquid lipid formulations that can be converted into liposomes by adding an aqueous phase [10,11].

Conclusion

When liposomes are evaluated in terms of usage areas, it is observed that they have a very wide range. Liposomes will continue to serve especially drug delivery systems by eliminating their stability problems or reducing them to a very small amount. Although pro-liposomes are produced for this purpose, they are new-generation drug delivery systems that aim to solve the stability problems of liposomes.

References

1. Stark, M., Silva, T. F., Levin, G., Machuqueiro, M., & Assaraf, Y. G. (2020). The lysosomotropic activity of hydrophobic weak base drugs is mediated via their intercalation into the lysosomal membrane. *Cells*, *9*(5), 1082.
2. https://lipozone.com.tr/#hangi-lipozone
3. Yurdakul, A., & Atav, R. (2007). Structures and classification of liposomes. *Textile and Apparel*, *17*(4), 243-247.
4. Singh, A. K., & Das, J. (1998). Liposome encapsulated vitamin A compounds exhibit greater stability and diminished toxicity. *Biophysical chemistry*, *73*(1-2), 155-162.
5. Zhang, X., Guo, S., Fan, R., Yu, M., Li, F., Zhu, C., & Gan, Y. (2012). Dual-functional liposome for tumor targeting and overcoming multidrug resistance in hepatocellular carcinoma cells. *Biomaterials*, *33*(29), 7103-7114.
6. Hickey, S., Roberts, H. J., & Miller, N. J. (2008). Pharmacokinetics of oral vitamin C. *Journal of nutritional & environmental medicine*, *17*(3), 169-177.
7. Marsanasco, M., Márquez, A. L., Wagner, J. R., Alonso, S. D. V., & Chiaramoni, N. S. (2011). Liposomes as vehicles for vitamins E and C: An alternative to fortify orange juice and offer vitamin C protection after heat treatment. *Food research international*, *44*(9), 3039-3046.

8. Koynova, R., & Caffrey, M. (1998). Phases and phase transitions of the phosphatidylcholines. *Biochimica et Biophysica Acta (BBA)-Reviews on Biomembranes*, *1376*(1), 91-145.
9. Sułkowski, W. W., Pentak, D., Nowak, K., & Sułkowska, A. (2005). The influence of temperature, cholesterol content and pH on liposome stability. *Journal of molecular structure*, *744*, 737-747.
10. Kobayashi, N., Nishikawa, M., & Takakura, Y. (2005). Gene therapy and gene delivery. Drug Delivery: Principles and Applications, 305-319.
11. Kırtıl, E., & Öztop, M. H. (2014). Liposomes as an encapsulation agent for food applications: structure, characterization, manufacture and stability. *Akademik Gida*, *12*(4), 41-57.

The role of uterine natural killer (uNK) cells in the endometrium of infertile women

Tiinçe Aksak[1]

[1] Toros University, Department of Medical Services and Techniques Health Services, Mersin, Türkiye, tiince.aksak@toros.edu.tr

Keywords
Infertility
Subfertility
Uterine Natural Killer Cell
Implantation
Recurrent Implantation
Failure

Abstract
Subfertility is defined as delayed conception with low fertility, while infertility is defined as inability to conceive naturally within one year despite unprotected sexual intercourse. The endometrium is the inner layer of the uterus where the blastocyst attaches and grows. The content of the endometrium and the number of immune system cells therein can be associated with infertility. The fact that most of the lymphoid cells in the endometrium are uterine natural killer (uNK) cells has drawn attention to the immune system in infertility. However, the roles of uNK cells have not yet been fully elucidated. Studies suggest that uNK cells, members of the lymphoid system, may play an important role in implantation and pregnancy. Although the high number of these cells, which are important for implantation and the continuation of pregnancy, is associated with infertility, there are also studies suggesting that there is no relationship between them. In our study, it was aimed to investigate studies examining the relationship of uNK cells with subfertility and infertility.

Introduction

Implantation occurs when the blastocyst adheres to and subsequently invades the endometrium during the implantation window that occurs in the late secretory stage of the endometrium. Successful implantation of the blastocyst into the endometrium is important for the continuation of the pregnancy. During implantation, adhesion molecules, various cytokines, growth factors and hormones are secreted. When these events are out of sync, implantation may fail [1,2]. Subfertility is defined as having low reproductive capacity and delay in getting pregnant, while infertility is defined as the inability to conceive naturally within one year despite unprotected sexual intercourse. The most common cause of subfertility is the mother's ovulation problem. At the beginning of ovulation problems are polycystic ovary syndrome (PCOS), advanced maternal age, decreased ovarian reserve due to medical reasons such as chemotherapy and hormonal problems. However, tubal uterine obstruction, endometriosis, inflammatory pelvic disease, gonorrhea, chlamydia infection, problems related to sperm structure and function have been associated with subfertility and infertility. Recent studies have shown that the framework of the endometrium, the adhesion molecules secreted and the number of immune system cells therein may be associated with subfertility and infertility. The presence of uterine Natural Killer cells, one of the immune system cells, in the endometrium shows that there is a relationship between infertility and the immune system. Natural Killer cells, which are members of the innate immune system, destroy tumor cells and virus-infected cells. They constitute 10% of the lymphocytes in the peripheral blood. These cells, which are morphologically characterized by their large cytoplasm containing azurophilic granules, can lyse cells without the need for immunoglobulin molecules. It is thought that increased blood levels of NK cells in women may affect implantation [3,4]. Most of the uNK cells consist of CD16-/CD56+ cells. These cells are called bright cells and they secrete cytokines. During pregnancy, uNK cells are involved in many important events such as the formation of the vascular structure of the placenta and trophoblast cells, as well as immune tolerance [5,6,7]. The number of natural killer cells in the uterus during the menstrual cycle may vary depending on the hormones secreted. In a study, it was observed that the number of uNK cells was highest in the early pregnancy period from the secretory phase to the late luteal phase [8]. These cells are found in areas very close to the implantation site during pregnancy, and studies have shown

that uNK cells are closely associated with trophoblasts. When pregnancy does not occur, uNK cells are destroyed by apoptosis. For a healthy pregnancy development, fetal trophoblasts invade the endometrium, move into the maternal arteries and provide blood flow to meet the needs of the fetus. If the invasion of trophoblasts does not occur adequately, pregnancy results in miscarriage or preeclampsia. In the literature, there are studies examining the functions of uNK cells in recurrent implantation failures. Some studies have found a high rate of abnormal expression of uNK cells and antigens in the endometrium of women with recurrent implantation failure. *In vitro* studies of endometrial specimens from women with recurrent implantation failure have demonstrated an increase in CD56 antigen immunohistochemically [9,10]. However, NK cell receptors and cytokines in peripheral blood and endometrium are very important for the implantation and maintenance of pregnancy [11]. uNK cells are large granular T lymphocytes located in the endometrium. Peripheral blood and uterine NK cells, which are known to have common CD56 antigens on their surfaces, differ according to the antigens they do not have on their surfaces. uNK cells do not have CD16 and CD3 antigens, whereas peripheral blood NK cells have these antigens NK cells are grouped as CD16+CD56d and CD16–CD56b. CD16–CD56b are cells found in the decidual endometrium. And it lacks the bright antigen and its receptors, which are usually found on lymphocytes involved in host defense [12]. Although it is argued that uNK cells migrate from the bone marrow and settle in the endometrium, there is controversy about their excessive proliferation in the endometrium before implantation. In this regard, it is more prevalent that approximately 50% of uNK cells are proliferative and reproduce themselves after migrating from the peripheral blood to the endometrium. These cells are particularly maximized in the mid, late luteal phase and early pregnancy endometrium [13]. In one study, an increase in genes controlling the proliferation of uNK cells was observed in the luteal phase endometrium [14]. uNK cells appear to be located around blood vessels, usually found in the endometrial stroma. Therefore, these cells are thought to be involved in the decidualization of the endometrial stroma or the remodeling of spiral arteries [15]. There is an opinion that the increased number of uNK cells in early pregnancy and their proximity to trophoblasts ensure that the fetus is not perceived as foreign by the mother and does not cause miscarriage [16]. uNK cells adjacent to fetal trophoblasts during early pregnancy express receptors that can recognize specific antigens on the surface of trophoblasts. It was observed that uNK cells in the mid-luteal phase of the endometrial cycle increased under the influence of progesterone and came to the uterus. Although uNK cells do not have progesterone receptors, they do contain prolactin, estrogen β and glucocorticoid receptors. Estrogen attracts cells to the uterus, while prolactin promotes the maturation and differentiation of cells. When uNK cells interact with trophoblasts, important cytokines such as Transforming Growth Factor Beta (TGFβ), Leukemia Inhibitory Factor (LIF) and Tumor Necrosis Factor-alpha (TNF-α) are released. These cytokines act on placental development and angiogenesis and show activation or inhibition properties.

uNK cells act as master regulators of decidual angiogenesis and control oxygen tension at the maternal-fetal interface [17]. It is thought that the endometrium is as effective as the blastocyst in implantation. In some studies, investigating the role of uNK cells in implantation, an increased number of uNK cells was observed in the endometrial stroma of preimplantation women [18,19]. Studies showing that the density of uNK cells can increase the angiogenesis factor suggested that increased and decreased decidual angiogenesis levels are associated with implantation failure and pregnancy loss. Some investigators point out that excessive accumulation and aggregation of uNK cells in the endometrium may cause dysfunction in the endometrium and a disordered environment of the stroma.

Material and Method

Electronic databases, Science Direct, Pubmed, Medline, Embase and Web of Science were searched. All searches were made from 1999 to February 2023. Keywords were infertility, subfertility, Natural killer cell, uterine natural killer cell, IVF, intracytoplasmic sperm injection (ICSI), embryo implantation, implantation failure, recurrent implantation failures (RIF) and recurrent pregnancy loss. There was no language restriction when searching for articles. All collected research and review articles formed the reference list.

Discussion

Infertility can occur depending on female, male and embryo factors. Genetic diseases, endocrine disorders, infectious diseases and immunological disorders can be shown among the reasons for the failure of embryo implantation. Although people diagnosed with infertility can enter the pregnancy process with *in vitro* fertilization (IVF) treatment, recurrent implantation failures in some patients negatively affect couples both financially and psychologically. For this reason, providing early prognostic markers and optimal options can contribute more positively to patients. The presence of uNK cells, one of the immune system elements in the endometrium, has recently attracted attention in reproductive physiology. In some studies examining implantation failure, an increase in the presence of uNK cells in the endometrium was observed before pregnancy. The presence of uterine Natural killer cells at the interface of the endometrium and trophoblast also suggests that trophoblasts may become targets for Natural killer cells during the implantation process. The proximity of uNK cells to trophoblasts

suggested that they could recognize trophoblasts fetally and regulate invasion [20,21,22]. However, a study showed that uNK cells are reduced before menstruation and there is also a decrease in the factors that protect the vasculature, which triggers menstrual disruption [23,24]. uNK cells regulate spiral arteries in the maternal-fetal bed by producing various angiogenic factors [25,26]. In a study, significant immunohistochemical differences were found in NK cells in endometrial samples, and it was stated that it would be important to establish a clinical standard for counting these cells [27,28]. In another study on NK cells, it was stated that immune tolerance is not limited to the decidua, but also affects the innate immune system in the periphery. Accordingly, they observed that T-helper 1 (Th1) cell-directed negative changes, one of the subcomponents of NK cells, were observed in blood samples before *in vitro* fertilization (IVF) and 1 week after IVF [29].

Conclusion

In recent years, there are studies that take attention to the fact that the presence of uterine Natural killer cells in the endometrium may take a role in the implantation process and at the same time, take part in the activity of trophoblasts in the maternal tissue. They stimulate growth in early development by synthesizing cytokines and remodeling maternal spinal arteries and providing trophoblast adhesion. However, an excessive increase in the number of uNK cells may also cause recurrent pregnancy loss. The pathophysiology of uNK cells in infertility and subfertility has not yet been fully elucidated. Therefore, there is a need for more preimplantation studies, especially measuring the levels of uNK cells at the molecular level and investigating them immunohistochemically

References

1. Mariee, N., Li, T. C., & Laird, S. M. (2012). Expression of leukemia inhibitory factor and interleukin 15 in endometrium of women with recurrent implantation failure after IVF; correlation with the number of endometrial natural killer cells. *Human reproduction*, *27*(7), 1946-1954.
2. Kolanska, K., Suner, L., Cohen, J., Ben Kraiem, Y., Placais, L., Fain, O., ... & Mekinian, A. (2019). Proportion of cytotoxic peripheral blood natural killer cells and T-cell large granular lymphocytes in recurrent miscarriage and repeated implantation failure: case–control study and meta-analysis. *Archivum immunologiae et therapiae experimentalis*, *67*, 225-236.
3. Shaulov, T., Sierra, S., & Sylvestre, C. (2020). Recurrent implantation failure in ivf: A canadian fertility and andrology society clinical practice guideline. *Reproductive biomedicine online*, *41*(5), 819-833.
4. Kolanska, K., Bendifallah, S., Cohen, J., Placais, L., Selleret, L., Johanet, C., ... & Mekinian, A. (2021). Unexplained recurrent implantation failures: Predictive factors of pregnancy and therapeutic management from a French multicentre study. *Journal of Reproductive Immunology*, *145*, 103313.
5. Quenby, S., Nik, H., Innes, B., Lash, G., Turner, M., Drury, J., & Bulmer, J. (2009). Uterine natural killer cells and angiogenesis in recurrent reproductive failure. *Human reproduction*, *24*(1), 45-54.
6. Erbaş, H., & Çetin, T. (2009). Tekrarlayan gebelik kaybı olan olgularda endometriyal CD 56+ Natural Killer hücrelerin araştırılması, Uzmanlık Tezi, Adana, Turkey.
7. Fukui, A., Funamizu, A., Fukuhara, R., & Shibahara, H. (2017). Expression of natural cytotoxicity receptors and cytokine production on endometrial natural killer cells in women with recurrent pregnancy loss or implantation failure, and the expression of natural cytotoxicity receptors on peripheral blood natural killer cells in pregnant women with a history of recurrent pregnancy loss. *Journal of Obstetrics and Gynaecology Research*, *43*(11), 1678-1686.
8. Sfakianoudis, K., Rapani, A., Grigoriadis, S., Pantou, A., Maziotis, E., Kokkini, G., ... & Simopoulou, M. (2021). The role of uterine natural killer cells on recurrent miscarriage and recurrent implantation failure: From pathophysiology to treatment. *Biomedicines*, *9*(10), 1425.
9. Tuckerman, E., Mariee, N., Prakash, A., Li, T. C., & Laird, S. (2010). Uterine natural killer cells in peri-implantation endometrium from women with repeated implantation failure after IVF. *Journal of reproductive immunology*, *87*(1-2), 60-66.
10. Lédée-Bataille, N., Dubanchet, S., Coulomb-L'hermine, A., Durand-Gasselin, I., Frydman, R., & Chaouat, G. (2004). A new role for natural killer cells, interleukin (IL)-12, and IL-18 in repeated implantation failure after *in vitro* fertilization. *Fertility and sterility*, *81*(1), 59-65.
11. Fukui, A., Funamizu, A., Yokota, M., Yamada, K., Nakamua, R., Fukuhara, R., ... & Mizunuma, H. (2011). Uterine and circulating natural killer cells and their roles in women with recurrent pregnancy loss, implantation failure and preeclampsia. *Journal of reproductive immunology*, *90*(1), 105-110.
12. Quenby, S., & Farquharson, R. (2006). Uterine natural killer cells, implantation failure and recurrent miscarriage. *Reproductive biomedicine online*, *13*(1), 24-28.
13. Bulmer, J. N., & Lash, G. E. (2005). Human uterine natural killer cells: a reappraisal. *Molecular immunology*, *42*(4), 511-521.

14. Clifford, K., Flanagan, A. M., & Regan, L. (1999). Endometrial CD56+ natural killer cells in women with recurrent miscarriage: a histomorphometric study. *Human reproduction*, *14*(11), 2727-2730.
15. Amrane, S., Brown, M. B., Lobo, R. A., & Luke, B. (2018). Factors associated with short interpregnancy interval among women treated with *in vitro* fertilization. *Journal of Assisted Reproduction and Genetics*, *35*, 1595-1602.
16. Croy, B. A., He, H., Esadeg, S., Wei, Q., McCartney, D., Zhang, J., ... & Yamada, A. T. (2003). Uterine natural killer cells: Insights to their cellular and molecular biology from mouse modelling. *Reproduction (Cambridge, England)*, *126*(2), 149.
17. King, A. (2000). Uterine leukocytes and decidualization. *Human reproduction update*, *6*(1), 28-36.
18. Trundley, A., & Moffett, A. (2004). Human uterine leukocytes and pregnancy. *Tissue antigens*, *63*(1), 1-12.
19. Laird, S. M., Tuckerman, E. M., & Li, T. C. (2006). Cytokine expression in the endometrium of women with implantation failure and recurrent miscarriage. *Reproductive biomedicine online*, *13*(1), 13-23.
20. Naruse, K., Lash, G. E., Innes, B. A., Otun, H. A., Searle, R. F., Robson, S. C., & Bulmer, J. N. (2009). Localization of matrix metalloproteinase (MMP)-2, MMP-9 and tissue inhibitors for MMPs (TIMPs) in uterine natural killer cells in early human pregnancy. *Human reproduction*, *24*(3), 553-561.
21. Tang, A. W., Alfirevic, Z., & Quenby, S. (2011). Natural killer cells and pregnancy outcomes in women with recurrent miscarriage and infertility: a systematic review. *Human reproduction*, *26*(8), 1971-1980.
22. King, A., & Loke, Y. W. (1999). The influence of the maternal uterine immune response on placentation in human subjects. *Proceedings of the Nutrition Society*, *58*(1), 69-73.
23. Igarashi, T., Konno, R., Okamoto, S., Moriya, T., Satoh, S., & Yajima, A. (2001). Involvement of granule-mediated apoptosis in the cyclic changes of the normal human endometrium. *The Tohoku Journal of Experimental Medicine*, *193*(1), 13-25.
24. Li, X. F., Charnock-Jones, D. S., Zhang, E. K. O., Hiby, S., Malik, S., Day, K., ... & Smith, S. K. (2001). Angiogenic growth factor messenger ribonucleic acids in uterine natural killer cells. *The Journal of Clinical Endocrinology & Metabolism*, *86*(4), 1823-1834.
25. Craven, C. M., Morgan, T., & Ward, K. (1998). Decidual spiral artery remodelling begins before cellular interaction with cytotrophoblasts. *Placenta*, *19*(4), 241-252.
26. Hanna, J., Goldman-Wohl, D., Hamani, Y., Avraham, I., Greenfield, C., Natanson-Yaron, S., ... & Mandelboim, O. (2006). Decidual NK cells regulate key developmental processes at the human fetal-maternal interface. *Nature medicine*, *12*(9), 1065-1074.
27. Tohma, Y. A., Musabak, U., Gunakan, E., Akilli, H., Onalan, G., & Zeyneloglu, H. B. (2020). The role of analysis of NK cell subsets in peripheral blood and uterine lavage samples in evaluation of patients with recurrent implantation failure. *Journal of Gynecology Obstetrics and Human Reproduction*, *49*(9), 101793.
28. Lash, G. E., Bulmer, J. N., Li, T. C., Innes, B. A., Mariee, N., Patel, G., ... & Laird, S. M. (2016). Standardisation of uterine natural killer (uNK) cell measurements in the endometrium of women with recurrent reproductive failure. *Journal of reproductive immunology*, *116*, 50-59.
29. Miko, E., Manfai, Z., Meggyes, M., Barakonyi, A., Wilhelm, F., Varnagy, A., ... & Szereday, L. (2010). Possible role of natural killer and natural killer T-like cells in implantation failure after IVF. *Reproductive biomedicine online*, *21*(6), 750-756.

Lifesaving open areas after earthquake and land management

Nurhan Koçan[*1]

1Bartın University, Faculty of Engineering, Architecture and Design, Department of Landscape Architecture, Bartin, nkocan@bartin.edu.tr

Keywords	**Abstract**
Natural disasters Earthquake Open green areas Land management Land use planning	Humans depend on the resources of nature since their existence. As human populations and technology advance, humans' impact on critical natural resources and natural areas, ecosystems, and atmospheric processes has grown. As society developed and urban life grew, people began to separate themselves from nature. Environmental disasters, most of which are natural disasters, have reminded people that they should use and manage natural areas and resources correctly. It is a constant need and responsibility for people and society to manage their relations with the environment. In the study, evaluations were made about the land use planning and land management of open spaces, which undertake many functions after earthquake disasters that cause devastating environmental, human and economic damages.

Introduction

Natural disasters such as floods, storms, earthquakes, forest fires cause many physical, economic, ecological and sociological damages and losses on natural areas, residential areas and people. The continuation of life after these disasters and the process of returning to normal is an issue that needs to be solved with the interdisciplinary cooperation of many sectors. The roots of interdisciplinary communication depend on the principles of scientific and engineering studies.

In order to protect and improve human health and environmental health, it is necessary to understand the interactions between human and environment. Knowing how natural systems work and reducing harmful effects helps prevent further disasters and environmental damage in the long run. In this respect, open green spaces are useful in natural and cultural structure with many functions in normal times, and they are life-saving with many functions after disasters.

Evaluation

All users and supporters, including the state, NGOs and the public, decide on the planning and management of the use of open spaces after the earthquake disaster. At the same time, these stakeholders are the first to be affected by the decisions, regulations and approaches. Plans and practices in which all of them decide together and coordinate are successful. All state institutions, aid organizations and civil aids that try to eliminate disaster damage use open spaces such as parks, squares, sports fields, recreation areas, gardens of public institutions and organizations in the disaster area for purposes such as gathering, sheltering, and carrying out various services. During the site selection process of existing areas for the re-establishment of the settlement, many issues such as the purpose for which they will be used and the impact of the type of use on the environment should be considered.

Governments take responsibility for issues related to measuring infrastructure, education and training impacts. The public and non-governmental organizations discuss project proposals on land use and land management with the state, and voice their suggestions on natural areas and resources. These responsible

activities are applications such as conservation designs, land use practices, pollution disposal, and land and water conservation approaches in site development. In some cases, these practices and designs result in creative plans, designs, and applications for services and landowners. Community participation is an indicator of the democratic political planning process. The success of implementation of projects and programs depends on public acceptance [1].

Planning and management of open spaces are activities such as developing or protecting resources, controlling pollution, using basic facilities, determining acceptable risk levels. The current and future status of the expense spent on investments is important for benefit-loss analysis. In this regard, it is thought that ecology economics will help to make the right decisions in the planning process [2-3].

Conclusion

The issues that need to be addressed in the planning and management of open spaces, which play an important role in the survival of the peoples after the earthquake, removal of the debris, arrangement of the physical environment, resettlement and establishment of the living space, are as follows.

1-People management and public participation

- Participants and roles in land use planning and management
- Reflection of social culture, values and ethics
- Interdisciplinary relations in land use planning (engineering, economics, cooperation, environmental law)
- Role of the planner (technical staff, public participation moderator, interdisciplinary negotiator, designer, observer)

2-Land usage planning

- Determination of development and settlement areas of urban
- Determination of development and settlement areas of rural
- Determination of development and settlement areas of public areas
- Determination of the effects of land use on environmental health
- Determination of the effects of land use on water systems
- Determination of the effects of land use on agricultural production areas
- Determination of the effects of land use on natural resources
- Determination of the effects of space use on energy and material consumption
- Determination of the effects of land use on cultural heritage and community identity

3-Land conservation and ecological conservation in open areas

- Criteria and scientific tools in land protection
- Ecological restoration
- Water and soil protection

4-Design for the development of sustainable, living and rational use of land

- Basic concepts of sustainable design
- Practices for sustainable and living design development (transportation solutions, parking areas, squares, urban forests, cemeteries, pedestrian paths, etc.)
- Design in accordance with the cultural structure and historical heritage

5-Rational growth management and land use control

- Determination and protection of soil usage characteristics and soil quality
- Prevention of loss of urban lands
- Determination of suitable settlement areas with scientific data

6-Environmental ınformation systems

- Data in land planning and management (open-closed areas to be used after the disaster, structural and open spaces of public spaces, manpower and task distribution, storage-distribution of materials, etc.)
- Identification of data limitations and uncertainties

7-Prevention of post-disaster environmental pollution

- Identifying areas where debris will be removed, stored and sorted

- Prevention of damage to soil and water resources of temporarily established shelters
- Disposal of waste and garbage to be formed in temporary shelter areas and prevention of damage to the environment

8-Planning and management of agricultural and animal production areas

- Supporting agriculture and livestock activities in rural life
- Supporting forestry activities

9-Integrative methods for field analysis

- Inventory collection
- Quick assessment
- Determination of carrying capacity
- Environmental impact assessment

References

1. Forester, J. (1989). Planning in the face of power. J*ournal of the American Planning Association*, 35(3).
2. McAllister, D.J. (1995). Affect and cognition based trust as foundations for ınterpersonel cooperation in organizations, *Academy of Management Journal,* 38(1)24-59.
3. Westman, W.E. (1985). Ecology, ımpact assessment, and environmental planning, ISBN: 978-0-471-80895-4.

Advanced Engineering Days

aed.mersin.edu.tr

Increase die life in hot forging process by using coating processes

Sait Gül *1 , **Adil Yağmur** 1 , **Esat Erdinç Önel** 1

1 ÇİMSATAŞ Çukurova Construction Machinery IND. TRADE. A.S. Mersin, Türkiye, foundry@cimsatas.com

Keywords
Wear Resistance
Die Life
Hardness
Hardenability
Coating
Tool Steels

Abstract
The aim of this study, indicate of optimum die life application for using some coating methods of forging die against to wear also as use different die steel and different coating materials. And another aim is decrease in the die costs which occurs wear of the die. Hot forging efficiency in direct proportion to wear of the die. At dies, workpiece is flowing on the die surface during forging processes, at a result of this causes friction between workpiece and surface of the die. At all of cycle, thermal loads and flow friction occur and this situation causes softening of the die as to be thermal. Therefore, surface hardness of the die will decrease. Losing of surface hardness and which occurs friction between die and work piece will negative effect life of the die. As to be die material, three different die steel will be used (DIN 1.2344 (ORVAR® 2 MICRODIZED) and DIN 1.2344 (UNIMAX®) At this time, different coating will be applied. These are FEXOY® and ABP+DIETOX®. As a result of coated operation, will follow cycle time proper die material will be selected.

Introduction

In all manufacturing processes, forging technology has a special place because of producing special parts with minimum waste material. During this operation, it will occur some plastic deformations on each cycle in die material. In hot forging process, thermal shock conditions will occur due to temperature difference between layers of the work piece and die whereby, surface coating have to on the die material. Failure of the dies occur which used in hot forging process, due to plastic deformation, abrasive wear, thermal shock and fatigue. Approximately %70 of failure of dies is which introduced as abrasive wear. Therefore, for estimate of die life in hot forging process, it is required to analyze the abrasive wear condition [1-4].

Die life effects many factors, metallographic composition of the material, forging operation temperature, die design, condition of the workpiece surface, hardness and toughness of the die. With changing a factor, die life can adversely effect. Therefore, in hot forging processes in general long die life is essential in order that reduce the unit fee of the product [5-7]. By improving the physical and thermal properties with this coating process, the desired optimum die life can be achieved.

Material and Method

In this study, the wear-related tool life of the dies and the cycle time during the forging process were observed and evaluated. ORVAR® 2M and UNIMAX® were selected as the die material. The experiment was applied to both uncoated and coated dies. The cycle time in uncoated dies was between 400 and 500, while in coated dies, this value varied between 2000 and 3500.

Die Materials

Die material should have long tool life and lowest crack risks due to excellent ductility and toughness. In addition to this, it should have good temper resistance, excellent hardenability, good dimensional stability

throughout heat treatment and coating operations. In addition to carbon, various alloying elements can be added to the steel structure in certain proportions to obtain higher strengths and structures that are more resistant to heat, cold, corrosion. UNIMAX® and ORVAR® 2M steel dies used in the process have improved properties compared to the reference hot work tool steel(H13) and high toughness under hot forging processes. Therefore, UNIMAX® and ORVAR® 2M tool steels have better properties when compared to H13 (1.2344) tool steel.

Table 1. Chemical Composition of Die Materials

Die Material		C	Si	Mn	Cr	Mo	V
	UNIMAX®	0,5	0,2	0,5	5	2,3	0,5
	ORVAR® 2M	0,39	1	0,4	5,3	1,3	0,9

Table 2. Hardness of the Die Materials

Die Material	UNIMAX®	56-58
	ORVAR® 2M	44-46
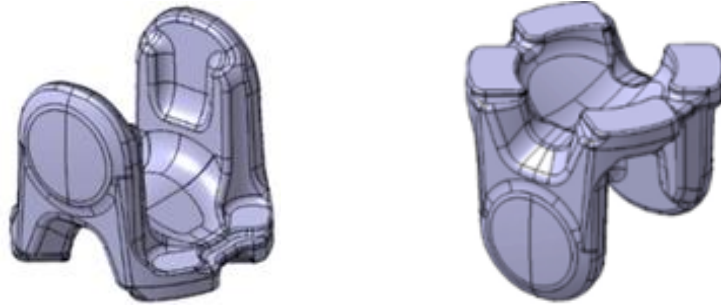
Figure 1. Part design in the CAD program

Uncoated Die

As tool steel, DIN1.2344A is used. After the forging process with 425 cycles, a fracture occurred in the radius region of the uncoated die. It has been observed that abrasions occur on the die surfaces along with breakage.

Figure 2. Coated Die situations after the forging process

Orvar® 2M (1.2344) Material FEXOY Coating

FEXOY® coating obtains wear resistance, excellent lubricated and it uses at hot forging dies and metal injection operations. Thickness range of the FEXOY® is 12-15 µm.

Figure 3. Coated Die situations before the forging process

ORVAR® 2M material preform top and bottom dies are coated with FEXOY® material. After forging process, grinding operation was not applied surface of the die material. Coated dies, at first forging operation was completed at 2438 cycle uneventfully. At second forging process was completed at 3499 cycles. However, after 2296 cycle and after 652 cycles, grinding operation was applied on surface of the die. After forging process, abrasive wear has been occurred at flange radius regions. Therefore, grinding operation was applied surface of that region.
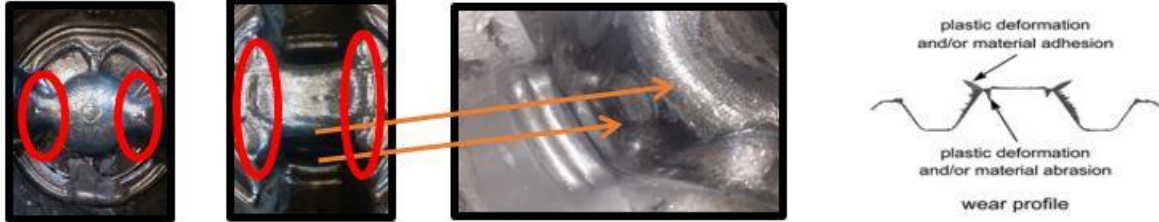
Figure 4. Abrasive wear surface of the die

Unimax® (1.2344) Material ABP+Dietox® Coating

ABP+Dietox® coating is a shot peening process that introduces compressive stress to the surface of material. It is a simple method for increasing fatigue and wear resistance of tooling materials. Coating material have similar properties with FEXOY® which applied to Unimax® die steel.

Figure 5. Coated Die situations before the forging process and Coated Die situations after the forging process

Unimax® preform top and bottom die material was coated with ABP+Dietox® coated material. Unimax® die material has 14 joule average toughness. With coating material preform dies worked up to 2177 cycle. As a result of these, it has been observed that die life of the coated preform die is higher than uncoated preform die. It has been observed that abrasive wear occurs on the radius of the coated die after 2177 cycles of forging. This die was then grinded and continued to be used again. Abrasive wear shows in Figure 5.

Results

In this article, it has been observed that the die life and performance of the preform die steels used in the forging process have increased with different coating techniques.

• After the uncoated dies worked for 400-500 cycles, breaks and cracks were observed.
• It has been observed that the dies with coating on the surface are subjected to grinding process after working for 2000-3500 cycles and continue to produce again.
• Fibering and abrasion were observed on the radius of coated and uncoated dies.
• It has been determined that the production is not interrupted frequently after the coating is applied and the total dies change time for the part is reduced.
• It has been observed that the die cost decreases with the die coating.

Conclusion

As a result of this study, the life of the preform dies to be used for the production of parts in the hot forging method and the cracks, abrasions and fibering formed on the die surface during the process were taken into account. The appropriate coating material has been selected by considering the hardness drop in the die caused by friction and thermal shocks caused by the material flow and other problems. Different coating techniques were applied to two different types of dies and maximum die life and number of cycles were determined in both dies according to uncoated die. Depending on the researches and applications made, it is observed that die coating

materials have a positive effect on die life. In addition, as a result of the work, there has been a noticeable decrease in die and labor costs.

References

1. Polat, H. (20069. *Comparisons of Different Methods Used For Improving Life of Hot Forging Dies,* 12-28.
2. Choi, C., Groseclose, A., & Altan, T. (2012). Estimation of plastic deformation and abrasive wear in warm forging dies. *Journal of Materials Processing Technology*, *212*(8), 1742-1752.
3. Rajiev, R., & Sadagopan, P. (2015). Plastic deformation analysis of wear on insert component and die service life in hot forging process. Indian Journal of Engineering & Materials Science, NISCAIR publication, 22, 686 – 692.
4. Pandya, V. A. (2021). *Investigation of Hot Forging Die to Improve its Life,* 2-3.
5. Zwierzchowski*, M. (2017). Factors affecting the wear resistance of forging tools,* Archives of Metallurgy and Materials, 62(3), 1567 – 1576.
6. Chander, S., & Chawla, V. (2017). Failure of hot forging dies–an updated perspective. *Materials Today: Proceedings*, *4*(2), 1147-1157.
7. Tanaka, T., Nakanishi, K., Yogo, Y., Kondo, S., Tsuchiya, Y., Suzuki, T., & Watanabe, A. (2005). Prediction of hot forging die life using wear and cooling model. R & D Review of Toyota CRDL, 40(1), 43-48

Flood modeling with FLO-2D: Mersin / Lamas River

Vahdettin Demir *1 , Abdulkadir Özcan 2

1 KTO Karatay University, Civil Engineering Department, Türkiye, vahdettin.demir@karatay.edu.tr, kadirozcan42@hotmail.com

Keywords
DEM
FLO-2D
Flood modeling
Mersin
Lamas River

Abstract
Floods are natural disasters that cause loss of life and property, when necessary, precautions are not taken. It is the first among meteorological disasters in our country, and it comes after earthquakes among all disasters. In order to prevent or reduce the losses caused by floods, flood models should be made and precautions should be taken. In this study, two-dimensional flood modeling was carried out for the Lamas River, which transfer its waters into the Mediterranean and is located in Mersin province. In the study, the FLO-2D model was carried out on the 5-meter resolution elevation model obtained from the General Directorate of Maps. In the study, Q_{100} and Q_{500} flow return periods were modeled, and flood maps were obtained. As a result of the study, it was determined that the study area within the city limits was affected by both floods and the agricultural greenhouses in this area were unprotected. In addition, it was stated that the DEM resolution used significantly affected the study results.

Introduction

Flood is a major natural disaster that affects many places in the world, including developed countries. In addition to loss of life, billions of dollars of property losses are experienced every year due to floods [1]. With flood models, it is possible to prevent or reduce all these losses by informing the public where will be flooded. These models are also very useful in flood-related relief and rescue operations [2]. 2D flood modeling is a newly developing subject in our country. In order to prevent or minimize the loss of life and property, flood maps should be prepared, and measures should be taken before floods occur. In this study, flood modeling is carried out by using a package program capable of hydraulic modeling, high-resolution topographic data, and some flood return periods obtained with various statistical distributions.

The aim of this study is to perform flood modeling with the help of the FLO-2D package program, which can make two-dimensional hydraulic modeling by using different recurring flow rates (100 and 500-year return periods) of the Lamas River, which is located within the borders of Mersin central district and empties into the Mediterranean.

Material and Method

Many input data are used in flood modeling [3]. As these parameters are detailed, the model can better express the real environment or the studied area. The main ones of these data are numerical surface or elevation model, flood recurrence rates or hydrograph and Manning roughness coefficient. For other data, the following source can be examined [3,4]. In this study, digital elevation model (DEM) data with a resolution of 5 meters was used. This data was obtained from the General Directorate of Mapping. The repeat flow rates were obtained from previous studies and the flow rates used in this study are given in Table 1 [5]. In the study, the Manning roughness coefficient was assumed to be a constant 0.04 like Demir et al. [6].

Table 1. Return period of flood flows [5]

Year	100	500
Peak Flows (m^3/s)	113.15	163.78

FLO-2D

FLO-2D is one of the package programs produced/developed by O'Brien, where 2D hydraulic models are made [7] .FLO-2D has been widely used in flood modeling in recent years [8–10]. It models the flow of water in terms of time. This model represents a simplified version of the stream containing particles of various sizes, the main components of which are solid and water materials [11].

Study Area

The surface area of Mersin is 15,853 km^2 and most of it is within the borders of the Eastern Mediterranean Basin. Mersin province, which is surrounded by the Mediterranean from the south, is separated from the inner parts of Anatolia by the high plateaus and peaks of the Western and Central Taurus Mountains from the north. Lamas River (Limonlu) is located in Erdemli district of Mersin. This river takes its source from Yüğlük Mountain and flow into the Mediterranean [6]. The study area and DEM are shown in Figure 1.
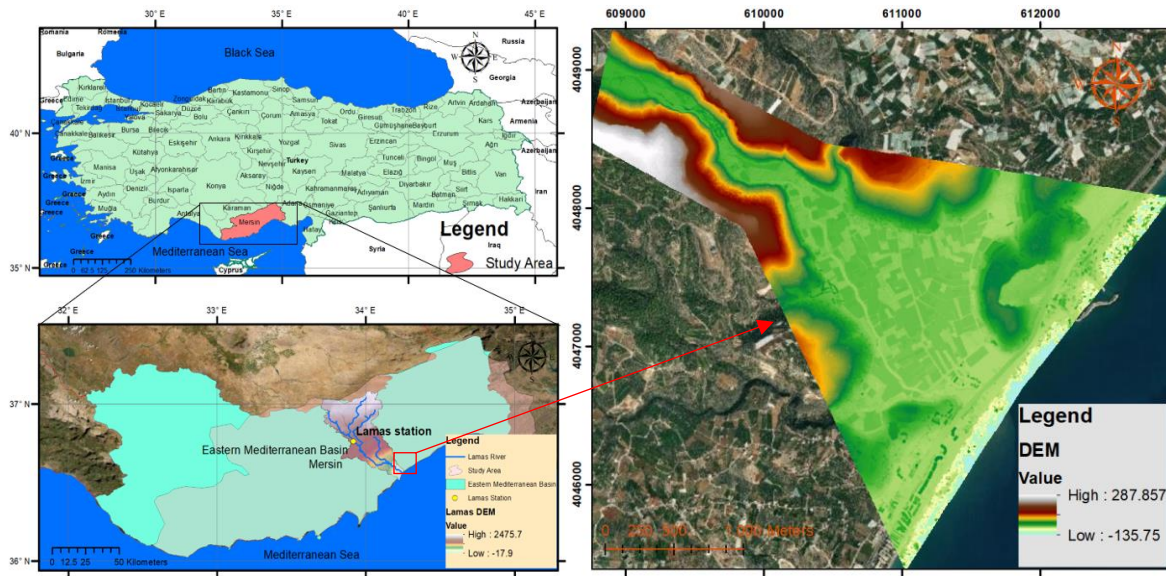
Figure 1. Study area and DEM, revised from [6]

Results

Flood modeling basically requires a digital elevation model, the calculated flow rates for the different recurrent times of the Lamas River, the baseline map of the region, and the Manning friction coefficients [6]. In this study, a 5-meter resolution DEM obtained from the General Directorate of Mapping was used. Flood flow rates were obtained from the literature and the Manning coefficient was assumed to be a constant 0.04 for the entire study area. In the study, 2 different recurring flow rates Q$_{100}$ and Q$_{500}$ were modeled using FLO-2D and the results are given in Figure 2 and Figure 3.

When Figure 2 and Figure 3 are examined, water heights of 11 meters at the upper elevations where the flow first begins, and 3 meters to 5 meters in places, in the region where the flow ends or exits to the Mediterranean, have been determined. At Q$_{100}$ flow rate, the flow generally follows the riverbed, but cannot follow downstream and spreads out of the river. At the Q$_{500}$ flow rate, many greenhouse areas are affected by the flow and water levels up to an average of 3 meters are observed.
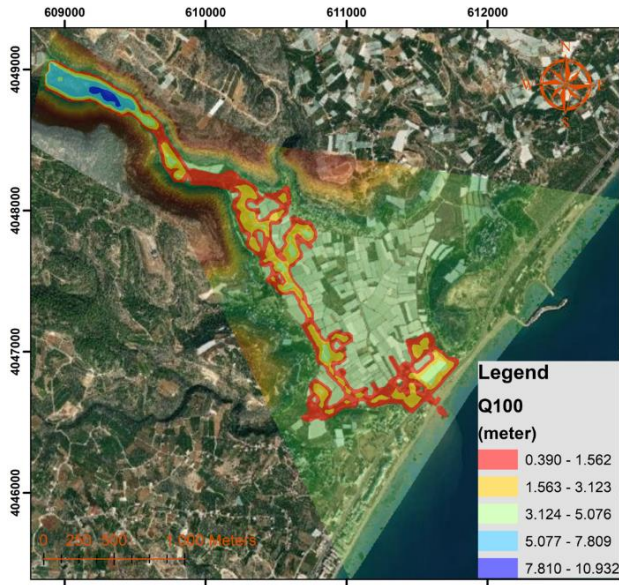
Figure 2. Flood propagation map for Q_{100}
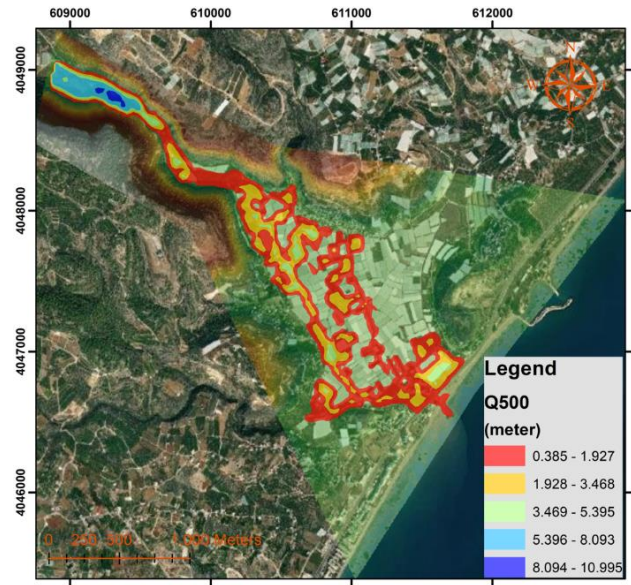
Figure 3. Flood propagation map for Q_{500}

Discussion

Another aim of the study is to compare the results of the model performed using HEC-RAS in this area with some of the criteria of this model [6]. In this study, 10-meter resolution DEM, 25-meter size mash, 0.04 constant Manning friction coefficient and Q_{100}=36.3 m^3/s, Q_{500}=51.5 m^3/s flow rates were used. As a result of the study, it is seen that almost all of the upstream region is under water. It was also determined that the river flow could not follow the riverbed in any way. In the current study, 5-meter resolution DEM, 25-meter size grid, 0.04 constant Manning friction coefficient and Q_{100}=113.15 m^3/s, Q_{500}=163.78 m^3/s flow rates were used. As a result of the study, it was observed that a part of the upstream section was affected by the flood and the water flow followed the river bed. This result shows that the DEM resolution used in flood models can greatly affect the study. In addition, the fact that the flood flow rate has increased by about 3 times shows that there may be an increasing flood trend in the region with the updated data. In order to protect the greenhouses in this region, which is important for the economy of the region, from possible floods, it is recommended to raise the river sections and to clean the sections at regular intervals.

Conclusion

In this study, two-dimensional flood modeling was carried out using FLO-2D and 5-meter DEM. In the modeling, 2 different recurring flow rates were used and the areas that would be affected by possible floods were determined in both flow rates. Contrary to the past records of climate change, serious floods are seen in some regions and extreme droughts are seen in some regions. For this reason, Q_{500} flow rate should be used as a reference model flow rate, especially in flood models to be made in urban centers, and cross-section and bridge arrangements-designs to pass this flow should be considered. In addition, digital surface model should be preferred instead of digital elevation model in modeling, and 5 meter resolution DEM data or more sensitive data should be used in modeling as in this study.

In future studies, it is considered to use smaller model grits (dimensions) for the same region and to simulate the flood using at least 2 different hydraulic models by calculating various recurrent flow rates. Thus, calibration problems will also be investigated. In addition, it is planned to obtain the Manning coefficient according to the topography characteristics and the COWAN method instead of a fixed value.

Acknowledgment

Funding

References

1. Demir, V., Ülke, K. A. (2022). Evaluation of Economic Damages of Floods (Samsun-Mert River Basin). International Journal of Engineering Research and Development. 14, 663–678. https://doi.org/10.29137/umagd.1090447
2. Demir, V., & Kisi, O. (2016). Flood Hazard Mapping by Using Geographic Information System and Hydraulic Model: Mert River, Samsun, Turkey. Advances in Meteorology. 2016. https://doi.org/10.1155/2016/4891015
3. Demir, V. & Ülke Keskin, A. (2022). Yeterince akım ölçümü olmayan nehirlerde taşkın debisinin hesaplanması ve taşkın modellemesi (Samsun, Mert Irmağı örneği). Geomatik, 7 (2), 149-162. https://doi.org/10.29128/geomatik.918502
4. Demir, V. (2020). Samsun Mert havzasında bir ve iki boyutlu modeller ile taşkın alanlarının belirlenmesi. Ondokuz Mayıs Üniversitesi, Doktora Tezi, Lisansüstü Eğitim Enstitüsü.
5. Öğsüz, E., & Demir, V. (2022). Mersin Lamas nehri taşkın tekerrür debilerinin istatistiki yöntemlerle belirlenmesi. International Congress on Art and Design Research. Kayseri, 73–74.
6. Demir, V., Alptekin, A., Çelik, M. Ö., & Yakar, M. (2021). 2D Flood modeling with the help of GIS: Mersin/Lamas River. *Intercontinental Geoinformation Days*, *2*, 175-178.
7. O'Brien (2006). FLO-2D user's manual, Version 2006.01. FLO Engineering, Nutrioso. 2006.
8. Haile, S., Worku, H., & Paola, F. De. (2018). Flood hazard mapping using FLO-2D and local management strategies of Dire Dawa city, Ethiopia. Journal of Hydrology: Regional Studies, 19, 224–239. https://doi.org/10.1016/j.ejrh.2018.09.005
9. Demir, V., Ülke Keskin, A. (2020). Obtaining the Manning Roughness with Terrestrial-Remote Sensing Technique and Flood Modeling using FLO-2D, a case study Samsun from Turkey. Geofizika. 2020. https://doi.org/10.15233/gfz.2020.37.9
10. Haltas, I., Tayfur, G., & Elci, S. (2016). Two-dimensional numerical modeling of flood wave propagation in an urban area due to Ürkmez dam-break, İzmir, Turkey. Natural Hazards. 2016. https://doi.org/10.1007/s11069-016-2175-6
11. Brien, K. (2006). Pocket Guide. FLO-2D Software, Inc. Nutrioso; 2006.

Advanced Engineering Days

aed.mersin.edu.tr

Internet of Things (IoT) in GIS

Çetin Önder İncekara*1

1BOTAŞ, Doç. Dr., Arazi Edinim Şube Müdürü, BOTAŞ Genel Müdürlüğü, Bilkent, Ankara, Türkiye, cetinincekara@gmail.com

Keywords	Abstract
Internet of Things GIS Smart Cities Disaster Management Building Information Modeling-BIM Fuzzy Logic Artificial Intelligence	Our world is transforming and rapidly becoming digital. Today, people are on the cusp of an IoT-driven technological revolution, affecting most sectors including energy industry. With billions of connected sensors deployed on assets and networks and in products around the world, companies are collecting and processing data at a higher frequency and velocity with the help of 6G (the sixth generation of wireless technology). GIS and IoT are interrelated and nested technologies. The challenge that continues to plague many organizations is how to make effective decisions with the help of 6G network technology. Organizations are facing many new challenges and looking toward technology to improve situational awareness, create operational efficiencies, and optimize all aspects of work. As IoT and GIS adoption increases and their applications mature, the future is becoming increasingly intelligent and automated. As IoT connects the data, and the GIS adds context around the asset, connecting the information model to other models and to its surroundings. GIS creates digital twins of the natural and built environment, and it can also be used to integrate many different digital representations of the real world.

Introduction

In the Digital era, evolution in technologies motivates and inspires us to live a better quality of life. Digitization has made once the impossible visions come true. Internet of Things (IoT) and Geographical Information System (GIS) are one of those technologies people witness today.

IoT is offering boundless opportunities for consumers and businesses. The connectivity between the objects and able to collect a considerable amount of real-time data has made it efficient. On the other hand, GIS has a foundation of data collected through IoT devices and digital maps.

With the help of 6G network technology, the data transfer will be faster. 6G will use higher frequency bands and agile, cloud-based networking technology to deliver record-breaking speeds and microsecond latency.

Internet of Things (IoT)

Internet of Things is a system that interconnects with a network of physical objects like sensors, computing devices, and software for transferring data over to other systems without any interference of human to human or human to computer interaction, i.e., smart homes. Growth of the Telecommunication Industry offers us new connectivity offerings like 6G service going to be connected soon.

The devices can connect with IoT range from ordinary household appliances to large industrial equipment. It is used for computing, and to minimize human intervention, with IoT, people automatically collect and share the data to align with your daily process with machinery or lifestyle.

Internet of Things can be defined as a network that allows things around us to interconnect and talk to each other. Things around us are smart, smartwatch, smart T.V, smart mobile and more. The future of IoT is vast and future will be based on IoT technologies.

6G Wireless Technology

6G is the sixth generation of wireless technology. 6G network follows up on 4G and 5G; 4G has the speed of approx. 33,88 Mbps, 5G has the speed of approx. 40-1,100 Mbps. 6G has the speed of upto 1 Tbps (1,000,000 Mbps). 6G is using higher frequency bands and agile, cloud-based networking technology to deliver record-breaking speeds and microsecond latency. The internet connectivity will become like air and this will come to true with the help of 6G technology.

6G will not only support mobile phones, but also it will be used for technology like automated cars and smart-home networks, helping create a seamless connectivity between the internet and everyday life.

Fusion of IoT and GIS

GIS is a technology used to keep tracks on the location of an object or user and store, manipulate the data for more digitized solutions. GPS on smartphones, traffic conditions on maps, Uber rides, food delivery exact locations are some of the famous examples of GIS technology. GIS and IoT are interrelated and nested technologies. Combining both gives a bigger picture with the range of objects, individual buildings and locations, and as well as large areas like smart cities, transit development, and disaster management. When GIS and IoT work together, it offers benefits such as an increase in flow efficiency, cost efficiency, and, most importantly, can get real-time information from the sensors without the need for human intervention.

Architecture of IoT and GIS

Flow chart in Figure 1 presents the system architecture of pairing IoT and GIS. IoT sensors are conventional sensors used to collect data from the environment, traffic conditions, and locations like individual buildings, roads, and smart cities.
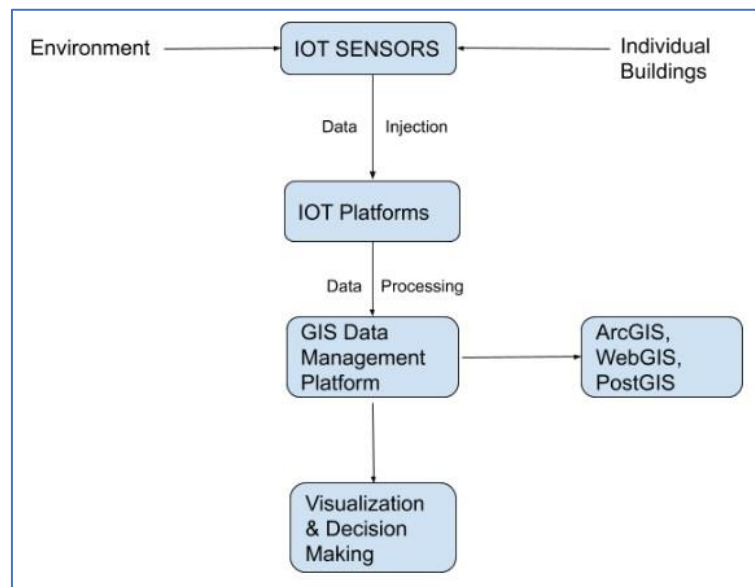
Figure 1. System architecture of pairing IoT and GIS Flow chart

Data Injection is storing the gathered information into the IoT platforms like technologies that manage, provision and connect with the IoT World. The next step is Data Processing, where the data gathered from the IoT are used in GIS platforms. The collected data is for manipulating, storing, and analyzing by WebGIS, PostGIS, and ArcGIS applications. Visualization and Decision making is to use all data into the mapping layers. From the Identified data, people can visualize the environment and locations. This process is providing solutions to the digital world.

Smart Mobility Solutions

Transportation plays a crucial role in our lifestyle. Earlier it wasn't easy, but people are traveling faster than time. IoT and GIS give solutions like GPS enabled vehicles and information about the route people need to travel, and people can also get applications for finding hotels, rest stops, filling stations on the go. By using IoT on Vehicles, people can connect to the LAN and connect with others. This tech takes control of the vehicle to avoid accidents. Also, it can report live data back to the relevant control room.

Smart Cities

An extensive range of data of whole cities can be collected by GIS and IoT sensors. From how many buildings, cars, and even lamp posts and reports of traffic, air, noise, GHG and more. This can help the government track the pollution and improve the pollution levels.

For this process, people need to collect large amounts of data, and IoT sensors are installed on cars, highways, roads, and buildings. In this way, people can track if any floods, forest fire, pollution or disease occurrence that are likely to happen on a full range scale. Also, this collaboration can be used to make city planners create routes for cycling and biking. Even for water and drainage routes for better control.

Disaster Management

The government can utilize GIS and IoT data to simulate the impact of natural disasters such as fire, earthquake and flooding. The government also takes preliminary decisions to determine the higher risks by analyzing the simulations of fire, flooding and earthquake. This will help the city planners to design better cities to eradicate these type disasters in advance by the help of the collected data via GIS and IoT.

Geospatial Information System (GIS) is a powerful set of tools that deal with capturing geospatial data, managing that data in a database, analyzing and pattern recognition, and finally visualizing information. IoT, as an emerging technology along with GIS, can result in advanced and user-friendly features in Smart Cities.

The connection between IoT and GIS is geographic location. Most devices combine their physical location from a GPS receiver giving real-time sensor information and positioning.

GIS and IoT-based systems are not only at developers' center of attention but also at officials' and organizations. With the wide range of applications provided by these integrated systems, they are being used in many aspects including urban and rural developments. These studies were categorized into seven groups of sectors and presented in Table 1.

Table 1. Industry share of GIS and IoT integrated applications

Industry/Sectors	GIS and IoT integrated applications
Urban Infrastructure	28
Environmental Monitoring	16
Utilities	16
Disaster Management	14
Agriculture	12
Transportation	9
Healthcare	5

Results

In literature Fuzzy Multi Criteria Decision Making Methods (FMCDM) are used in different fields by many researchers [1-25] by using MATLAB program.

As it is presented in Table 1, the percentages are: Urban Infrastructure 28%, Environmental Monitoring 16%, Transportation 9%, Agriculture 12%, Disaster Management 14%, Utilities 16%, Healthcare 5%. Urban Infrastructure mostly including smart city-related studies has been the most frequent domain of applications. Environmental Monitoring and Utilities shared the same frequency of 16%. On the other hand, less attention was paid to the Healthcare industry in GIS and IoT integrated point of view. These industry shares can be compared with the estimated market share of IoT applications by 2025 in which Healthcare is projected to have the most economic influence. Therefore, it would be a great opportunity to focus on the Healthcare industry to use the great functionality of GIS simultaneously with IoT.

Conclusion

GIS and IoT, this fusion has some confronting challenges ahead of them. To name a few, they are Data Integration, Data Security, Data Storage, and hardware ruggedization. Storage and integration of the data is the biggest challenge. The data are collected in different formats, such as images and videos, and more. Securing information is the most significant challenge as it includes the whole data of the real world of cities, which is now used for better business, improving decisions, and enhanced quality of life. The two technologies will lead the ways for a better world.

While large-scale deployments of IoT have improved the availability and timeliness of data, it can be difficult to connect these sometimes discrete and unstructured datasets. Every sensor, asset, or network has one thing in

common: it is located somewhere. Location provides a common reference system to create relationships. GIS location technology interconnects GIS information via IoT.

Industry and government organizations are facing challenges in every area of their business. They work hard to adapt to and leverage digital technology. Yet they often face today's challenges with yesterday's methods. In the struggle to remain relevant and thrive, they are looking to update to modern advanced information technology (IT) and operational technology (OT) solutions. To achieve these transformation objectives, they need to reinvent the way they do business and change many legacy operating models and processes. To affect the desired change, organizations need scalable solutions that not only meet today's challenges but also align to their strategic future vision. As IoT and GIS adoption increases and their applications mature, the future is becoming increasingly intelligent and automated. GIS and IoT technologies are connecting systems and data in new ways, which is enabling the transformation of many organizational workflows. The innovation and integration of these technologies are creating the nervous system and enabling real-time integrated digital twins.

Digital twins are used to represent accurate historical views, observe and monitor current performance, and predict future states. A digital twin of a fixed asset or real-world system benefits directly from the inclusion of GIS and IoT data about the asset. The IoT connects the data, and the GIS adds context around the asset, connecting the information model to other models and to its surroundings. GIS creates digital twins of the natural and built environment, and it can also be used to integrate many different digital representations of the real world.

In the last several years, the convergence of GIS technology; IoT; and, more recently, building information modeling (BIM) has created interactive 3D visualizations, which are redefining what a digital twin is and the value it brings to organizations. A digital twin is not a single product or solution; it is a complex network of technology and systems. It must work in harmony to achieve the desired transformational outcomes and return on investments that organizations desire. ArcGIS location technology is a proven way to create a framework to bring data together using location and to deploy big data accurately and intelligently against real-world problems and bring IoT data to life in spatial context.

References

1. Chan F. T. S., & Kumar, N. (2007). Global Supplier Development Considering Risk Factors Using Fuzzy Extended AHP-based Approach. Omega International Journal of Management Science, 35, 417-431.
2. İncekara, Ç. Ö., & Oğulata, S. N. (2011). Enerji darboğazında ülkemizin alternatif enerji kaynakları. Sosyal ve Beşeri Bilimler Dergisi, 3(1).
3. İncekara, C. O. & Oğulata, S. N. (2012). EU and Turkey's Energy Strategies. International Journal of Economics and Finance Studies, 4(2), 35-43.
4. İncekara, Ç. Ö., & Oğulata, S. N. (2017). Turkey's energy planning considering global environmental concerns. Ecological Engineering. Elsevier, A.B.D., 589-595.
5. Incekara, C. O. (2018). Ülkemizdeki Enerji Santral Yatırımlarının AHP Yöntemi ile Değerlendirilmesi. Çukurova Üniversitesi Mühendislik Fakültesi Dergisi, 33 (4), 185-196.
6. Incekara, C. O. (2019). Use of an Optimization Model for Optimization of Turkey's Energy Management by inclusion of Renewable Energy Sources. International Journal of Environmental Science and Technology, Springer, 121-133.
7. İncekara, Ç. Ö. (2019). Türkiye ve AB'nin Enerji Stratejileri ve Politikaları. Journal of Turkish Operations Management, 3(2), 298-313.
8. Incekara, C. O. (2019). Turkey's Energy Management Plan by Using Fuzzy Modeling Approach. Scholars' Press, ISBN-10: 6138829697, Book, 38-52.
9. Incekara, C. O. (2020). Türkiye' nin Elektrik Üretiminde Doğalgaz Talep Tahminleri. Journal of Turkish Operations Management, 3(2), 298-313.
10. İncekara, Ç. Ö. (2020). Evaluation of Turkey's International Energy Projects by Using Fuzzy Multi-Criteria Decision Making Methods. Euroasia Journal of Mathematics, Engineering, Natural & Medical Sciences, 7(9), 206-217. https://doi.org/10.38065/euroasiaorg.143
11. İncekara, Ç. Ö. (2020). Turkey's natural gas demand projections. EJONS Internatıonal Journal, 4(15), 489-505. https://doi.org/10.38063/ejons.269
12. Incekara, C. O. (2020). Bulanık Mantık ile Sanayii Sektöründe ISO 50001 Enerji Yönetim Sistemi Uygulaması. Afyon Kocatepe Üniversitesi Fen ve Mühendislik Bilimleri Dergisi, 20(6), 991-1013.
13. İncekara, Ç. Ö. (2020). Enerji Sektöründe Faaliyet Gösteren Bir İşletmede İş Sağlığı ve Güvenliği Yönetim Sistemi. Mehmet Akif Ersoy Üniversitesi Uygulamalı Bilimler Dergisi, 4(1), 152-177.
14. İncekara, Ç. Ö. (2021). Bulanık TOPSIS ve Bulanık VIKOR yöntemleriyle bir enerji şirketinde kurumsal hafızanın oluşturulması. Euroasia Journal of Mathematics, Engineering, Natural & Medical Sciences, Cilt 8, Sayı 17, (2021), 1-20. https://doi.org/10.38065/euroasiaorg.589
15. Incekara, C. O. (2021). Post-COVID-19 Ergonomic School Furniture Design under Fuzzy Logic. Work, 69, 1197–1208.

16. İncekara, Ç. Ö. (2021). Dünyanın ve Türkiye' nin Doğal Gaz Talep Senaryosu. Euroasia Journal of Mathematics, Engineering, Natural & Medical Sciences, 8(17), 44-57. https://doi.org/10.38065/euroasiaorg.610
17. İncekara, Ç. Ö. (2021). Global Natural Gas Demand Projections under Fuzzy Logic. EJONS Internatıonal Journal, Vol. 5, No. 18 (2021): EJONS Journal, 367-385. (https://doi.org/10.38063/ejons.430)
18. Incekara, C. O. (2022). Designing Ergonomic Post-Covid-19 School Furniture. South African Journal of Industrial Engineering, 33(2), 211–224.
19. İncekara, Ç. Ö. (2022). Sigorta Eksperlerinin Dask Sigortası Değerlendirmelerinin Bulanık Mantık Altında İncelenmesi. Euroasia Journal of Mathematics, Engineering, Natural & Medical Sciences, 9(21), 14-41. https://doi.org/10.38065/euroasiaorg.952
20. Incekara, Ç. Ö. & Lala, S. (2022). Enerji projelerinde arazi edinim faaliyetleri ve arazi değerlemesi. Geomatik, 8(1), 61-71.
21. Kumar Sahu, A., Datta S., & Mahapatra S. S. (2016). Evaluation and selection of resilient suppliers in fuzzy environment. Benchmarking: An International Journal, 23(3), 651-673.
22. Satrovic, E. (2018). The Human Development Relies on Renewable Energy: Evidence from Turkey. 3rd International Energy & Engineering Congress, 19-27.
23. Shukla, A. K (2014). Interpretability Assessment in Fuzzy Rule Based Systems. International Journal of Scientific & engineering Research, Volume 5, Issue 7, 506-509.
24. Wang, C. (2015). A Study of Membership Functions on Mamdani-Type Fuzzy Inference System For Industrial Decision-Making. PhD Theses and Dissertations. Lehigh University, (Paper:1665).
25. İncekara, Ç. Ö. (2022). Industrial internet of things (IIoT) in energy sector. Advanced Engineering Days (AED), 5, 181-184.

Synthesis of cobalt-doped bead type catalyst for hydrogen production via hydrolysis reaction of NaBH4

Filiz Akti[*1]

[1]*Hitit University, Chemical Engineering Department, Türkiye, filizakti@hitit.edu.tr*

Keywords
Cobalt
Bead
NaBH4
Hydrogen

Abstract
Cobalt-doped bead type catalyst was synthesized for hydrogen generation from sodium borohydride hydrolysis reaction by using sodium hydroxide. Synthesized catalyst was characterized using XRD (X-ray diffraction), nitrogen adsorption/desorption isotherm and FTIR (Fourier transforms infrared) analyses techniques. XRD pattern showed presence of chitosan in the structure, while cobalt species were not observed. Nitrogen adsorption/desorption isotherm was exhibited a behavior indicating of micro-mesoporous structure. The surface area, total pore volume and pore diameter values of catalyst were determined as 35.0 m^2/g, 0.03 cm^3/g and 3.4 nm, respectively. FTIR spectra showed existence of peaks related to chitosan. The catalyst was test in sodium borohydride hydrolysis reaction and hydrogen production rate was determined as 28 mL. min^{-1}. g^{-1}.

Introduction

Nowadays, the search for new and renewable clean energy sources continues due to the decrease in fossil fuels and their harmful effects on the environment. Hydrogen still attracts attention as an environmentally friendly clean energy source. Sodium borohydride ($NaBH_4$) is the most widely used metal hydride source due to its high hydrogen storage capacity (10.8 by wt%), stability in alkaline solution, pure hydrogen generation and easy reproduction from by-products. The catalytic hydrolysis reaction of $NaBH_4$ is an exothermic reaction and it produces two times as much hydrogen than its content at the end of the reaction [1,2]. The self-hydrolysis reaction of $NaBH_4$ without a catalyst is quite slow. Although noble metals such as platinum, palladium, rhodium and ruthenium have been widely used due to their excellent catalytic activity, their rarities and the resulting high cost have caused to the development of alternative catalysts. However, the direct use of these metals causes agglomeration problem and low surface area. This situation can reduce the catalytic activity by affecting the catalytic active centers. In addition, the problem of separating the catalysts from the reaction medium reduces the reusability of the catalyst and increases the cost at this rate. Therefore, synthesized catalysts using support structure largely eliminates these disadvantages. In general, zeolite, metal oxides, clay, activated carbon, graphene, carbon nitride, silica, alumina, aerogel and hydrogel materials were used as catalyst support materials [3-5].

In this study, cobalt which is cheap and having high catalytic activity were preferred catalyst active metal. Aforementioned problems were tried to be eliminated by synthesizing the catalyst active components in the form of bead using chitosan.

Material and Method

Synthesis of catalyst

$CoCl_2.6H_2O$ was chosen as catalyst active component. Chitosan was used to obtain the bead structure. First, 0.2 g $CoCl_2.6H_2O$ was dissolved in 50 mL acetic acid (1% v/v) and then chitosan (2% w/v) was added and mixture was stirred for 3 hours at room temperature until a clear homogeneous viscous solution was obtained. The resulting

gel was kept for one night to elimination of bubbles and then it was dropped into the 1 M NaOH solution using a syringe and stirred for 2 hours to form a stable bead structure. The resulting beads were filtered using filter paper, washed several times with distilled water and dried at room conditions. The catalyst was coded as Co@C. The all chemicals were of analytical purity and supplied from Sigma-Aldrich.

Characterization of catalyst

X-ray diffraction (XRD) pattern of catalyst was recorded by a Philips PW 3040 diffractometer equipped with CuKα radiation (λ=0.15406 nm) in the 2θ range of 10–90° with 0.02° step size and 1°/min scan speed.

Nitrogen adsorption/desorption isotherm was obtained with a Quanthrocrome®ASiQwin™ instrument at -196 °C after degassing the catalyst for 3 h at 120 °C. Before analysis catalyst was waited in an oven for overnight at 110 °C. Multi point BET (Brunauer Emmet Teller) surface area was calculated using adsorption data in the range of $0.05 < P/P_o < 0.30$. Total pore volume was determined at relative pressure of $P/P_o = 0.99$. Pore diameter was estimated by Barrett-Joyner-Halenda (BJH) method [6].

The FTIR (Fourier transforms infrared) spectra of the catalyst was recorded on a Thermo Scientific/Nicolet IS50 device with ATR (attenuated total reflectance) in the wavelength range of 600-4000 cm^{-1}.

Catalytic activity test

The performance of catalyst was tested in the NaBH$_4$ hydrolysis reaction for hydrogen generation. In the reaction experiments, firstly a mixture containing 5 mL water, 1.0 wt% NaOH and 1.0 wt% NaBH$_4$ were prepared after that the 30 mg of catalyst was added. Generated hydrogen volume was measured using a classical water displacement method. The hydrogen generation rate was calculated from the slope of the volume-time plot in the linear region using formula HGR=V/(t*m). Where HGR is hydrogen generation rate (mL.min^{-1}.g$_{cat}^{-1}$), V is generated hydrogen volume (mL), t is time (min) and m is weight of the catalyst (g).

Results and Discussion

XRD pattern of catalyst is given in Fig.1a. The catalyst exhibited amorphous structure, it was determined that the broad peaks obtained at Bragg angle values of ∼ 20 º and 40 º belong to chitosan [7]. The peaks corresponding to cobalt was not observed, this situation suggested that the metals might be embedded in the chitosan structure.

The nitrogen adsorption/desorption isotherm is given in Fig. 1b and the structural properties determined from the isotherms are inset in Figure 1b. The catalyst exhibited Type IV isotherm behavior, representing porous materials containing micro and mesopores, according to the IUPAC classification [6]. Amount of adsorbed gas volume increased with relative pressure for catalyst. Total adsorbed gas volume for Co@C was approximately 19 cm^3/g. The surface area, total pore volume and pore diameter values of catalyst were determined as 35.0 m^2/g, 0.03 cm^3/g and 3.4 nm, respectively.
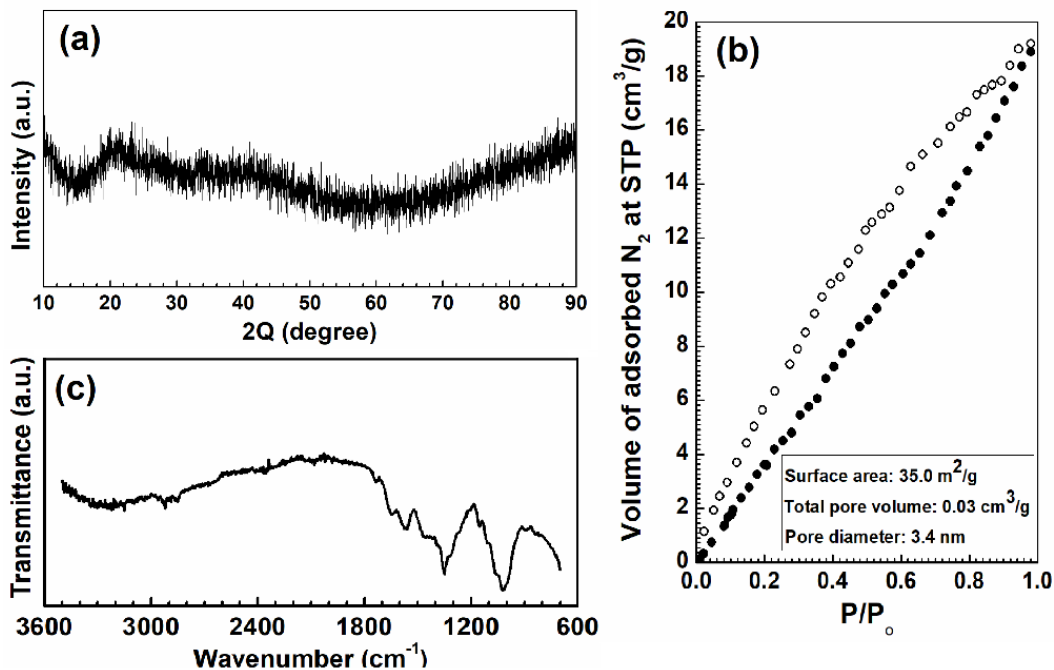
Figure 1. (a) XRD patterns (b) Nitrogen adsorption/desorption isotherms (STP: Standard temperature and pressure) (c) FTIR spectra of Co@C catalyst

The FTIR spectra of the catalyst is shown in Figure 1c. Functional groups related with chitosan were clearly observed in catalyst. The peak observed around 1030 cm^{-1} indicates C-O vibration, the peaks obtained at 1350 and 1460 cm^{-1} show C-H vibration originating from the CH_2/CH_3 groups. In addition, the peak at 1644 cm^{-1} was assigned to C=O bond in the chitosan structure, and the peaks at 1557 and 3270 cm^{-1} to N-H group [7, 8].

Catalytic activity test of catalyst is given in Figure 2. Hydrogen generation was not observed in the first 60 min over Co@C catalyst. It was thought that the reason for this might be due to the contact time of the catalyst surface with reactants or the pore diffusion resistance [9]. During the NaBH$_4$ hydrolysis reaction, BH$_4^-$ ions, which are first separated from NaBH$_4$, are adsorbed on the catalyst surface, and H$^-$ ions transfer to metal ions, and hydrogen is released at the end of a series of reactions [10]. Hydrogen production volume with cobalt catalyst was measured as 124 mL within 210 min. The hydrogen production rate was determined as 28 mL. min^{-1}. g^{-1}.
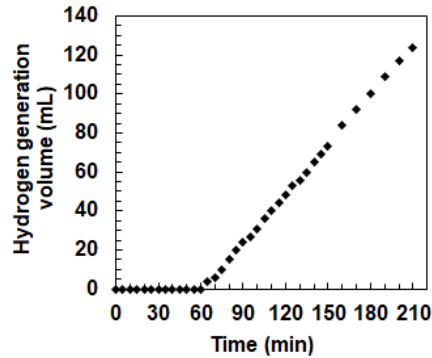
Figure 2. Catalytic activities of Co@C catalyst

Conclusion

Cobalt-doped bead type catalyst was synthesized using chitosan. Characterization results showed that catalyst was prepared successfully. Hydrogen generation rate was 28 mL. min^{-1}. g^{-1}. In present study, the development of cobalt-doped bead type catalysts for hydrogen production might be initiative for next studies.

Acknowledgements

References

1. Patel, N., & Miotello, A. (2015). Progress in Co–B related catalyst for hydrogen production by hydrolysis of boron-hydrides: A review and the perspectives to substitute noble metals. *International journal of hydrogen energy*, *40*(3), 1429-1464.
2. Kilinc, D. (2022). Co complex modified on Eupergit C as a highly active catalyst for enhanced hydrogen production. *International Journal of Hydrogen Energy*, *47*(23), 11894-11903.
3. Saka, C., Eygi, M. S., & Balbay, A. (2020). CoB doped acid modified zeolite catalyst for enhanced hydrogen release from sodium borohydride hydrolysis. *International Journal of Hydrogen Energy*, *45*(30), 15086-15099.
4. Li, Y. T., Zhang, X. L., Peng, Z. K., Liu, P., & Zheng, X. C. (2020). Highly efficient hydrolysis of ammonia borane using ultrafine bimetallic RuPd nanoalloys encapsulated in porous g-C3N4. *Fuel*, *277*, 118243.
5. Xu, D., Zhang, Y., Cheng, F., & Zhao, L. (2014). Enhanced hydrogen generation by methanolysis of sodium borohydride in the presence of phosphorus modified boehmite. *Fuel*, *134*, 257-262.
6. Lowell, S., Shields, J. E., Thomas, M. A., & Thommes, M. (2006). *Characterization of porous solids and powders: surface area, pore size and density* (Vol. 16). Springer Science & Business Media.
7. Abdeen, Z., Mohammad, S. G., & Mahmoud, M. S. (2015). Adsorption of Mn (II) ion on polyvinyl alcohol/chitosan dry blending from aqueous solution. *Environmental Nanotechnology, Monitoring & Management*, *3*, 1-9.
8. Kumirska, J., Czerwicka, M., Kaczyński, Z., Bychowska, A., Brzozowski, K., Thöming, J., & Stepnowski, P. (2010). Application of spectroscopic methods for structural analysis of chitin and chitosan. *Marine drugs*, *8*(5), 1567-1636.
9. Xu, D., Dai, P., Liu, X., Cao, C., & Guo, Q. (2008). Carbon-supported cobalt catalyst for hydrogen generation from alkaline sodium borohydride solution. *Journal of Power Sources*, *182*(2), 616-620.
10. Narasimharao, K., Abu-Zied, B. M., & Alfaifi, S. Y. (2021). Cobalt oxide supported multi wall carbon nanotube catalysts for hydrogen production via sodium borohydride hydrolysis. *International Journal of Hydrogen Energy*, *46*(9), 6404-6418.

Advanced Engineering Days

aed.mersin.edu.tr

Precise point positioning technique with single frequency raw GNSS observations using different products on android smartphones

Barış Karadeniz[*1] , **Hüseyin Pehlivan** [1] , **Barışcan Arı** [1]

[1]*Gebze Technical University, Department of Geomatics Engineering, Türkiye, b.karadeniz@gtu.edu.tr, hpehlivan@gtu.edu.tr, b.ari2021@gtu.edu.tr*

Keywords
Low-cost GNSS
PPP
Smartphone

Abstract
In recent years, the proliferation of low-cost Global Navigation Satellite System (GNSS)-enabled smartphones, updates in GNSS systems, and advancements in positioning algorithms have led to increased research into the contributions of smartphones to positioning studies. The aim of this study was to test the positioning performance of single-frequency GPS/GLONASS observations using the Precision Point Positioning (PPP) technique with different products (Final, Rapid, and Real-Time) offered by Wuhan University. To provide a reference for comparison, post-process PPP solutions were obtained using geodetic-grade GNSS receivers and Final products, which have demonstrated centimeter-level accuracy in previous studies. The analysis of the GPS/GLONASS observations using the three different products revealed consistent the Root Mean Square Error (RMSE) values in the centimeter-level when all the observations in the epoch-differenced time series were examined. Moreover, after the convergence of the time series generated from the smartphone data, an improvement ranging from 76% to 98% was observed for the horizontal and vertical components at a level of 0.5 cm and 1 cm, respectively. These results suggest that GNSS-enabled smartphones using PPP techniques with appropriate products can achieve accurate positioning performance.

Introduction

The release of the first Android smartphones in 2008 marked the beginning of a new era in mobile technology, which has rapidly evolved to become ubiquitous in many application areas. The accuracy of smartphone positioning has improved in proportion to the advancements in satellite systems. However, until 2016, raw GNSS observations were not available to users, and only position, velocity, azimuth, and time information could be obtained from smartphones [1]. In 2016, Google announced the availability of raw GNSS data to users with the Android N (Nougat=Version 7) version, which was a significant milestone for positioning studies on smartphones [2].

Until 2018, positioning, navigation, and timing applications on smartphones were based on single-frequency GNSS observations. However, in May 2018, Xiaomi launched the Mi8 model smartphone, which was the first smartphone capable of collecting dual-frequency GNSS raw observation data [3]. This development opened up new possibilities for precise positioning performance evaluation using smartphones with different positioning techniques, such as Real-Time Kinematic and Precise Point Positioning [4-7].

In this study, using different satellite orbit and clock corrections produced by Wuhan University, solutions were produced with PPP technique, both with a smartphone and with a geodetic-grade GNSS receiver. Experiments were carried out to investigate the contribution of products produced by the same analysis center at different time intervals to the literature, to both single-frequency and multi-GNSS observations. In addition, it is aimed to

evaluate the positioning performance in terms of the process by using post-process (Final and Rapid) and near-real-time (Real-Time) products in the experiments.

Material and Method

The solution of the PPP technique using the raw observation data (via Geo++RINEX Logger) collected from the Android smartphone and the satellite orbit and clock correction parameters provided via the internet is shown schematically in Figure 1 [8]. The satellite orbit and clock correction information required in post-process and near real-time solutions based on PPP technique is obtained via the internet by the WHU (Wuhan University) analysis center produced. In the RTKPOS application of RTKLIB software, raw GNSS observation data and necessary products are processed. In the experiment description, data was collected with a Xiaomi Redmi Note 8 smartphone, which can collect single-frequency GPS and GLONASS raw observation data with a sampling interval of 1 Hz. On the other hand, raw observation data was recorded under the same conditions with the geodetic-grade CHC I80 receiver to test the position accuracy of the smartphone. Experiments were carried out in Gebze Technical University, Department of Geomatics Engineering in November 2022 for approximately one and half hour.
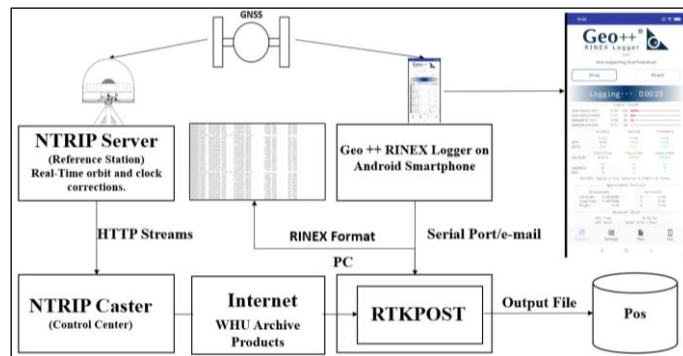
Figure 1. Schematic view of the PPP method with an Android smartphone.

Results and Discussion

In this section, the performance of positioning accuracy on Android smartphones is examined using 3 different products of both GPS and GPS/GLONASS satellite constellations. However, the epoch difference time series obtained using only real-time products and the histogram distributions related to these solutions are shown in Figure 2 and Figure 3. In Figure 2, the epoch differenced time series of the solutions generated from both the geodetic-grade GNSS receiver and the smartphone during the whole experiment are shown. In addition, statistical histograms of the epoch differenced obtained from the smartphone are given by taking the solutions obtained with the geodetic-grade GNSS receiver as reference. In the first row of the figure, the epoch differenced time series of the north, east and up components, respectively, based on only-GPS observations are shown. In the second row of the figure, with reference to the epoch differences obtained from the CHC I80 GNSS receiver, RMSE values and histogram distributions of the three different components of the epoch differenced produced from the Xiaomi 8 smartphone are given. Unlike the first line of the figure, the epoch difference time series of GPS/GLONASS observations is presented in the third line, and the statistical values of the observations obtained from the smartphone are presented in the fourth line. According to the results, due to the integer phase uncertainty due to the nature of the PPP-based solution, the convergence time causes fluctuations as seen in the time series. Despite being a static solution, these fluctuations persisted between approximately 800 (s) and 1000 (s) periods, although different for the three components. The reason for this short duration is that the measurement was made without recording data for about 15-20 minutes before the experiment. Therefore, from the instant that the fluctuations fall below 0.5 cm in the horizontal component and below 1 cm in the vertical component, the epoch differenced time series and statistical histograms are shown as seen in Figure 3. It has been observed that the RMSE values of GPS-only and GPS/GLONASS solutions, for which the post-convergence period difference is taken, have improved compared to the results obtained during the whole experiment. In addition, in Table 1, the position accuracy of the smartphone was evaluated by making both GPS and GPS/GLONASS satellite observations by using Final, Rapid and Real-Time products produced by Wuhan University at certain times. As a reference, the raw GPS/GLONASS observation data obtained from the geodetic-grade GNSS receiver and the solution obtained using the Final products were taken. The results showed that while the position accuracy was below about 10 cm in the solutions obtained throughout the experiment, the position accuracy decreased sub-centimeter after the convergence of the integer phase ambiguity. In this study, for a fair assessment, a single geodetic-grade GNSS receiver was used as a reference to the PPP technique, which has been proven to be at the centimeter level in many studies. However, after convergence, it was observed that the solutions obtained from 3 different products gave consistent and successful results at the millimeter level.
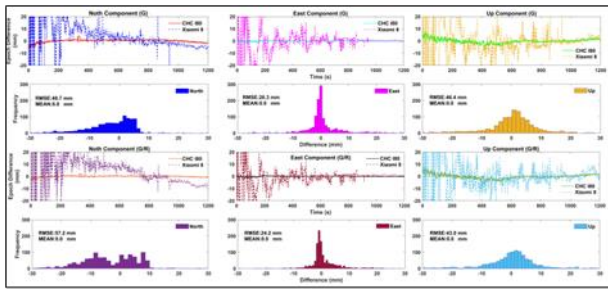
Figure 2. The epoch differenced time series and histogram distributions throughout the experiment
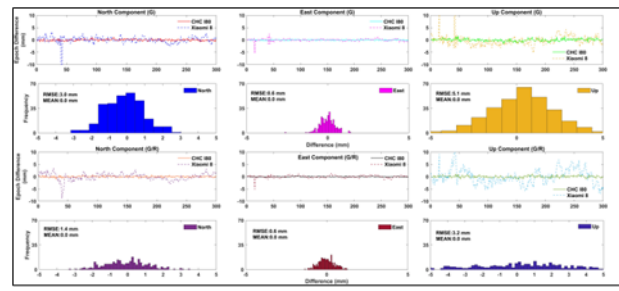
Figure 3. The epoch difference time series and histogram distributions after convergence

Table1. RMSE values of North, East and Up components for Xiaomi 8 smartphone

	GPS			GPS/GLONASS		
	North (mm)	East (mm)	Up (mm)	North (mm)	East (mm)	Up (mm)
Real-Time	49.7	26.3	46.4	57.2	24.2	43.0
Rapid	47.8	28.1	85.4	62.7	22.3	81.9
Final	48.5	29.0	86.4	62.8	22.7	83.6
Real-Time	3.0	0.6	5.1	1.4	0.6	3.2
Rapid	5.8	3.2	20.8	3.8	2.9	14.9
Final	5.6	1.8	11.2	2.9	2.1	9.9

Conclusion

In this research, the positioning performance of the smartphone was evaluated in static mode by using the parameters of the single-frequency PPP-based solution produced by the same analysis center at different times. The results were tested with the raw data collected from the geodetic quality GNSS receiver, whose positioning accuracy has been proven at the centimeter level in many studies, simultaneously with the smartphone and with the PPP-based solution using the final products as a reference. According to the results, it was observed that the RMSE values obtained with the GPS/GLONASS satellite combination after convergence were better than the RMSE values obtained with only-GPS satellite observations. However, in the raw observation data collected according to the smart phone's geodetic GNSS receiver; It is seen that the positioning performance of smartphones is significantly affected due to disadvantages such as the number of satellites due to satellite locking, hardware-related data quality, signal-to-noise ratio and duty cycle. Therefore, in future studies, it is recommended to use smartphones with the developer option that disables the duty cycling feature in Android 9 and higher versions for continuous carrier phase measurement. This will contribute to faster convergence and improve positioning accuracy. In addition, it is considered to investigate the effect of different satellite system combinations in real-time positioning studies on smartphones with dual-frequency data collection feature.

References

1. Aggrey, J., Bisnath, S., Naciri, N., Shinghal, G. & Yang, S. (2019). Multi-GNSS precise point positioning with next-generation smartphone measurements. Journal of Spatial Science, 65, 79–98.
2. Banville, S., & Diggelen, F. (2016). Precise GNSS for everyone: precise positioning using raw GPS measurements from Android smartphones. GPS World, 27(1), 43–48.
3. Chen, B., Gao, C., Liu, Y., & Sun, P. (2019). Real-Time Precise Point Positioning with a Xiaomi MI 8 Android Smartphone. Sensors, 19, 2835.
4. Liu, Q., Gao, C., Peng, Z., Zhang, R., & Shang, R. (2021). Smartphone positioning and accuracy analysis based on real-time regional ionospheric correction model. Sensors, 21(11), 3879.
5. Odolinski, R., & Teunissen, P. (2019). An assessment of smartphone and low-cost multi-GNSS singlefrequency RTK positioning for low, medium and high ionospheric disturbance periods. Journal of Geodesy, 93(5), 701-722.
6. Robustelli, U., Baiocchi, V., & Pugliano, G. (2019). Assessment of dual frequency GNSS observations from a Xiaomi Mi 8 Android smartphone and positioning performance analysis. Electronics, 8(1), 91.
7. Wu, Q., Sun, M., Zhou, C., & Zhang, P. (2019). Precise point positioning using dual-frequency GNSS observations on smartphone. Sensors, 19(9), 2189.
8. Pehlivan, H., Karadeniz, B., & Ari, B. (2022). Near-Real-Time Precise Point Positioning Technique with Single-Frequency Raw GNSS Observations on Android Smartphones. 5th Intercontinental Geoinformation Days (IGD'2022), 14-15 December, New Delhi, India.

Advanced Engineering Days

aed.mersin.edu.tr

Deep learning based poplar tree detection and counting using multispectral UAV images

Ismail Colkesen[*1] , **Taskin Kavzoglu** [1] , **Umut Gunes Sefercik** [1] , **Osman Yavuz Altuntas**[1] , **Mertcan Nazar** [1] , **Muhammed Yusuf Ozturk** [1] , **Mustafacan Saygı** [1]

[1] *Gebze Technical University, Engineering Faculty, Department of Geomatics Engineering, Kocaeli, Türkiye, icolkesen@gtu.edu.tr*

Keywords
Poplar trees
Deep learning
Tree detection
Tree counting
YOLOv7

Abstract
Poplars (Populus sp.), a member of fast-growing and short-lived tree species, have been widely planted since ancient times. Identification and mapping of poplar planted areas on global and local scales, as well as the automatic crown detection and counting of individual poplar trees in a given area provide valuable information to decision-makers in developing strategies for planting area estimation, growth monitoring and yield estimation. At this point, offering significant advantages compared to traditional methods, remote sensing technologies, especially unmanned aerial vehicle (UAV) systems, have become a prominent data source in individual tree crown detection. In this study, one of the latest You Only Look Once (YOLO) algorithms, YOLOv7, was applied to high-resolution multispectral UAV captured images to detect and count individual poplar (P. deltoides) trees. For this purpose, a UAV-derived orthomosaic image covering dense hybrid poplar tree plantations in the Akyazı district of Sakarya province was used as the primary data source. Training and validation datasets were created from the orthomosaic with a total of 260 images and 19.989 instances. Results showed that the YOLOv7 model achieved the precision, recall, mean average precision, and F-score values for the bounding boxes of poplar trees as 86.50%, 86.80%, 87.80%, and 88.20%, respectively.

Introduction

Poplar trees, a leading member of the family of fast-growing trees, are extensively used as raw material (e.g., timber and fibre), especially in the forest industry, and are also of great importance in terms of environmental and agricultural benefits [1]. Therefore, identification and mapping of poplar planted areas on global and local scales, as well as the automatic crown detection and counting of individual poplar trees in a given area provide valuable information to decision-makers in developing strategies for planting area estimation, growth monitoring and yield estimation. At this point, offering significant advantages compared to traditional methods, remote sensing technologies, especially unmanned aerial vehicle (UAV) systems, have become a prominent data source in individual tree crown detection studies in the literature [2-5]. The availability and widespread use of very high-resolution imagery has led to a proliferation of studies around the application of machine learning techniques, including deep learning (DL) models, due to their robustness in information extraction from the imagery [6]. Various DL models have been successfully applied in the literature, reporting the effectiveness in tree crown detection and counting. For example, Yu et al. [7] evaluated the performance of the Mask Region-based Convolutional Neural Networks (Mask R-CNN) model in broad-leaved tree crown extraction from multispectral-UAV imagery. Zhu et al. [8] applied the YOLO (You Only Look Once) v4 algorithm for fruit tree detection from very high spatial resolution UAV imagery, while Yildirim et al. [9] utilized the YOLOv4 to detect stone pine crowns from the RGB-UAV imagery. Gan et al. [3] utilized DeepForest and Detectree2 DL-based algorithms to delineate individual tree crowns from the UAV-captured RGB imagery. In this study, YOLOv7, the relatively new state-of-the-art DL-based object detection model, was applied to detect and count individual poplar trees using multispectral UAV-derived images.

Study area and dataset

The study area covering dense hybrid poplar tree plantation sites is located in Çıldırlar neighbourhood of Akyazı district, Sakarya province, Türkiye (Figure 1). Although agriculture is the main economic activity, poplar cultivation is an essential forestry activity for the region's economy. In order to achieve the ultimate goal of this study, five bands multispectral (MS) (red, green, blue, red edge and near-infrared) images of the study area were taken by DJI Phantom 4 MS UAV on 05 November 2021. The UAV has a RTK GNSS receiver and own positioning capability that means, no need ground control points for absolute orientation of the aerial photos. The spatial resolution of the UAV camera is 2.08 MP however, by means of the short focal length, the ground sampling distance (GSD) reaches half of the 20 MP RGB UAV cams. The aerial photos were collected from 90 m flight altitude with 80% forward and %60 side overlap, resulting in GSD of 4.86 cm. Structure from motion (Sfm)-based image matching software Agisoft Metashape Professional was used for geometric correction, camera reflectance calibration and whole photogrammetric processing. Finally, a 16-bit resolution orthomosaic was produced in original grid spacing.
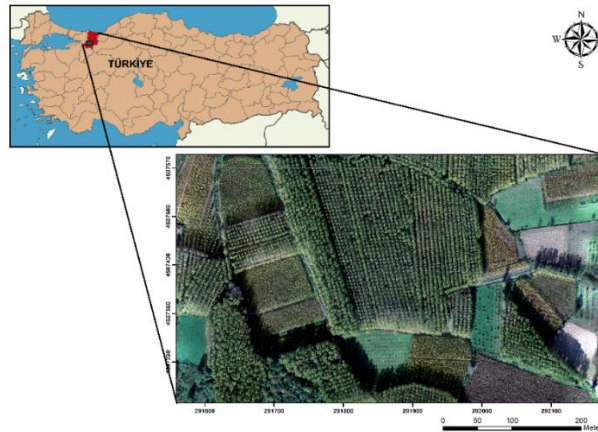
Figure 1. The location of the study area and the UAV ortho-mosaic imagery

Methodology

In this study, individual poplar trees were detected and counted from the multispectral orthomosaic using the YOLOv7 deep learning model. The YOLO model structure usually consists of backbone, neck, and head parts. In YOLO models, image frames are highlighted thanks to the backbone [10]. Another purpose of the backbone part is to extract the basic features of the image. Therefore, the selection of backbone architecture is essential to increase object detection accuracy [11]. The features extracted from the backbone are fused and mixed in the neck part and transmitted to the head of the network. The final estimate was utilized using the non-maximum suppression technique. The technique mainly removes the boxes with low overlap by selecting the most appropriately represented among the duplicate and overlapping suggestion boxes of the objects [12]. Following these steps, YOLO models estimate the probabilities of the location and class membership for each object detected with bounding boxes. Among the real-time object detection models, the recently released YOLOv7 has been introduced as an improved model concerning processing speed and prediction accuracy compared to its previous versions [13]. Unlike its previous versions, YOLOv7 uses enhanced efficient layer aggregation networking (E-ELAN) architecture in the backbone part, based on expand, shuffle, and merge cardinality for continuously increasing the learning ability of the model.

Results

To construct a YOLOv7 model, 50 images of 640x640 and 1280x1280 pixel sizes were selected from the orthomosaic and labelled as poplar polygons in Roboflow. Data augmentation methods (i.e., Gaussian blur, vertical and horizontal cropping, 90 degrees clockwise, and counter-rotation) were also applied to increase the labelled training data size artificially. As a result, 260 images containing 19.989 poplar samples were created, and the dataset was randomly divided into 80% training and 20% validation. PyTorch deep learning framework was used to construct the YOLOv7 model and implemented on a high-capacity workstation with NVIDIA GeForce RTX 3090 graphics card, Intel® Core™ i9-12900K 3.2GHz 24-Core ~3.2GHz processor, and 128GB Ram available at GTU Geomatics Engineering Department's Advanced Remote Sensing Technology Laboratory (ARTLAB). The model parameters to be set by the user side in the training phase were selected as 640x640 image size, 1000 epoch, 4 batch size, 0.01 learning rate, 0.937 momentum, and 0.005 weight decay.

Two loss measures, including the bounding box and objectiveness, were calculated for the YOLOv7 model in the training and validation processes. No overfitting was observed in the constructed model, and loss values showed a decreasing trend during the training stage (Figure 2). Standard accuracy measures, namely precision, recall, mean average precision (mAP), and F-score values, were also calculated for the validation dataset, and the accuracy values for the bounding boxes of poplar trees were found to be 0.8650, 0.8680, 0.8780, and 0.8820, respectively. In order to further evaluate the performance of the model, precision, recall, and F-Score values were also estimated for the two test datasets covering different areas with varying image sizes selected apart from the training and validation dataset. First test image contained 1024x1024 pixels and 115 samples labelled as poplar trees. When the constructed YOLOv7 model was applied to the test image, 111 True Positive (TP), 4 False Positive (FP) and 4 False Negative (FN) trees were predicted. As a result, precision, recall and F-score values for poplar trees were 0.9652, 0.9652 and 0.9652, respectively. The second test image comprised 512x512 pixel sizes and 54 samples labelled as poplar trees. The trained YOLOv7 model correctly predicted 48 test samples as poplar trees (TP), whereas the remaining 6 were miss-detected (FP). For this test dataset, estimated precision, recall and F-score values were 0.8888, 1.0000 and 0.9411, respectively.
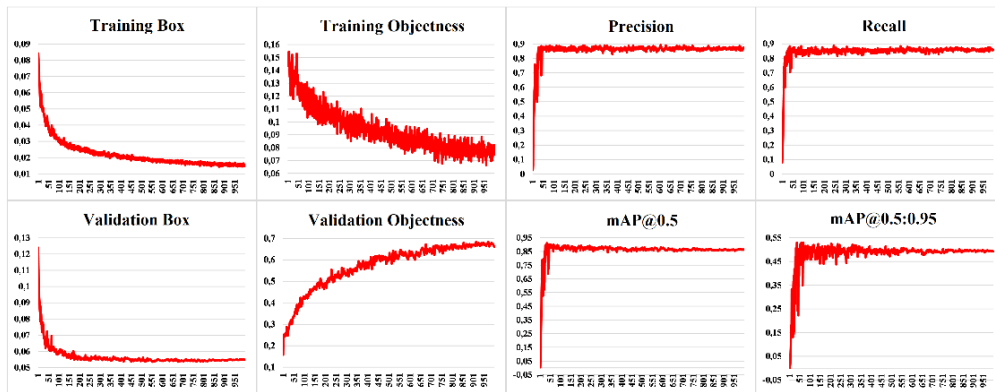
Figure 2. Loss graphs of the trained YOLOv7 model.

To visually analyze the performances of the trained YOLOv7 model, the resulting predictions representing bounding boxes for detected poplar trees for the first test image were shown in Figure 3 where the red boxes represent the accurately detected poplar trees, whereas the blue and purple boxes indicate FP and FN predictions, respectively. If the bounding boxes predicted by the model overlapped more than 50% with ground truth, the detected bounding boxes were marked as TP, otherwise as FP. On the other hand, other land cover types or trees miss-detected as poplar by the model were labelled as FN. As can be seen from the figure, poplar trees that are very close to each other were labelled as false positives, while some other broadleaf trees in the area were detected as false negatives. Finally, 119 objects were detected in the first test image, 111 of which were correctly labelled as poplar trees.
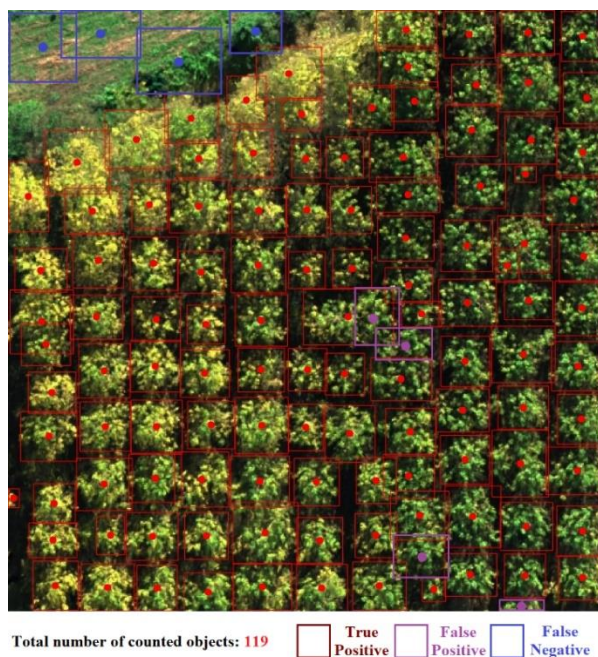
Figure 3. The results of poplar detection and counting on the UAV image

Conclusion

The main goal of this study is to automatically detect and count individual poplar trees from the UAV-derived multispectral imagery using the state-of-art YOLOv7 deep learning-based object detection model. The qualitative and quantitative evaluations based on accuracy measures and visual interpretation showed that the YOLOv7 model with mAP of about 88% showed robust performance in detecting individual poplar trees from the UAV-derived imagery. Accuracy results calculated for the two test images indicated that the YOLOv7 model correctly detected the individual poplar trees over the %94 in terms of the F-score measure. While the results verified the usefulness and effectiveness of the DL-based model in automatic individual tree detection and counting problems, comparative studies are required to assess the performances of different DL models on poplar tree detection and segmentation of tree crowns using very high-resolution remotely sensed imagery.

References

1. Isebrands, J. G. & Richardson, J. (2014). Poplars and Willows: Trees for Society and the Environment CAB International and Food and Agriculture Organization of the United Nations (FAO), CABI, p. 634.
2. Ke, Y., & Quackenbush, L. J. (2011). A review of methods for automatic individual tree-crown detection and delineation from passive remote sensing. International Journal of Remote Sensing, 32(17), 4725-4747.
3. Gan, Y., Wang, Q., & Iio, A. (2023). Tree Crown Detection and Delineation in a Temperate Deciduous Forest from UAV RGB Imagery Using Deep Learning Approaches: Effects of Spatial Resolution and Species Characteristics. Remote Sensing, 15(3), 778.
4. Ateşoğlu, A., Kavzoğlu, T., Çölkesen, İ., Özlüsoylu, Ş., Tonbul, H., Yılmaz, E. Ö. & Öztürk, M. Y. (2022). Türkiye'de Hızlı Büyüyen Türlere Ait Spektral Kütüphane Kurulması: Kavak Türleri Çalışması. Bartın Orman Fakültesi Dergisi, 24 (2), 324-338.
5. Colkesen, I., Kavzoglu, T., Atesoglu, A., Tonbul, H., & Ozturk, M. Y. (2022). Multi-seasonal evaluation of hybrid poplar (P. Deltoides) plantations using Worldview-3 imagery and state-of-the-art ensemble learning algorithms. Advances in Space Research. https://doi.org/10.1016/j.asr.2022.10.044
6. Diez, Y., Kentsch, S., Fukuda, M., Caceres, M. L. L., Moritake, K., & Cabezas, M. (2021). Deep learning in forestry using UAV-acquired RGB data: A practical review. Remote Sensing, 13(14), 2837.
7. Yu, K., Hao, Z., Post, C. J., Mikhailova, E. A., Lin, L., Zhao, G., ... & Liu, J. (2022). Comparison of classical methods and mask R-CNN for automatic tree detection and mapping using UAV imagery. Remote Sensing, 14(2), 295.
8. Zhu, Y., Zhou, J., Yang, Y., Liu, L., Liu, F., & Kong, W. (2022). Rapid Target Detection of Fruit Trees Using UAV Imaging and Improved Light YOLOv4 Algorithm. Remote Sensing, 14(17), 4324.
9. Yildirim, E., Nazar, M., Sefercik, U. G., & Kavzoglu, T. (2022). Stone Pine (Pinus Pinea L.) Detection from High-Resolution UAV Imagery Using Deep Learning Model. In IGARSS 2022-2022 IEEE International Geoscience and Remote Sensing Symposium (pp. 441-444). IEEE.
10. Vimal, S., & Subbulakshmi, P. (2016). Secure data packet transmission in MANET using 18 enhanced identity-based cryptography. International Journal of New Technologies in Science and Engineering, 3(12), 35-42.
11. Chen, Y., Yang, T., Zhang, X., Meng, G., Xiao, X., & Sun, J. (2019). Detnas: Backbone search for object detection. Advances in Neural Information Processing Systems, 32.
12. Rothe, R., Guillaumin, M., & Van Gool, L. (2015). Non-maximum suppression for object detection by passing messages between windows. In Computer Vision–ACCV 2014: 12th Asian Conference on Computer Vision, Singapore, Singapore, November 1-5, 2014, Revised Selected Papers, Part I 12 (pp. 290-306). Springer International Publishing.
13. Chen, J., Liu, H., Zhang, Y., Zhang, D., Ouyang, H., & Chen, X. (2022). A Multiscale Lightweight and Efficient Model Based on YOLOv7: Applied to Citrus Orchard. Plants, 11(23), 3260.

Advanced Engineering Days

aed.mersin.edu.tr

Analyzing of court decisions cancelling land readjustments due to implementation boundary

Hüseyin Pehlivan*1 , Seyfullah Aybal 2

¹Gebze Technical University, Department of Geomatics Engineering, Turkey, hpehlivan@gtu.edu.tr
²Gebze Technical University, Department of Geomatics Engineering, Turkey, s.aybal2020@gtu.edu.tr

Keywords

Zoning Application
Aplication of Article 18
DOP rate
Land Readjustment
Development
Readjustment Share (DRS)
Implementation Boundary

Abstract

Many land readjustment projects are subject to cancellation by courts due to parcel boundaries within the scope of application or non-compliance with relevant laws, regulations, and guidelines. Such cancellation decisions can cause significant hardship to parcel owners and impose both time and financial burdens. The objective of this study is to examine court decisions related to urban development projects with the aim of preventing potential cancellations in the future. In this context, a sample urban development project was analyzed, application limits were established based on relevant court decisions, and the land readjustment process was reconsidered. The examination revealed that the land readjustment did not impact social amenities areas and protected the rights of property owners. Consequently, it was concluded that court decisions canceling land readjustment projects, when not altering the outcome from legal and technical perspectives, can introduce additional time and cost burdens.

Introduction

In all cities around the world where people reside, two crucial aspects, land planning, and land regulation, play a critical role in improving living standards and achieving balanced development. In this regard, it is important that urban plans are created, taking into account the economic, social, cultural, and other unique circumstances of cities, as well as their physical topography and spatial characteristics [1]. In the plans prepared in accordance with these criteria as a vision for the future, it is most ideal approach to apply them to the land, taking into account the state of ownership and the spatial conditions of use.

However, while land regulation practices or land readjustments (LR) have achieved a certain standard in developed countries, they have not yet reached desired levels of standards in many parts of the world [2]. Consequently, numerous studies have been conducted and continue to be carried out globally concerning the successful and unsuccessful outcomes of LR methods. For example, Suza et al. (2018) extensively researched the land readjustment approach in urban development. They examined how land readjustment experiences in Japan and other countries have been applied and improved in developing nations [3]. Soliman (2017) explored land readjustment programs as a tool to reduce the adverse effects of random urban development in Egypt [4]. Based on a case study, he sought ways to conduct land readjustments optimally by considering human needs, demands, obligations, and government policies. Turk and Turk (2011) examined the serious consequences of legal or technical errors in LR applications involving a specific procedural process. They investigated why LR projects implemented in Turkey were canceled by administrative courts and their repercussions [5].

In Turkey, the primary objective in implementing urban plans is to create urban parcels that adhere to minimum building standards while simultaneously unveiling social and public spaces in line with design principles. This ensures that essential elements such as roads, parks, municipal service areas, recreational spaces,

educational facilities, social and cultural areas, and more, which are needed by urban residents, become public property. However, despite a rich history and knowledge regarding property and land-use models, land readjustment (LR) activities are not always implemented successfully [2]. Until today, many urban planning applications have been halted by court decisions, resulting in both suspensions of executive actions and cancellations. This has not only increased the workload for both the administration and relevant courts but also caused financial and temporal distress for property owners. Consequently, the transfer of public spaces to the public in urban plans is becoming increasingly challenging and slow.

The main reasons for the annulment decisions regarding land and urban regulation by the Council of State and administrative courts are twofold. To subject an LR process to a cancellation lawsuit, there must either be a violation of a legal rule or a technically incorrect procedure [6]. In a study examining lawsuits against LR practices, it was observed that when decisions made by local courts were reviewed by the higher court, the Council of State, in terms of authority, form, cause, subject, and purpose 44% of them were canceled. For this reason, it has been emphasized that local courts should specialize in their field and, otherwise, the process may take longer and lead to irreparable consequences [7].

Within the scope of this study, a case study based in the Pendik district of Istanbul Province, Turkey, has been examined. Specifically, this study focuses on a LR application (application of Article 18 of Law No. 3194 on Zoning and Urban Planning) that was canceled due to a technical deficiency. The examination has been conducted by reviewing the Land and Zoning Regulation, relevant Cadastral Directives, previous research on similar topics, and relevant publications. Additionally, solutions have been sought.

Material and Method

Under the implementation of Article 18 of Construction Law Numbered 3194, cadastral parcels within the Istanbul Province Pendik District, specifically in the Kaynarca 4th Region Zoning Application area, have been incorporated into the zoning arrangement for this section. Figure 1 illustrates the registered subdivision plan of the area that has been included into the LR application. As a result of the application of Article 18 to the 67 cadastral parcels that are now included in the regulation process a total of 41 zoning parcels have been created, excluding those not required for registration.
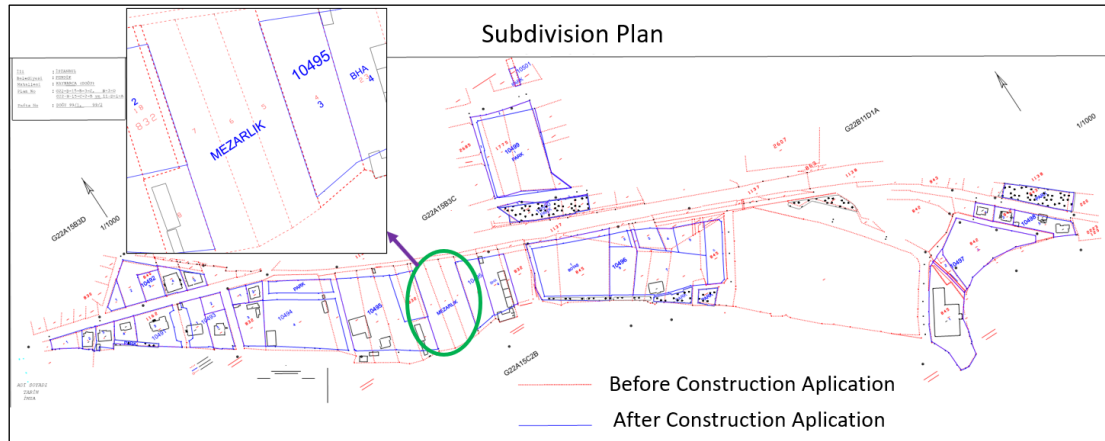
Figure 1. Aplication of article 18 implemented Subdivision Plan.

Furthermore, there are three parcels, not included within the LR boundaries for various reasons, as depicted in Figure 1. There are four zones where the LR application boundaries have been exceeded. As a result of this LR application, twelve lawsuits has been initiated. Due to the failure to define parcels within the LR boundaries and in accordance with the relevant laws, regulations, and directives, as well as within the limits of the zoning regulation, the zoning applications were canceled based on the argument that they did not meet the area's needs.

In this context, the cancellation of a registered land and zoning regulation often leads to irreversible consequences or unworkable situations, marking the beginning of a series of subsequent issues. These issues include property owners being unable to apply for construction permit, parcels remaining within the reserved area unable to utilize their zoning rights within the building block, resulting in the distress of property owners within social amenity areas. As a consequence, legal actions such as expropriation without compensation cases have been filed against municipalities. In light of the provisions related to the zoning boundaries in the court decision concerning the examined LR application, a new zoning boundary was established, including all parcels not previously included. Subsequently, the LR application was re-implemented. Following this re-implemented LR application, it was observed that there was no change in the legal or technical nature of the parcels subject to cancellation decisions, as per the court rulings.

Results and Discussion

In this study, it was emphasized that in administrative cases filed for the application of article 18 of the Construction Law Numbered 3194, experts and courts should not look only at the formal appearance and characteristics of the regulatory boundary of the zoning application subject to the lawsuit when making their final decisions. In addition, it has been shown that it is necessary to investigate the cadastral histories of parcels that are not included in the zoning application and cause the regulation boundary to be disconnected.

In the case of re-implemented LR applications, it has been observed that the additional parcels introduced into the plan have no impact on any calculations, outcomes, or steps in the process, such as the DOP ratio or allocated area. In other words, the sole alteration involves a formal adjustment of the zoning boundary and the inclusion of new parcels. This results in changes only to the plot and parcel numbers for the owners of the newly added parcels, while the actual land areas remain unchanged. Consequently, this situation imposes unnecessary administrative burdens on public authorities and, furthermore, may lead to the loss of zoning rights for parcel owners who did not initiate legal action because of cancellation decisions.

As a solution to all these situations, It can be considered that an advisory board should be formed, which consists of people who are experts in their field and who know the technical and legal legislation well, where jurisprudence can be taken, except for courts, and which will make decisions according to these jurisprudence in the courts. Otherwise, our colleagues are left alone with the problems and if there is no precedent decision of the Council of State taken in this direction, they are left alone with the situation of experiencing by living. In this respect, as a solution, it can be considered that the experts have a good command of the legislation technically and legally, and that a commission consisting of experts of this nature can take case law in the decision-making process of the courts. Thus, even if there is no precedent decision regarding the problems faced by the Administration, this commission will be consulted, and the right and healthy decision will be made.

Conclusion

In this study, it has been emphasized that the importance of administrative court cases filed regarding the implementation of Article 18 of Law No. 3194 on Zoning and Urban Planning should not solely focus on the form and nature of the zoning boundary. Through the investigation of the cadastral backgrounds of parcels that are not included in the urban planning and contribute to the disconnection of the zoning boundary, it has been observed that technical and legal aspects can be identified. This process has revealed valid reasons for non-inclusion and has shown that including such parcels would not affect the procedure. Consequently, court decisions concerning the subject of the case have favored the defendant administration.

This study aims to contribute to preventing future cancellations by examining an LR case example. However, further research is needed to explore the impact of canceled LR applications on construction applications and their effects on parcel owners. This will help prevent cancellations that can lead to irreparable errors and avoid time and financial losses.

References

1. Meşhur, M. Ç. (2008). Arazive arsa düzenlemesi (18. madde uygulamasi) süreciṅin kentsel mekân oluşumu açisindan irdelenmeṡi. Metu Journal of the Faculty of Architecture, 25(2).
2. Turk, S. S. (2007). An analysis on the efficient applicability of the land readjustment (LR) method in Turkey. Habitat International, 31(1). https://doi.org/10.1016/j.habitatint.2006.04.001
3. Souza, F. F., Ochi, Takeo., & Hosono, A. (2018). Land Readjustment: Solving Urban Problems Through Innovative Approach. In Japan International Cooperation Agency Research Institute (Issue March).
4. Soliman, A. M. (2017). Land readjustment as a mechanism for New Urban Land Expansion in Egypt: experimenting participatory inclusive processes. International Journal of Urban Sustainable Development, 9(3). https://doi.org/10.1080/19463138.2017.1382497
5. Turk, S. S., & Turk, C. (2011). The annulment of land readjustment projects: An analysis for Turkey. Town Planning Review, 82(6). https://doi.org/10.3828/tpr.2011.39
6. Karaca, A. G. E. (2018). İmar Planı Uygulama Yöntemlerinden Arazi ve Arsa Düzenlemesinin İlgili Mevzuat Çerçevesinde İncelenmesi. Uyuşmazlık Mahkemesi Dergisi, 11., 217-261. https://doi.org/10.18771/mdergi.435754
7. Pamuk, H. (2016). The Reasons for Cancellation of Land Readjustment in Turkey. Master Thesis, Yıldız Technical University.

Improving GNSS data accuracy using DBSCAN, moving averages, and Hampel identifier

Hüseyin Pehlivan*

Gebze Technical University, Department of Geomatics Engineering, Türkiye, hpehlivan@gtu.edu.tr

Keywords
GNSS data
Filtering
Hampel
Moving average
DBSCAN

Abstract

There is a common issue in GNSS (Global Navigation Satellite System) data, which is the presence of outliers that can affect the accuracy of positional measurements. In this study, three methods for outlier detection and removal in GNSS data were compared: Hampel filter, moving average, and DBSCAN (Density-Based Spatial Clustering of Applications with Noise) algorithm. Both synthetic and real GNSS datasets were used to test these methods. The Hampel filter and moving average were first applied to clean the data, and then the DBSCAN algorithm was used to detect outliers. The results were evaluated using the RMS error criterion. The study found that DBSCAN was effective with appropriate parameter settings, but the combination of Hampel filter and moving average was the most successful method. The Hampel filter was particularly efficient in filtering outliers in low-quality GNSS data. These findings suggest that the combination of multiple methods can result in more accurate and reliable outlier detection and removal in GNSS data.

Introduction

In Outliers in GNSS (Global Navigation Satellite System) data can cause problems in data analysis and processing, especially in situations where measurement capabilities are limited. While accurately identifying outliers from time series is important in general, it is also widely used in data mining, machine learning, and many other applications. Many methods have been proposed for outlier detection, but methods such as the Hampel filter, moving average, and DBSCAN (Density-Based Spatial Clustering of Applications with Noise) algorithm are popularly used.

There are many studies that have utilized Hampel filter, moving average, and DBSCAN algorithms for outlier detection and cleaning in GNSS data. For example, Yang and Rizos [1] proposed the use of Hampel filter and Grubbs test for outlier detection in GNSS data to improve accuracy. Rana and Tiwari [2] suggested the use of moving average and double difference technique to detect and remove biases in GNSS data. Hou and Chen [3] showed that DBSCAN algorithm was an effective method for outlier detection and cleaning in GNSS data. However, each of these studies employed different approaches for identifying and removing outliers in GNSS data. In particular, Hampel filter has been used for many years as a statistical method for detecting and removing outliers [4], while moving average is a commonly used method for signal smoothing [5]. DBSCAN algorithm is a density-based clustering method that can also be used to identify outliers [6].

Additionally, Tang et al. [7] and Zhu et al. [8] are among the many studies that have utilized these methods for outlier detection and cleaning in GNSS data. In this study, we propose that the combination of Hampel filter and moving average may be more effective for outlier detection, and we also investigate the effectiveness of DBSCAN algorithm for this purpose. Our goal is to create an overall algorithm for outlier detection using the Hampel filter, moving average, and DBSCAN methods. The cleaned data with Hampel filter and moving average were then used for outlier detection with the DBSCAN method, and the obtained results were compared using the RMS error criterion. The effectiveness of the results and the advantages of combining these methods for outlier detection compared to other methods were also evaluated.

Material and Method

The main research question of this study is to investigate the effectiveness of the combination of Hampel filter, moving average, and DBSCAN algorithm in detecting and removing outliers in GNSS data. The hypothesis is that the combined approach will result in more accurate and reliable data compared to using any of the methods individually. The study is designed in three stages to test this hypothesis.
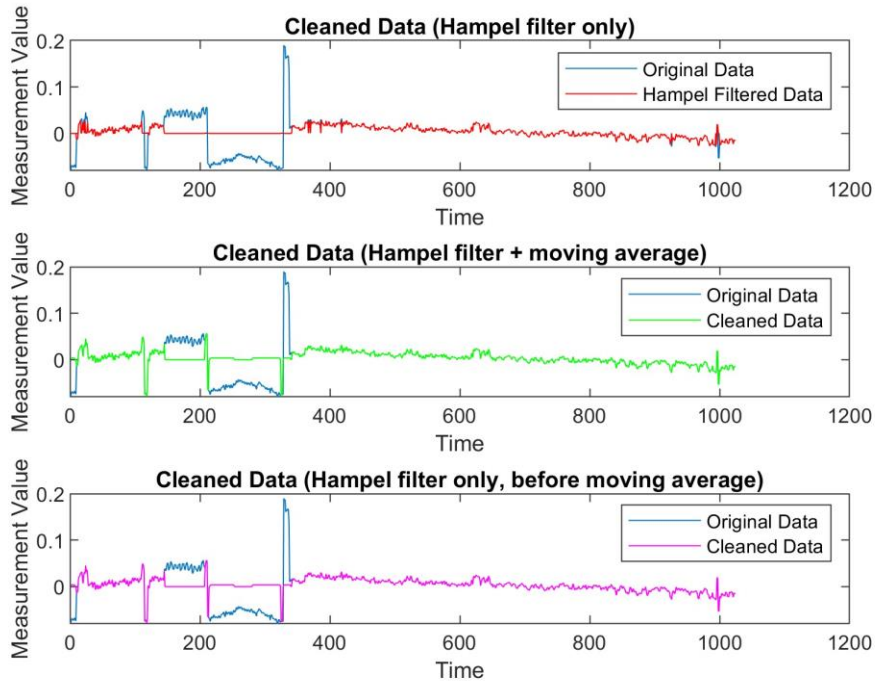
Figure 1. Detection of outliers using Hampel filter and moving average algorithms
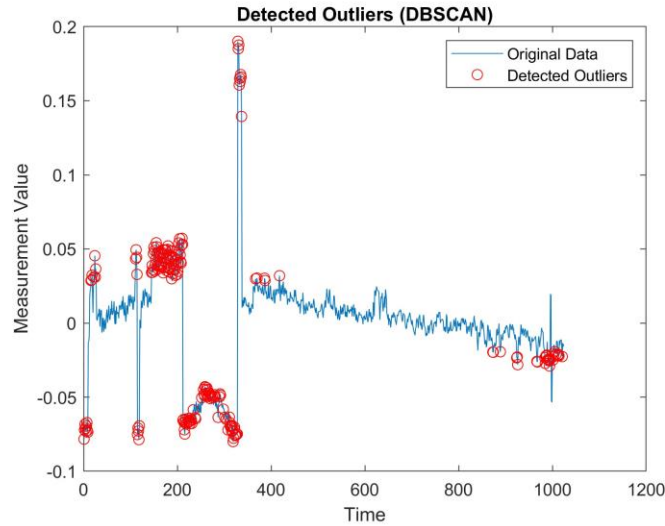
Figure 2. Detection of outliers using the DBSCAN algorithm.

In the first stage, Hampel filter and moving average methods were applied to the dataset to remove initial outliers (Figure 1). In the second stage, DBSCAN algorithm was used to detect remaining outliers in the data (Figure 2). In the final stage, statistical analysis was conducted on the results to evaluate the effectiveness of DBSCAN, Hampel filter, and moving average methods in outlier detection after their application to the data. Root Mean Square (RMS) error criterion was used to compare the filtered data with the original data in order to evaluate the effectiveness of DBSCAN algorithm, Hampel filter, and moving average methods (Table 1).

Table 1. RMS Errors

Simulated data	Real GNSS data
RMS error for Hampel only: 1.1744	RMS error for Hampel only: 0.029785
RMS error for Hampel + moving average: 1.0057	RMS error for Hampel + moving average: 0.028788
RMS error for DBSCAN non-outlier: 0	RMS error for DBSCAN non-outlier: 0
RMS error for DBSCAN outlier: 1.5875	RMS error for DBSCAN outlier: 0.061354

Results and Discussion

Method: Outliers were detected in low-quality GNSS data and synthetic datasets of the same size using Hampel filter, moving average, and DBSCAN algorithms. For Hampel filter, the num_sigma and window_size parameters were optimized. For moving average, the num_mov parameter was optimized. For DBSCAN algorithm, the epsilon and minPts parameters were optimized.

Simulated Data: The given results are the outcome of operations on a simulated signal. The RMS error obtained when using only the Hampel filter is 1.1744. The RMS error obtained when using both the Hampel filter and moving average is 1.0057. These results show that using both the Hampel filter and moving average results in a lower RMS error. The RMS error obtained using DBSCAN algorithm is 1.5875 for outlier data and 0 for non-outlier data. These results indicate that the DBSCAN algorithm performs well in detecting outlier data, but may fail to determine accurate non-outlier data. Overall, the results indicate that using the Hampel filter and moving average together yields better results, while the DBSCAN algorithm performs well in detecting outlier data, but may not provide accurate results for non-outlier data.

Real GNSS Data: Assuming the data is real GNSS data, outlier detection performed using both the Hampel filter and moving average has yielded better results compared to the DBSCAN algorithm. Outlier detection using both the Hampel filter and moving average has lower error rates compared to the DBSCAN algorithm. However, the DBSCAN algorithm has provided accurate results for all outlier data. These results indicate that using multiple methods for outlier detection may be better than using a single method to obtain accurate results.

Conclusion

This study compared DBSCAN, Hampel filter, and moving average methods for outlier detection in GNSS data. The results showed that the combination of Hampel filter and moving average was the most successful approach, while DBSCAN algorithm was less effective than the combined method. The combined method also required less computation than DBSCAN. Therefore, the Hampel filter and moving average combination was found to be the most effective approach for outlier detection, especially for large datasets. To improve the performance of DBSCAN algorithm, different distance metrics and parameter adjustments could be considered. Hampel filter could be combined with other statistical methods or used as a preprocessing step for other outlier detection methods. Moving average method could be applied with different window sizes or to more predictable datasets. In general, combining multiple outlier detection methods can provide more accurate and robust results than using a single method. Further research is needed to develop and evaluate more advanced and effective outlier detection methods for GNSS data.

References

1. Yang, K., & Rizos, C. (2007). GNSS data quality control using Hampel filter and Grubbs test. Journal of Global Positioning Systems, 6(1-2), 23-30.
2. Rana, S., & Tiwari, R. K. (2018). Identification of GNSS multipath outliers using moving average and double difference technique. Journal of Applied Geodesy, 12(2), 85-94.
3. Hou, M., Li, Y., & Chen, Z. (2018). Outlier detection in GPS surveying data using DBSCAN algorithm. International Journal of Geomechanics, 18(7), 04018043.
4. Hampel, F. R. (1974). The influence curve and its role in robust estimation. Journal of the American Statistical Association, 69, 383-393.
5. Chatfield, C. (2019). The Analysis of Time Series: An Introduction. CRC Press.
6. Ester, M., Kriegel, H. P., Sander, J., & Xu, X. (1996). A density-based algorithm for discovering clusters in large spatial databases with noise. In Proceedings of the 2nd International Conference on Knowledge Discovery and Data Mining (pp. 226-231).
7. Tang, W., Zhang, X., Dai, W., & Tang, L. (2019). A New Method for Outlier Detection in GPS Precise Point Positioning. IEEE Access, 7, 105404-105414. https://doi.org/10.1109/ACCESS.2019.2936687
8. Zhu, X., Wang, L., & Li, Y. (2017). A study on detecting outliers in GPS time series. Measurement, 110, 190-198. https://doi.org/10.1016/j.measurement.2017.05.018

Explainable artificial intelligence empowered landslide susceptibility mapping using Extreme Gradient Boosting (XGBoost)

Alihan Teke[*1] , **Taskin Kavzoglu** [1]

[1]*Gebze Technical University, Department of Geomatics Engineering, Türkiye, a.teke2020@gtu.edu.tr, kavzoglu@gtu.edu.tr*

Keywords
Landslide susceptibility
XAI
SHAP
XGBoost
Sapanca

Abstract
Up to now, a wide variety of non-linear machine learning models with black-box nature have been intensively utilized to spatially predict landslide susceptibility in a given geographical context. However, the results obtained from these models can be difficult to interpret, making it challenging to identify the reasons for false positives and take corrective action. To address this problem, this study makes use of the XGBoost algorithm to predict landslide susceptibility in a lake basin and its surrounding areas. Additionally, the Shapley additive explanation (SHAP) approach as an explainable artificial intelligence (XAI) tool was used to increase the interpretability of the model's predictions. The accuracy of the XGBoost model was evaluated and found to have an OA of 92.44% and an AUC score of 98.73%. The SHAP analysis showed that slope was the most influential factor in predicting landslide susceptibility. Additionally, the dependence plot highlighted that the impact of slope angle on the model's output was consistent within the range of 8° to 21°. The findings of this study demonstrate the potential benefits of incorporating XAI techniques into the modeling process to increase transparency.

Introduction

Until the last decade, landslide susceptibility mapping was often carried out using traditional methods such as manual inspection, expert judgment, and statistical analysis, which are often subjective and time-consuming, and can lead to inconsistent results. However, with the advent of artificial intelligence and machine learning, predictive models can now be used to generate landslide susceptibility maps with improved accuracy and efficiency. Nonetheless, most operate in a "black box" manner, meaning that the reasoning behind their predictions is not transparent nor easily interpretable [1]. This lack of transparency poses significant concerns regarding the potential biases and errors that may be introduced during the modeling process, ultimately impacting the accuracy and validity of the results. For instance, if a predictive model used to generate a landslide susceptibility map results in a false positive, it could lead to the evacuation of residents or the halt of development activities in a certain area. Thus, it is crucial to develop transparent and interpretable models for landslide susceptibility mapping practices, such as explainable artificial intelligence (XAI) [2]. These models can provide an explanation for their predictions, making it easier to understand how they arrived at their conclusions and to identify any potential biases or flaws in the data or algorithms used.

Taking Lake Sapanca Basin and its surrounding as an example, this study aims to create a landslide susceptibility map that maintains its accuracy while incorporating XAI tools such as Shapley Additive Explanations (SHAP). This will be achieved by utilizing a gradient-based machine learning algorithm called XGBoost, which is considered a black-box model. A total of 14 landslide-related parameters were selected by taking into consideration of the overall characteristics of the study area.

Material and Method

The region of Lake Sapanca Basin and its surroundings, located in the Catalca-Kocaeli region of the eastern Marmara area of Turkey, is experiencing rapid urbanization and industrialization. The area of interest is located between longitudes 29° 59′ and 30° 23′ to the east, and latitudes 40° 36′ and 40° 53′ to the north, covering an approximate area of 945 km². Topographically, the north-facing section of the Samanli Mountains, which extend in the east-west direction and are situated in the south of the basin, comprises steep slopes, indicating the presence of relatively unstable landscape structures. The study employed a geospatial dataset consisting of 14 parameters related to landslides, including aspect, convergence index (CI), elevation, lithology, plan curvature, profile curvature, distance to rivers, road density, distance to roads, slope, soil type, topographic position index (TPI), topographic wetness index (TWI), and valley depth.

Extreme Gradient Boosting (XGBoost)

XGBoost is a highly optimized and distributed gradient-boosting algorithm designed to efficiently and effectively implement gradient-boosting models [3]. It uses an ensemble of decision trees, where each tree predicts the residual errors of the previous tree to arrive at the final prediction. Its flexible API allows users to customize and fine-tune the algorithm and perform complex operations, and it supports parallel processing, making it well-suited for large datasets and distributed computing environments. However, it is generally considered a black-box algorithm because its internal workings are difficult to interpret. Since XGBoost relies on the combination of many decision trees, it is challenging to determine how each feature contributes to the final prediction, making it hard to understand how the algorithm arrived at a specific prediction.

Shapley Additive Explanation (SHAP)

Shapley Additive Explanation (SHAP) is an approach to interpret the output of machine learning models developed by Lundberg and Lee [4]. It works by attributing the impact of each feature on a prediction, individually and not as a group [5]. The SHAP values give a comprehensive explanation of a model's predictions, taking into account the contribution of each feature and the interaction between features. This leads to a better understanding of how a model makes predictions. The SHAP values have a probabilistic interpretation, as they sum up to the difference between the expected and actual output for a given instance. This interpretation helps to compare the contribution of different features to a prediction and to evaluate the uncertainty in the explanation.

Results and Discussion

The XGBoost algorithm was used to generate landslide susceptibility maps for a region located in the Lake Sapanca Basin, utilizing 14 landslide-related parameters. The accuracy of the resulting map was assessed using four metrics: overall accuracy (OA), true positive rate (TPR), true negative rate (TNR), and area under curve (AUC) score. The XGBoost model produced a landslide susceptibility map with an OA of 92.44% and an AUC score of 98.73%, indicating a high level of accuracy. The XGBoost algorithm achieved TPR and TNR scores of 96.85% and 88.03%, respectively, demonstrating its strong intraclass separability power. The produced landslide susceptibility map highlighted that the high-risk areas were predominantly located in the northwestern parts of the basin and the northern slopes of the Samanli Mountains, while the areas with very low to low risks were mostly found in the interior of the area.
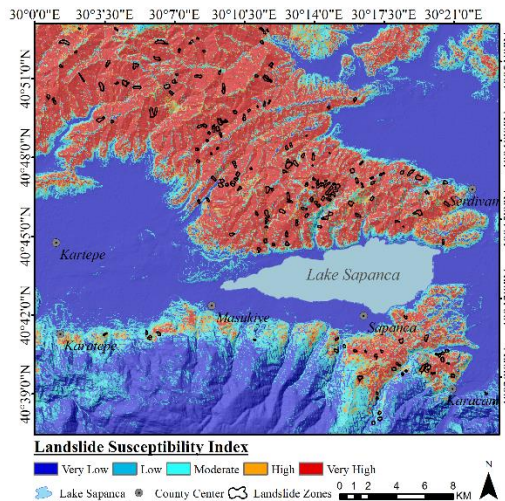
Figure 1. Landslide susceptibility map produced with XGBoost algorithm

With the application of the SHAP analysis, two different explanation results were obtained: summary plot and dependence plot. The former explains the overall impact of each feature on the model's output, while the latter shows how a single feature affects the predictions made by the model. Specifically, the dependence plot displays the relationship between a selected feature and the SHAP values for that feature across the entire dataset, allowing us to understand how changes in that feature's value impact the model's predictions. The summary plot revealed that the slope had the strongest impact on the model's output, followed by elevation and lithology, respectively. In contrast, TWI and CI had the lowest contribution to the XGBoost model's prediction. On the other hand, the dependence plot highlighted that the effect of slope angle on the model's output is consistent across the range between 8° and 21°, but not across its entire range of values.

(a)   (b)
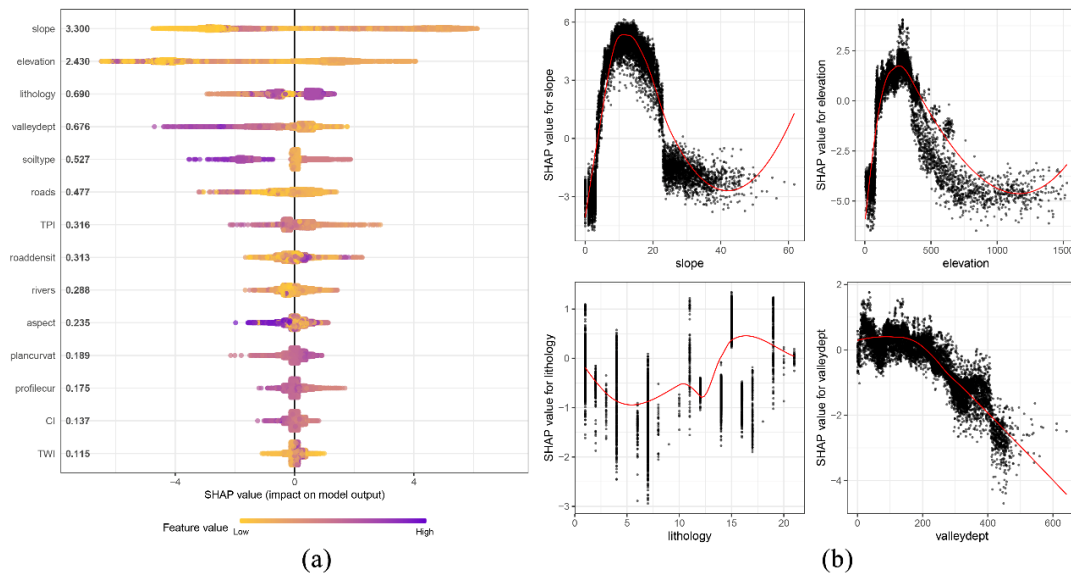
Figure 2. (a) SHAP summary plot for whole geospatial covariates and (b) dependence plots for slope, elevation, lithology, and valley depth

Conclusions

Using Lake Sapanca Basin and its surrounding regions as a case study, this study seeks to establish a landslide susceptibility map that employs an XAI tool while maintaining high levels of accuracy. To summarize, the principal conclusions of this work can be encapsulated as follows:

- The XGBoost algorithm successfully generated accurate landslide susceptibility maps for the Lake Sapanca Basin region, achieving an OA of 92.44% and an AUC score of 98.73%.
- The SHAP analysis allowed for a better understanding of the XGBoost model's output by providing two different explanation results: the summary plot and the dependence plot. The summary plot revealed that slope, elevation, and lithology were the most influential factors in predicting landslide susceptibility, while TWI and CI had the least contribution to the model's output.
- The produced landslide susceptibility map indicated that high-risk areas were predominantly located in the northwestern parts of the basin and the northern slopes of the Samanli Mountains, while very low to low-risk areas were mostly found in the interior of the area and the western parts of Lake Sapanca.

References

1. Kavzoglu, T. (2009). Increasing the accuracy of neural network classification using refined training data. *Environmental Modelling & Software*, 24(7), 850–858. doi: https://doi.org/10.1016/j.envsoft.2008.11.012
2. Kavzoglu, T., & Teke, A. (2022). Advanced hyperparameter optimization for improved spatial prediction of shallow landslides using extreme gradient boosting (XGBoost). *Bulletin of Engineering Geology and the Environment, 81(5), 201*. https://doi.org/10.1007/s10064-022-02708-w
3. Chen, T., & Guestrin, C. (2016). XGBoost: A Scalable Tree Boosting System. In Proceedings of *22nd ACM SIGKDD International Conference on Knowledge Discovery and Data Mining*, San Francisco, CA, USA, 13–17 August, 785–794.
4. Lundberg, S. M., & Lee, S. I. (2017). A unified approach to interpreting model predictions. *Advances in Neural Information Processing Systems*, Long Beach, CA, USA, 4–9 December, 4766–4775.
5. Kavzoglu, T., & Teke, A. (2022). Predictive Performances of Ensemble Machine Learning Algorithms in Landslide Susceptibility Mapping Using Random Forest, Extreme Gradient Boosting (XGBoost) and Natural Gradient Boosting (NGBoost). *Arabian Journal for Science and Engineering*, 47, 7367–7385. https://doi.org/10.1007/s13369-022-06560-8

Advanced Engineering Days

aed.mersin.edu.tr

GIS-based real estate legislation information system design: The case of İzmir, Foça

Mert Kayalık*1 , **Zeynel Abidin Polat** 1

1*İzmir Katip Çelebi University, Geomatics Engineering, Turkey, mert.kayalik@ikcu.edu.tr; zeynelabidin.polat@ikcu.edu.tr*

Keywords
Real estate
Legislation
Multi-criteria
GIS
Ownership

Abstract
Due to the rapidly increasing world population, the management of limited and non-renewable land is an inevitable reality for the whole world. While planning the land management, the management of the real estates (e.g. building, parcel) is another topic that needs to be planned. While the real estates are used by the citizens for purposes such as agricultural production, accommodation and lease, they have been the subject of tax due to the economic value they have for the central and local governments. Therefore, the need to legally evaluate, define and registry real estates has appeared. The main motivation in the current study is to present the legal legislations (e.g. law, regulation) that the real estate is responsible for due to different main criteria (e.g. owner, location, type, intended use, acquisition form, encumbrance) on a single platform. In this context, İzmir/Foça was chosen as the study area. Then, the spatial and attributive features of each real estate were determined. The legislation information that is responsible for these features was introduced in the attribute table together with the router link. In this way, the originality of the study, which distinguishes it from the existing applications, has been revealed. As a result, legislative information that will enable more accurate decisions to be made for each real estate has been presented with a user-friendly interface.

Introduction

Land is a resource that should be used in a planned manner due to the rapid increase in the world population. During this planning, the need to legally evaluate, define and registry the real estate should also be resolved. In this context, a GIS based information system has been designed in which the real estate and the legislation are related. In this information system, building/parcel geometries, and laws in areas such as property, inheritance and tax were used. The main reason for the design of the mentioned information system is the existence of too many legal legislations that will cause legislative inflation and the fact that these legislations are carried out by different institutions. These two situations make difficult for real estate owners and many professional groups (e.g. lawyers, real estate specialists, engineers, planners, appraisers, experts) to understand and follow the legislation. Cases on real estate, the processes of preparing valuation reports, and the decision-making processes of experts will be shortened with the use of the designed information system. In addition, real estate owners will be more aware in protecting and using their legal rights.

Another reason for designing the information system is that the real estate-centered legislation studies in the literature are mainly related to the determination and classification of the legislation. For example, Çete [1] has determined that as of 2008, there were 88 laws, decree laws and bylaws related to land in our country. İşiler [2] has determined the laws concerning the first degree land management. Candaş [3] has examined successful samples (e.g. Germany, Netherlands, Spain) for the real estate valuation together with the legislation forms. İban [4] has modeled legislation for rural areas (e.g. agriculture, pasture and forest lands) in a spatial data infrastructure. Polat and Alkan [5] have revealed that more harmonious and mass legislation arrangements can be made by using the "Co-Concepts and Co-Citation Methods", which enables the determination of the most related laws with each other. The studies that identify the legislation associated with land management and classify them

in subtitles have been listed in sequence. No study and/or application has been met that shares the legal legislations due to the real estate location, attribute, and property form. In the current study, an information system was designed and presented to eliminate this relative missing part.

Material and Method

The legislation of the real estate is a very important research topic in terms of determining the rights and responsibilities. However, no meaningful information has been presented to the public on this topic. In the current study, the relationship between real estate and legislation was presented in a GIS-based information system. At every stage of this information system the ArcGIS software, which is the product of ESRI company, has been used effectively. The main question that guided the study was "Is it possible to access the legal legislations that the real estate is responsible due to its spatial and attributive feature through a single platform?". In this context, some web-based applications (e.g. parcel inquiry, title deed information inquiry, ATLAS) were examined and the relative user needs were determined in these applications. The examination result is that the mentioned applications don't provide any legal legislation about the real estate. Then, the study area was determined as İzmir, Foça. The study area is a coastal town with a total area of 58.75 km² and a coastline of 25 km. The study area was shared in Figure 1 with the building/parcel geometries and the land cover digitized from 1: 100,000 scale environmental plan.

In the continuation of the study, the main criteria (e.g. owner, location, type, intended use, acquisition form, encumbrance) were determined based on the spatial and attributive features of the real estates. Three of these main criteria consist of imaginary data set (e.g., owner, acquisition form, encumbrance), while three of them consist of an actual data set (e.g. location, type, intended use). The graphical and verbal data of the main criteria consisting of actual data sets were obtained from various data sources (e.g., base maps, web-based applications, closed source public data). The data projected in the same coordinate system were generalized for the intended use and stored in the geodatabase. Then, according to the main criteria, legal legislation associated with the real estate was determined and a comprehensive legislation inventory was created. Subsequently, some analysis processes (e.g., overlay analysis, buffer analysis, digitizing, select by attribute/location) were carried out. In this way, the attribute table of the real estate containing the legislation information was made ready for the user.
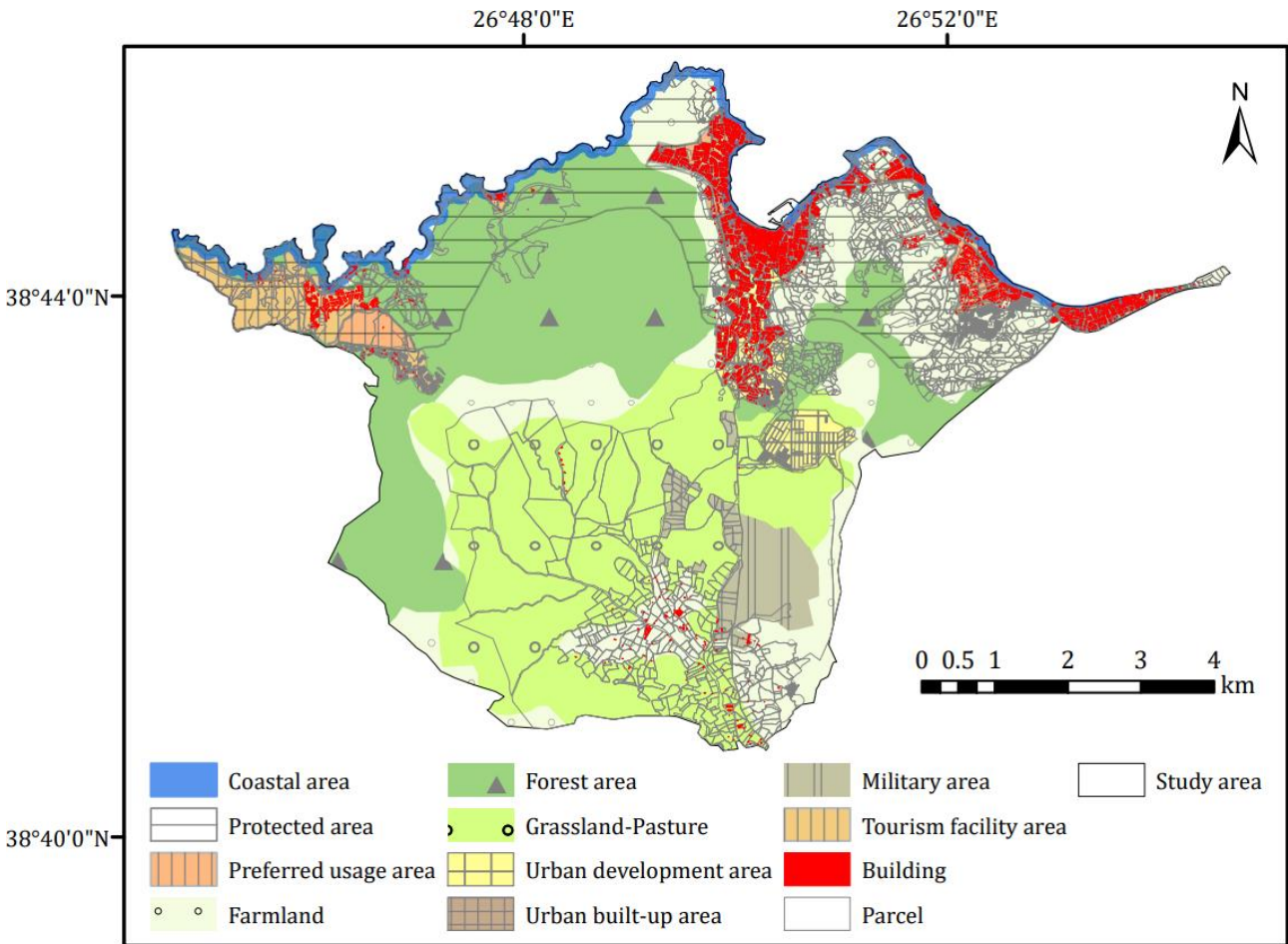
Figure 1. Study area

Results and Discussion

Each real estate in the region of interest has been related with the legislation spatially and attributive. In order to better understand the relationship, sample queries of six main criteria were made on the same real estate. For the real estate located in İzmir province, Foça county, Yenifoça neighborhood, 10729 block, 10 parcel; owner is naturel person so "Turkish Civil Code No. 4721 of 2001" and "Expropriation Law No. 2942 of 1983" (Figure 2a); location is urban built-up area so "Zoning Law No. 3194 of 1985" (Figure 2b); type is construction servitude so "Turkish Civil Code No. 4721 of 2001" and "Condominium Law No. 634 of 1965" (Figure 2c); intended use is residence so "Zoning Law No. 3194 of 1985" and "Condominium Law No. 634 of 1965" (Figure 2d); acquisition is purchase and sale so "Turkish Civil Code No. 4721 of 2001" and "Land Registry Law No. 2644 of 1934" (Figure 2e); encumbrance is family housing annotation and management plan and single space number change statement so "Turkish Civil Code No. 4721 of 2001" and "Condominium Law No. 634 of 1965" (Figure 2f) appears in the attribute table with the router link. These inquiries are proof that a real estate may be subject to more than one law at the same time due to the spatial and attributive features.
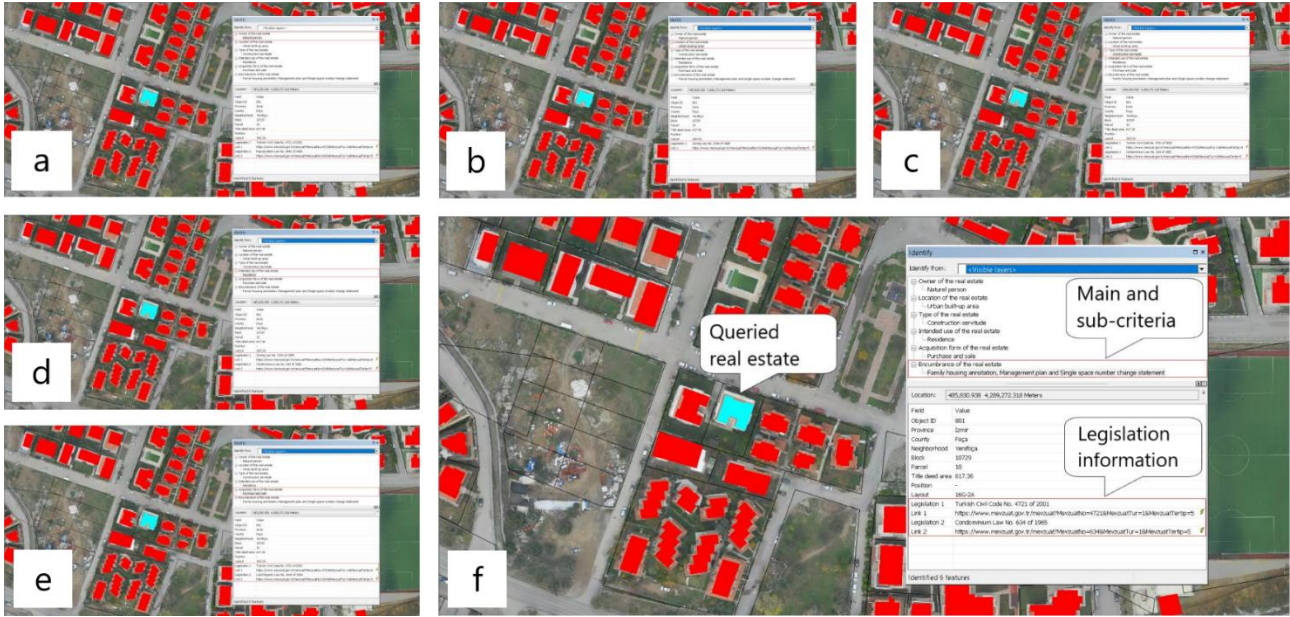
Figure 2. Sample queries of six main criteria

Conclusion

The legislation information of the real estates was presented with the attribute tables. In this way, the real estate owners who do not have technical and legal information and the professional groups interested in the real estate will reach the legal legislation. Thus, the public will use its legal rights more consciously. In addition, decision-making processes in real estate lawsuits, valuation report preparation processes and acquisition procedures will be shortened. In addition, pecuniary loss and intangible damages (e.g. penalties, usage constraints, loss of immovable) will be reduced in the cases, carried out in accordance with the incorrect legislation. Designed information system has also been a guide for possible updates that can be made in some applications (e.g. parcel inquiry, title deed information inquiry, ATLAS). As a result, the mentioned system should be supported by public power and presented to users. In this way, the diversity of the service provided to the public will increase and a more sustainable real estate-legislation management will be established.

References

1. Çete, M. (2008). An approach for Turkish land administration system. *Karadeniz Technical University Graduate School of Natural and Applied Sciences* (Doctoral Thesis).
2. İşiler, M. (2012). Legislation analysis about land management in Turkey. *İstanbul Technical University Graduate School of Natural and Applied Sciences* (Master's Thesis).
3. Candaş, E. (2012). Design of a real estate valuation legislation infrastructure model. *İstanbul Technical University Graduate School of Natural and Applied Sciences* (Master's Thesis).
4. İban, M. C. (2019). Modelling the spatial data infrastructure towards the land use in Turkey. *İstanbul Okan University Graduate School of Natural and Applied Sciences* (Doctoral Thesis).
5. Polat, Z. A., & Alkan, M. (2015). Using the Co-Concepts and Co-Citation methods on detection of similarity of land management legislation. *Electronic Journal of Map Technologies*, 7(2), 43-55.

Advanced Engineering Days

aed.mersin.edu.tr

A brief evaluation regarding the use of street view images for urban studies

Mehmet İşiler[*1] , **M. Oğuz Selbesoğlu** [1]

1Istanbul Technical University, Department of Geomatics Engineering, Türkiye, isiler@itu.edu.tr

Keywords
Urban environment
Street View Images
Visual Perception

Abstract
Street view images (SVIs) have the great potential to obtain essential data for assessing the urban street's environmental conditions. SVI enables visualization of the urban landscape through a human-centric view. Therefore, some vertical detail about streets not detected by traditional remote sensing methods can be easily obtained and analyzed. street view images can be available freely through several web services. In addition, with the advances in digital image analysis and deep learning techniques, the results from SVI analysis can be improved. This new data source has been used in many types of urban studies in recent years. This study highlights the potential of SVIs as a new data tool for urban planning by presenting recent street-level urban studies based on SVIs analysis.

Introduction

Today, economic, social, and cultural activities have become increasingly complex due to globalization trends, technological advancements, and widespread communication options [1]. In this regard, the nature of the needs in the cities has gradually changed. With the parallel of this transformation in urban areas, spatial planning requires a comprehensive land management approach addressing social-economic needs, healthy lifestyles, protecting natural resources, and energy issues to design the urban environment.

Thanks to technological developments, it is now possible to use various data sources for geo-information science [2]. Unmanned aerial vehicle (UAV) techniques, satellite images, and digital globes providing street view perception are common data collection techniques in urban studies. Despite the advantages of UAV and satellite data acquisition techniques, they have some constraints in obtaining vertical details of urban areas with sufficient accuracy. In this case, Street view images can be effectively used in vertical urban research to understand street spatial characteristics and identify urban features.

Street view images can provide crucial information for understanding urban conditions. SVI allows the visualization of urban landscapes from a human-centered perspective. Recently, street view images can be accessed freely through several web services such as Google, Microsoft, Baidu, and Tencent [3]. With the enhancement in computer vision techniques and deep-learning strategies, the visual perception of streets provides more meaningful information for supporting urban planning and land policy making.

This study aims to show the potential of SVIs as a new data tool for street-level urban studies. This study also aims to classify urban studies based on SVIs to create a comprehensive overview.

Street View Images for Urban Studies

This new data source has become a central part of many types of research. These studies have primarily focused on assessing visual space qualities of the urban streets [3-8], detecting trees and other types of plants in urban areas [1-13], visualizing the climatic conditions and air pollution for a specific time [14-16], walkability [17,18], and obtaining building-level information [4, 19-21].

Virtual space qualities of urban streets

Virtual quality is a function of the connection between landscape elements and individual residence perception [9]. The visual perception of built-up urban areas has a strong influence on the quality of urban residents' life [3]. Therefore, developed countries consider designing and analyzing visual perception elements in urban areas. Many studies have focused on developing visual perception parameters to analyze urban environment quality. The visual quality of cities can be described by different urban features such as greenery, pedestrian space, motorization, traffic density, cleanliness, and sky openness. In recent years, SVIs have become an effective tool for measuring visual perception metrics.

Chang et al. revealed the potential of using Tencent Street View images to automatically analyzed the visual perception of the Jianye District of Nanjing City in China according to visual entropy, green view index, and sky-openness index [3]. Gong et al. calculated the main view factors describing the urban thermal environment in the high-density streets of Hong Kong based on Google Street View (GSV) images and a deep learning feature extraction algorithm [4]. Ye et al. analyzed the perceptual-based visual quality of streets, including the building frontage, greenery, sky view, pedestrian space, motorization, and diversity, using screenshots from Baidu Street View and a machine learning algorithm [6].

These mentioned studies show that SVIs obtained through different online services can be utilized for urban street quality analyses. In addition, these kinds of analyses can be easily automated with the help of a deep-learning approach,

Detecting trees and other plants in urban areas

The existence of street greenery has crucial effects on mitigating climate change, reducing urban pollution, protecting urban resources, and improving human health [10,11]. Recent studies have emphasized the benefits of SVIs as a new data source for determining the characteristics of urban trees.

Seiferling et al. tested their model to obtain vertical information, that cannot be detected from traditional long-range remote sensing methods, on the urban tree cover from the perspective of pedestrians by using GSV images [11]. In another study, Li and Yao presented a 3D system for determining tree inventory with geographic locations in Hong Kong based on GSV panorama images by combining a deep learning approach [12]. Ringland et al. showed the availability of using GSV images and RetinaNet, an object-detection method, to map plant species widely grown in home gardens facing the roads in Thailand [13].

According to these studies, SVIs can be a good choice for obtaining the spatial distribution of plant inventory in the cities. This information can be efficiently used in upper-scale planning.

Visualizing the climatic condition and air pollution for a specific time

SVIs may enable an analysis of urban meteorological conditions and air pollution levels in cities. The meteorological dynamics of cities can present the urban population and environment interaction. The relation between street visual metrics and air pollution [14] can be analyzed. Furthermore, weather conditions can be extracted for a specific period using street-view images [15]. It should be noted that the quality of SVIs is an important issue that can adversely affect experiment results.

Walkability

Walkable streets contribute the social life and environment-friendly mobility. SVIs are popular data sources for walkability analysis. SVIs have recently improved the walkability analysis from the street scale to the large scale by combining sensor technology and digitization [17]. For instance, Yin et al. conducted a study to detect and count pedestrians from GSV images using a deep-learning method [18]. Therefore, pedestrian volume and traffic conditions [18] can be analyzed at the street level.

Obtaining building-level information

Many studies have asserted the advantages of using SVIs for mapping places [19], classifying building functions [20,21], and identifying landscape features at the street level [4]. Li et al. achieved classifying residential and non-residential buildings using GSV images [20]. This study used three image feature descriptors to represent GSV images of different buildings [20]. Zhang et al. develop an approach to analyze the relationship between building dominant color and building functions including residential, public services, commercial services, and other facilities.

Conclusion

These academic studies indicate that utilizing SVIs to investigate the interaction between humans and urban environments yields comprehensive and accurate results. Accessible SVIs can be easily used for understanding the dynamics of the outdoor environment on a street-level scale for urban areas, it is seen that the machine learning techniques used in these studies improve image analysis performance as well. Some critical information describing buildings and their functions can be obtained through the SVIs without field survey data collection and manual interpreting. SVIs provide an opportunity to obtain meaningful and comprehensive data for urban planning.

References

1. İşiler, M., Yanalak, M. & Selbesoğlu, M. O. (2022). Arazi yönetimi paradigması çerçevesinde Türkiye'de binalar için enerji kimlik belgesi uygulamasının değerlendirilmesi. Niğde Ömer Halisdemir Üniversitesi Mühendislik Bilimleri Dergisi, 11 (3), 689-705
2. Donmez, S. O., & Ipbuker, C. (2018). Investigation on agent based models for image classification of land use and land cover maps. 39th Asian Conference on Remote Sensing- Proceeding (ACRS 2018). 4, 2005-2008.
3. Cheng, L., Chu, S., Zong, W., Li, S., Wu, J., & Li, M. (2017). Use of tencent street view imagery for visual perception of streets. *ISPRS International Journal of Geo-Information*, *6*(9), 265.
4. Gong, F. Y., Zeng, Z. C., Zhang, F., Li, X., Ng, E. & Norford, L. K. (2018) Mapping sky, tree, and building view factors of street canyons in a high-density urban environment. Building and Environment, 134, 155–167.
5. Middel, A., Lukasczyk, J., Zakrzewski, S., Arnold, M. & Maciejewski, R. (2019) Urban form and composition of street canyons: A human-centric big data and deep learning approach. Landscape and Urban Planning, 183, 122–132.
6. Ye, Y., Zeng, W., Shen, Q., Zhang, X. & Lu, Y. (2019) The visual quality of streets: A human-centered continuous measurement based on machine learning algorithms and street view images. Environment and Planning B: Urban Analytics and City Science. 46(8), 1439–1457.
7. Liu, M., Han, L., Xiong, S., Qing, L., Ji, H. & Peng, Y. (2019) Large-scale street space quality evaluation based on deep learning over street view image. In Proceedings of the International Conference on Image and Graphics, Beijing, China, 23–25 August 2019; 690–701.
8. Wang, M., He, Y., Meng, H., Zhang, Y., Zhu, B., Mango, J. & Li, X. (2022) Assessing street space quality using street view imagery and function-driven method: the case of Xiamen, China. ISPRS Int. J. Geo-Inf. 2022, 11, 282.
9. Ozkan, U.Y. (2014) Assessment of visual landscape quality using IKONOS imagery. Environmental Monitoring and Assessment, 186, 4067.
10. Xia, Y., Yabuki, N., & Fukuda, T. (2021). Development of a system for assessing the quality of urban street-level greenery using street view images and deep learning. *Urban Forestry & Urban Greening*, *59*, 126995.
11. Seiferling, I., Naik, N., Ratti, C., & Proulx, R. (2017). Green streets– Quantifying and mapping urban trees with street-level imagery and computer vision. *Landscape and Urban Planning*, *165*, 93-101.
12. Li, M., & Yao, W. (2020). 3D map system for tree monitoring in hong kong using google street view imagery and deep learning. *ISPRS Annals of the Photogrammetry, Remote Sensing and Spatial Information Sciences*, *3*, 765-772.
13. Ringland, J., Bohm, M., Baek, S. R., & Eichhorn, M. (2021). Automated survey of selected common plant species in Thai homegardens using Google Street View imagery and a deep neural network. *Earth Science Informatics*, *14*, 179-191.
14. Wu, D., Gong, J., Liang, J., Sun, J., & Zhang, G. (2020). Analyzing the influence of urban street greening and street buildings on summertime air pollution based on street view image data. *ISPRS International Journal of Geo-Information*, *9*(9), 500.
15. Ibrahim, M. R., Haworth, J., & Cheng, T. (2019). WeatherNet: Recognising weather and visual conditions from street-level images using deep residual learning. *ISPRS International Journal of Geo-Information*, *8*(12), 549.
16. Qi, M., & Hankey, S. (2021). Using street view imagery to predict street-level particulate air pollution. *Environmental Science & Technology*, *55*(4), 2695-2704.
17. Yin, L., & Wang, Z. (2016) Measuring visual enclosure for street walkability: using machine learning algorithms and google street view imagery. Applied Geography. 76, 147-153.
18. Yin, L., Cheng, Q., Wang, Z., & Shao, Z. (2015). 'Big Data' for pedestrian volume: exploring the use of google street view images for pedestrian counts. Applied Geography. 63, 337–345.
19. Rangel, J. C., Cruz, E., & Cazorla, M. (2022). Automatic Understanding and Mapping of Regions in Cities Using Google Street View Images. *Applied Sciences*, *12*(6), 2971.
20. Li, X., Zhang, C., & Li, W. (2017) Building block-level urban land-use information retrieval based on google street view images. GIScience & Remote Sensing. 54, 6, 819-835.
21. Zhang, J., Fukuda, T., & Yabuki, N. (2021). Development of a city-scale approach for façade color measurement with building functional classification using deep learning and street view images. *ISPRS International Journal of Geo-Information*, *10*(8), 551.

Advanced Engineering Days

aed.mersin.edu.tr

Sentinel-2 derivatives are rewriting land-cover history

Arif Oguz Altunel[1]* , Durmus Ali Celik[2]

[1]Kastamonu University, Faculty of Forestry, Forest Engineering, Turkiye, aoaltunel@kastamonu.edu.tr
[2]Kastamonu University, Arac Vocational School, Forestry, Turkiye, dcelik@kastamonu.edu.tr

Keywords
Sentinel-2
10 m multispectral
Hi-resolution
Land cover

Abstract
The terms, land-use, land-cover and change detection, gained their full meanings and came to researches' attentions after NASA's first Landsat, the Earth Resource Technology Satellite, was launched in July 1972, started monitoring the Earth and collecting data. Successional namesake satellites have continued Earth monitoring missions, even today. They have later been challenged by SPOT and IRS missions, being also continued by France's and India's respected institutions. Famous CORINE land cover maps which have been released by Copernicus Land Monitoring Service for five periods since 1990 primarily used the imagery captured by these missions. In the last coverage of 2018, though, a new imagery amassed by a completely new mission called Sentinel-2, has taken over the task only to be complemented by Landsat-8 for gap filling across the Europe. 10 m multispectral imagery has surpassed expectations in all arenas and has helped in the formation of new global land-cover datasets. This study aimed to present three new such global datasets, Dynamic World by World Research Institute, Google; World Cover by ESA and Land Use/Land Cover Time-series coverages by ESRI, their specifications and field verification results.

Introduction

Land use/land cover maps have mostly been transformed to frequently updated, considerably reliable global datasets displaying the changes occurring in ecosystems, habitats, regions, etc. Monitoring the biodiversity, the health of natural resources, carbon cycle and sequestration, favorable or adverse effects of human endeavors on natural any anthropogenic processes, the effects of shifting climate on agricultural production and natural forest loss/gain can effectively be performed utilizing such maps [1-3].

The concept has always been on the spotlight [4], however the satellite image qualities that have been used to construct such datasets have mostly been configured for specific tasks, so not very many discernable classes were present in earlier such datasets [5-7].

ESA's launch of Sentinel-2A in June, 2015 has started a new era in global land-cover monitoring. With the inclusion of Sentinel 2B in March 2017, the tandem satellites quickly amassed enough data for Google World Research Institute's Dynamic World datasets produced using deep learning [8], European Space Agency's World Cover datasets produced using machine learning [9], and ESRI's Land Cover datasets produced again using deep learning methodologies [10-11].

Material and Method

Three global land-cover datasets were acquired from their respective portals [12-14]. Area of interest was determined as a rectangle plot within downtown Kastamonu; 33.791 and 33.771 Eastern Latitudes, 41.417 and 41.401 Northern Longitudes. 2021 coverages from each dataset was visually compared to the corresponding year's hi-resolution Google Earth imagery.

Results
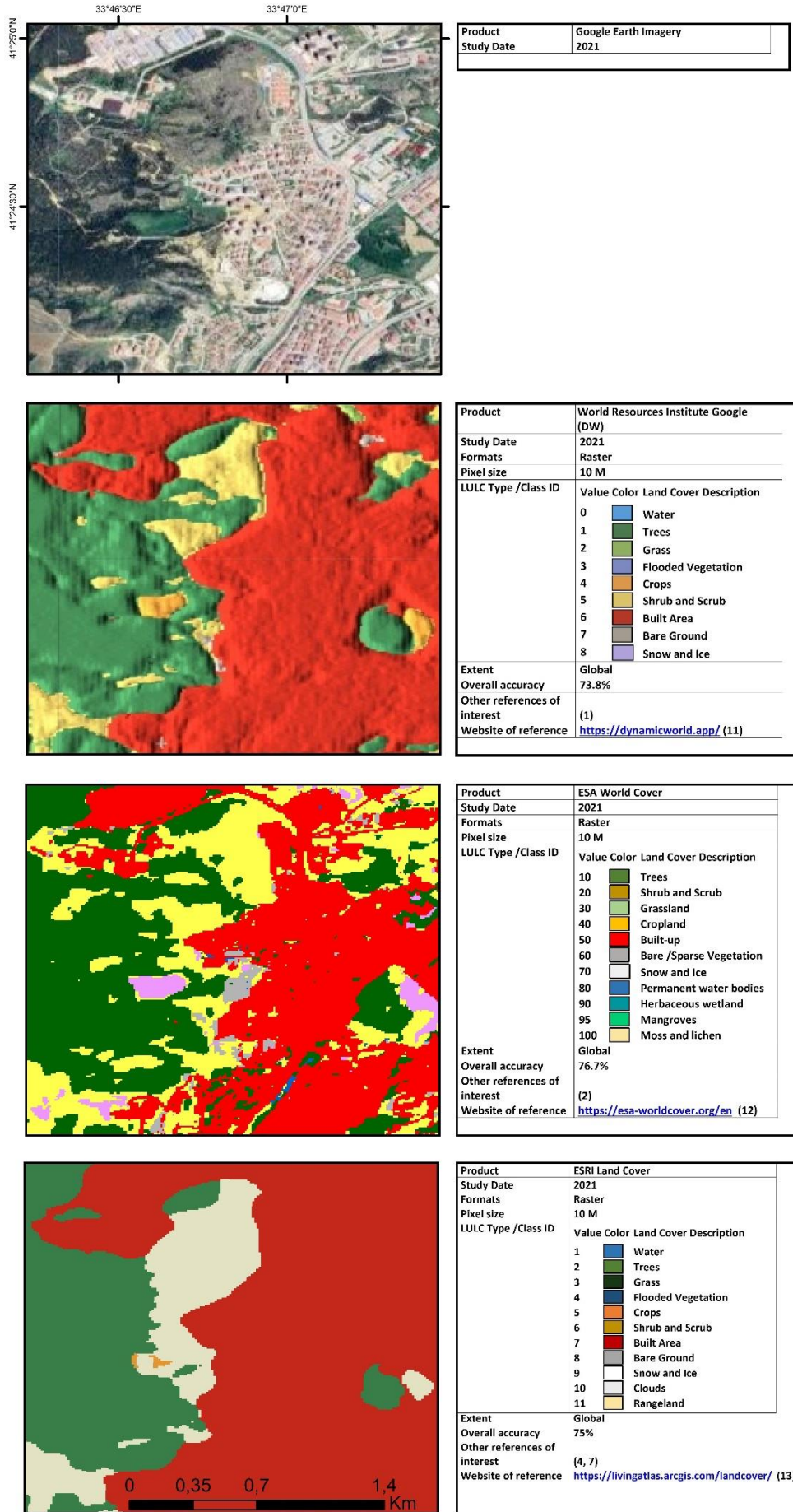
Figure 1. Google earth, Dynamic world, ESA world-cover and ESRI land-cover over Kastamonu study plot

Discussion and Conclusion

Although similar in overall accuracies, ESA world-cover and Google dynamic-world clearly surpassed ESRI land-cover apparent from simple visual comparison. Despite the fact that the very same data, Sentinel-2, were the only imagery used in the construction of all datasets, the different methodologies used in each were the reason that the first two were aesthetically coinciding with the actual land cover parcels and partitions in studied plot while ESRI land-cover fell short in defining them as much precisely. Owing to the exceptionally good quality of Sentinel-2 imagery, such rather detailed land-cover maps that have been produced either with global intentions or with regional interests, will keep surfacing as the satellites operational life-time continues. Near future is ripe for fierce competition in global land cover mapping racing.

References

1. Feddema, J. J. (2005). The Importance of Land-Cover Change in Simulating Future Climates. Science, 310, 1674–1678.
2. Ramachandran, R. M., Roy, P. S., Chakravarthi, V., Joshi, P. K., & Sanjay, J. (2020). Land use and climate change impacts on distribution of plant species of conservation value in Eastern Ghats, India: a simulation study. Environmental monitoring and assessment, 192, 1-21.
3. Roy, P. S., Ramachandran, R. M., Paul, O., Thakur, P. K., Ravan, S., Behera, M. D., ... & Kanawade, V. P. (2022). Anthropogenic land use and land cover changes—A review on its environmental consequences and climate change. Journal of the Indian Society of Remote Sensing, 50(8), 1615-1640.
4. García-Álvarez, D., & Lara Hinojosa, J. (2022). Global Thematic Land Use Cover Datasets Characterizing Vegetation Covers. *Land Use Cover Datasets and Validation Tools: Validation Practices with QGIS*, 373-398.
5. Townshend, J. R., Masek, J. G., Huang, C., Vermote, E. F., Gao, F., Channan, S., ... & Wolfe, R. E. (2012). Global characterization and monitoring of forest cover using Landsat data: opportunities and challenges. *International Journal of Digital Earth*, *5*(5), 373-397.
6. Shimada, M., Itoh, T., Motooka, T., Watanabe, M., Shiraishi, T., Thapa, R., & Lucas, R. (2014). New global forest/non-forest maps from ALOS PALSAR data (2007–2010). Remote Sensing of environment, 155, 13-31.
7. Akturk, E., Altunel, A. O., Atesoglu, A., Seki, M. & Erpay, S. (2023) How good is TanDEM-X 50 m forest/non-forest map? Product validation using temporally corrected geo-browser supplied imagery through Collect Earth, International Journal of Geographical Information Science,1-28. https://doi.org/10.1080/13658816.2023.2183959.
8. Brown, C. F., Brumby, S. P., Guzder-Williams, B., Birch, T., Hyde, S. B., Mazzariello, J., ... & Tait, A. M. (2022). Dynamic World, Near real-time global 10 m land use land cover mapping. Scientific Data, 9(1), 251.
9. ESA (2020) https://worldcover2020.esa.int/data/docs/WorldCover_PUM_V1.1.pdf.
10. Karra, K., Kontgis, C., Statman-Weil, Z., Mazzariello, J. C., Mathis, M., & Brumby, S. P. (2021). Global land use/land cover with Sentinel 2 and deep learning. In 2021 IEEE international geoscience and remote sensing symposium IGARSS (pp. 4704-4707). IEEE.
11. Venter, Z. S., Barton, D. N., Chakraborty, T., Simensen, T., & Singh, G. (2022). Global 10 m Land Use Land Cover Datasets: A Comparison of Dynamic World, World Cover and Esri Land Cover. Remote Sensing, 14(16), 4101.
12. https://dynamicworld.app/, last accessed on 03/03/2023.
13. https://esa-worldcover.org/en, last accessed on 03/03/2023.
14. https://livingatlas.arcgis.com/landcover/, last accessed on 03/03/2023.
.

Advanced Engineering Days

aed.mersin.edu.tr

3D modeling of Mersin Akyar Cliffs with wearable mobile LIDAR

Atilla Karabacak *[1] [iD], Murat Yakar [2] [iD]

[1]Mersin University, Vocational School of Technical Sciences, Türkiye, atilakarabacak@mersin.edu.tr
[2]Mersin University, Geomatics Engineering Department, Türkiye, myakar@mersin.edu.tr

Keywords
Remote sensing
Wearable Mobile Lidar
Photogrammetry
Laser Scanning
3D

Abstract
LiDAR (Light Detection and Ranging) is a remote sensing technology that measures distance a laser light on objects and catching the light reflected back. The rapid change in navigation systems and technology, the introduction of sensors into our lives have brought new systems that map the environment in the cartography profession. The lidar scans the area and measures the time it takes the light to reach various objects and return. Wearable Mobile Lidar designed for indoors and outdoors, complex sites, underground mines, multi-floor buildings, forests, urban areas, stockpile volumes. In this study, a 3D model was produced by scanning the Akyar cliffs in Silifke district of Mersin with Wearable Mobile LIDAR (GML). It has been experienced from our previous studies that LIDAR pulses make different reflections and affect the measurement when they hit the water. In the study, it was seen that the effect of the measurements made at the seaside on the SLAM algorithm was reduced by using the Ground Control Point (GCP).

Introduction

Mersin is an important tourism city in Turkey. Akyar cliffs are located in Silifke district of Mersin province. Domestic and foreign tourists coming to the region come here to see these natural wonders. In this study, cliffs were modeled in 3D and using GML at the seaside and its effect on LIDAR data and using Ground Control Point GCP were examined.

There is limestone from carbonate rocks in the cliffs, and there is more than 50% CaCO3 in carbonate rocks [1].

Material and Method

The WML Gexcel Heron we used in this study is a Wearable 3D Mobile Mapping System. The system started to be used in 2015. The system, which uses the SLAM algorithm, is designed to be used in places where a person can walk. The system is used to measure all kinds of natural and artificial objects such as tunnels, mines, cultural heritage. The system can capture 3D point cloud and 5K panoramic images.

Gexcel Heron WML emits infrared laser beams with a wavelength of 903 nm. A 16-channel Velodyne Puck LITE laser scanner provides 300,000 points per second in single rotation mode from 360-degree horizontal vision and 30-degree vertical vision. It has a range of 100 meters. The laser scanner sensor is combined with an XSens MTI, IMU, whose data is used in system trajectory prediction. While measuring, the scan head is mounted on a telescopic carbon fiber pole, connected to a battery and a control unit. The LIDAR scanner head is used by mounting on a pole. Range rod is carried upright by hand or by placing it in a pocket attached to the belt [2-3].

Gexcel Heron is a wearable or handheld mobile laser scanner. It uses SLAM Algorithm. It can be used in all kinds of walkable areas. It can be used in places such as indoor and outdoor, underground mines, geospatial applications, structures, tunnels, cultural heritage sites, forensic events, forests, urban areas. Captures 3D point clouds and 5K panoramic images to collect both geometry and color information together.

The portable Mobile laser scanner tested in this study is the Heron wearable Lidar device manufactured by Gexcel. It is a 16-channel Velodyne Puck LITE laser scanner that emits infrared laser beams at a wavelength of 903 nm and provides 300,000 points per second in single rotation mode from 360 degrees horizontal vision and 30 degrees vertical vision. Range measurements are performed on the time-of-flight principle with a maximum measurable distance of 100 m. The laser scanner sensor is combined with an XSens MTI, IMU, whose data is used in system trajectory prediction. While surveying, the scan head is mounted on a telescopic carbon fiber pole, connected to a battery and a control unit. According to the manufacturer's specifications, the system provides a local accuracy of 3 cm and a final global accuracy of 5 cm. By the presence of system loops and closures, as well as the characteristics of the scanned environment, the SLAM algorithm may be affected and the accuracy may drop to 20-50 cm [2-3].

Today, there have been significant developments in measurement technologies. Unmanned aerial vehicles, 3D laser scanners and lidar technology, and photogrammetric methods have made significant contributions to measurement technology [4-20].

Scanning was performed by creating open and closed routes using and without Ground Control Point for cliff measurement.

Working methods in the field

Akyar cliffs are located in Narlıkuyu town of Silifke district of Mersin. In the study, 5 ground control points were placed on the land. Two of the ground control points were measured with GNSS and the other points were measured with a total station (Figure 1).

Figure 1. Images from fieldworks in Akyar cliffs

3D modeling of cliffs using ground control points (GCP)

A route passing through all control points was followed in the fieldwork. The route was followed as a closed route and the starting point was reached again. The route was completed in about 5 minutes. As a result of the transformation and adjustment, the largest RMS value was 3 cm and the average was 2 cm (Figure 2).
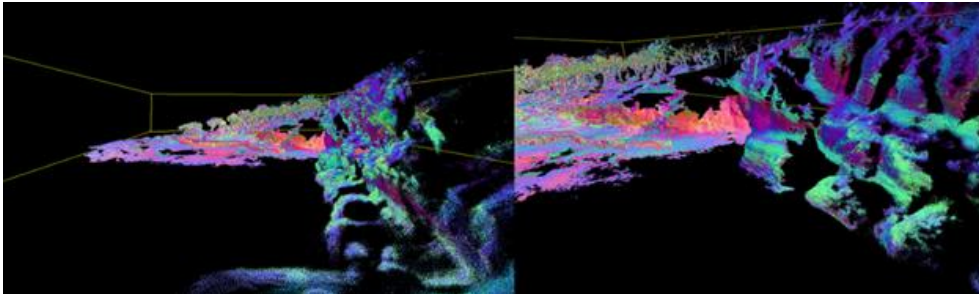
Figure 2. 3D model of Akyar cliffs

Open route 3D modeling of cliffs with GCP

The route was completed in about 3 minutes. As a result of the transformation and adjustment, the largest RMSD value was 6.5 cm and the average was 3 cm (Figure 3).
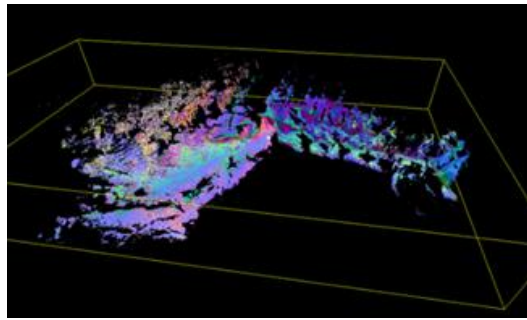
Figure 3. Akyar cliffs 3D model

It was observed that RMS values and bond errors increased in the open route between working as a closed route and working as an open route in the same study area.

3D Modeling of Akyar Cliffs with Closed Route without GCP

The route measurement was completed in approximately 5 minutes (Figure 4).
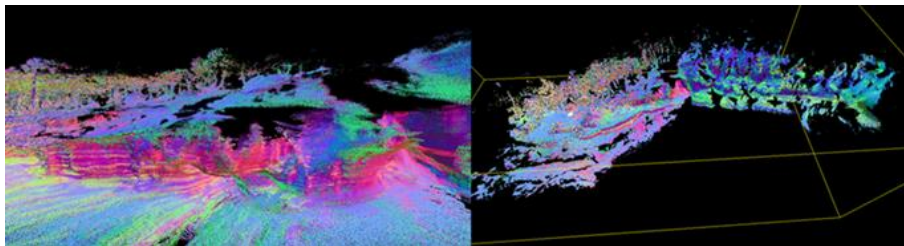
Figure 4. The 3D model produced without the closed route GCP

All ligaments together have an average of 3.5 cm adjusted RMS square root error between 5 cm and 2 cm.

Results

To interpret the results of the methods used, the orthophotos produced in each method were compared in Figure 5 (Table 1).
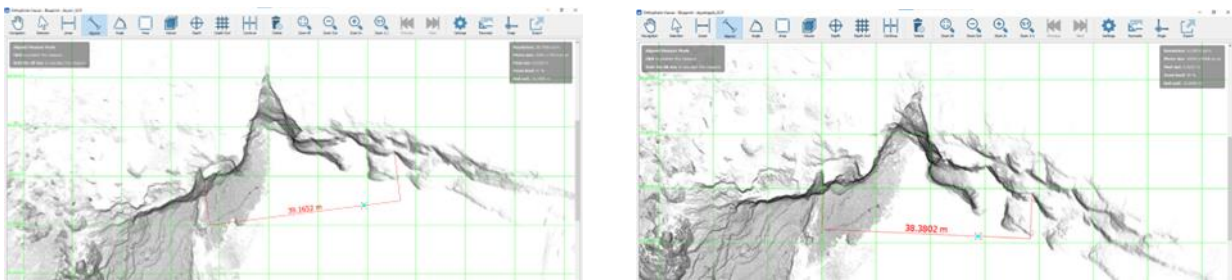
Figure 5. Orthophotos from left to right 1. With GCP 2. Without GCP, taken with closed route

Table 1. Base lengths found by different methods

Survey type	With GCP open	With GCP closed	Without GCP closed
Base lenght	39,18m	39,17 m	38,38m

While there is a 1 cm difference between the measurement methods used at GCP points, there is a difference of approximately 80 cm on the route without GCP.

Discussion

GML scans using a GCP point show little to no difference. However, when GCP is not used in the measurement, the difference exceeds the given error rate of GML. There was no difference between the open and closed routes made by taking GCP. In studies without GCP, the baseline length was found to be incorrect. It exceeds the error rate expected from GML. The fact that the deviation is too much is due to the reflections from the sea surface disrupting the SLAM algorithm.

Conclusion

As a result, using GML without using GCP does not give reliable results since the water surface breaks the SLAM algorithm at the water's edge. In the future, it is necessary to carry out studies to determine the cliff deformations on the 3D model.

References

1. Alptekin, A., & Yakar, M. (2020). Mersin Akyar Falezi'nin 3B modeli. *Türkiye Lidar Dergisi*, *2*(1), 5-9.
2. Karabacak, A., & Yakar, M. Giyilebilir Mobil LİDAR Kullanım Alanları ve Cambazlı Kilisesinin 3B Modellemesi. Türkiye Lidar Dergisi, 4(2), 37-52.
3. https://paksoyteknik.com.tr/index.php/paksoy-topcon/lazer-tarama/gexcel-heron
4. Yılmaz, H. M., Karabörk, H., & Yakar, M. (2000). Yersel fotogrametrinin kullanım alanları. *Niğde Üniversitesi Mühendislik Bilimleri Dergisi*, *4*(1), 1.
5. Yakar, M., Orhan, O., Ulvi, A., Yiğit, A. Y., & Yüzer, M. M. (2015). Sahip Ata Külliyesi Rölöve Örneği. *TMMOB Harita ve Kadastro Mühendisleri Odası*, *10*.
6. Yakar, M., & Yilmaz, H. M. (2008). Using in volume computing of digital close range photogrammetry. *The International Archives of the Photogrammetry, Remote Sensing and Spatial Information Sciences. Vol. XXXVII. Part B3b*.
7. Alptekin, A., & Yakar, M. (2021). 3D model of Üçayak Ruins obtained from point clouds. *Mersin Photogrammetry Journal*, *3*(2), 37-40.
8. Alptekin, A., & Yakar, M. (2020). Determination of pond volume with using an unmanned aerial vehicle. *Mersin photogrammetry journal*, *2*(2), 59-63.
9. Karataş, L., Alptekin, A., Kanun, E., & Yakar, M. (2022). Tarihi kârgir yapılarda taş malzeme bozulmalarının İHA fotogrametrisi kullanarak tespiti ve belgelenmesi: Mersin Kanlıdivane ören yeri vaka çalışması. *İçel Dergisi*, *2*(2), 41-49.
10. Kanun, E., Alptekin, A., & Yakar, M. (2021). Cultural heritage modelling using UAV photogrammetric methods: a case study of Kanlıdivane archeological site. *Advanced UAV*, *1*(1), 24-33.
11. Şasi, A., & Yakar, M. (2017). Photogrammetric modelling of sakahane masjid using an unmanned aerial vehicle. *Turkish Journal of Engineering*, *1*(2), 82-87.
12. Yakar, M., & Doğan, Y. (2017). Mersin Silifke Mezgit Kale Anıt Mezarı fotogrametrik rölöve alımı ve üç boyutlu modelleme çalışması. *Geomatik*, *2*(1), 11-17.
13. Karataş, L., Alptekin, A., & Yakar, M. (2022). Creating Architectural Surveys of Traditional Buildings with the Help of Terrestrial Laser Scanning Method (TLS) and Orthophotos: Historical Diyarbakır Sur Mansion. *Advanced LiDAR*, *2*(2), 54-63.
14. Ulvi, A., Yakar, M., Toprak, A. S., & Mutluoglu, O. (2014). Laser scanning and photogrammetric evaluation of Uzuncaburç Monumental Entrance. *International Journal of Applied Mathematics Electronics and Computers*, *3*(1), 32-36.
15. Yilmaz, H. M., & Yakar, M. (2006). Lidar (Light Detection and Ranging) Tarama Sistemi. *Yapı Teknolojileri Elektronik Dergisi*, *2*(2), 23-33.
16. Kanun, E., Alptekin, A., Karataş, L., & Yakar, M. (2022). The use of UAV photogrammetry in modeling ancient structures: A case study of "Kanytellis". *Advanced UAV*, *2*(2), 41-50.
17. Korumaz, A. G., Dülgerler, O. N., & Yakar, M. (2011). Kültürel mirasin belgelenmesinde dijital yaklaşimlar. *Selçuk Üniversitesi Mühendislik, Bilim ve Teknoloji Dergisi*, *26*(3), 67-83.
18. Yilmaz, H. M., Yakar, M., Yildiz, F., Karabork, H., Kavurmaci, M. M., Mutluoglu, O., & Goktepe, A. (2009). Monitoring of corrosion in fairy chimney by terrestrial laser scanning. *Journal of International Environmental Application & Science*, *4*(1), 86-91.
19. Karataş, L. (2023). Yersel lazer tarama yöntemi ve ortofotoların kullanımı ile kültür varlıklarının cephelerindeki malzeme bozulmalarının dokümantasyonu: Mardin Mungan Konağı örneği. *Geomatik*, *8*(2), 152-162.
20. Karataş, L., Alptekin, A., & Yakar, M. (2022). Analytical Documentation of Stone Material Deteriorations on Facades with Terrestrial Laser Scanning and Photogrammetric Methods: Case Study of Şanlıurfa Kışla Mosque. *Advanced LiDAR*, *2*(2), 36-47.

3D modeling of Mersin Sarisih Caravanserai with wearable mobile LIDAR

Atilla Karabacak *1 [iD], **Murat Yakar** 2 [iD]

¹Mersin University, Vocational School of Technical Sciences, Türkiye, atilakarabacak@mersin.edu.tr
²Mersin University, Geomatics Engineering Department, Türkiye, myakar@mersin.edu.tr

Keywords
Remote sensing
Wearable Mobile Lidar
Photogrammetry
Laser Scanning
3D

Abstract
A 3D model was produced by scanning the Sarşıh Caravanserai in Tarsus, Mersin with a Wearable Mobile LIDAR (GML). In the study, it has been seen that the effect of disrupting the SLAM algorithm in areas where walking is difficult due to terrain obstacles is reduced by using Ground Control Point (GCP). Cultural heritage can be documented with GML and in this way, our immortal culture can be inherited to future generations with its 3D model.

Introduction

Sarisih Caravanserai is our cultural heritage, which is thought to have been built during the Principalities Period. Sarisih Caravanserai is located in the Sarisih neighborhood of Çukurbağ village, approximately 50 km north of Tarsus. Its geographical coordinates are at 37012'55'' north latitude, 34048'25'' east meridian, and it is located on the side of the Tarsus-Ankara highway. It is known that the building was used as a factory for soda production for a while. Small boat-shaped pools were built inside the building. It is reported that the building was later used as an animal barn by the villagers. The original state of the interior of the building has deteriorated. It is understood from the changes in the wall thickness of the building, which has eight arches, that the building was repaired at different times, and the difference in the stones used. Horosan mortar was used in the building, the stone top of the building was covered with concrete [1].

Nowadays, it has become a necessity to use modern technologies in documentation studies. Laser scanning, unmanned aerial vehicles and photogrammetric methods are used extensively for measuring historical artifacts and surveying [2-18].

Sarşıh Caravanserai was scanned with GML and modeled in 3D. In the study, SLAM errors were tried to be reduced by using GCP.

Material and Method

The WML Gexcel Heron Wearable 3D Mobile Mapping System we used in this study. Gexcel Heron System was launched in 2015. The system, which uses the SLAM algorithm, can be used wherever a person can walk. The system can be used to measure anything visible to the non-moving eye during scanning. System offers 3D point cloud and 5K panoramic view.

Gexcel Heron WML is a 16-channel Velodyne Puck LITE laser scanner that emits infrared laser beams at a wavelength of 903 nm and provides 300,000 points per second in single rotation mode from 360 degrees horizontal vision and 30 degrees vertical vision, has a range of 100 m. The laser scanner sensor is combined with an XSens MTI, IMU, whose data is used in system trajectory prediction. While surveying, the scan head is mounted on a telescopic carbon fiber pole, connected to a battery and a control unit. The LIDAR scanner head is used by mounting on a pole. Jalon can be carried upright by hand or placed in a pocket attached to a belt [19-20].

The mobile laser scanner used in this study is the Heron wearable Lidar device produced by Gexcel. It is a 16-channel Velodyne Puck LITE laser scanner that emits infrared laser beams at a wavelength of 903 nm and provides 300,000 points per second in single rotation mode from 360o horizontal sight and 30o vertical sight. Its range is 100 m. The laser scanner sensor presents the data by combining it with an XSens MTI, IMU used in system trajectory prediction. While surveying, the scan head is mounted on the fiber mast, connected to a battery and a control unit. According to the manufacturer's specifications, the system provides a local accuracy of 3 cm and a global accuracy of 5 cm [19-20].

For the measurement of the caravanserai, scanning was carried out by creating an open and closed route using and without the Ground Control Point.

Methods of working in the field

A total of 4 GCPs, two GCPs each inside and outside the caravanserai, were established. A controlled method was followed by stopping by the GCP in the form of an open route, considering that the land does not allow passage to go around the structure and the route would be unnecessarily long (Figure 1). Two of the ground control points were measured with GNSS and the other points were measured with a total station (Figure 2).
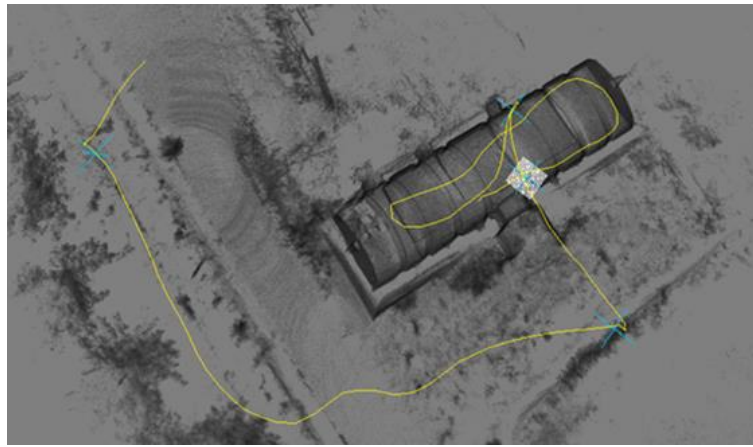
Figure 1. The shape of the route and the caravanserai (marked places GCP)

Images obtained from the caravanserai and field studies are shown in Figure 2.

Figure 2. GCP measurement and GML

3D modeling of the caravanserai using GCP

A clear route was followed across the terrain, passing through all checkpoints. The route was completed in about 6 minutes. As a result of the transformation and balancing, the largest RMS value was 4 cm. The 3D point cloud of the Sarisih caravanserai is shown in Figure 3.
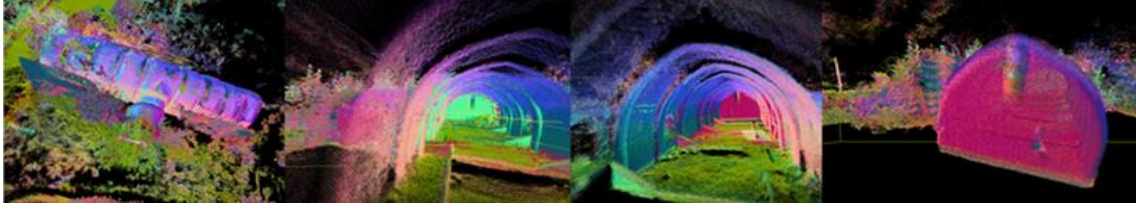
Figure 3. Sarisih Caravanserai 3D point Cloud

The distance between two opposing columns in the field was 7.00 m. The same length was measured as 7.01 m on the 3D model, and 6.99 m in the horizontal section taken on the point cloud. In the field, the distance between two adjacent columns was measured as 3.83 m. The same length was measured as 3.82 m on the 3D model, and 3.85 m in the horizontal section taken on the point cloud. The distance between two opposing columns in the field was 6.97 m. The same length measured 6.93 m on the 3D model. The average of the wall thickness on the façade, where the south entrance door of the building is located, was measured as 1.50 m in the horizontal section (Figure 4).
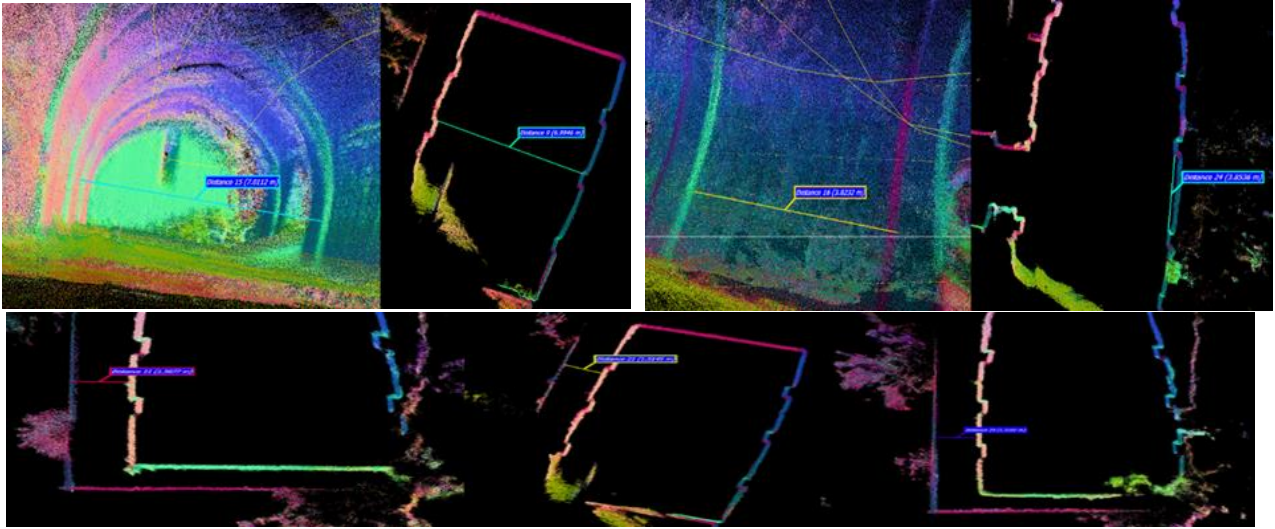
Figure 4. Length measurement in section and 3D models

Results

Comparing the lengths measured in the field with the lengths measured from the model, it was calculated below 5cm.

Discussion

In the process stages of the study, it was observed that the faults in the defected lands and the vineyards grew. in this case, errors are reduced when using the GCP point.

Conclusion

In order to obtain the correct data in documentation studies, documentation studies have now left their place to modern documentation techniques with the developing technology. One of these technologies is GML technology.

In this study, as a result, it has been seen that it is possible to document and map the historical heritage in 3D with GML technology using the GCP point.

References

1. Çalışkan, M., Aydın, A., Aydınoğlu, Ü., & Kerem, F. (2009) Mersin Ören Yerleri Kaleleri Müzeleri, T.C. Mersin Valiliği, Seçil Ofset II. Baskı, İstanbul

2. Yılmaz, H. M., & Yakar, M. (2006). Yersel lazer tarama Teknolojisi. *Yapı teknolojileri Elektronik dergisi*, *2*(2), 43-48.

3. Yılmaz, H. M., Karabörk, H., & Yakar, M. (2000). Yersel fotogrametrinin kullanım alanları. *Niğde Üniversitesi Mühendislik Bilimleri Dergisi*, *4*(1), 1.

4. Yakar, M., Orhan, O., Ulvi, A., Yiğit, A. Y., & Yüzer, M. M. (2015). Sahip Ata Külliyesi Rölöve Örneği. *TMMOB Harita ve Kadastro Mühendisleri Odası*, *10*.

5. Yakar, M., & Yilmaz, H. M. (2008). Using in volume computing of digital close range photogrammetry. *The International Archives of the Photogrammetry, Remote Sensing and Spatial Information Sciences. Vol. XXXVII. Part B3b.*

6. Alptekin, A., & Yakar, M. (2021). 3D model of Üçayak Ruins obtained from point clouds. *Mersin Photogrammetry Journal*, *3*(2), 37-40.

7. Alptekin, A., & Yakar, M. (2020). Determination of pond volume with using an unmanned aerial vehicle. *Mersin photogrammetry journal*, *2*(2), 59-63.

8. Karataş, L., Alptekin, A., Kanun, E., & Yakar, M. (2022). Tarihi kârgir yapılarda taş malzeme bozulmalarının İHA fotogrametrisi kullanarak tespiti ve belgelenmesi: Mersin Kanlıdivane ören yeri vaka çalışması. *İçel Dergisi*, *2*(2), 41-49.

9. Kanun, E., Alptekin, A., & Yakar, M. (2021). Cultural heritage modelling using UAV photogrammetric methods: a case study of Kanlıdivane archeological site. *Advanced UAV*, *1*(1), 24-33.

10. Şasi, A., & Yakar, M. (2017). Photogrammetric modelling of sakahane masjid using an unmanned aerial vehicle. *Turkish Journal of Engineering*, *1*(2), 82-87.

11. Yakar, M., & Doğan, Y. (2017). Mersin Silifke Mezgit Kale Anıt Mezarı fotogrametrik rölöve alımı ve üç boyutlu modelleme çalışması. *Geomatik*, *2*(1), 11-17.

12. Karataş, L., Alptekin, A., & Yakar, M. (2022). Creating Architectural Surveys of Traditional Buildings with the Help of Terrestrial Laser Scanning Method (TLS) and Orthophotos: Historical Diyarbakır Sur Mansion. *Advanced LiDAR*, *2*(2), 54-63.

13. Ulvi, A., Yakar, M., Toprak, A. S., & Mutluoglu, O. (2014). Laser scanning and photogrammetric evaluation of Uzuncaburç Monumental Entrance. *International Journal of Applied Mathematics Electronics and Computers*, *3*(1), 32-36.

14. Yılmaz, H. M., & Yakar, M. (2006). Lidar (Light Detection And Ranging) Tarama Sistemi. *Yapı Teknolojileri Elektronik Dergisi*, *2*(2), 23-33.

15. Karataş, L., Alptekin, A., & Yakar, M. (2022). Analytical Documentation of Stone Material Deteriorations on Facades with Terrestrial Laser Scanning and Photogrammetric Methods: Case Study of Şanlıurfa Kışla Mosque. *Advanced LiDAR*, *2*(2), 36-47.

16. Alptekin, A., & Yakar, M. (2020). Mersin Akyar Falezi'nin 3B modeli. *Türkiye Lidar Dergisi*, *2*(1), 5-9.

17. Kanun, E., Alptekin, A., Karataş, L., & Yakar, M. (2022). The use of UAV photogrammetry in modeling ancient structures: A case study of "Kanytellis". *Advanced UAV*, *2*(2), 41-50.

18. Korumaz, A. G., Dülgerler, O. N., & Yakar, M. (2011). Kültürel mirasin belgelenmesinde dijital yaklaşımlar. *Selçuk Üniversitesi Mühendislik, Bilim ve Teknoloji Dergisi*, *26*(3), 67-83.

19. Karabacak, A., & Yakar, M. Giyilebilir Mobil LİDAR Kullanım Alanları ve Cambazlı Kilisesinin 3B Modellemesi. *Türkiye Lidar Dergisi*, *4*(2), 37-52.

20. https://paksoyteknik.com.tr/index.php/paksoy-topcon/lazer-tarama/gexcel-heron

Advanced Engineering Days

aed.mersin.edu.tr

Production of road maps in highway projects by unmanned aerial vehicle (UAV)

Fatih Tükenmez *[1] , **Murat Yakar** [2]

[1]5th Regional Directorate of Highways, Chief Survey, Project and Environmental Engineering, Mersin, Türkiye, f.tukenmez@hotmail.com
[2] Mersin University, Engineering Faculty, Geomatics Engineering Department, Türkiye, myakar@mersin.edu.tr

Keywords
UAV
DTM
Photogrammetry
Bitumen
Highway Project

Abstract
Unmanned aerial vehicles (UAVs), which are used in many areas of use today and are among the contemporary measurement systems, have recently been used in highway projects. In highway projects, there is a direct correlation between the accuracy and precision of the existing digital maps and the calculation of the geometric components of the horizontal and vertical (profile-long-section) lines of the project route, followed by the determination of the excavation filling amounts (cubage), also expressed as soil movement. The data collected by the unmanned aerial vehicle was used in this study to conduct research for the creation of route maps (strip data), which serve as the foundation for highway projects. The study region, which was 2 km of the Mersin-Findikpinar Provincial Road project route, was part of the road system of the 5th Regional Directorate of Highways. According to the pre-determined flight plan, the UAV was flown at a height of 195 meters to capture 70% transverse and 85% longitudinal superimposed pictures in a 200 m wide corridor roughly 100 m to the right and 100 m to the left of the route chosen in the study area. A Digital Terrain Model and Route Map of the chosen corridor were created as a consequence of the photogrammetric analysis of these images. The volume computation was carried out using a sample highway project in a common area established between the high-accuracy 1/1000 scale baseline maps of the study area produced by the terrestrial method and the baseline maps produced by the UAV photogrammetry method. Digital Terrain Models (DTMs) have been contrasted. The location accuracy of the orthophoto map created by determining the coordinates of the detail points in the field with the RTK GPS technique was measured in addition to the YKN used as a reference, and an approximation cost comparison between the two techniques was made.

Introduction

Transportation is generally defined as the displacement of passengers and goods [1-4]. The highway, which is one of the transportation routes, is the land strips, bridges, tunnels, all kinds of art structures, protection structures, and other areas open to the public in order to allow traffic flow for the safe, fast, and comfortable transportation of passengers and goods. Highways, as in the past, have a great share in the development and prosperity of societies today [5-8]. The contribution of this system, which is realized with a large investment, to the national economy depends on the appropriate selection of the highway route and low construction, maintenance, and operating costs. In this respect, there is a need for those who use the highway to study and know the elements constituting it very well.

The existing maps, which are used as a base for highway projects, are composed of streams, hills, roads, ETL, etc., covering a corridor with a width of approximately 200 m. They are strip-like maps showing structures. Stream, ditch, slope, etc., which are defined as critical land sections on the highway project routes in the current maps in question. In order for the sections to reflect the real terrain and for the accurate calculation of the soil volume amounts, it is important that the current map digital elevation model sensitivity is high [8-10].

In the production of highway route maps and digital terrain models, generally, labor-intensive traditional terrestrial methods or classical aerial photogrammetry are used. In addition to these methods, the use of advanced

technology remotely controlled UAVs (Unmanned Aerial Vehicles) is also important when evaluated in terms of time and workforce [10-15].

The highway is one of the most important infrastructure investments made by human beings. The common space of human beings is the forward journey of societies. The history of the roads starts with the first person and goes on and on, developing from the past to the future. The path to this cause is the most important infrastructure that forms the basis for the development of a country and the socio-economic development of society. The use of UAV technology on highways, especially on the routes where mountainous and dense forest areas are hit, enables the production of maps at a low cost in a short time. UAVs on Highways; production of digital base maps of project routes, production of maps of landslide areas, production of maps of intersection areas, etc. frequently used in applications.

Material and Method

In addition to the polygon stones, 51 YCP points were established in the study area, 23 of them were used in Balancing and 51 of them were used as check notes in orthophoto accuracy analysis. The desired land topography is an undulating land structure so that the soil movements (excavation and fill amounts) on the highway project routes can balance each other. For this reason, this section of Mersin Fındıkpınarı Provincial Road, which has a wavy land structure, was preferred in order to make a more accurate comparison in the soil movement evaluation (excavation-fill) of the DTM (Digital Terrain Model) to be obtained in this study as the study area. Before the field studies, the UAV (Revolving Wing) to be used in the application, digital camera (integrated with the UAV), GNSS device, and (cloth tarpaulin and line paint) to be established as ground control points in the evaluation of the photographs obtained by the UAV were provided (Figure 1).

Figure 1. Ground Control Point Facilities view

Results

In this study, the cubage of the project route was determined by using digital terrain models produced in both methods of a route of approximately 1.5 km in the section of Mersin Fındıkpınarı Provincial Road, which was produced by the digital method in 2014, with the terrestrial method. Inroads running under the MicroStation V8I program were used in this sample project work. Highway project route geometric elements outline; consists of Horizontal Geometry, Vertical Geometry, superelevation, and cross-section. In this study, the DTM model produced by the terrestrial method using the same design parameters of the same route, and the DTM produced by the UAV Photogrammetry method was used. The excavation volume of 107682.456 m³ and the fill volume of 75908.986 m³ were calculated at the project site, which was obtained by using DTM produced by the Terrestrial Method, and there is an excess of 31773.469 m³ of excavation. 108951.136 m3 excavation and 74768.338 m³ fill volume were calculated on the project route obtained by using DTM produced by the UAV Photogrammetry method (Figure 2). The amount of soil advance obtained as a result of the application was calculated and the comparison results are given in Table 1.

Table 1. Excavation Fill Amounts Comparison.

Items	Geodetic DTM	UAV DTM	Difference
Splitting Volume (m³)	107686.456	108951.136	1268.68
Fill Volume (m³)	75908.98	74768.338	-1140.648
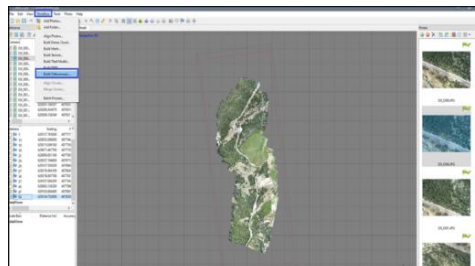
Figure 2. Agisoft Workspace DTM and Orthomosaic Build Menu

Conclusion

In the accurate evaluation of the orthophoto map produced with Agisoft Photoscan software, the GCP points were established in the study area, and in addition to these points, 30 points in total, 81 points from which GPS/RTK measurement technique coordinates were obtained in the field. In the determination of these 30 detail points, the existing building corners, wall points, mid-road line details, etc. points are used. The coordinates of these points, which are accepted as exact coordinates, on the orthophoto map were determined using NetCAD software. The square mean errors and mean position errors of these points used in the orthophoto map accuracy assessment were calculated as my = ± 2.76 cm, mx = ±2.64 cm and mP = ± 3.81 cm. When these results are examined, the calculated values are; According to Large Scale Map and Map Information Production Regulation and Technical Specification for Highways Terrestrial and Photogrammetric Map Engineering Services, it was observed that it remained within the error limit (± 7 cm) determined under the heading of detail measurement accuracy. A cost evaluation was made between the terrestrial method and UAV Photogrammetry in the production of the current map of the study area, which has an area of approximately 50 hectares. The approximate cost of the map produced using the Rotary Wing UAV was found to be 4682.10 TL, and the approximate cost of the map produced by the terrestrial method was 9648.53 TL.

Acknowledgement

References

1. Yakar, M., & Yilmaz, H. M. (2008). Using in volume computing of digital close range photogrammetry. *The International Archives of the Photogrammetry, Remote Sensing and Spatial Information Sciences. Vol. XXXVII. Part B3b*.
2. Yakar, M., Yılmaz, H. M., & Mutluoğlu, Ö. (2010). Comparative evaluation of excavation volume by TLS and total topographic station based methods. Lasers in Engineering, 19, 331–345
3. Alptekin, A., & Yakar, M. (2020). Heyelan bölgesinin İHA kullanarak modellenmesi. Türkiye İnsansız Hava Araçları Dergisi, 2(1), 17-21.
4. Yılmaz, H. M., & Yakar, M. (2008). Computing of volume of excavation areas by digital close range photogrammetry. The Arabian Journal for Science and Engineering, 33, (1A), 63-79.
5. Yilmaz, H. M., Yakar, M., & Yildiz, F. (2008). Digital photogrammetry in obtaining of 3D model data of irregular small objects. The International Archives of the Photogrammetry, Remote Sensing and Spatial Information Sciences, 37, 125-130.
6. Yılmaz, H. M., Karabörk, H., & Yakar, M. (2000). Yersel fotogrametrinin kullanım alanları. Niğde Üniversitesi Mühendislik Bilimleri Dergisi, 4(1), 1.
7. Kusak, L., Unel, F. B., Alptekin, A., Celik, M. O., & Yakar, M. (2021). Apriori association rule and K-means clustering algorithms for interpretation of pre-event landslide areas and landslide inventory mapping. *Open Geosciences*, *13*(1), 1226-1244.
8. Alptekin, A., & Yakar, M. (2020). Heyelan bölgesinin İHA kullanarak modellenmesi. *Türkiye İnsansız Hava Araçları Dergisi*, *2*(1), 17-21.
9. Unal, M., Yakar, M., & Yildiz, F. (2004, July). Discontinuity surface roughness measurement techniques and the evaluation of digital photogrammetric method. In Proceedings of the 20th international congress for photogrammetry and remote sensing, ISPRS (Vol. 1103, p. 1108).
10. Alptekin, A., & Yakar, M. (2021). 3D model of Üçayak Ruins obtained from point clouds. Mersin Photogrammetry Journal, 3(2), 37-40.
11. Yakar, M., & Yilmaz, H. M. (2008). Using in volume computing of digital close range photogrammetry. *The International Archives of the Photogrammetry, Remote Sensing and Spatial Information Sciences. Vol. XXXVII. Part B3b*.
12. Ünel, F. B., Kuşak, L., Çelik, M., Alptekin, A., & Yakar, M. (2020). Kıyı çizgisinin belirlenerek mülkiyet durumunun incelenmesi. Türkiye Arazi Yönetimi Dergisi, 2(1), 33-40.
13. Alptekin, A., & Yakar, M. (2020). Determination of pond volume with using an unmanned aerial vehicle. Mersin photogrammetry journal, 2(2), 59-63.
14. Yakar, M., & Karabacak, A. (2019). Bilgisayar Destekli Harita Çizimi (Netcad 5.0). 1. Baskı, Atlas Akademi.
15. Karataş, L., Alptekin, A., Kanun, E., & Yakar, M. (2022). Tarihi kârgir yapılarda taş malzeme bozulmalarının İHA fotogrametrisi kullanarak tespiti ve belgelenmesi: Mersin Kanlıdivane ören yeri vaka çalışması. İçel Dergisi, 2(2), 41-49.

Modeling of the historical monument with mobile phone-based photogrammetry method

Abdurahman Yasin Yiğit*1 , **Murat Yakar1**

1Mersin University, Engineering Faculty, Geomatics Engineering Department, Türkiye, ayasinyigit@mersin.edu.tr, myakar@mersin.edu.tr

Keywords
Cultural heritage
Photogramemtry
Mobile-phone
3D

Abstract
Efforts to obtain accurate and healthy data in the documentation of cultural heritages have led to the emergence of new techniques in the field of documentation. With the developing technology, traditional methods have left their place for modern documentation techniques, and this has allowed documentation techniques to progress rapidly. One of these developing techniques is the photogrammetry technique. With the photogrammetry technique, in digital documentation, a detailed examination of a structure with limited or complex access and 3D models of the elements can be obtained. The basic material of the photogrammetry technique photographs. All cultural artifacts should be documented digitally and photogrammetry is one of the best methods. In this study, a small-scale historical monument was photographed with a mobile phone camera and documented by the photogrammetry method.

Introduction

Cultural heritages are generally historical buildings, modern structures, bridges, statues, monuments, etc., that constitute the wealth of a place and its population due to its historical, cultural, and artistic significance [1-6]. It is defined as a set of related entities such as the Conservation and restoration of cultural heritage including the preservation of historical buildings using new technologies to preserve their original condition for as long as possible and to pass this knowledge on to future generations. Often, geometric research is associated with tracing and documenting heritage [7]. The protection of cultural heritage objects is a complex and multidisciplinary activity. A large number of cultural heritage studies are obtained by monitoring the risks to which a cultural heritage property may be exposed, or by recommendations on preventing or minimizing damage. Therefore, although the degree of importance of these works is a criterion, each work must be documented. Recently, experts in the documentation of cultural heritage have made various studies in the documentation of historical artifacts with photogrammetric applications [8]. When the literature is reviewed, studies on the documentation of cultural heritage generally stand out as the production of photogrammetric 3D or 2D models of the exteriors of buildings with different approaches [9-15]. However, there are few studies on the documentation of small works of historical importance. With the photogrammetry technique, in digital documentation, a detailed examination of a structure with limited or complex access and 3D models of the elements can be obtained. The basic material of the photogrammetry technique photographs. In this study, a column base was modeled in 3D from photographs obtained by photogrammetry using a mobile phone camera.

Material and Method

In photogrammetry, the 3D coordinates of points on an object's surface are determined by the camera positions and external orientation parameters of the overlapping images. External orientation parameters can be calculated if the overlapping images have at least three control points. Internal orientation parameters have to be known

beforehand, but thanks to new algorithms such as Structure from Motion (SfM), the necessity of knowing internal orientation parameters is eliminated with the self-calibration technique. Thanks to SfM algorithm-based photogrammetric software, 3D modeling and reconstruction of surfaces from photographs taken with conventional cameras have become quite easy. SfM; A photogrammetric technique or algorithm that automatically solves the geometry of the scene, camera positions, and orientation without requiring pre-definition of a target mesh with known 3D positions. SfM is a measurement method based on computer visualization techniques; With the use of digital cameras, video cameras, or smart phones with cameras in this area, it has gained popularity with its frequent use in various studies by many disciplines. For this reason, its use in scientific research has become very common and has had a transformative effect on earth science research due to its low cost, extremely fast results, and easy 3D measurement capability. In the SfM method, a series of overlapping picture frames are used to create 3D structures. It works by finding and matching commonalities across a series of overlapping photos. This study has tried to document a monument of historical importance with the methods of close-range photogrammetry. In total, 41 images were collected. The photos were taken with a mobile cell phone camera with a resolution of 12 megapixels (Table 1). The 3D model of the monument was made with the Agisoft Meteshape software.

Table 1. Smartphone camera specifications

Parameters	Value
Focal length	27 mm
Aperture	F1.8
Camera Resolution	12 MP - 1.25µm
Number of pixels	16 Million

Results

In the study, as shown in Figure 1, photographs were taken as superimposed and 360 degrees around the work. Overlay ratios are set completely manually.
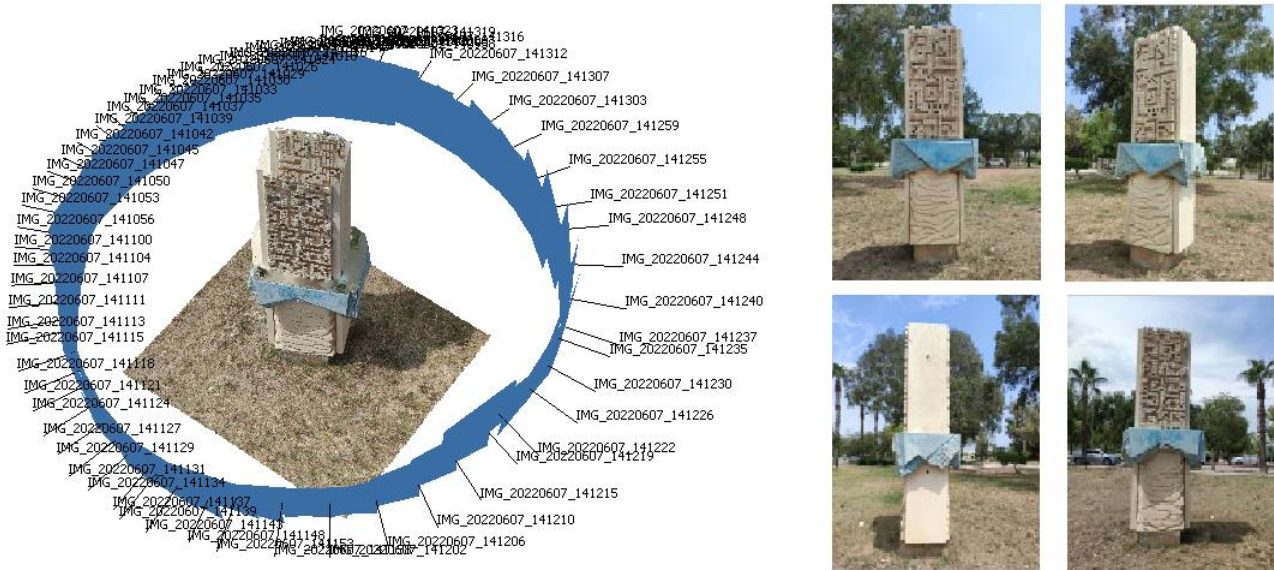
Figure 1. Photograph capturing method and sample photos

Then the photos taken were transferred to the software. First, a sparse point cloud was produced by applying the self-calibration method and the images were aligned. Then, a dense point cloud was created with the SfM algorithm (Figure 2/a). Finally, the 3D Mesh and 3D Wire Frame models necessary to produce the 3D model were created (Figure 2/b).
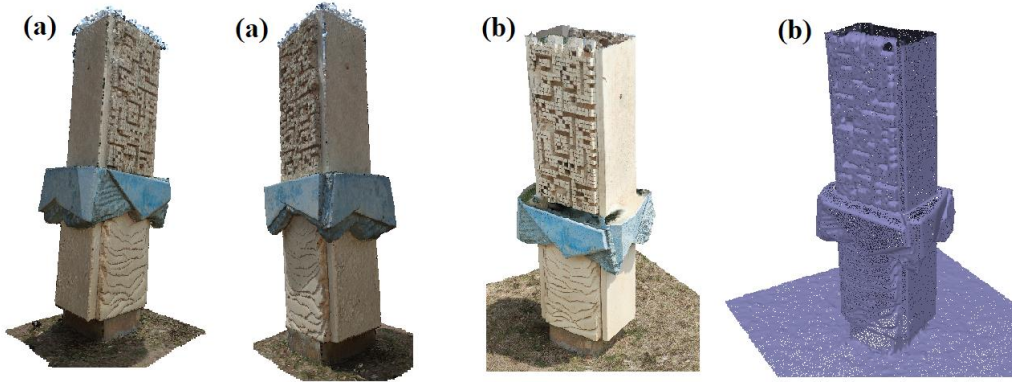
Figure 2. Dense point cloud (a) and 3D model (b)

Conclusion

The development of computer technology and software has contributed positively to the determination of the behavior of complex structures by 3D modeling, and the digital model of the structure has become easily created. 3D models are frequently used in documentation studies because they contain many details of the structure. 3D models created with the photogrammetry method are formed in real size and appearance. Photogrammetric measurement systems enable the determination of the actual object geometry as well as the modeling of the object. In addition, these technologies enable 3D models with real images, especially since they are processed with the real image of the object.

References

1. Yakar, M., & Yilmaz, H. M. (2008). Using in volume computing of digital close range photogrammetry. The International Archives of the Photogrammetry, Remote Sensing and Spatial Information Sciences. Vol. XXXVII. Part B3b.
2. Yakar, M., Yılmaz, H. M., & Mutluoğlu, Ö. (2010). Comparative evaluation of excavation volume by TLS and total topographic station based methods. Lasers in Engineering,19, 331–345
3. Yılmaz, H. M., & Yakar, M. (2008). Computing of volume of excavation areas by digital close range photogrammetry. The Arabian Journal for Science and Engineering, Volume 33, Number 1A, 63-79.
4. Yilmaz, H. M., Yakar, M., & Yildiz, F. (2008). Digital photogrammetry in obtaining of 3D model data of irregular small objects. The International Archives of the Photogrammetry, Remote Sensing and Spatial Information Sciences, 37, 125-130.
5. Yılmaz, H. M., Karabörk, H., & Yakar, M. (2000). Yersel fotogrametrinin kullanım alanları. Niğde Üniversitesi Mühendislik Bilimleri Dergisi, 4(1), 1.
6. Kusak, L., Unel, F. B., Alptekin, A., Celik, M. O., & Yakar, M. (2021). Apriori association rule and K-means clustering algorithms for interpretation of pre-event landslide areas and landslide inventory mapping. Open Geosciences, 13(1), 1226-1244.
7. Yakar, M., L. Kuşak, F. B. Ünel, and M. Oğuz. 2019. Küçük-Yan Nokta ve Kesişim Hesabı (Çözümlü Örnekler). 1. Baskı, Atlas Akademi.
8. Unal, M., Yakar, M., & Yildiz, F. (2004, July). Discontinuity surface roughness measurement techniques and the evaluation of digital photogrammetric method. In Proceedings of the 20th international congress for photogrammetry and remote sensing, ISPRS (Vol. 1103, p. 1108).
9. Korumaz, A. G., Dülgerler, O. N., & Yakar, M. (2011). Kültürel mirasin belgelenmesinde dijital yaklaşimlar. *Selçuk Üniversitesi Mühendislik, Bilim ve Teknoloji Dergisi*, *26*(3), 67-83.
10. Ünel, F. B., Kuşak, L., Çelik, M., Alptekin, A., & Yakar, M. (2020). Kıyı çizgisinin belirlenerek mülkiyet durumunun incelenmesi. Türkiye Arazi Yönetimi Dergisi, 2(1), 33-40.
11. Yakar, M., & Karabacak, A. (2019). Bilgisayar Destekli Harita Çizimi (Netcad 5.0). 1. Baskı, Atlas Akademi.
12. Kanun, E., Alptekin, A., Karataş, L., & Yakar, M. (2022). The use of UAV photogrammetry in modeling ancient structures: A case study of "Kanytellis". *Advanced UAV*, *2*(2), 41-50.
13. Yilmaz, H. M., & Yakar, M. (2006). Yersel lazer tarama Teknolojisi. *Yapı teknolojileri Elektronik dergisi*, *2*(2), 43-48.
14. Cengiz, A., Semra, A., & Yakar, M. (2010). Measurement of petroglyhps (rock of arts) of Qobustan with close range photogrammetry. *International Archives of Photogrammetry, Remote Sensing and Spatial Information Sciences*, *38*(Part 5), 29-32.
15. Mohammed, O., & Yakar, M. (2016). Yersel Fotogrametrik Yöntem İle İbadethanelerin Modellenmesi. *Selcuk University Journal of Engineering Sciences*, *15*(2), 85-95.

An overview of organic pollutants concentrations in the port of Durres, Adriatic Sea

Esmeralda Halo[*1] , **Aurel Nuro** [1] , **Bledar Myrtaj**[1] , **Jonida Tahiraj** [1] , **Sonila Kane** [1]

University of Tirana, Faculty of Natural Science, Department of Chemistry, Albania, esmeraldahalo647@gmail.com

Keywords
Port of Durres
OCPs
PCBs
PAHs
Water analyze
GC/ECD/FID

Abstract
The findings reported here belong to a study on determination of organochlorine pesticides (OCPs), polychlorinated biphenyls (PCBs) and polycyclic aromatic hydrocarbons (PAH) concentrations in water samples of the port of Durres which is the largest port of Albania. In it are processed the main part of commercial and passengers shipping in Albania. These substances that present high risks are classified as priority substances. Although the production and use of these substances has been banned for decades, their presence continues to be reported due to their high persistence in the environment. Water samples were taken in 12 different stations of the port of Durres in two periods (May and July 2022). Organochlorine compounds were extracted simultaneously using liquid-liquid technique using hexane as extracting solvent. Also, PAHs were extracted also using liquid-liquid technique using dichloromethane and hexane (two steps) as extracting solvent. Chlorinated pollutants were determined by gas chromatography electron capture detection (GC/ECD) while PAH by gas chromatography flame ionization detector (GC/FID). Organochlorine pesticides (mostly their metabolites) were detected almost in all water samples because of their previous use. Also, PCBs and PAHs were found almost for all analyzed samples. Their presence could be because of elevated activity and ship transport in port area. The found levels for these priority substances in waters of Port of Durres was higher / comparable with reported levels of them from others stations of Adriatic Sea, Albania part.

Introduction

In this study was determined some priority substances concentrations in water samples of the port of Durres. The Port of Durres is the largest seaport of Albania, located in Adriatic Sea. It is an artificial basin that is formed between two moles. The Port is located at the north end of the Bay of Durres, an extensive body of water between Castel of Turra and Cape Durres. As of 2014, the port ranks as the largest passenger port in Albania and one of the largest passenger port in the Adriatic Sea, with annual passenger volume of more than 1.5 million.

Organochlorine pesticides (OCPs), polychlorinated biphenyls (PCBs), polycyclic aromatic hydrocarbons (PAH) and some other pollutants are classified as Persistent Organic Pollutants (POP), because they are persistent for many years after their application [1, 2]. Great concern was caused by chlorinated compounds, which proved to be extremely persistent in the environment and after that in the food chain [2, 3, 5]. For more than 50 years (after the Second World War to 90') organochlorine pesticides were used widely in Albania against malaria vector and for agricultural purposes. PCBs have not been used in Albania since 90s. They can only be found in some electrical transformers that were used in the early 1990s, but they were reported in many water ecosystems of our country because of atmospheric depositions. PAHs are pollutants generated by automobiles transport, extracting/processing of oil industry, coal mine and other industries. PAH could be found in marine water because of ship transport or some accident spills of hydrocarbons. Forest burning and their natural background make them very often in environment. Organochlorine pollutants (OCP and PCB) and PAHs have high stability, high bioaccumulation capacity and the ability to spread out far away from the application site. Generally, these compounds are difficult to degrade and can persist for many years in particular in water ecosystems [3, 6, 7, 8].

Material and Method

Sampling: Water samples from the port of Durres were taken in 12 different stations of the port of Durres (10 inside and 2 outside its area). Water samples were taken in in two sampling periods (May and July 2022). A volume of 2.5l of water were taken from each station in Teflon bottles. The sampling method was based on UNEP/MED Wg. 128/2, 1997. Water samples were tranported and conserved at +4°C before being analyzed.

Analyzes of pesticides and PCBs by GC/ECD: Liquid-liquid extraction was used for extraction of OCPs and PCBs from water samples. One liter of water and 40 ml n-hexane as extracting solvent were added in a separator funnel. After extraction, the organic phase was dried with anhydrous Na_2SO_4 for water removing. A florisil column was used for the sample clean-up. 20 ml n-hexane/dichloromethane (4/1) was used for their elution. After concentration up to 1 ml, the samples were injected in GC/ECD. OCPs and PCBs were analyzed simultaneously using capillary column model Rtx-5 (30 m long x 0.25 mm i.d. x 0.25 μm film thicknesses) on a gas chromatograph model Varian 450 GC equipped with μECD detector. The organochlorine pesticides detected were DDT-related chemicals (o,p-DDE, p,p-DDE, p,p-DDD, p,p-DDT), HCHs (a-, b-, γ- and d-isomers), Heptachlor's (Heptachlor and Heptachlorepoxide); Aldrin's (Aldrine, Dieldrine and Endrin) and Endosulfanes (Endosulfan alfa, Endosulfan beta and Endosulfan sulfat). Analysis of PCBs was based on the determination of the seven PCB markers (IUPAC Nr. 28, 52, 101, 118, 138, 153 and 180). Their quantification was based on external standard method [4-9].

Analyzes of PAHs by GC/FID: Liquid-liquid extraction was used for extracting PAHs from marine water samples. In a volume of 1 liter of water that was put in a separation funnel was added 30 ml dichloromethane first and after that 30 ml hexane as extracting solvent were added in it. After extraction, the organic phase was dried and concentrated to 1 ml using Kuderna-Danish and then were injected in GC/FID for their quantification. Gas chromatographic analyses of PAH in water samples were realized with a Varian 450 GC instrument equipped with a flame ionization detector and PTV detector. VF-1 ms capillary column (30 m x 0.33 mm x 0.25 μm) was used to isolate and determine 13 PAHs according to EPA 525 Method. Acenaphthylene, Fluorene, Phenanthrene, Anthracene, Pyrene, Benzo [a] anthracene, Chrysene, Perilene, Benzo [b] fluoranthene, Benzo [k] fluoranthene, Indeo [1,2,3-cd] pyrene, Dibenzo [a, b] anthracene and Benzo [g, h, i] perylene were determined in seawater samples. Quantification of PAH was based on external standard method [7, 9].

Results

In this study were analyzed marine water samples from port of Durres, which is located in Adriatic Sea. Samples were taken in May and July 2022. This is the main port of Albania for passengers and commercial shipping. Organochlorine pesticides and PCB markers were analyzed using GC/ECD while PAH by using GC/FID techniques. These substances were classified as priority substances because of their stability and toxicity. The processed data on OCP classes, total of pesticides, PCBs and PAHs were shown in Table 1.

Table 1. Statistical data on OCPs, PCBs and PAHs for water samples of the port of Durres in May and July 2022

	May 2022					July 2022				
	Mean	**Median**	**STDEV**	**Min**	**Max**	**Mean**	**Median**	**STDEV**	**Min**	**Max**
HCHs	0.19	0.09	0.25	N.D.	0.66	1.37	0.54	1.67	0.09	5.65
DDTs	0.08	0.06	0.08	N.D.	0.25	0.47	0.23	0.58	N.D	2.15
Aldrin's	0.49	0.28	0.52	0.05	1.46	0.61	0.43	0.56	0.05	2.10
Heptachlor's	0.06	0.02	0.08	N.D.	0.26	0.49	0.28	0.56	N.D.	1.72
Endosulfane's	0.11	0.08	0.10	N.D.	0.34	0.27	0.12	0.35	N.D.	1.25
Pesticides	1.17	1.05	0.79	0.29	2.22	3.61	3.56	1.51	1.63	6.59
PCBs	2.14	1.48	2.08	0.27	7.63	1.73	0.66	3.82	0.15	13.79
PAHs	1.03	0.83	0.91	0.29	3.35	4.57	4.86	2.22	1.97	8.61

Discussion

Pesticides were present in all water samples of Durresi's port. Their maximum was in water samples of July around 3 times higher than in May 2022. Their presence could be because more intense agricultural activity in this period. New arrival from the rivers (rivers of Ishmi, Erzeni, Shkumbini, Semiani, etc.) could be another factor in found concentrations. Their total for all analyzed samples was lower than 50 ng/l, a limit values for the total of pesticides in surface waters based on 2013/39 EU Directive. Lindane and its isomers (alpha-, beta-, and delta-hexachlorocyclohexanes-HCHs) were found in higher concentrations (around 8 times higher) in July seawater samples. Notes that Lindane was found only in 25% of all analyzed samples. Delta-, alfa- and beta-HCH isomers were found to be in majority for all seawater samples. Their origin could be because of their presence as an impurity in other pesticide formulations or because it's physical – chemistry properties. Also, HCH isomers could

be found because of degradation of other pesticides, new arrivals by rivers and urban wastes. For all stations, total of HCHs was lower than permitted level (0.04 ug/l) conforming to EU Directive 2013/39. DDTs (4,4'-DDT, 4,4'-DDD and 4,4'-DDE) were found in 67% water samples for the port of Durres for both periods. The higher DDT levels were found in July (around 3 times higher than in May). Note that DDT degradation products (DDD and DDE) were found in higher concentration in all stations, Average of DDTs in port area was lower compare with other stations on Adriatic Sea [5, 6, 8]. DDT was lower than permitted level (0.01 ug/L) in marine water based on Albanian and EU norms. Aldrine's were found almost in all water samples for the port of Durres. A slight higher levels of Aldrines were found in May 2022. This fact is connected with the use of Aldrins in this period, any punctual source or because on new arrival by rivers or effluents near the port area. Sweater currents inside/outside the port and momentum values are not excluded. Aldrins were found in lower levels than EU directive 2013/39 and Albanian norms. Heptachlors were found in higher concentrations in July. The higher levels in all analyzed samples were found Heptachlor epoxide, its degradation products. This fact is connected with the previous use of Heptachlor. Heptachlors in all samples were lower than EU Directive 2013/39. Total of Endosulfanes were 2 times higher in July samples. Their total was higher at stations inside the port area. These data could be the result of their previous use or and Endosulfan's punctual source near port of Durres. Endosulfan concentrations for water samples of Durresi port were lower than permitted level based on EU Directive 2013/39.

PCBs were found in all analyzed water samples. Their total was higher in May 2022. Presence of PCB markers in seawater samples can be related to the elevated mechanical and industrial activity in port area. For all water samples, volatile congeners (PCB 28 and PCB 52) were found at higher level. PCB concentrations for water samples of Durresi's port were comparable levels than the reported data on previous studies on the same stations [6, 7, 8].

PAHs were detected for all analyzed water samples. PAH were found 3 times higher in July 2022. Their presence could be because of elevated ship transport in this area. Automobilist transport and any possible accident could be another source of PAH pollution in marine water samples of Durres port. The presence of some individual PAHs in higher level was noted. Also, this could be a momentum value of PAHs. PAH levels in seawater samples were in the same range/higher than the reported levels for other stations of Adriatic Sea, Albania [8, 9]. The presence of some individual PAHs was higher than permitted level according to Albanian and EU norms.

Conclusion

Organochlorine pesticides, their residues, PCBs and PAHs were found in all water samples of Durresi port, for both periods. The higher levels of these pollutants were found mostly in July 2022. It was noted presence of degradation products of pesticides in higher levels compare to their active products. This fact is related with the previous use of pesticides in Albania and their degradation process. Aldrine's (in May) and HCHs (in July) were shown to be in high level in all samples. This pesticide could be in use in near port area or because of new arrivals by terrestrial or water currents inside-outside port of Durres. PCBs volatile were found at high levels for all seawater samples. Their presence could be because of their atmospheric deposition. Some water samples were detected heavy PCB. This could be connected with punctual sources of PCBs in these stations. PAHs were found in all water samples because of ship transport, automobilist transport and any possible accident of hydrocarbons near the area of Durres port. Momentum values of them are not excluded. Generally, concentrations of organochlorine pesticides, PCBs and PAHs were lower than permitted levels for surface waters according to EU Directive 2013/39 and Albanian norms. Monitoring of organic pollutants in water of Durres port should be continuous because of its importance in Albanian economy overall.

References

1. Lekkas, T., Kolokythas, G., Nikolaou, A., Kostopoulou, M., Kotrikla, A., Gatidou, G., ... & Lekkas, D. F. (2004). Evaluation of the pollution of the surface waters of Greece from the priority compounds of List II, 76/464/EEC Directive, and other toxic compounds. *Environment international*, *30*(8), 995-1007.
2. Vryzas, Z., Vassiliou, G., Alexoudis, C., & Papadopoulou-Mourkidou, E. (2009). Spatial and temporal distribution of pesticide residues in surface waters in northeastern Greece. *Water research*, *43*(1), 1-10.
3. Wells, D. E., & Hess, P. (2000). Determination and evaluation of chlorinated biphenyls. *Sample handling and trace analysis of pollutants, techniques, applications and quality assurance. Elsevier, Amsterdam*, 239-285.
4. Konstantinou, I. K., Hela, D. G., & Albanis, T. A. (2006). The status of pesticide pollution in surface waters (rivers and lakes) of Greece. Part I. Review on occurrence and levels. *Environmental Pollution*, *141*(3), 555-570.
5. Borshi, X., Nuro, A., Macchiarelli, G., & Palmerini, M. G. (2016). Analysis of Some Chlorinated Pesticides in Adriatic Sea: Case Study: Porto-Romano, Durres, Albania. *Journal of International Environmental Application and Science*, *11*(3), 270-276.

6. Çomo, E., Nuro, A., Murtaj, B., Marku, E., Shehu, E., & Emiri, A. (2013). Study of some organic pollutants in water samples of Shkumbini River, Albania. *Journal of International Environmental Application & Science*, *8*(4), 573-579.
7. Nuro, A., Marku, E., Murtaj, B., & Mance, S. (2014). Study of organochlorinated pesticides, their residues and PCB concentrations in sediment samples of Patoku Lagoon. *Journal of International Environmental Application & Science*, *9*(3), 452-458.
8. Murtaj, B., Nuro, A., Como, E., Marku, E., & Mele, A. (2013). Study of Organochlorinated Pollutants in Water Samples of Karavasta Lagoon. Science Bulletin of Faculty of Natural Sciences, Tirane, 14, 178-185.
9. Directive 2008/105/EC Of The European Parliament and of the Council on environmental quality standards in the field of water policy, amending and subsequently repealing Council Directives 82/176/EEC, 83/513/EEC, 84/156/EEC, 84/491/EEC, 86/280/EEC and amending Directive 2000/60/EC of the European Parliament and of the Council.

Determination of volatile organic pollutants in water samples of White Drin River, Kosovo

Aferdita Camaj[*1] , **Arben Haziri** [1] , **Aurel Nuro** [2] , **Arieta Camaj Ibrahimi** [3]

[1]*University of Pristina "Hasan Prishtina", Faculty of Natural Sciences, Department of Chemistry, Kosovo, aferditacamaj@gmail.com, arben.haziri@uni-pr.edu*
[2]*University of Tirana, Faculty of Natural Sciences, Department of Chemistry, Albania, aurel.nuro@fshn.edu.al*
[3]*University of Peja "Haxhi Zeka", Faculty of Agribusiness, Kosovo, arietacibrahimi@gmail.com*

Keywords
White Drin River
Chlorbenzene's
BTEX
Head Space
SPME
GC/ECD/FID

Abstract
In this paper, the concentrations of some volatile organic compounds (VOC) in water samples from the White Drin River (Kosovo) are presented. The White Drin River is one of the largest river in Kosovo and one of the largest in the Balkans. Water of the river could be affected by anthropogenic pollutions that comes mainly by directly discharges of urban wastewaters. The volatile organic pollutants that were analyzed were chlorobenzenes (mono-, di-, tri-, tetra-, penta- and hexachlororbenzene) and BTEX (Benzene, Toluene, Ethylbenzene, ortho-, meta- and para-Xylenes). Water samples were taken in February 2023, at 15 different stations from Drini Waterfall (near Peja to Albanian border). The head space solid phase micro-extraction (HS/SPME) method was used for the extraction and quantitative analysis of chlorobenzenes and BTEX followed by gas chromatography (GC) techniques. This method presents advantages for the analysis of volatile pollutants because it eliminates the use of organic solvents and different sample treatment steps that often lead to erroneous results. The sensitivity and reproducibility of HS is favorable for volatile organic pollutants. The adsorption of organic pollutants was carried out on a polydimethyl siloxane (PS) fiber at a temperature of 50ºC for 30 minutes. Desorption process was carried out in the injector of the gas chromatograph at high temperature (250ºC for 10 seconds). The qualitative and quantitative analysis of chlorobenzenes (mono-, di-, three-, tetra-, penta- and hexachlorobenzene) was realized in the GC/ECD apparatus, while the analysis of BTEX was carried out in the GC/FID apparatus. VOC were present almost in all analyzed samples. BTEX presence is related to the high intensity of transport near the river. The presence of chlorobenzenes can be a consequence of urban spills, of cleaning/sanitization processes, as degradation products of other compounds (pesticides, PCBs, etc.).

Introduction

Head-space (HS) technique is commonly used mainly for the concentration (extraction) and analysis of volatile organic compounds. In this technique the sample first establishes a balance between the gas phase (above in the head-space) and the sample which may be liquid or solid. This balance is established using moderate temperatures (30 - 70°C) to create the opportunity for volatile compounds to pass into the gas phase. After that, a polymer fiber which has high adsorption capabilities (Solid Phase Micro-Extraction or SPME) is used to fix homogeneous gas sample and pass it directly to the injector of the gas chromatograph (GC). The injector carries out the passage of the sample from the polymer fiber to the column of the apparatus through the desorption process at high temperature (220 - 280°C). Chromatographic columns enable the separation of all volatile compounds found in the sample. The head-space technique can be used in static and/or dynamic mode, Today, HS technique is fully automated. The advantage of HS technique is operation without the use of solvents and in a single step the extraction and analysis of the sample compounds is performed [1-2]. HS/SPME analysis followed by GC analysis consists of two steps: Adsorption of the compound from the sample and transfer of the sample directly to the gas

chromatograph by desorption process. The amount of analyte transferred to the instrument is proportional to the volume of the gas phase, and to the concentration of the analyte, accepting that the space above the sample is in equilibrium with the sample [3, 4].

Material and Method

Water sampling in Drini i Bardhe River: Water samples were taken in 15 different stations of the White Drin River. Water samples were sampled and analyzed in February 2023. A quantity of 2.5 litre of water from each station in Teflon bottles. The sampling method was based on ISO 5667-3: 2018. Water samples were tranported and conserved at +4°C prior to their analyze.

Analyzes of BTEX in water samples: For the determination of BTEX, 5 ml of water samples were taken from the stations of the White Drin River in SPME bottles with a volume of 10 ml. The bottles were equipped with Teflon stoppers suitable for their analysis by Head-space technique. The manual SPME syringe equipped with a 100 um PDMS (Polydimethyl siloxane) fiber was inserted through the Teflon stopper into the top of the sample. The bottle was placed at a temperature of 50°C for 30 minutes. PDMS fiber was transferred to the gas chromatograph injector where desorption process was carried out at 250°C for 10 seconds. For the qualitative and quantitative determination of BTEX, the Varian GC 450 apparatus equipped with a flame ionization detector (FID) and a PTV injector was used. The separation of BTEX was performed in VF-1ms (30m length x 0.33mm internal diameter x 0.25μm film), suitable for their separation [5-7].

Analyzes of chlorobenzenes in water samples: For the chlorobenzenes analyze, 5 ml of water samples were taken in SPME bottles with a volume of 10 ml. The bottles were equipped with Teflon stoppers suitable for their analysis by Head-space technique. The manual SPME syringe equipped with a 100 um PDMS (Polydimethyl siloxane) fiber was inserted through the Teflon stopper into the top of the sample. The bottle was placed at a temperature of 50°C for 30 minutes. The process of desorption for the chlorobenzenes was realized to the gas chromatograph injector at 260°C for 10 seconds. Qualitative and quantitative determination of chlorobenzenes was realized in a Varian GC 450 apparatus equipped with electron capture detector (ECD). The separation of chlorinated benzene derivates was performed by using a RTX-5 capillary column (30m length x 0.25mm internal diameter x 0.25μm film), suitable for their separation [8, 9].

Results

In this study, water samples from the White Drin River, which is one of the largest river in Kosovo, were analyzed. The water samples were taken in February 2023. The analysis of volatile organic compounds was carried out using the HS/SPME technique followed by gas chromatography technique. The qualitative and quantitative analysis of BTEX was realized by means of GC/FID, while the analysis of chlorobenzenes was realized by means of GC/ECD. The processed data for BTEX and chlorobenzenes in the water of the river are shown in Tables 1 and 2.

Table 1. BTEX data in water samples of White Drin River, February 2023

BTEX	Mean	STDEV	Median	Min	Max
Benzene	0.256	0.052	0.223	N.D.	1.187
Toluene	0.141	0.047	0.135	N.D.	1.583
m-Xylene	0.026	0.011	0.028	N.D.	0.186
p-Xylene	0.105	0.028	0.103	N.D.	0.748
o-Xylene	0.039	0.586	0.038	N.D.	0.102
Ethylbenzene	0.089	0.009	0.086	N.D.	0.211

Table 2. Data of chlorobenzenes in water samples of White Drin River, February 2023

Chlorobenzene	Mean	STDEV	Median	Min	Max
Chlorobenzene	0.428	0.103	0.418	N.D.	2.158
1,2-Dichlorobenzene	0.075	0.026	0.069	N.D.	0.126
1,3-Dichlorobenzene	0.052	0.013	0.055	N.D.	0.284
1,4-Dichlorobenzene	0.036	0.017	0.038	N.D.	0.206
1.3.5-Trichlorobenzene	0.129	0.029	0.131	N.D.	0.245
1.2.3-Trichlorobenzene	0.068	0.016	0.057	N.D.	0.355
1.2.4-Trichlorobenzene	0.227	0.047	0.225	N.D.	0.954
Tetrachlorobenzene	0.124	0.049	0.128	N.D.	0.850
Pentachlorobenzene	0.210	0.058	0.223	N.D.	1.147
Hexaclorbenzene	0.364	0.086	0.354	N.D.	2.352

N.D. – Not Detected or lower than Limit of detection (LOD)

Discussion

BTEX were detected in all analyzed samples. The highest level was found for station near the border to Albania (station 15) and the minimum near Drini Waterfall (station 1). Presence of BTEX in the water of the river could be

related to the automobilist transport, the spilling/accidents of hydrocarbon near the river and beyond, and the impact created by mechanical businesses (car service) in the area of river. Waste from other businesses operating in this area is also not excluded. It was noted presence of Benzene in higher quantities than other volatile compounds. Its presence is a consequence of its identification in high quantity at some stations where there may be some point source of it. This could also be the value of the moment of this compound or spillage of hydrocarbon waste from any vessel. Benzene levels do not exceed the permitted rate for surface waters according to EU 2008/105.

The presence of chlorobenzenes were noted in all analyzed water samples. Their maximum was noted in several stations located near cities or villages while the minimum in waterfall of White Drin station. Their presence may be a consequence of direct discharges of liquid urban waste from houses and/or buisnesses, due to hygiene/cleaning products, as a consequence of the degradation of large organic molecules with chlorine (pesticides, PCBs, etc.) At a higher level were found chlorobenzene, pentachlorobenzene and hexachlorbenzene, whose presence was identified at a higher level at several stations near of urban centers or agricultural areas. The presence of these compounds may be mainly by wastewater discharges or degradation products of pesticides and other molecules. The levels of volatile organic pollutants in the water of the port of Durres were similar to the levels reported in previous works for Balkan area [8-10].

Conclusion

In this study, water samples from the White Drin River, which is one of the largest river in Kosovo, were analyzed. The analysis of chlorobenzenes and BTEX was carried out by HS/SPME technique followed by GC/FID/ECD technique. Volatile organic pollutants were present in almost all analyzed water samples. BTEX presence is related mainly to the intensity of automobilist transport near the river. Spills of hydrocarbon by gas stations, agro-mechanicals or mechanical businesses operating in this area are not excluded. Momentum values and the influence of water flow are not excluded. Benzene was the compound that was most frequently identified in the highest quantity for all samples. Chlorobenzenes were also detected for most of the samples analyzed. Chlorobenzene, pentachlororbenzene and HCB were identified at higher level in several stations of the river. The presence of chlorobenzenes can be a consequence of urban spills, of cleaning/sanitization in houses and businesses, as degradation products of other compounds (pesticides, PCBs, etc). The levels of VOC in the water of White Drin River were similar to the levels reported in previous works for the water of some Albanian rivers. The presence of BTEX and chlorobenzenes in the water samples of the White Drin River shows that the monitoring of this area should be continuous.

References

1. Ukoha, P. O., Ekere, N. R., Timothy, C. L., & Agbazue, V. E. (2015). Benzene, toluene, ethylybenzene and xylenes (BTEX) contamination of soils and water bodies from alkyd resin and lubricants industrial production plant. *Journal of Chemical Society of Nigeria*, *40*(1), 51-55
2. Osuji, I., & Achugasim, O. (2010). Trace metals and volatile aromatic hydrocarbon content of Ukpeliede-I oil spillage site, Niger Delta, Nigeria. *Journal of Applied Sciences and Environmental Management*, *14*(2), 17-20
3. Ezquerro, O., Ortiz, G., Pons, B., & Tena, M. T. (2004). Determination of benzene, toluene, ethylbenzene and xylenes in soils by multiple headspace solid-phase microextraction. *Journal of chromatography A*, *1035*(1), 17-22.
4. Beltrán, J., López, F. J., & Hernández, F. (2000). Solid-phase microextraction in pesticide residue analysis. *Journal of chromatography A*, *885*(1-2), 389-404.
5. Directive 2008/105/EC of the European Parliament and of the Council on environmental quality standards in the field of water policy, amending and subsequently repealing Council Directives 82/176/EEC, 83/513/EEC, 84/156/EEC, 84/491/EEC, 86/280/EEC and amending Directive 2000/60/EC of the European Parliament and of the Council
6. ISO 5667-3:2018, Water quality — Sampling — Part 3: Preservation and handling of water samples
7. Dukaj, A., Shkurtaj, B., & Nuro, A. (2015). Determination of MTBE, TBA, BTEX and PAH in sediment and water samples of Karavasta lagoon. *Journal of International Environmental Application & Science*, *10*(2), 162-167.
8. Duka, A., Shkurtaj, B., & Nuro, A. (2015). Chlorbenzenes, Organochlorinated Pesticides and PCB in Biota samples of Karavasta Lagoon. *International Journal of Ecosystems and Ecology Science (IJEES)*, *5*(2), 217-228.
9. Nuro, A., Marku, E., & Murtaj, B. (2019). Organic pollutants in Hot-Spot area of Porto-Romano, Albania. In *International Scientific Conference "Kliment's Days"* (Vol. 104, pp. 243-255).
10. Borshi, X., Nuro, A., Macchiarelli, G., & Palmerini, M. G. (2016). Determination of PAH and BTEX in water samples of Adriatic Sea using GC/FID. *International Journal of Current Microbiology and Applied Sciences*, *5*(11), 877-884.

Study of chemical profile for essential oil of *Salvia officinalis* L. plants by using CO₂ supercritical extraction

Miranda Misini*1 , **Arben Haziri 1** , **Fatmir Faiku 1** , **Aurel Nuro2**

¹University of Prishtina "Hasan Prishtina", Faculty of Natural Sciences, Department of Chemistry, Kosovo, miranda.misini@uni-pr.edu, arben.haziri@uni-pr.edu, fatmir.faiku@uni-pr.edu
²University of Tirana, Faculty of Natural Sciences, Department of Chemistry, Albania, aurel.nuro@fshn.edu.al

Keywords
Salvia officinalis
Essential oil
Supercritical extraction
GC/FID

Abstract
This study shows chemical profile of *Salvia officinalis* L. plants by using CO2 supercritical extraction method. Samples of sage plants were selected by natural population of Gjilan, Kosovo. Sage samples were obtained in August 2022. The dried and ground plants were subjected of CO₂ supercritical extraction techniques in a modified Clevenger apparatus, to obtain the essential oil of *Salvia officinalis* plants. Chemical profiles for all sage samples were performed using the GC/FID technique. Capillary column VF-1ms (30 m x 0.33 mm x 0.25 um) was used for the separation and isolation of compounds found in sage plants. In the analyzed chromatograms from sage samples, 30-45 compounds were identified. In the study, the 20 main compounds that make up over 90% of the total identified compounds were considered. Oxygenated monoterpenes were the main group of monoterpenes because of higher values for alpha + beta-Thujones and Camphor. Sesquiterpenes were the second group while bicyclic monoterpenes were third group of terpenes. Percentages of monocyclic, aliphatic and aromatic monoterpenes were found in non-considerable level. Chemical profile of Salvia officinalis plants from Kosovo was the same with other reported studies from Balkan and Mediterranean area.

Introduction

Kosovo is located on the Balkan Peninsula. As part of this area and due to its favorable geographical position, it has a rich vegetation, with over 2500 different types of plants. This development of the flora is favored by the great diversity of plain, hilly, and mountainous relief forms, as well as by its climate. From this diverse vegetation, about 300 species are aromatic and medicinal plants, which constitute a good and important natural economic resource for Kosovo [1, 2]. Medicinal plants of Kosovo are distinguished by their active ingredients and essential oils. These plants are known and used since ancient times. They are widely used in traditional medicine and culinary [1, 2]. The activity of gathering aromatic-medicinal plants constitutes one of the main incomes for the livelihood of poor families in rural areas. *Salvia officinalis*, known as sage, is a perennial plant of the pre-mountainous Mediterranean area. It grows from 25-80 cm in height. It blooms in the May-July period, depending on the climatic subzone where the plant's biotope is located. This plant is found on stony soils, rising above limestone karst rocks with slightly basic to slightly acidic pH. It grows in dry, cool soils that stretch along the submontane Mediterranean zone. It is found at altitudes of 150-1200 m above sea level.

Sage has found many uses in the cosmetic industry, the essence of the leaves is used as a flavoring agent for perfumes and soaps. In the kitchen, it is used as a spice in various meat dishes. Sage has different properties such as: astringent, antiseptic, aromatic, carminative, estrogenic, antisudorific, tonic, stimulant, antispasmodic, etc. Cures nervous disorders, dizziness, fainting, depressive states. It stimulates the entire organism, regulates the secretions of the digestive tract, soothes diarrhea due to its astringent properties, regulates menstrual flow and soothes painful reactions by fighting the disorders brought about by menopause. The combination of antiseptic, soothing and astringent properties make it ideal for almost all types of sore throats and widely used for gargling. It is also used for mouth and gum ulcers [1, 3, 4, 5, 6].

Material and Method

Sampling of *Salvia officinalis*

The samples of *Salvia officinalis* plants (aerial parts) were taken from the wild populations of the area of Anamorava, Gjilan in the southern area of Kosovo. *Salvia officinalis* plants were collected in August 2022. Sage sampling stations were at an altitude of 1000 – 1200 m above sea level. At each station, the aerial parts of the *Salvia officinalis* plant were selected. The plants of each station were dried in the shade so as not to lose morphological characteristics. The plant material after drying was chopped in a grinder into small pieces < 0.5 cm for further analysis [5, 6, 7].

Isolation of essential oils by CO2 supercritical technique

The plant material of *Salvia officinalis* (50 g of plants from the aerial parts of *Salvia officinalis*) was subjected to CO_2 supercritical in a modified Clevenger apparatus. CO_2 temperature was 33°C and the pressure was 100 bar. The isolation of the essential oil was done for 30 minutes. The essential oil was collected in 2 ml of Toluene as extraction solvent. The extract was treated with 1 g of anhydrous sodium sulfate. It was stored in dark vials at +4°C. The essential oil of *Salvia officinalis* in organic solvents was subjected to GC/FID analysis [6, 8, 9].

Gas chromatographic apparatus and analysis

Gas chromatographic analysis of the essential oil of *Salvia officinalis* was performed on a Varian 450 GC apparatus, equipped with a PTV injector and a flame ionization detector (FID). Injector and detector temperatures were set at 280°C and 300°C, respectively. 2ul of essential oil of Salvia officinalis dissolved in Toluene was injected in split mode (1:250). Nitrogen was used as carrier gas (1 ml/min) and as make-up gas (25 ml/min). Hydrogen and air were the flame gases in the detector at 30 ml/min and 300 ml/min, respectively. VF-1ms capillary column (30 m x 0.33 mm x 0.25 mu) was used to isolate the essential oil compounds. The oven temperature was programmed as follows: from 40°C (held for 2 minutes at 40oC) to 150°C at 4°C/min, further to 280°C at 10°C/min, at 280°C held for 2 minutes. The identification of compounds was based on the comparison of retention time (RT) with Kovats indices which together with literature data were used to identify the main compounds. The quantitative data of the analyzed compounds are given in % against the total areas of the piks [6, 7, 8, 10, 11, 12].

Results

In this study, sage plants from the area of Gjilan (Anamorava), Kosovo, were analyzed. The chemical components of sage plants have been analyzed using the CO_2 supercritical technique with the Clevengar apparatus. The chemical profile of the *Salvia officinalis* samples was performed using the GC/FID technique. In the analyzed chromatograms from sage samples, 30-45 compounds were identified. In the study, the 20 main compounds that make up over 90% of the total identified compounds were considered. Some of the main compounds identified to the all samples were: alpha-Thujone, beta-Thujone, Camphor, Cineole and Camphene. Chemical profile for 20 main compounds and for the main groups of terpenes were shown in above figures.
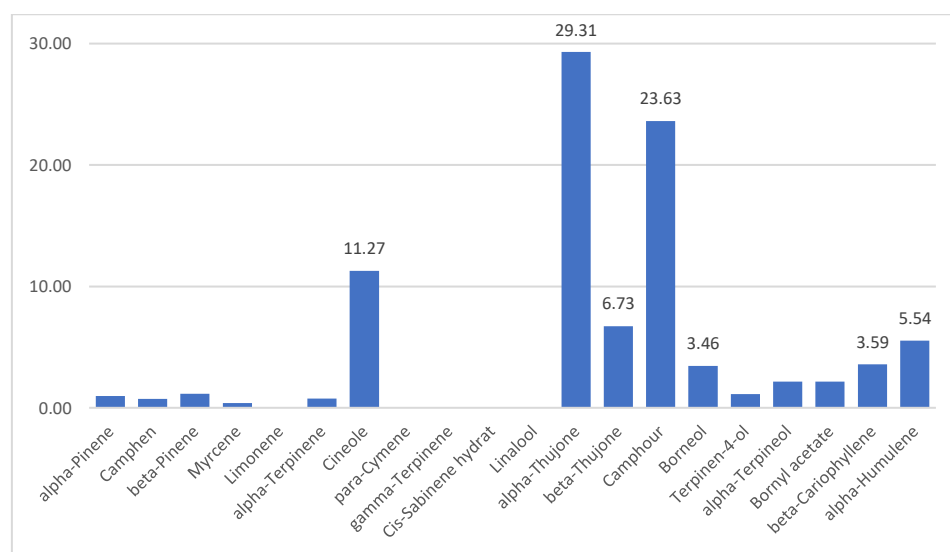

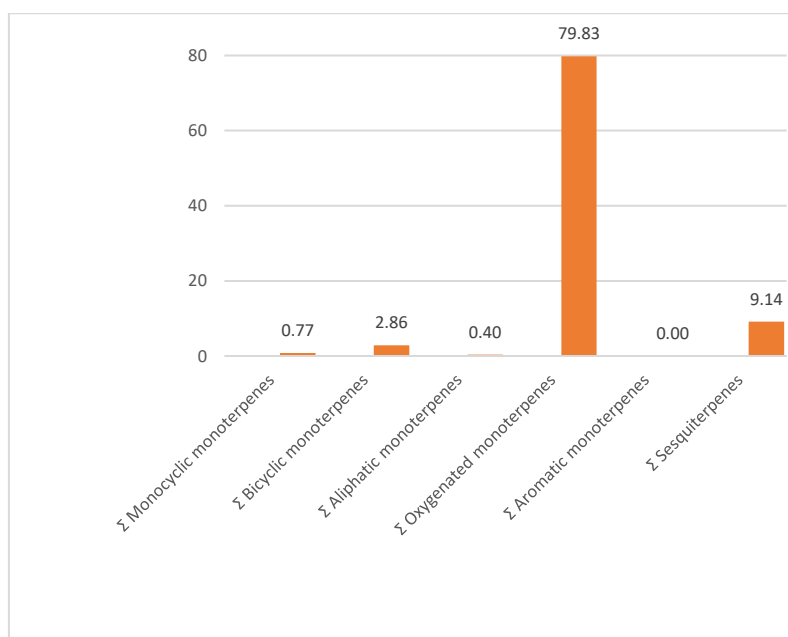**Figure 1.** Chemical profile of Salvia officinalis samples

Figure 2. Terpene groups in sage samples

Discussion

Chemical profile of *Salvia officinalis* from Kosovo area by using CO_2 supercritical extraction techniques was: alpha-Thujone > Camphour > Cineole > beta-Thujone > alpha-Humulene > beta-Cariophyllene > Borneol. Other compounds were found lower than 2%. The main compound was alha-Thujone for all sage samples with average values of 29.3%. Total of Thujones (alpha + beta isomers) was 36%. Thujone values were the same with reported values for classical techniques of hydro-distillation technique based on Pharmacopeia instructions. The second compound found in sage samples was Camphor (23.6%). This value was higher than hydro-distillation process. This difference could be because of the affinity for the CO_2 supercritical for this compound. The same was noted for alpha-Humulene (5.6%) but for the other compounds was the opposite. This profile was almost the same with reported values for *Salvia officinalis* plants from Kosovo and other countries of Balkan areas [6, 7, 8, 10].

Note that, the main place in all samples was occupied by monoterpenes. The total of monoterpenes in the analyzed samples was 83.4%. The profile of monoterpenes was: oxygenated monoterpenes were found in most abundance, followed by bicyclic monoterpenes, monocyclic monoterpenes, aliphatic monoterpenes and aromatic monoterpenes. Sesquiterpenes (beta-Caryophyllene and alpha-Humulene) were identified in sage samples as the second group of terpenes. Oxygenated monoterpenes (Cineole, Linalool, alpha-thujone, beta-Thujone, Borneol, Terpinen-4-ol, alpha-Terpineol and Bornyl acetate) was the main group of monoterpenes with 79.8%. The higher percentage was found because the higher values for alpha + beta-Thujones and Camphor. Sesquiterpenes (beta-Cariophyllene and alpha-Humulene) was the second group of terpenes with 9.2%. Bicyclic monoterpenes (alpha + beta-Pinene, Camphene and Sabinene hydrate) was third group of terpenes with 2.9%. Monocyclic, aliphatic and aromatic monoterpenes were found lower than 1%. This profile was the same with other reported studies from Balkan and Mediterranean area [5, 6, 7, 9, 10].

Conclusion

Salvia officinalis essential oil samples from the area of Anamorava (Gjilan), Kosovo 2022 were analyzed using the CO_2 supercritical technique with the modified Clevengar apparatus. Their quantification was performed by GC/FID. In the analyzed chromatograms from sage samples, 30-45 compounds were identified. In the study, the 20 main compounds that make up over 90% of the total identified compounds were considered. Some of the main compounds identified in all solvents were: alpha-Thujone, beta-Thujone, Camphor, Cineole and Camphene. The main compound was alha-Thujone for all sage samples. Total of Thujones (alpha + beta isomers) was the same with reported values for sage samples from this area measured by hydro-distillation. Camphor and alpha-Humulene were found higher than hydro-distillation process but for the other compounds was the opposite. The main compounds in all samples were monoterpenes. The profile of monoterpenes was: oxygenated monoterpenes were found in most abundance, followed by bicyclic monoterpenes, monocyclic monoterpenes, aliphatic monoterpenes and aromatic monoterpenes. Oxygenated monoterpenes was the main group of monoterpenes because of higher values for alpha + beta-Thujones and Camphor. Sesquiterpenes were the second group while bicyclic monoterpenes were third group of terpenes. Percentages of monocyclic, aliphatic and aromatic

monoterpenes were found in non-considerable level. Chemical profile of Salvia officinalis plants from Kosovo was the same with other reported studies from Balkan and Mediterranean area [5, 6, 7, 9, 10].

References

1. Asllani, U. (1998). Bimët eterovajore dhe mjekësore që rriten në Shqipëri
2. Kathe, W., Honnef, S., & Heym, A. (2003). Medicinal and aromatic plants in Albania, Bosnia-Herzegovina, Bulgaria, Croatia and Romania: a study of the collection of and trade in medicinal and aromatic plants (MAPs), relevant legislation and the potential of MAP use for financing nature conservation and protected areas.
3. Daferera, D. J., Ziogas, B. N., & Polissiou, M. G. (2000). GC-MS analysis of essential oils from some Greek aromatic plants and their fungitoxicity on Penicillium digitatum. *Journal of agricultural and food chemistry*, *48*(6), 2576-2581.
4. Sell, C. (2005). Chapter 12. Natural Product Analysis in the Fragrance Industry. The Chemistry of Fragrances (2nd ed.). Royal Society of Chemistry Publishing. pp. 214–228. ISBN 978-0-85404-824-3.
5. David, F., Scanlan, F., Sandra, P., & Szelewski, M. (2002). Analysis of essential oil compounds using retention time locked methods and retention time databases. *Food and Flavors*.
6. König, W. A., Bülow, N., & Saritas, Y. (1999). Identification of sesquiterpene hydrocarbons by gas phase analytical methods. *Flavour and Fragrance Journal*, *14*(6), 367-378.
7. Adams, R. P. (2017). *Identification of essential oil components by gas chromatography/mass spectrometry. 5 online ed*. Texensis Publishing.
8. Khedher, M. R. B., Khedher, S. B., Chaieb, I., Tounsi, S., & Hammami, M. (2017). Chemical composition and biological activities of Salvia officinalis essential oil from Tunisia. *EXCLI journal*, *16*, 160.
9. Oniga, I., Oprean, R., Toiu, A., & Benedec, D. (2010). Chemical composition of the essential oil of Salvia officinalis L. from Romania. *Revista Medico-chirurgicala a Societatii de Medici si Naturalisti din Iasi*, *114*(2), 593-595.
10. Damyanova, S., Mollova, S., Stoyanova, A., & Gubenia, O. (2016). Chemical composition of Salvia officinalis L. essential oil from Bulgaria. *Ukrainian food journal*, (5, Issue 4), 695-700.
11. Bernotienė, G., Nivinskienė, O., Butkienė, R., & Mockutė, D. (2007). Essential oil composition variability in sage (Salvia officinalis L.). *Chemija*, *18*(4), 38-43.
12. Awen, B. Z., Unnithan, C. R., Ravi, S., Kermagy, A., Prabhu, V., & Hemlal, H. (2011). Chemical composition of Salvia officinalis essential oil of Libya. *Journal of Essential Oil Bearing Plants*, *14*(1), 89-94.

Influence of the instability form on the traffic safety of freight rolling stock

Angela Shvets *1 ID

1Ukrainian State University of Science and Technologies, Department of Engineering and Design Specialized Department «Microprocessor-Based Control Systems and Safety in the Railway Transport» (EDSD MBCSS), Ukraine, angela_shvets@ua.fm

Abstract
The purpose of the paper is a theoretical study of the influence of longitudinal forces of a quasi-static nature and the instability form of freight wagons in a train on the wheel derailment stability. Knowledge of the laws of train movement under various control modes is necessary when programming the equations of train movement when it is necessary to determine the exact position of the train on the railway track and the stability of the wagons at the time of interest. As a result of theoretical studies, the values of the factor of stability against lift by longitudinal forces were obtained, taking into account the forms of instability. The relevance of this study relates to the need to control the longitudinal forces arising during the train movement, taking into account the increase in speeds, masses, and lengths of trains (especially freight trains) and the locomotive power increase.

Introduction

Elevating the maximum speeds makes it necessary to increase the braking efficiency of the rolling stock. The main limitation of the magnitude of the braking force of the rolling stock is the force of adhesion of the wheels to the rails and the stability of the wheel from the derailment. Numerous studies make it possible to obtain the absolute values of the longitudinal dynamic forces during braking and also demonstrate that the forces depend on the weight and length of the train, brake parameters, train speed, braking mode, characteristics, and condition of the draft gear, the size of the gaps in the shock absorbing elements and traction devices, and their distribution along the length of the train at the time of the start of braking [1-3].

Knowledge of the laws of movement of a slowed-down train is necessary when programming the equations of train movement when it is necessary to determine the exact position of the train on the railway track at the point of interest. In the presence of correctly compiled train motion equations, it is not particularly difficult to accurately calculate the length of the braking distances and evaluate the effectiveness of various braking systems.

Ensuring the safety of the movement of heavy trains is possible only if there is a well-controlled brake that does not cause large longitudinal forces in the composition under any braking modes. Therefore, it is necessary to more accurately investigate the dependence of the wheel stability coefficient on derailment on various factors and develop measures to increase the braking efficiency of the rolling stock. The purpose of the paper is a theoretical study of the influence of longitudinal forces of a quasi-static nature and the instability form of freight wagons in a train on the stability of a wheel from the derailment.

Material and Method

It is known that when carrying out traction calculations and solving problems related to the optimization of energy costs for traction, the train is considered as a one-dimensional mechanical system of solid bodies connected by elastic-viscous bonds. An increase in the weight and length of trains leads to the need to consider

the body of a freight wagon, taking into account the tare weight of the wagon and weight of the cargo, as an elastic massless beam carrying a uniformly distributed load (Figure 1) [4-5].
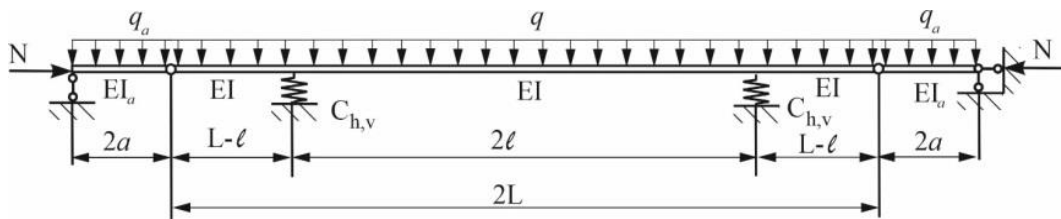

Figure 1. Scheme of a freight wagon, taking into account its weight and loading mode

Here q_a – own weight of two coupler assemblies, respectively related to two lengths of coupler bodies; q – the empty weight of the wagon body together with the suspended equipment and two bolsters in an empty state, referred to its length. When taking into account the loading, the cargo weight is added to the body weight and is considered to be evenly distributed along the entire length; 2ℓ – wheelbase; $2L$ – the distance between coupler followers; $2a$ –automatic coupler body double length from a pulling face to the shank end; $C_{h,v}$ – the horizontal (vertical) stiffness of spring suspension of one bogie.

The nominal bending stiffness of a gondola wagon body is approximately equal to three times the stiffness of the center sill (in the corresponding directions) [4]. In works [4, 6], the most unfavorable sections of an automatic coupler from the point of view of strength were established. Rod system in the displacement method has a degree of static indeterminacy equal to 6. The table of reactions of compressed-bent rods from single displacements and loads is given in the work [7]. The basic system of the displacement method, taking into account the symmetry of the rod system, is shown in Figure 2.
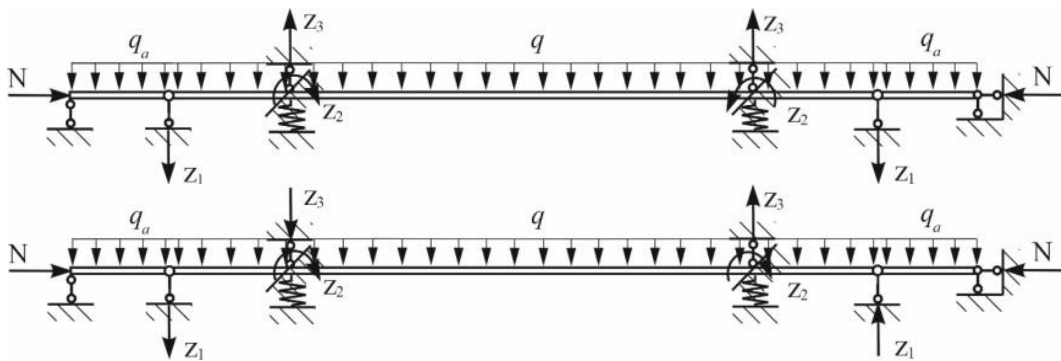
Figure 2. The basic system of the displacement method, taking into account the symmetry of the rod system

When searching for the minimum critical forces of a symmetrical and symmetrically loaded system, it suffices to find two smaller critical parameters for a direct-symmetrical and skew-symmetrical grouping of unknowns. Expressions for the functions of the displacement method for compressed-bent rods are taken in accordance with [7]. The critical parameter v_i or the length reduction factor, which depends on the instability form, is determined by expanding the determinant composed of expressions for the coefficients at unknown [4-5].

A theoretical study [5] made it possible to obtain dependences for determining the critical parameter for some instability forms, taking into account the rigidity, the weight of the elements of the hinge-rod system, and the gap in the rail track.

Results

Most of the existing methods used to assess the safety of the movement of wagons set permissible limits for the values of the parameters, beyond which there is a possibility of an emergency situation. The stability factor of wagons against derailment, as is known, is estimated by the ratio of horizontal transverse (lateral) forces to vertical forces acting at the point of contact of the wheel flange with the rail head [7-8].

Let us calculate the stability of the wheelset of a wagon under the action of compressive longitudinal forces according to the dependences for straight [4] and curved sections of the railway track [7-8] in the presence of a difference in the heights of the axles of two adjacent wagons. It is envisaged that the loss of stability of wagons occurs according to the I-st (loaded front bogie) and according to the II-nd form (unloaded front bogie). The calculations took into account the difference in height between the longitudinal axles of automatic couplers in a freight train from 0 to 0.1 m with a step of 0.02 m. Behind the wagon under study, the difference between the axle levels of the automatic couplers is taken equal to Δ_2=0.04 m.
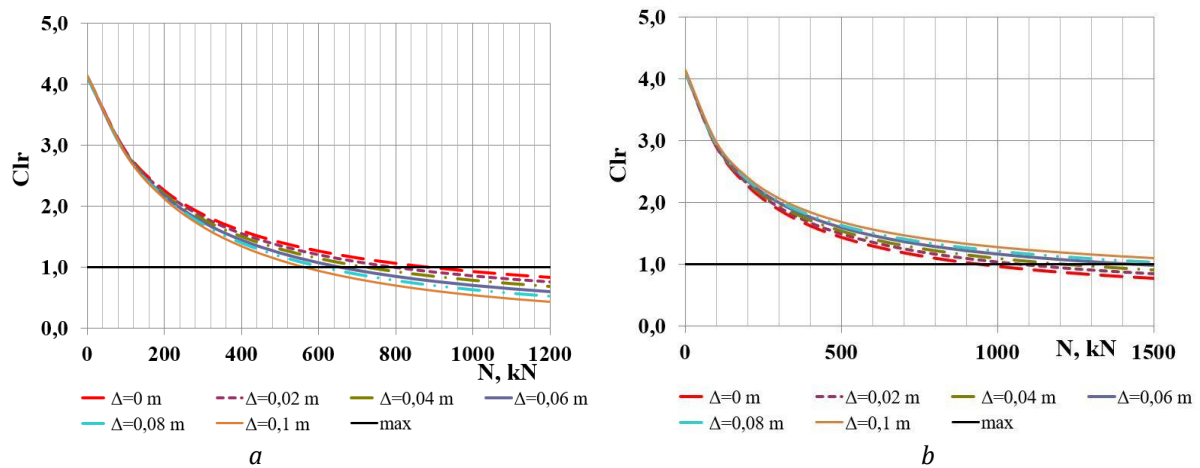
Figure 3. Resistance coefficient of an empty wagon lift: *a* – unloaded front bogie; *b* – loaded front bogie

The given results confirm that the loss of stability of wagons in the I-th and II-nd form occurs with a significant difference in the magnitude of the longitudinal compressive force. Consequently, the stability loss of freight wagons as part of a train should be divided into two stages: stability loss of the body on suspension springs and the stability loss of the wheelset, which results directly in the derailment.

Conclusion

The use of the method of determining the critical parameter for the I-th and II-nd forms of instability under the action of quasi-static longitudinal forces will allow us to justify the cause of the derailment, as well as to develop and put into practice the technical measures to prevent the lift of the carriages, widening and shear of the track. Using the methodology in compiling the process flow diagrams for driving the trains will make it possible to recommend rational train driving not only at the lowest energy costs but to implement technical measures to improve the stability of freight rolling stock, which in turn will allow removing some existing restrictions on permissible speeds and increasing the train speed.

In order to carry out continuous analysis in train conditions of the value of the resulting longitudinal compressive forces and to prevent large compressive forces, it is necessary to equip locomotives with a system for monitoring and recording longitudinal forces arising on the automatic coupler of the wagons.

References

1. Cheli, F., Di Gialleonardo, E., & Melzi, S. (2017). Freight trains dynamics: effect of payload and braking power distribution on coupling forces. *Vehicle system dynamics*, *55*(4), 464-479. https://doi.org/10.1080/00423114.2016.1246743.
2. Crăciun, C., & Cruceanu, C. (2018). Influence of resistance to motion of railway vehicles on the longitudinal trains dynamics. In *MATEC Web of Conferences* (Vol. 178, p. 06003). EDP Sciences. https://doi.org/10.1051/matecconf/201817806003.
3. Zhang, H., Zhang, C., Lin, F., Wang, X., & Fu, G. (2021). Research on Simulation Calculation of the Safety of Tight-Lock Coupler Curve Coupling. *Symmetry*, *13*(11), 1997. https://doi.org/10.3390/sym13111997.
4. Shvets, A. (2022). Stability of a car as a hinged-rod system under the action of compressive longitudinal forces in a train. *Journal of Modern Technology and Engineering*, *7*(2), 96-123.
5. Shvets, A. O. (2022). Determination of the form of loss the freight cars stability taking into account the gap in the rail track. *Strength of Materials and Theory of Structures*, 109, 485-500. https://doi.org/10.32347/2410-2547.2022.109.485-500.
6. Shvets', A. O. (2022). Investigation of coupling strength at non-central interaction of railcars. *Strength Mater*, 54(2), 233–242. https://doi.org/10.1007/s11223-022-00396-1.
7. Shvets, A. O. (2020). Stability of freight wagons under the action of compressing longitudinal forces. *Science and Transport Progress*, *1*(85), 119-137. https://doi.org/10.15802/stp2020/199485.
8. Shvets, A. O., Shatunov, O. V., Dovhaniuk, S. S., Muradian, L. A., Pularyia, A. L., & Kalashnik, V. O. (2020). Coefficient of stability against lift by longitudinal forces of freight cars in trains. IOP Conference Series: Materials Science and Engineering, 985, Paper 012025. https://doi.org/0.1088/1757-899X/985/1/012025.

How hospitals response to disasters; a conceptual deep reinforcement learning approach

Ardeshir Mirbakhsh[*1]

[1]*New Jersey Institute of Technology, Department of Transportation Engineering, USA, Am2775@njit.edu*

Abstract
During a disaster the requests for using ambulance services increases. Efficient assignment of the ambulances leads to lowering the patients' travel time. Simulating these environments is very complex and needs a solid framework. This paper uses a Deep Reinforcement Learning approach to better schedule ambulance dispatch problem during those disasters. The concept of a call and assignment of ambulances are illustrated and the elements of states, rewards, and actions in the formulations are described. The algorithm steps for solving this problem are also presented. This paper can help disaster planners to have a better idea for better scheduling ambulances.

Introduction

In the disaster situation there is a need for public health service to transfer the patients facing an emergency situation. In the disaster situation, resources should be allocated differently and new policies should be used [1]. Sample of these situation is hospital responses to Covid-19 surge of the patients where hospital allocation needs a special allocation [2]. Another example is hospitals facing with cyber-attacks where the patients should be transferred to another healthcare until full recovery of the hospital [3]. These planning totally can improve regional capacity of the hospitals in response to disaster situation [4]. During the Covid-19 fever and cough increased and the request for ambulances increased. In this situation the pickup time of the patients are very important to serve patients efficiently.

Therefore, the problem of dispatching the ambulances plays a significant role in managing this situation. Previous researchers tried to address this problem. For example, some of them used a Multi-Agent Q-Network framework by reformulating the ambulance dispatch problem with a multi-agent reinforcement learning framework and designing a simulator to control ambulance status and produce patient's request [5].

In this paper we aim to provide a deep reinforcement learning approach using a deep q-learning framework to find the optimal planning of the ambulances. In other words, this research aims to lower the patients' pickup time by a deep reinforcement learning approach.

Method and materials

Deep reinforcement learning is an approach to dynamically optimize the problem while the agents try to take actions to maximize the rewards and minimize the costs and is used in different fields [6]. We use the method implemented in Investigating lake drought prevention using a DRL-based method which is illustrated in the next sessions [7]. In each time step, the agent uses a reward-maximization policy to lower the penalties. Figure1 shows the general framework for deep reinforcement learning (DRL) which is used in a variety of fields. This framework uses a trial-and-error approach to finding the strategies that maximize the objective function value. Figure 2 shows the component of a conceptual dispatching problem in which a Covid-19 patient calls 911 and requests an ambulance. Then agent in the ambulance station assesses the situation and assigns the ambulance to the patient and then transfers them to the hospital and returns to the ambulance center. In this network, the patients calling have several elements in their data structure including geographic status and urgency level of the calls. When a patient requests an ambulance 911 center should decide to assign which ambulance. The ambulance entity has information like geographic status and status which shows if the ambulance is free or not.
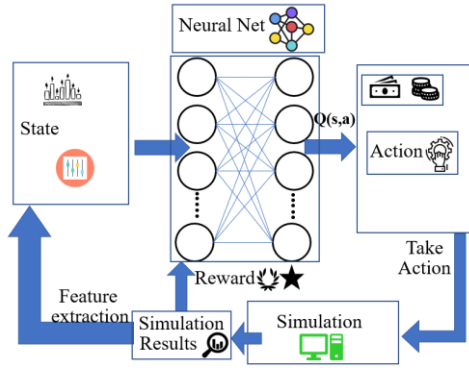
Figure 1. ……………..
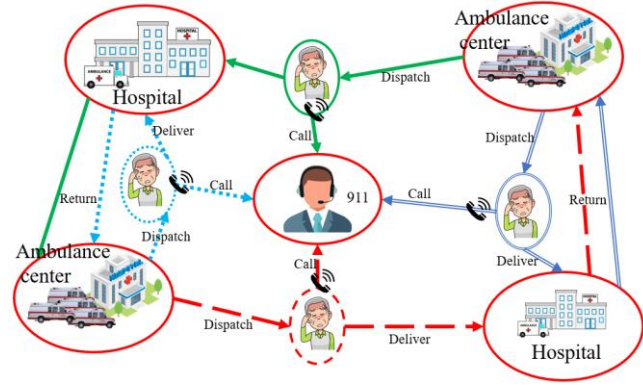
Figure 2. ………………

Elements of deep Q-network

In a simple reinforcement learning the goal is to maximize the value function in a sequential decision-making process. But in the deep reinforcement learning approach, a deep neural network approximates the Q-Function and updates the buffer information. In this framework, the loss function is provided in the Equation 1.

$$L(\theta) = \left(\left(r + \gamma \max_{a_t+1} Q(s_{t+1}, a_{t+1}; \theta^-) \right) - Q(s, a, \theta^{pred}) \right)^2 \qquad (1)$$

Where parameters $(s_t, a_t, \gamma_t s_{t+1})$ are random parameters which are selected from reply memory. Following algorithm shows psuedocode for solving this problem, where the Q-Values are estimatd by a deep nueral network approximation. In this algorithm and formulas, $Q(s, \theta')$ is the target network while $Q(s, \theta)$ is the current network. using $Q(s, \theta)$ the actions and $Q(s, \theta')$ is evaluated. In this algorithm steps 0-3 is initializatuion, spets 7-12 are experlearning steps, steps 7-12 are experience learning. In this algorithm step 5 and step 7 count episodes and steps respectively.

Algorithm 1: Training of the Deep Reinforcement algorithm
0   Inputs (Memory size, batch size, Episode and step numbers
1   Initialize parameters θ for the simulation
2   Initialize parameters θ' for the simulation
3   Initializing memory
4   **for** each episode:
5   **for** each simulation set:
6   *Actions and simulating */
7   **if** $random() < \varepsilon$ **then***:
8   Select a random action a:
9   **else**:
10   Select $a = max\ Q(s, a; \theta)$:
11   **end**
12   Get short-term reward R and new state s' by simulating action a;
13   Save state transition data (s, a, s', R);
/* Updating Q-network parameters*/
14   Sample batch state transition $\{(s, a, s', R)\}$;
if simulator terminated **then**:
$Q^* = R$
else:
$Q^* = R + \gamma\ max_{a'}\ Q(s', a'; \theta)$
End
Use equation 1 to perform using gradient descent on the loss $L(\theta)$ based on Q^*;
end
End

In this algorithm the states are the times that the ambulances finnish their serices which are treatment or drop offthe patients. The actions are different options that the agent can use to go to the next steps. In other word the actions here are the stations or dispatch areas that ambulance finnish their work and stay for future work. The agent aims to minimize the time and distance between pispatch points and call points. The ambulance moves to the targe location with the specified speed to the location. Rewards in this algorithm is squared diference of the arrival time and dispatch time. In Equation 2, agent tries to get maximum rewards that can get from different actions:

$$R(s, a) = -(T_{Ar} - T_{Dis})^2 \tag{2}$$

Where T_{Ar} is the arrival time of ambulance and T_{Dis} is the dispatch time of the ambulnce. The agent tries to minimize the difference between these times.

Simulation

A reinforcement learning is used to find the optimal solution for this problem. The goal is to minimize the difference time between the request and the arrival time. the calls for ambulances are due to different reasons including accident, hearth attack, Covid-19 related calls. Call requests are time dependant and usually follow the daily traffic patern. The reason is probably due to increase in the accidents in the peak trafic periods. For simulating this problem python packages can be used. The learning part can be implemented using open source package named Pytorch. For the deep reenforcement learning section a neural network can be developed with some hidden layers and layers. The number of actions are equal to the number of the stations. First agent is trained over some episodes with a predifined buffer size and discount factor and learning rate. At the beginning of the simulation, the states, actions, rewards and next states are initialized to let the environment save the experiences for the future learning.

Conclusion

This paper provided a framework for an efficient ambulance dispatching problem using a Q-learning reinforcement algorithm. The elements of this simulation including actions, states, and rewards have been illustrated. The results reduce the time between the ambulance request and ambulance arrival time. The algorithm for solving this problem also has been presented.

Future works can extend this work by adding more realistic constraints to provide insights for hospital managers using a deep reinforcement learning approach. This research can help them plan ambulance scheduling in response to pandemics.

References

1. Shahverdi, B., Miller-Hooks, E., Tariverdi, M., Ghayoomi, H., Prentiss, D., & Kirsch, T. D. (2022). Models for Assessing Strategies for Improving Hospital Capacity for Handling Patients during a Pandemic. Disaster Medicine and Public Health Preparedness, 3(2), 1–26. https://doi.org/10.1017/dmp.2022.12
2. Ghayoomi, H., Miller-Hooks, E., Tariverdi, M., Shortle, J., & Kirsch, T. D. (2022). Maximizing hospital capacity to serve pandemic patient surge in hot spots via queueing theory and microsimulation. IISE Transactions on Healthcare Systems Engineering, 0(0), 1–19. https://doi.org/10.1080/24725579.2022.2149936
3. Ghayoomi, H., Laskey, K., Miller-Hooks, E., Hooks, C., & Tariverdi, M. (2021). Assessing Resilience of Hospitals to Cyberattack. Digital Health, 7, 20–25. https://doi.org/10.1177/20552076211059366
4. Shahverdi, B., Ghayoomi, H., Miller-Hook, E., Tariverdi, M., & D. Kirsch, T. (2022). Regional Maximum Hospital Capacity Estimation For Covid-19 Pandemic Patient Care In Surge Through Simulation. Proceedings of the Winter Simulation Conference, 30–44. Singapore: IEEE Press.
5. Liu, K., Li, X., Zou, C. C., Huang, H., & Fu, Y. (2020). Ambulance Dispatch via Deep Reinforcement Learning. Proceedings of the 28th International Conference on Advances in Geographic Information Systems, 123–126. New York, NY, USA: Association for Computing Machinery. https://doi.org/10.1145/3397536.3422204
6. Bazmara Maziyar, Mianroodi Mohammad, & Silani Mohammad. (2023). Application of Physics-informed neural networks for nonlinear buckling analysis of beams. Acta Mechanica Sinica. https://doi.org/10.1007/s10409-023-22438-x
7. Ghayoomi, H., & Partohaghighi, M. (2023). Investigating lake drought prevention using a DRL-based method. Engineering Applications, 2(1), 49–59.

The impact of hybrid cars on reducing urban pollution and global warming

Ledia Bozo*[1] , Asllan Hajderi[2] , Fatmir Basholli [3]

[1]University of Tirana, Faculty of Natural Sciences, Department of Informatics, Tirana, Albania
[2]Universiy College of Business, Department of Higher Technical Studies, Tirana, Albania ahajderi@kub.edu.al
[3]Albanian University, Department of Engineering, Tirana, Albania, fatmir.basholli@albanianuniversity.edu.al

Keywords

Vehicle exhaust gases
Hybrid/electric cars
Pollution on human health
Environmental pollution

Abstract

In this report, the problem of environmental pollution in urban intersections, from vehicle gases and the impact of hybrid automobiles on its reduction and global warming is analyzed. For this purpose, it is proposed to change the fleet of vehicles, introducing electric hybrid vehicles into circulation. From the analysis of the types of hybrid cars, it is proposed to import plug-in hybrid electric vehicles, which can reduce the level of pollution up to 5 times. Then, the amount of polluting gases caused by vehicles was calculated, for the current structure of vehicles in circulation at a city intersection and for the proposed structure, removing vehicles manufactured before 2005 and adding 5% plug in hybrid electric vehicles. The results show that the level of pollution at the intersection for the current vehicle fleet is high over 2100 kg (CO+NOx+HC+PM) per day and over 370 tons of CO_2 in day. While for the proposed structure the level of pollution at the intersection can be reduced by over 22% and the reduction of carbon dioxide to 12%. In order to implement the proposed structure, it is proposed that the customs tax, road tax and environmental tax be removed for hybrid electric cars.

Introduction

Economy is the main pillar of humanity, while transport is the skeleton of its development, without which economic production cannot be realized [1].

The growth of production in the world but also in our country has always relied more and more on road transport. The use of conventional vehicles has been increasing a lot in the world, reaching in 2012 in over 1 billion and it is expected that in 2050 this number will exceed around 2 billion [2]. Thus, in the USA over 30.7% of energy is consumed in the transport sector and 82% of this by vehicles [1].

From vehicle engines are released into the atmosphere gases CO_2, CO , NOx , HC and PM particles, which affect the deterioration of human health and the creation of the greenhouse effect and global warming [3]. Air pollution is the biggest health and environmental problem of all big cities.

The European Environment Agency's report on air quality in Europe for 2016 has published that for Albania the number of premature deaths as a result of air pollution reached in 2120 people in 2016, when in 2013, there were 776 deaths. So this has almost tripled [4-5]. Statistics show that deaths from air pollution are 2 times higher than those caused by road accidents. The peoples at least have breathing problems, inhaling this polluted air, then there are high possibilities of heart attacks, autism, schizophrenia, up to insanity . So the lives of citizens are in danger, because life expectancy is being shortened, due to air pollution from two to three years

To change this situation, people should resign from using cars, but this cannot happen, because it has become an indispensable means of transportation.

Until 1996, the problem of reducing polluting gases was posed in general, where the production of CO_2 from vehicles was considered a gas of perfect combustion. Now the problem lies in the reduction of CO_2 through the

reduction of fuel consumption and the use of alternative energies. This evolution has gone from 200 g/km before 1995, to 186 g/km in 1995, to 130 g/km in 2015 and to 95 g/km in 2021 according to the CE regulation [5].

Therefore, the challenge in transport is to reduce energy consumption and CO_2 emissions in the conditions of the increase in the number of cars until 2050.

Solving this problem requires finding low-emission cars. For this purpose, the production of hybrid cars was experimented in years 1993-2001. So, in 2015, out of 80 million cars produced per year, 1.2 million are hybrid vehicles, mainly in the USA and Japan. Recently, production has increased and production costs have decreased. A hybrid car not only saves fuel, but also produces less CO_2 emissions and other pollution [6].

The lack of knowledge about hybrid/electric cars has created doubts among many users about the possibility to completely replace conventional vehicles in human activity. This constitutes the object of this report, to increase interest in the use of hybrid/electric cars, with the aim of reducing the level of pollution and improving human life.

Material and Method

Analysis of hybrid/electric cars

From the analysis of hybrid electric cars regarding the benefits with fuel economy, emission reduction, fuel cost while driving [6] of practical interest are plug-in hybrid electric vehicles (PHEVs) because:
- Fuel economy is better because these use 40% - 60% less fuel than conventional vehicles
- Emissions are lower than hybrid cars and conventional vehicles and the reduction is about 38% in the city and 20% on the highway
- The cost of driving is 2 times less than a hybrid car and 5 times less than a conventional vehicle. The cost of driving is very small, 0.02 - 0.04 $ per mile, while for conventional vehicles, it costs 0.10 - 0.15 $ per mile.

While for electric cars (EV) we have:
- Fuel economy is better, because the vehicle has no fuel.
- Emissions in marmites are zero, because they only use electricity
- The cost of driving is very small, 0.02 -0.04 $ per mile

Structure of vehicles in circulation

The number of vehicles in circulation in Albania has increased a lot, reaching at the end of 2022 in total to 588,766 for the whole country, which according to the years of production can be grouped as in Figure 1 [7]. The number of imported vehicles is around 50,000 per year, which can renew old vehicles that are out of circulation.
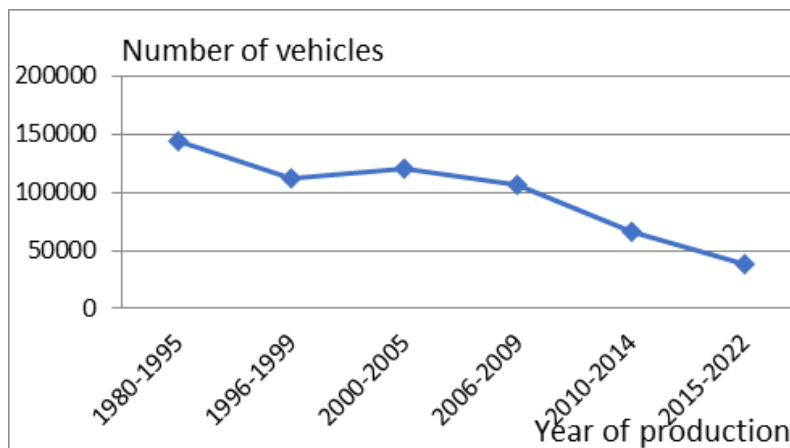
Figure 1. The number of vehicles in circulation in Albania, according to years of production

We propose to import about 25,000 hybrid electric vehicles (PHEV) every year

Determining the amount of pollution at the İntersection

Accepting that the vehicles in circulation are cars with diesel engines, (cars with petrol engines are very small) the calculation of the amount of pollution caused by the vehicles will be done accepting that the vehicles have pollution levels within the limits allowed by the EU regulations, given in table 1 in g/km [8].

From the measurements carried out at the intersection "21 Dhjetori" [9] it results N_h = 4800 car/hour, crossing time T_{av} =2 min and speed V= 0.1 km/min. For this speed, the pollution values of CO, NOx+HC, PM particles and CO_2 produced, calculated in g/min according to the years of production are given in Table 1.

Table 1. Pollution values for speed v = 0.1km/min

Standard	Year of production	CO g/min	NOx+HC g/min	PM (g/min)	CO_2 (g/min)
Euro 1	July 1992	0.316	0.113	0.018	21.1
Euro 2	July 1996	0.10	0.090	0.01	18.1
Euro 3	January2000 January 2005	0.064	0.056	0.005	15.2
Euro 4	September2009	0.0500.050	0.030	0.005	14.6
Euro 5	September2014	0.050	0.023	0.005	13.1
Euro 6			0.017	0.005	12.6

For the structure of vehicles in circulation, the intersection pollution amounts in g/hour for the pollutant CO, HC+NOx and PM particles can be calculated [9]:

$$G_h = (G_1 P_1 + G_2 P_2 + G_3 P_3 + G_4 P_4 + G_5 P_5 + G_6 P_6) T_{av} 60 N_h [g/h] \qquad (1)$$

Where:
- G_1, G_2, G_3, G_4, G_5, G_6 - are the pollution measures in g/min for every polluting according to 6 groups of production years, namely before 95, 1996-1999, 2000-2005, 2006-2009, 2009-2014 and after 2014 given in Table 2.
- P_1, P_2, P_3, P_4, P_5, P_6 - are the percentages of vehicles in circulation according to 6 groups of production years, namely before 96, 1996-1999, 2000-2005, 2006-2009, 2009- 2014 and after 2014, calculated for the corresponding situation given in fig. 1, which are: P_1 =25%, P_2 =19%, P_3 =20%, P_4 =18 %, P_5 =11% and P_6 =6%

For the proposed structure, the number of vehicles manufactured before 1995 (25,000) will be replaced with PHEV vehicles. Then the new percentages will P'_1 =20%, P'_2 =19%, P'_3 = 20% P'_4 = 18 %, P'_5 = 11%, P'_6 =11%. While the pollution of PHEV cars will be zero, because in the city they use electricity.

Results

Hourly pollution amounts for the main pollutants CO, NOx+HC and PM, calculated according to formula 1 for the current state of vehicles in circulation and for the proposed structure, with PHEV, are shown in figure 2.

The results show that the amount of daily pollution caused by vehicles at the "21 Dhjetori" intersection is extremely high and amounts go to 1350 kg CO, 675 kg (NOx+CH) and 75 kg PM particles per day with a total pollution of 2100 kg per day. While the amount of CO_2 produced by vehicles is about 23 tons/hour, or about 370 tons/ day. The results show that with the introduction of 5 % PHEV into circulation the production of CO_2 will decrease to 20 tons/hour, or 320 tons/ day.
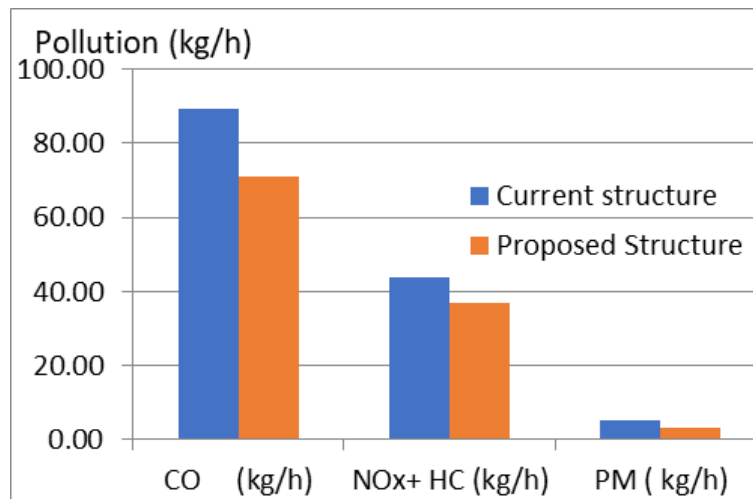
Figure 2. Amounts of pollution in kg/hour during the day for the current and the proposed structure

Discussion

This high level of pollution at the intersection is mainly caused by vehicles manufactured before 1996, which in our country predominate in circulation and have a pollution rate more than 3 times higher than those manufactured after 2005. While with the introduction of PHEV, the daily pollution amounts will be 1040 kg CO, 520 kg (NOx+HC) and 50 kg PM particles per day.

The results show that with the introduction of 5 % PHEV into circulation, we have a reduction in pollution of around 22%. This shows that if this scheme is implemented for 2 years, we halve the pollution rate in the city. In this direction, a great help is the initiative of the Municipality of Tirana to review the current legislation and creating facilities for hybrid electric vehicles.

Based on the obligations of the agreement according to the [2], Albania should have introduced more than 25,000 hybrid/electric cars into circulation by 2020. This becomes possible if buyers of these cars are stimulated by reducing customs duties. In the meantime, we propose to remove the road tax and environmental pollution tax for electric hybrid vehicles. For this purpose, legal acts must be prepared in advance for these types of cars and must to set the tasks to create the necessary infrastructure for electricity supply, the preparation of specialists with the necessary knowledge for the maintenance of hybrid vehicles. This requires to set the tasks to introduce knowledge about hybrid/electric vehicles in vocational schools.

Also, to motivate citizens to buy hybrid cars, government incentive programs can be used, giving special credits and discounts to support the purchase and use of hybrid cars,, such as reduced insurance premiums and free or reduced parking.

Conclusion

High environmental pollution from vehicles at intersections in the city is caused by vehicles manufactured before 1996, which have a pollution rate over 3 times higher than those manufactured after 2005 and prevail in circulation in Albania. Also, the amount of CO_2 produced by these vehicles is very high.

The proposed structure with the introduction of 5% of PHEV in circulation, which replace vehicles produced before 1996, ensure a reduction of environmental pollution in urban intersections up to 22% and a reduction of CO_2 up to 12%

The introduction of hybrid/electric vehicles in Albania can be achieved by helping vehicle owners with the removal of customs tax, road tax and the reduction of environmental tax, insurance premium, parking tax to zero, as well as by used incentive programs from the government for their purchase.

References

1. Heinberg, R. (2015). The end of economic growth. New York, USA
2. IEA (April 2015). Hybrid and Electric Vehicles. Electric Drive Delivers Implementing Agreement for Co-operation on Hybrid and Electric Vehicle Technologies and Programmes. On the basis of a decision by the German Bundestag. www.ieahev.org
3. Car Exhaust, Air Pollution, Combustion Engines, (2020 February,) http://www.nutra.med.com/environment/carsepa.htm
4. IEA (2013), Hybrid and Electric Vehicles, www.ieahev.org
5. European Environment Agency, (2020). Monitoring CO_2 emissions from passenger cars and vans in 2018, ISBN: 978-92-9480-222-4
6. Vehicle technologies program (2011). Energy Efficient & renewable energy, USA DE
7. GDRTS (2022), Archive's central of General Directorate of Road Transport Services www.dpshtrr.org.al
8. Hillier, V. A. W., & Coombes, P. (2016). Hillier's Fundamentals of Motor Vehicle Technology 5th edition Book 1. P.233
9. Hajderi, A. Bozo, L. (2014). Air pollution from vehicles and their effect on human health in urban areas. Revista: International Journal of Engineering Science and Innovative Technology (IJESIT), 3(3), 41-47

Health care cyber security: Albania case study

Dolantina Hyka*[1] , Fatmir Basholli*[2]

[1]Mediterranean University of Albania, Department of Information Technology, Albania, dolantina.hyka@umsh.edu.al
[2]Albanian University, Department of Engineering, Tirana, Albania, fatmir.basholli@albanianuniversity.edu.al

Abstract
Nowadays real time communication is defining and at the same time conditioning our daily life. Increasing the volume of communications constitutes an added value to the economic and social development of a country, but at the same time exposes it to cyber risks. Health care is a favorite area to attack. Violation of healthcare data is a growing threat to the healthcare industry, causing not only data loss and monetary theft, but also attacks on medical equipment and infrastructure. An important aspect is the context of the place where the phenomenon is being studied. Albania is a developing country with a high middle income. it is important to note that Albania has experienced rapid development in terms of information and communication technology (ICT) in the last decade. During this time the number of internet users has increased spectacularly. The purpose of this paper is to analyze information security practices in Albanian public and private hospitals, in order to determine the level of Information Security in this sector, and to provide suggestions for improvements.

Introduction

The purpose of this paper is to analyze the state of information security in Albanian public institutions by providing a clearer picture of the level of development of information security and the steps that need to be taken to further advance.

The entire public and private health system through the systems they use and the services they provide are the users and in a sense also the owners of personal data of the entire population of a country. They contain very important information in electronic version that should be protected from serious threats which may be abuse as well as illegal actions with the data, but also their destruction [1-2]. The rapid development of information-threatening techniques poses a serious risk to information [3-4]. Developing and managing ongoing protection is necessary to keep information as secure as possible.

For users of information systems it is important to ensure the security of their data whether personal or not. It is therefore essential that users have a good knowledge and awareness of information security practices based on regulations, policies and practices. This study will reflect the state of this documentation in the health system and provide suggestions on how improvements can be made.

This study helps healthcare leaders reduce hospital sensitivity by detailing the results that come from strategic online safety development decisions. It also helps cyber security professionals to understand the complexities of developing internet security capability in hospitals. In this rapidly changing and evolving environment, information as a valuable asset is always under threat.

Material and Method

a. Identify, define and discuss information security management practices and what are the factors that can influence the implementation and development of information security management in Albanian public institutions;
b. Understand the importance of the components identified and how they interact with each other;

c. Determine the level of information security awareness in public institutions and determine whether improvements can be made in information security management;

This are the objectives of this paper.

In order to achieve the objectives of this study, we have considered the following research questions
1. What are the security management practices of information in the health system?
2. What are the factors that influence the effectiveness of information security management practices?
3. How can information security be improved in the Albanian health system?

This question seeks to lay out concrete steps that need to be taken to improve information security in the Albanian health system based not only on the literature, but also on the common characteristics that these institutions have.

Other factors that give importance to this study are:

1 Lack of studies on information security in Albania;
2 Relatively new developments in terms of information security in the health care system in our country.

As limitations of this study we can mention the lack of academic studies in the field of safety in the health system in Albania. The questionnaire design phase took longer than anticipated as there were difficulties in completing the questionnaire in its initial version in the pilot phase. The data collection phase of the study also took longer than anticipated due to the difficulty in obtaining the response of the respondents. Reasons may include lack of familiarity with the questionnaires, low culture of collaboration in such studies, lack of information and misunderstanding of the purpose of this study.

Results

In this study responded 71 people, students in the faculty of medicine in the field of pharmacy. Interesting is the fact that they understood the importance of information security and had doubts whether this information was being used by others. Most of them were pursuing higher education or had completed them. However most of these respondents were mostly around 19-25 years old.

Most of the respondents indicated that there are still problems and uncertainties in the health system about information security. However, regarding the management of information security in the country by hospitals, 71.8% answered that they do not trust the information system in the country, it is also noted that respondents do not have information about digitalization of health. 38% answered that I am not sure if digitalization would bring information insecurity and make it even more easily accessible by illegal organizations or structured groups of hackers dealing with information theft

Also, 46.5% of respondents do not read private matters at all when they become part of the health system in the country.

Discussion

The literature on information security management emphasizes the need to address technical and non-technical issues related to information security. Especially in developing countries there is a lack of attention in the literature to address these issues as well as the level of awareness on information security. Appropriate measures must therefore be taken to protect the critical assets of the health organization.

This question seeks to identify and understand the factors associated with information security management by doing a literature review in general and for the health system in particular focusing on developing countries

Conclusion

From the analysis of the questionnaires for the analysis of trust in the health system as well as the security of information in Albania, we identified that:

i. The largest percentage of respondents are women with 81.4%, this large percentage of women as the field where we are focused to do this study is mostly chosen by women, the respondents are medical students in the field of pharmacy;

ii. The 19-25 age group is 90% of the respondents, this was known in advance as the respondents are students. This age group was chosen to be surveyed as they are more inclined in the field of information technology and have more knowledge about digital medicine;

iii. Respondents were also asked about their education and almost 70% of them had a bachelor's degree, most of them were still studying. A very small part of them were employed;

iv. A considerable part of them did not understand the term cybernetics even though they are the age group of technology, they had problems in filling out the forms and little known for this category even though they are students in the field of pharmacy. This further complicates healthcare digitalization as pharmacists should be the first to use this system to see prescriptions issued by doctors in a future where healthcare will be digitized. This brings many obstacles on the way to a total digitalization of it;

v. Only a small number of them knew how polyclinics worked, and a large number of them had no idea how to book a place for a polyclinic analysis.

from polyclinics in the country. A large proportion of about 62% of respondents have never had a check-up at a polyclinic. 21% who had had this type of control had a pronounced lack of confidence that their analysis would be safe in health systems;

vi. Nearly 83% of them were not aware of where the card analysis data or medical prescriptions were stored, they are not fully informed. Polyclinics in the country have never asked permission to use the data of their clients, this is noted in the survey we conducted where 83% of them say that this type of request has never been made, except in cases where polyclinics have asked to do any specific statistics. But there are also many cases where the data is used without the consent of the person who owns this data;

References

1. Kruse, C. S., Frederick, B., Jacobson, T., & Monticone, D. K. (2017). Cybersecurity in healthcare: A systematic review of modern threats and trends. *Technology and Health Care*, *25*(1), 1-10.
2. Alharam, A. K., & Elmedany, W. (2017, May). The effects of cyber-security on healthcare industry. In *2017 9th IEEE-GCC Conference and Exhibition (GCCCE)* (pp. 1-9). IEEE.
3. Jalali, M. S., & Kaiser, J. P. (2018). Cybersecurity in hospitals: a systematic, organizational perspective. *Journal of medical Internet research*, *20*(5), e10059.
4. Ahmad, A. (2012). Type of security threats and it's prevention. *Int. J. Computer Technology & Applications*, *3*(2), 750-752.

Complex network approach to detect faults in photovoltaic plants: Albanian case study

Xhilda Dhamo[*1] , **Eglantina Kalluçi** [1] , **Eva Noka** [1] , **Darjon Dhamo** [2]

[1]University of Tirana, Department of Applied Mathematics, Albania, xhilda.merkaj@fshn.edu.al; eglantina.kalluçi@fshn.edu.al; eva.jani@fshn.edu.al
[2] Polytechnic University of Tirana, Department of Electrical Engineering, Albania, darjon.dhamo@gmail.com

Keywords
Complex network
PV plant
Fault detection
Node strength

Abstract

With the trend towards photovoltaic plants in energy production, it is often difficult to describe the system status and fault conditions using traditional methods. We used machine learning and deep learning to predict PV production, but here we are focused on detecting faults in PV plants. Complex networks analysis is presented as an approach which succeeds in detecting faults in PV plants. Our case study is a photovoltaic plant installed in a factory in Albania. Firstly, we use sliding windows for different periods of time and construct a weighted directed network (functional graph) when each node represents a sensor and each edge represents the strength between the two signals which is determined by the mutual information measure. We have used in total 29 different signals from 4 different inverters for a period of six months (June 2022- December 2022). Secondly, we compute the node's strength for the signals corresponding to voltage, current and irradiance and show that when a fault occurs the weighted degree centrality of the irradiance node decreases while the voltage and current weighted degree centrality increases.

Introduction

The use of renewable energy has many potential benefits, including a reduction in greenhouse gas emissions, the diversification of energy supplies and a reduced dependency on fossil fuel markets. Based on the Eurostats statistics solar is the fast- growing energy source in Europe. Even in Albania, the capacity of PV plants has been growing exponentially over recent years. Albania has more than enough solar power projects in the pipeline to meet the 220.4 MW in the combined capacity of wind power and photovoltaic that transmission system operator OST (Transmission System of Electricity) expects to connect by 2023.

In order for the PV plants to have good performance and long lifetime it is important that the time to detect the fault and repair or substitute the faulty component is fast. These factors are related also with profitability. For that reason the case study of this paper is fault diagnosis of a 125 kW PV system which is installed on a rooftop of a factory in Tirana, Albania. The data are obtained by Fronius Solar. web database every 5 minutes for a period of six months (June 2022- July 2022).

Complex networks have been successfully used to model real-world problems and data in more than 11 areas. The idea of using complex networks as an approach for detecting faults in PV plants. In this paper, complex network analysis is used to model the sensor network described in the previous paragraph as a weighted network based on the mutual information matrix which is computed to the signals and measures the amount of information taken from one signal by knowing the outcome of the other one.

Material and Method

The data collected from the PV plant consists of 29 signals taken from 4 different inverters. Table 1 shows all the signals used in this study.

Table 1. PV plant variables for 4 inverters

Signals	Measuring unit
Active Power	W
DC Current	A
L1 AC Voltage	V
L2 AC Voltage	V
L3 AC Voltage	V
PV production	Wh
Ambient temperature	℃
Wind speed	m/s
Irradiation	W/m^2
Module temperature	℃

Figure 1 shows schematically all the steps from the time series data up to the construction of comparative time series and weighted node strength plots.
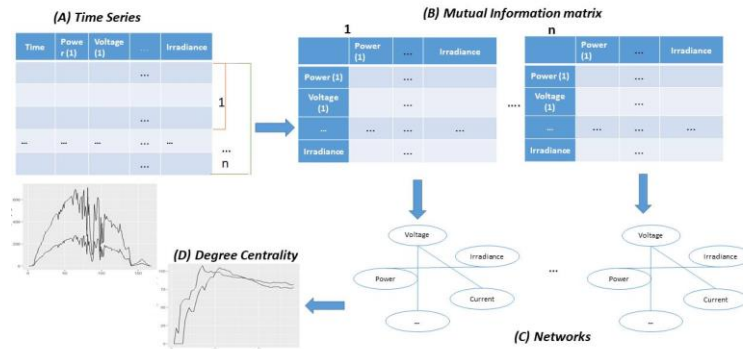
Figure 1. Weighted network construction from time series data

Firstly, considering that there are m samples and *n* different signals, the mutual information matrix with dimensions *nxn* is constructed. Each of its components gives the strength between two distinct signals. The mutual information matrix is computed for different periods of times, sliding the window from the beginning of the data up to the entire monitoring interval. The time interval used in this study is 10 hours and in total are used 125 sliding windows.

Secondly, for each of these sliding windows a directed weighted network (functional graph) is constructed [1-3]. In this paper, we are focused just on the nodes representing the DC Current, AC Voltage and Irradiation for the inverter where the fault is detected. This network is used to compute the weighted node centrality and divide the centralities in two groups corresponding to the period before and after the fault occurs.

All the analysis is performed in RStudio.

Results

In this paper we have considered one fault that happened in the first inverter on 27 August 2022. The fault happened at 05:04 PM and the time interval considered is from 07:25AM up to 05:45 PM, using in total 125 sliding windows. The fault alert is "No feed in for 24 hours".

In the first plot, we consider 0 the initial time studied (07:25) and increment by one for each of the 5 minutes. Whereas, in the second plot, the first sliding window is considered the initial moment 0 and incremented by one for each of the sliding windows.

In the first plot, irradiation and the DC current increases proportionally with each other before the fault occurs. In the time when fault happens (moment 82 corresponding to time 02:55 PM) the current decreases immediately to 0, while irradiance decreases normally as the evening is coming.

Figure 2. Comparison between signals time series data and weighted degree centralities

In the second plot it is clear that weighted node degree centralities are positively correlated to each other before the fau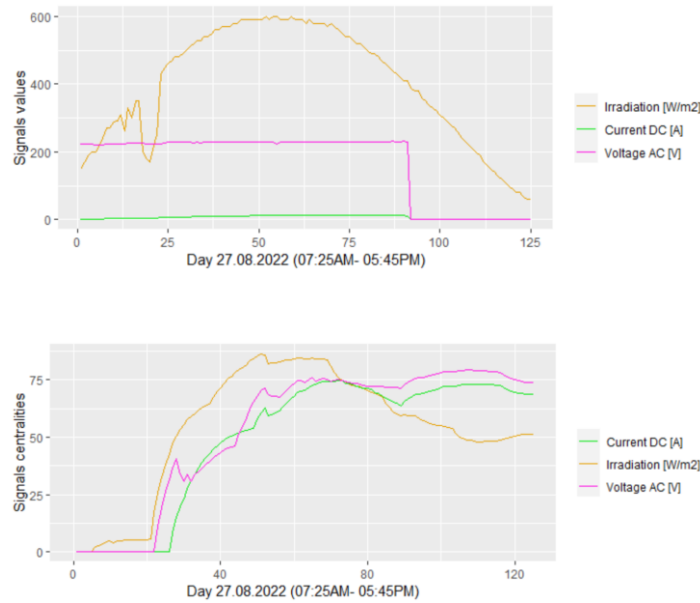lt happens. After the fault, it is seen that the irradiation decreases while the DC current and AC voltage increases and remain positively correlated with each other.

Discussion

In this study we have considered one fault and taken in consideration only one inverter. Furthermore, we are based only on the weighted node centralities of the networks constructed. Our intention for future work is to use all the information obtained from the sensors in the PV plants and to analyze if we can extract more valuable information about the time and the sensor where a fault occurs by extending our focus from the weighted degree centrality to other centralities and to the usage of modularity to detect communities in networks, where these communities may be time intervals or sensors where a fault is detected.

Conclusion

We have shown in this study that complex network analysis can be a powerful tool in identifying faults in photovoltaic plants. We concluded that we can reveal meaningful information from the weighted degree centralities and these are important in detecting the moment when a fault occurs. One fault in PV plants implies that the weighted degree centrality of the irradiation is not positively correlated with the weighted degree centrality of the power and voltage. Table 2 shows the changes in the correlation before and after fault occurs.

Table 2. Correlations between weighted degree centralities before and after fault occurs

	Irradiance	DC Current	L1 AC Voltage
Irradiance	1	0.89062/ **-0.36066**	0.90268/ **-0.19876**
DC Current	0.89062/ **-0.36066**	1	0.97493/ 0.98425
L1 AC Voltage	0.90268/ **-0.19876**	0.97493/ 0.98425	1

References

1. Dhamo, D., Dhamo, X., Spahiu, A., & Panxhi, D., (2022). PV production forecasting using machine learning and deep learning techniques: Albania case study. Advanced Engineering Days, 5, 68-70.
2. Bonacina, F., Corsini, A., Cardillo, L., & Lucchetta, F. (2019). Complex Network Analysis of Photovoltaic Plant Operations and Failure Modes. *Energies*, *12*(10), 1995. MDPI AG. Retrieved from http://dx.doi.org/10.3390/en12101995.
3. Geng, Zh., Wang, Z., Hu, H., Han, Y., Lin, X., & Zhong, Y., (2018). A fault detection method based on horizontal visibility graph-integrated complex networks: Application to complex chemical processes. Wiley Online Library, https://doi.org/10.1002/cjce.23319.

Advanced Engineering Days

aed.mersin.edu.tr

Hand gesture and voice-controlled mouse for physically challenged using computer vision

Aarti Morajkar*1 ⓘ, Atheena Mariyam James 2 ⓘ, Minoli Bagwe3 ⓘ, Aleena Sara James4ⓘ, Aruna Pavate1ⓘ

1University of Mumbai, St Francis Institute of Engineering, Information Technology, India, morajkaraarti41@gmail.com, arunaapavate@gmail.com, atheenajames96@gmail.com, minolibagwe@gmail.com, aleenajames998@gmail.com

Keywords	Abstract
HCI Gesture AI Media pipe Virtual Mouse	A Human-Computer Interface (HCI) is presented in this paper to allow users to control the mouse cursor with hand gestures and voice commands. The system uses computer vision EfficientNet B4 architecture with no code ml to identify different hand gestures and map them to corresponding cursor movements. The objective is to create a more efficient and intuitive way of interacting with the system. The primary purpose is to provide a reliable and cost-effective alternative to existing mouse control systems, allowing users to control the mouse cursor with hand gestures and voice commands. The system is designed to be both intuitive and user-friendly, with a simple setup process. The highly configurable system allows users to customize how it works to suit their needs best. The system's performance is evaluated through several experiments, which demonstrate that the hand gesture-based mouse control system can accurately and reliably move the mouse cursor. Overall, this system can potentially improve the quality of life and increase the independence of individuals with physical disabilities.

Introduction

Artificial intelligence is putting intelligence to make machines intelligent and capable of performing logical tasks designed by humans. Computer vision is part of AI that uses image samples to train machines. Computer vision provides different solutions such as disease prediction [1-2], landmine detection [3], designing adversarial samples to make machine learning models more robust [4-5], Lip reading recognition [6], and many more.

AI has a massive impact on people with disabilities to improve their lifestyles, providing the same access and services regardless of their disabilities. Gesture recognition is a technology that interprets hand gestures as commands using images. The voice assistant interface enables the hands-free operation of digital devices. This work aims to develop a new Human-Computer Interaction System that utilizes natural and intuitive hand gestures and voice commands rather than external mechanical devices such as a mouse. The proposed research introduces a novel system that utilizes hand gestures and voice commands to facilitate computer mouse movements for users. Voice assistants are hands-free and require minimal effort, allowing fast response times. This system benefits teachers, clinicians, and other users who can benefit from the hands-free operation and physically challenged people.

Many HCI systems capture human biological information as input, such as bioelectricity and speech signals, resulting in richer HCI modes. These new interactive methods made the HCI process more user-friendly and convenient. The field of human-computer interaction improved in terms of branching and interaction quality. Many researchers concentrated on using multimodality, intelligent adaptive interfaces rather than command/action-oriented ones, and active rather than passive interfaces instead of conventional interfaces [7].

This research aims to develop a cutting-edge Human-Computer Interaction System that simplifies the usage of natural and intuitive hand gestures and voice commands rather than relying on an external mechanical device like a mouse. Our proposed system utilizes hand gestures and voice assistant technology to enable users to efficiently

control computer mouse movements, with the benefits of hands-free, effortless operation and speedy response times. This system has potential applications in various fields, such as education, healthcare, and defense, to enhance user experience and accessibility. Specifically, this system can benefit individuals with physical disabilities, in-car systems, and military operations. The objectives of the proposed system are:

1. To replace direct mouse clicks and points with gestures to control computers and other devices to simplify completing tasks.
2. To offer a cost-effective alternative to existing mouse control systems by eliminating the need for costly hardware such as additional sensors and special controllers using a deep learning model.

The remaining work is organized as follows: section II discusses the related work, section III describes the methodology, section IV concludes the work.

Literature Review

In recent years, a growing interest has been in developing new human-computer interaction (HCI) systems that replace traditional input devices such as the mouse with more natural and intuitive alternatives. One such alternative is hand gesture-based mouse control, which allows users to control cursor movements and perform mouse functions using hand gestures. In this paper, we present a review of the current state of the art in hand gesture-based mouse control, including recent developments in gesture recognition algorithms, sensing technologies, and applications of this technology in various fields.

Kabid et al. proposed [7] to create a novel mouse cursor control system that employs a webcam and a color-detecting technique. The system records every frame the webcam captures until the project is completed by implementing an infinite loop. Color-caught frames from the webcam captured frames are used to detect the color pixels on the fingertips. The distance between two detected colors is calculated using the OpenCV function. For clicking events, the proposed system uses close gestures. However, the system's efficiency could be improved due to the difficulties and complexity associated with background interference.

Rokhsana et al. [8] proposed a real-time vision-based gesture-controlled mouse system. It employs color-based image segmentation for detecting hands, and contour extraction is performed to obtain the boundary information of the desired regions. The system uses a MATLAB function for moving operations, which calculates the centroid of the hand region. This approach is not limited to only controlling a mouse; it can control other devices such as televisions, robots in dangerous nuclear reactors, and other industrial setups. The system's sensitivity to surrounding noise and brightness can also be increased.

Kollipara et al. [9] proposed a system that utilizes libraries such as OpenCV, NumPy, and sub-packages. The model is built using computer vision techniques, and the detection and movement of the mouse are based on color fluctuations. The color detection model can be designed to identify a particular color from a colored image, which can improve the system's accuracy.

Reddy et al. [10] proposed a model for recognizing motions, detecting fingers, and controlling mouse operations. The OpenCV library is used for image processing, and the PyAutogui module is used for mouse control. The algorithm's implementation involves two different approaches for mouse control: one using color caps and the other recognizing gestures made with bare hands. It involves integrating the video and processing the photos through backdrop removal. Background subtraction helps by ignoring steady items and only considering foreground objects. Fingertip detection includes finger guessing, circle recognition, and color identification. Gesture recognition involves identifying the skin tone, detecting contours, forming convex hulls, and inferring the gesture.

Sugnik et al. [11] proposed a technology that uses hand gesture recognition and image processing to create a virtual mouse and keyboard. The mouse operates using a convex hull technique, where gestures are detected or recorded and used to map the mouse's functionalities. The keyboard function uses a hand position system that records the user's hand position in a video. However, the Convex Hull algorithm may encounter issues and lose accuracy if there is external noise or flaws within the webcam's operational range.

Shibly et al. [12] aims to develop a hand gesture-based virtual mouse system that allows users to control a computer cursor using hand gestures instead of a traditional physical mouse. The methodology used in this study involved designing and developing a prototype system that captures and processes the hand gestures of the user using a camera and a machine learning algorithm. The work describes the various components of the system, including the hardware and software used and the algorithms utilized for hand gesture recognition.

Sharma et al. [13] used video processing techniques to track the position of the user's hand and translate its movements into corresponding movements of the computer cursor. To achieve this, the authors used a computer vision algorithm called skin color segmentation to detect the user's hand from the video stream. The authors applied a motion estimation algorithm based on the Lucas-Kanade method to track the movement of the hand. The authors also used a machine learning algorithm called K-Nearest Neighbour (KNN) to recognize hand gestures. This algorithm classifies hand gestures based on the fingers' and palm coordinates. The authors trained the algorithm using a dataset of hand gesture images and achieved a recognition rate of 95%.

Mishra et al. [14] used a deep convolutional neural network (CNN) called YOLOv3 to detect and localize the fingertips in the video frames. The authors used a custom-built data collection system that captured egocentric video of a user's hand performing various gestures. The annotated frames with fingertip locations used this annotated data to train and evaluate the YOLOv3 model. The proposed system showed promising results in terms of accuracy and efficiency. It could be applied to various applications involving hand gesture recognition, such as virtual or augmented reality interfaces.

The reviewed work has highlighted several issues and challenges related to hand gesture-based mouse control systems. For instance, one study [10] identified the problem of the model's sensitivity to specific color detection, leading to detection errors. Another study [11] reported limitations in detecting hand movements in a pre-defined zone and the lack of advanced mouse functionalities. Additionally, the system's accuracy is affected by various lighting conditions, further reducing the effectiveness of color and shape-based algorithms. To address these challenges, the proposed approach by the authors provides solutions that improve accuracy and efficiency and provide more advanced mouse functions for users.

Methodology

Gesture-controlled virtual mouse implementation using deep learning involves creating a pipeline to detect hand gestures and map them to mouse actions. The following are the steps:

1. Collection and processing of the Data: - This is the initial stage of gathering information on the hand motions to operate the virtual mouse. The collected images are transformed into tensors of nodes. The data is preprocessed to remove pertinent details like hand position and orientation before being captured using a depth sensor or camera.
2. Gesture Recognition Model training: - The model is trained using examples of labeled hand movements. A machine learning model recognized the hand motions.
3. Model: A Convoluted Neural Network (CNN) using the Efficientnet4 model is used for gesture recognition. The EfficientnetB4 trained on a custom dataset to accommodate customized gestures.
4. Run the model and Map Gestures to Mouse Actions: - After building the pipeline, it is executed on a device to detect hand gestures in real time. The detected gestures were mapped to mouse actions, such as clicking, scrolling, or moving the cursor.
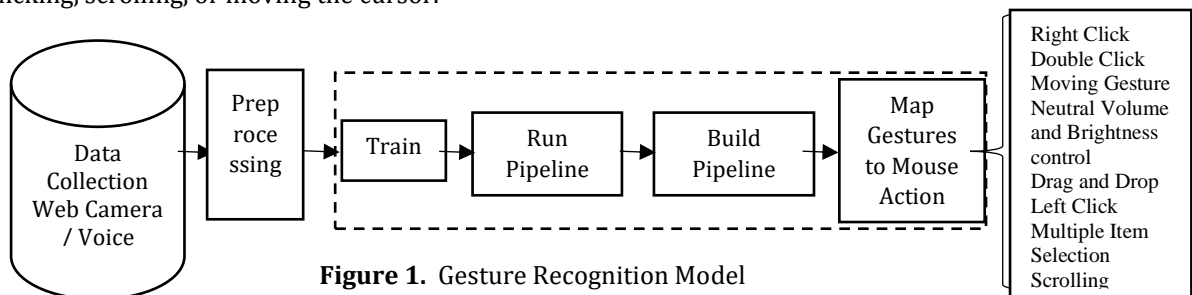
Figure 1. Gesture Recognition Model

A voice assistant can be added to a gesture-controlled virtual mouse implementation using MediaPipe. To do this, a voice recognition module can be included in the pipeline to detect and recognize voice commands from the user. The recognized voice commands can then be mapped to mouse actions or other actions, such as opening a file or launching an application. Figure 1 illustrates the implementation of a gesture-controlled virtual mouse with a voice assistant using MediaPipe. The hand gestures are captured using a depth sensor or a camera and preprocessed to extract relevant features such as hand position and orientation. The gesture recognition model is trained to recognize hand gestures from the collected data. It received the hand gesture as input and output as recognized gestures. The mouse action mapping module mapped the recognized hand gestures to mouse actions such as clicking, scrolling, or moving the cursor. It receives recognized hand gestures and the tracked hand position and orientation as input and outputs the mapped mouse actions. The virtual mouse module simulated the mouse's actions on the computer by accepting mouse actions as input. The voice recognition module detects and recognizes voice commands from the user. The implementation involved capturing and preprocessing hand gestures, recognizing the hand gestures using a machine learning model, tracking the hand in the video stream, mapping the recognized gestures and voice commands to the mouse and other actions, and executing the mapped actions on the computer.

Results and Discussion

The hand gesture and voice recognition system incorporate ten gestures: neutral gesture, moving cursor, left click, right-click, double click, scrolling, drag and drop, multiple item selection, volume control, and brightness control. The voice assistant performs launch/stop gesture recognition, and content search on Google, identifies a location, navigates files, displays the current date and time, copies and pastes, sleeps/wakes up, and exit actions. In the proposed system, authors aimed to enhance human-computer interaction using computer vision.
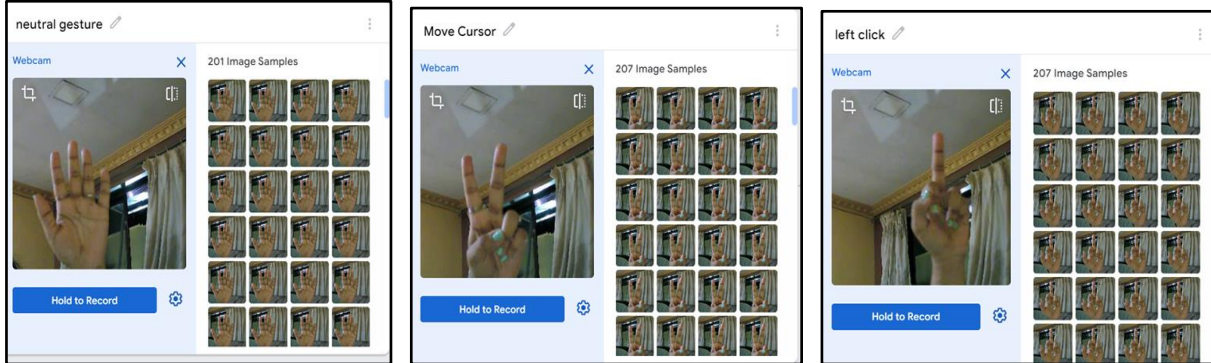

Figure 2. Hand Gestures incorporated by Gesture Recognition System

The webcam is positioned at various distances from the user to monitor hand motions and gestures to detect fingertips as shown in Figure 2. Gesture's ability is assessed under diverse lighting conditions such as bright light settings, low-light configurations, at a much farther distance from the camera, at a closer distance from the camera, with a left hand, right hand, both hands in camera, different backgrounds, and different hands of individuals of varying ages. The Voice Assistant is tested by providing diverse input via the mic and executing various functions such as location, file navigation, current time and date, copy and paste, sleep/wakeup, google search, and start and exit under various conditions.
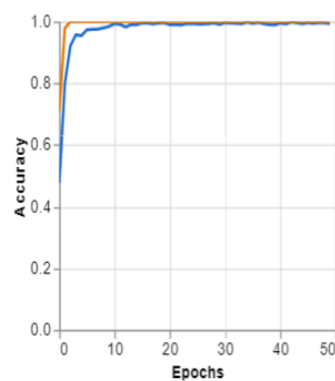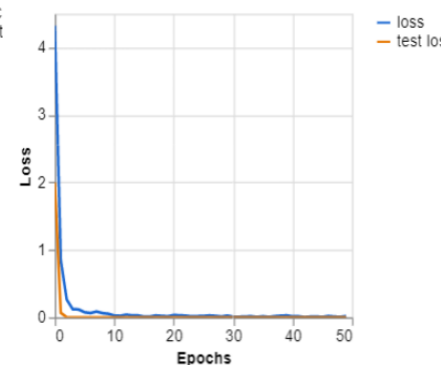
Figure 3. Performance of the model represented by accuracy per class and loss obtained by the model

It is observed that every mouse action gives a few seconds of delay, but apart from that, all the gestures had excellent and high accuracy for all the classes as shown in the Figure 3. The hand gestures are captured using an automated training machine learning model, showing promising results. Using hand gestures to control a mouse can increase productivity and ease of use, particularly for individuals with disabilities or those who find traditional mouse controls difficult. The automated training machine learning model accurately detects and classifies hand gestures, allowing for smooth and precise cursor control. While further research and testing may be necessary to optimize the system's performance, the results thus far suggest that a hand gesture-controlled mouse could become a valuable tool for computer users in the future.

Conclusion

Human-Computer Interaction was a rapidly evolving technological sector. New technological advances were produced every year, and new efforts were taken toward seamless, natural contact between the computer and the user. It has progressed from the traditional keyboard and text-based interface to the more powerful mouse and

touch-based interactions. With this study, we want to move forward to the next phase of virtual touchless interactions. This work developed a system for controlling the mouse cursor with a real-time camera. The technology was based on computer vision techniques such as CNN and could perform all mouse functions. However, due to the wide range of lighting and skin colors, it was impossible to obtain consistent results.

This method improves presentations for physically disabled individuals and enhances reliability. The system provides a comfortable PC and laptop experience for physically challenged persons. Future research involves eye movements to control mouse actions for those who cannot use their hands and introducing more functions to improve system performance.

References

1. Pavate, A., Mistry, J., Palve, R., & Gami, N. (2020). Diabetic Retinopathy Detection-MobileNet Binary Classifier.
2. Pavate, A., & Ansari, N. (2015). Risk Prediction of Disease Complications in Type 2 Diabetes Patients Using Soft Computing Techniques. 2015 Fifth International Conference on Advances in Computing and Communications (ICACC), 371-375.
3. Kumar, A., Pavate, A., Abhishek, K., Thakare, A. R., & Shah, M. (2020). Landmines Detection Using Migration and Selection Algorithm on Ground Penetrating Radar Images. 2020 International Conference on Convergence to Digital World - Quo Vadis (ICCDW), 1-6.
4. Pavate, A., & Bansode, R. S. (2020). Performance Evaluation of Adversarial Examples on Deep Neural Network Architectures.
5. Pavate, A., & Bansode, R. (2023). Design and Analysis of Adversarial Samples in Safety–Critical Environment: Disease Prediction System. In: Gupta, M., Ghatak, S., Gupta, A., Mukherjee, A.L. (eds) Artificial Intelligence on Medical Data. Lecture Notes in Computational Vision and Biomechanics, vol 37. Springer, Singapore.
6. Shi, B., Hsu, W., Lakhotia, K., & Mohamed, A. (2022). Learning Audio-Visual Speech Representation by Masked Multimodal Cluster Prediction. ArXiv, abs/2201.02184.
7. K. H. Shibly, S. Kumar Dey, M. A. Islam and S. Iftekhar Showrav, "Design and Development of Hand Gesture Based Virtual Mouse," 2019 1st International Conference on Advances in Science, Engineering and Robotics Technology (ICASERT), Dhaka, Bangladesh, 2019, pp. 1-5. https:doi.org/10.1109/ICASERT.2019.8934612.
8. Titlee, R., Rahman, A. U., Zaman, H. U., & Rahman, H. A. (2017). A novel design of an intangible hand gesture controlled computer mouse using vision based image processing. In 2017 3rd International Conference on Electrical Information and Communication Technology (EICT) (pp. 1-4). Khulna, Bangladesh.
9. Varun, K. S., Puneeth, I., & Jacob, T. P. (2019). Virtual Mouse Implementation using Open CV. In 2019 3rd International Conference on Trends in Electronics and Informatics (ICOEI) (pp. 435-438). Tirunelveli, India.
10. Reddy, V. V., Dhyanchand, T., Krishna, G. V., & Maheshwaram, S. (2020). Virtual Mouse Control Using Colored Finger Tips and Hand Gesture Recognition. In 2020 IEEE-HYDCON, Hyderabad, India (pp. 1-5).
11. Chowdhury, S. R., Pathak, S., & Praveena, M. D. A. (2020). Gesture recognition based virtual mouse and keyboard. In 2020 4th International Conference on Trends in Electronics and Informatics (ICOEI)(48184) (pp. 585-589). Tirunelveli, India.
12. Sharma, Neeta & Gupta, Aviral. (2020). A Real Time Air Mouse Using Video Processing. International Journal of Advanced Science and Technology, 29, 4635 - 4646.
13. Mishra, P., & Sarawadekar, K. (2019, December). Fingertips detection in egocentric video frames using deep neural networks. In *2019 International Conference on Image and Vision Computing New Zealand (IVCNZ)* (pp. 1-6). IEEE.

Advanced Engineering Days

aed.mersin.edu.tr

Machine learning algorithms for predicting life expectancy

Miranda Harizaj*[1] , Olgerta Idrizi [2] , Alfons Harizaj [3]

[1]Polytechnic University of Tirana, Faculty of Electrical Engineering, Albania, miranda.harizaj@fie.edu.al
[2]Mediterranean University of Albania, Faculty of Informatics, Albania, idriziolgerta@gmail.com
[3]Canadian Institute of Technology, Faculty of Engineering, Albania, alfons.harizaj@cit.edu.al

Keywords
Life expectancy
Machine Learning
Algorithms
Linear Regression
KNN

Abstract
In the last years SARS-Covid has had a big impact on mortality rate and also on life expectancy. Today the artificial intelligence techniques and machine learning algorithms can analyze large amounts of data and can be used to predict life expectancy. Life expectancy (LE) models have an immense effect on the social and financial structures of many countries around the world. This paper is an attempt to find the most efficient algorithm and methodology to predict it. Life expectancy depends on various variables like mortality rate, life expectancy from the past years, alcohol consumption rate, infant death, covid mortality and other illness that affect life expectancy rate. In this analysis it is reviewed different machine learning algorithms that have achieved better accuracy based on pertinent features of the datasets. Based on the analyze of simple linear regression and k-nearest neighbors (KNN) algorithms, machine learning techniques were applied in order to develop an accurate prediction solution for life expectancy with the effect COVID-19. By comparing these machine learning algorithms, it is analyzed which among them is more accurate to predict life expectancy.

Introduction

Everything in this world has a limited life expectancy. Humans also have a limited life span to survive. Life span prediction has a greater impact in the modern society because of food habits, different types of diseases, environmental conditions and other factors. After Covid 19, unfortunately, life expectancy was decreased. It has been the impact of the increase of mortality rate in this last years, because of Covid 19 pandemic.

Life expectancy is always defined statistically as the average number of years remaining at a given age. During the last years, life expectancy at birth has risen rapidly, due to many factors [1].
During the last century, statistics show the continuous increase in life expectancy at birth, resulted because of economic development and the improvement lifestyles, progresses in healthcare and medicine etc. There are a lot of factors that affect in life expectancy and mortality rate like gender, genetics, lifestyle, hygiene, access to health care, diet, exercise etc. Evidence-based studies indicate that longevity is based on two major factors, genetics, and lifestyle choices [2].

In this paper it is presented how machine learning and data science can help in predicting life span on the future. With the use of machine learning algorithms and data analytics can be prognosticated and examined the life span of the individual human being and can be used different classification algorithms for this prediction to accomplish higher accuracy.

Linear Regression

A correlation heat map is a graphical representation of correlation matrix representing the correlation between different variables and this helps understanding the linear dependencies of variables. The range of Correlation is (-1,1) and is calculated between two variables. Correlation value near to zero means the two variables are unrelated and close to 1 means the two variables are perfectly related.
As first step it is required adapt a supervised regression algorithm that fits the task requirements. Today there are a bunch of algorithms for regression tasks, and among them each has its pros and cons. The algorithm can result

in superior outcomes compared to others but might deficiency in terms of explain ability. Even that, the deployment of such complex algorithms is not an easy task. There is a trade-off between accuracy, model complexity and model explain ability.

Linear Regression is a comparatively simple and explainable algorithm. Deployment of Linear Regression requires minimal efforts, but on the contrary, it lacks accuracy when the data is non-linear. Complex algorithms perform better on non-linear datasets, but then the model lacks explain ability [3].

LR is a regression algorithm with a linear approach and can be used to predict a continuous value of a given data point by simplifying the given data. The linear part indicates the linear approach for the generalization of data.
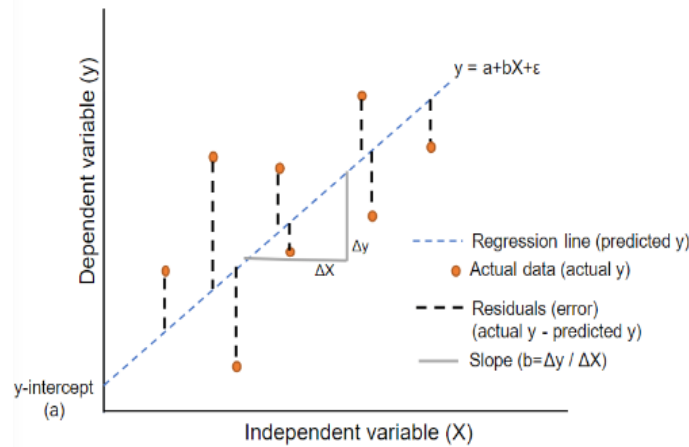

Figure 1. Linear regression [3]

In this algorithm it is predicted the dependent variable (y) using a given independent variable (x). A residual error is measured with the difference of the real value from the regression line that is the difference between a predicted value and the observed value.

If the coefficient of determination R-square came out to be closer to 1, this can indicate that the model optimally predicts the Life expectancies.

KNN Algorithm

In statistics, the k-nearest neighbors algorithm (k-NN) is a non-parametric supervised learning method first developed by Evelyn Fix and Joseph Hodges in 1995, and later expanded by Thomas Cover. It is one of the simplest ML Algorithms and is used for classification and regression. In both cases, the input consists of the k closest training examples in a data set. The output depends on whether k-NN is used for classification or regression:

It is needed to determine which k data points out of training are closer to the data point in order to get a prediction for. In k-NN classification, the output is a class membership. An object is classified by a plurality vote of its neighbors, with the object being assigned to the class most common among its k nearest neighbors (k is a positive integer, typically small). If k = 1, then the object is simply assigned to the class of that single nearest neighbor. It is supposed that the data are the lowing:

$$X_{11}, X_{12}, X_{13}, X_{1m}, Y_1$$
$$................................$$
$$X_{n1}, X_{n2}, X_{n3}, X_{nm}, Y_n$$

(1)

In the above array with n rows and m+1 columns, the first m columns are the attributes used to predict assuming that all attribute values x are numerical while the label values y are categorical. Then it is calculated the distance between data points. The Euclidean distance is a good choice for such a distance function if the data is numerical.

$$d(s, x_j) = \sqrt{(s_1 - X_{j1})^2 + \cdots.. (s_m - X_{jm})^2}$$

(2)

In k-NN regression, the output is the property value for the object. This value is the average of the values of k nearest neighbors. If k = 1, then the output is simply assigned to the value of that single nearest neighbor and is the reason why calculating training errors are useless.

The k-NN algorithm is a type of classification where the function is only approximated locally and all computation is accepted until function evaluation. If the features represent different physical units or come in

much different scales then normalizing the training data can improve its accuracy dramatically, since this algorithm relies on distance for classification [4].

A useful methodology can be to assign weights to the contributions of the neighbors, so that the nearer neighbors contribute more to the average than the more distant ones for both, classification and regression.

A peculiarity of the k-NN algorithm is that it is sensitive to the local structure of the data.

Results and Conclusion

In this paper it is analyzed how the artificial intelligence techniques and machine learning algorithms can predict life expectancy. By employing data through datasets, the correlation between attributes like mortality rate, life expectancy from the past years, alcohol consumption rate, Infant death, Covid mortality and other illness are monitored.

In this paper are reviewed different machine learning algorithms that have achieved better accuracy based on pertinent features of the datasets. Machine learning techniques were applied in order to develop an accurate life expectancy after COVID-19 based on those variables.

Advantages:

Linear Regression
- It performs good for linearly separable data
- It is simple to implement, interpret and efficient to train
- It handles overfitting pretty well using dimensionally reduction techniques, regularization, and cross-validation
- extrapolation beyond a specific data set

KNN Algorithm
- It is simple to implement.
- It is robust to the noisy training data
- It can be more effective if the training data is large [3].

Disadvantages:

Linear Regression
- The assumption of linearity between dependent and independent variables
- It is often quite prone to noise and overfitting
- Linear regression is quite sensitive to outliers
- It is prone to multicollinearity

KNN Algorithm
- Always needs to determine the value of K which may be complex some time.
- The computation cost is high because of calculating the distance between the data points for all the training samples [4].

The inclusion and dependency of these suggested features on life expectancy is still a matter of debate and a future part of research in this particular domain. Furthermore, the future enhancement can be made by using deep learning algorithm which may give better solution. Depending on the dataset, and other variables, the best adaptation is made.

References

1. Scholey, J., Aburto, J. M., Kashnitsky, I., Kniffka, M., Zhang, L., Jaadla, H., Dowd, J. & Kashyap, R. (2022). Life expectancy changes since COVID-19. Avaiable: https://www.nature.com/articles/s41562-022-01450-3
2. Bali, V., Aggarwal, D., Singh, S., & Shukla, A. (2021). Life Expectancy: Prediction & Analysis using ML, ICRITO.
3. Predicting Life Expectancy using Liner Regression. Avaiable: https://www.enjoyalgorithms.com/blog/life-expectancy-prediction-using-linear-regression
4. K-Nearest Neighbor (KNN) Algorithm for Machine Learning. Available: https://www.javatpoint.com/k-nearest-neighbor-algorithm-for-machine-learning

Finding the closest and lowest price pharmacy over a given location

Julian Imami *1

1Polytechnic University of Tirana, Faculty of Technology of Information, Albania, julian.imami@fti.edu.al

Keywords	**Abstract**
Pharmacy website Database PostgreSQL Python Huffman	If an object is required, people will buy it, but they will search for a seller who is deserving of their cash. Timing and approval are not very important factors when making a buy. Negotiating a lower price is essential because it might make them happier. You may be wondering why drugstore prices differ so much. The cost of treatments, even those that aren't prescribed, can vary considerably. These expenses change because various pharmacy benefit managers (PBMs) bargain prices on behalf of pharmacies and drug companies. When there are numerous PBMs and shops, drug prices frequently fluctuate. The purpose of this paper is to provide customers with the opportunity to input their desired medication and location in order to find the nearest (driving distance) pharmacy that will provide their desired medications at a reduced price.

Introduction

Customers should look for the pharmacy with the best prices in a particular area for a number of factors. One justification is to lower their out-of-pocket costs for prescribed drugs. Drug costs can differ considerably between pharmacies, says a Consumer Reports article [1]. Therefore, customers can save money on their prescription medications by looking around for the lowest price pharmacy.

In an effort to retain customers, some pharmacies also provide specific medications for free or at a very low cost, especially high-volume prescription drugs [2]. Additionally, the cost of the same medicine can vary significantly between pharmacies. For instance, when compared to Walmart and Kroger, Target/CVS had the lowest rates for a particular market basket of prescription drugs [3].

Customers can use resources like prescription discount cards or pharmacy search tools, like those offered by RxSaver and Health Peek [4-7], to discover the lowest-priced pharmacy. Customers can then evaluate prices at various pharmacies in their neighborhood and select the one with the best deal for their required medication. Customers may also think about buying prescribed drugs from foreign online pharmacies that adhere to strict guidelines for pharmacy practice and have been approved by the PharmacyChecker Verification Program [8].

STEPS OF DEVELOPMENT

Although PostgreSQL is a strong relational database system, it does not come with built-in support for location-based search. However, location-based searches can be executed using PostGIS' spatial extension [9]. Here are some steps you can take to use PostgreSQL to locate the nearby, lowest-priced pharmacy near a specific location:
   1. Gather information about pharmacy locations, such as prices and addresses.
   2. Transfer the data into a PostgreSQL database with PostGIS support.
   3. To locate the pharmacy with the best deal near a specific place, run a database query combining spatial and aggregation functions. We use the MIN function to locate the pharmacy with the lowest price within a certain

distance range and the ST Distance function to determine the distance between the given location and each pharmacy. To make sure the locate of the pharmacy that is nearest to each location, are grouped the pharmacies by their locations.

Lets suppose we have 2 tables which contains multiple possible combinations between the respective id-s.

```
SELECT FirstMap.id1, SecondMap.*
FROM   map1 FirstMap
CROSS  JOIN LATERAL (
SELECT  ST_HausdorffDistance(FirstMap.cordinates1, SecondMap. cordinates2) AS  h_dist, SecondMap.id2,
SecondMap. cordinates2
FROM   map2 SecondMap
WHERE  ST_HausdorffDistance(FirstMap. cordinates1, SecondMap. cordinates2) < 2
ORDER  BY 1, 2
LIMIT  2
) m2;
```

Depending on the minimal Hausdorff distance, returns 1 or 2 rows for each row in FirstMap, along with the top 2 corresponding rows in SecondMap and the minimum Hausdorff distance between them. No row is returned if SecondMap doesn't contain any rows with Hausdorff distances less than 2.

HAUSDORFF DISTANCE

The Hausdorff distance, also referred to as the Hausdorff metric, is a measurement of the separation between two groups of a metric space. It can be used to compare shapes and find variations between them in mathematics and computer science. Felix Hausdorff and Dimitrie Pompeiu invented the distance, which bears his name.

The Hausdorff distance [10] calculates the greatest distance possible between any two points in a rectangle. The infinity of all integers dH(f(X), g(Y)) for all metric spaces M and all isometric maps f and g is used to define this distance. If every point of one set is close to some point of the other set, and vice versa, two sets are said to be close in the Hausdorff distance. The Hausdorff distance transforms a metric space's collection of non-empty compact subsets into a separate metric space [11].

Numerous computer science applications, especially in the areas of image processing and computer vision, make use of the Hausdorff distance [12-13]. It is used to assess medical picture segmentation techniques and compare binary images and portions of them [14-15]. The Frechet distance, on the other hand, is more appropriate for curves because it is less susceptible to outliers [16].

Hausdorff dimension, which is a measurement of roughness or fractal dimension, should not be confused with Hausdorff distance, it is essential to note [17]. Additionally, in a Hausdorff space, every pair of unique points has a neighborhood that is disconnected from the other [18].

Briefly stated, the Hausdorff distance is a mathematical measure of how comparable two shapes are in a metric space. It has a wide range of uses in computer science and other disciplines.

Other Options

It could be possible to make the data visualisation even through some Python libraries as per below:

Matplotlib: For making static, interactive, and animated visualizations in Python, Matplotlib is one of the most popular libraries. It offers numerous layout types, such as line, bar, scatter, pie, and many more. Seaborn: Seaborn is a Matplotlib-based Python data visualization tool. It offers a sophisticated user interface for producing visually appealing and educational statistical images. Plotly is a web-based application for data visualization that works with Python, R, and MATLAB. It offers many dynamic plot types, such as scatter, line, bar, and more. Online sharing of dynamic plots can be done using Plotly. Bokeh: Bokeh is a Python library that gives contemporary web browsers access to dynamic visualization tools. For the creation of interactive plots like scatter, line, and bar charts, it offers a high-level UI. Altair: For the purpose of producing declarative statistical graphics, Altair is a Python library. By offering a clear and succinct API, it enables users to concentrate on the data rather than the specifics of the visualization. ggplot: Based on the R package ggplot2, ggplot is a Python library. Using a syntax of graphics, it offers a high-level interface for producing statistical graphics. Pygal: A Python tool called Pygal is used to create SVG (Scalable Vector Graphics) charts. It offers a straightforward API for making various types of plots, such as line, bar, pie, and more. 4. Another possibility is utilizing a geocoding API to transform the user's location into coordinates prior to querying the database.

Results

PostGIS is an effective tool that can be used to carry out location-based searches, such as locating the pharmacy with the best prices in a specific area. As a spatial database extender for PostgreSQL, PostGIS makes the PostgreSQL database more compatible with geographic objects and spatial searches [19].

You will need a dataset with information on the locations and costs of pharmacists in order to run this query. Once you have this information, you can use PostGIS to run spatial searches to identify the pharmacy with the best prices nearby. Spatial searches can be carried out using a variety of PostGIS functions. To determine whether a point is inside a polygon, for instance, use the ST Contains method [20]. This feature can be used to locate every pharmacy in a specific area. When you have this list of pharmacies, you can use SQL searches to identify which has the best deal. Additionally, PostGIS has tools for computing the separations between locations. To determine the separation between two locations, use the ST Distance function [19]. This function can be used to determine how far pharmacies are from a particular location. Once you know how far something is from another location, you can use SQL queries to locate the pharmacy with the best deal nearby.

It's important to remember that PostGIS, when used correctly, can be quite quick for spatial queries. For instance, PostGIS nearest neighbor support can deliver results with significantly improved performance when a spatial index is present [18]. Additionally, PostGIS enables you to write a small amount of SQL code to build location-aware queries [17]. In summation, PostGIS can be used to run location-based queries, such as locating the pharmacy with the best prices in a specific area. You will need a da-taset that lists the locations and costs of shops in order to accomplish this. Once you have this information, you can use PostGIS to run spatial searches to identify the pharmacy with the best prices nearby.

Conclusion

In conclusion, customers who want to save money on their prescribed medications should search for the lowest cost pharmacy in the area. Customers can use a variety of resources and tools to evaluate prices at various pharmacies and select the one that charges the least for the prescription drugs they require. In this paper is discussed the possibility to use the PostgreSQL DB over locating the nearby, lowest-priced pharmacy near a specific location. There are created a list of necessary steps to be followed and discussed different ways that possible to make the data visualization of the nearest location required.

References

1. https://www.postgresql.org
2. https://books.google.com/books/about/PostGIS_in_Action_Third_Edition.html?id=dhs-EAAAQBAJ
3. https://www.crunchydata.com/blog/a-deep-dive-into-postgis-nearest-neighbor-search
4. http://cgm.cs.mcgill.ca/~godfried/teaching/cg-projects/98/normand/main.html
5. https://www.wikiwand.com/en/Hausdorff_distance
6. https://www.sciencedirect.com/topics/computer-science/hausdorff-distance
7. https://pubmed.ncbi.nlm.nih.gov/31329113/
8. https://courses.cs.duke.edu/spring07/cps296.2/scribe_notes/lecture23.pdf
9. https://en.wikipedia.org/wiki/Hausdorff_dimension
10. https://en.wikipedia.org/wiki/Hausdorff_space
11. https://www.consumerreports.org/drug-prices/shop-around-for-better-drug-prices/
12. https://www.verywellhealth.com/free-low-cost-prescription-drugs-stores-2615299
13. https://reviews.cheapism.com/pharmacies/
14. https://www.rxsaver.com/blog/cheapest-pharmacy-to-fill-prescriptions
15. https://www.wellrx.com/discount-pharmacy-prices/
16. https://www.wellrx.com/prescriptions/
17. https://www.health-peek.com/pharmacy-lowest-prescription-drug-prices/
18. https://money.com/mark-cuban-pharmacy-drug-prices-comparison/
19. https://www.businessnewsdaily.com/3455-cheap-prices-customers.html
20. https://www.pharmacychecker.com/

Advanced Engineering Days

aed.mersin.edu.tr

Detection and prevention of intrusions into computer systems

Fatmir Basholli*1 , Adisa Daberdini 2 , Armand Basholli 3

1Albanian University, Department of Engineering, Tirana, Albania, fatmir.basholli@albanianuniversity.edu.al
2Aleksander Xhuvani University, Informatics Department, Elbasan, adisa.daberdini@uniel.edu.al
3Vodafone Albania/Safety & Security Lead, Tirana, Albania, armand.basholli@vodafone.com

Keywords
Intrusion detection
Denial of Service
Network-based
Interventions
Detection systems

Abstract
Historically, the concept of ownership has dictated that individuals and groups tend to protect valuable resources. No matter how much protection is given to the property, there is always a weak point, where the security provided at certain points fails.
This general notion has guided the concept of systems security and defined the disciplines in cyber security and especially that of computer networks. Computer network security consists of three principles: prevention, detection and reaction/response. Although these three are the basic components of security, the main focus is on detection and prevention resources because if we are able to detect and prevent all security threats, then there is no need for reaction and response. Intrusion prevention is the art of preventing unauthorized access to system resources. The two processes are related in a sense, where intrusion detection passively watches for intrusions into the system, and intrusion prevention actively filters network traffic to prevent intrusion attempts. In the continuation of the treatment, we will focus on these two processes.

Introduction

The notion of detecting intrusions in computer networks is a phenomenon born around 1980 and treated continuously by many researchers with works on "Computer security, computer networks, monitoring and surveillance of threats" etc. In their studies, it has been emphasized that through computer audit trails we gain vital information that can be valuable in tracking misuse and understanding user behavior. An intrusion is a deliberate unauthorized attempt, successful or not, to break the security, gain access, manipulate or misuse some valuable information and where the misuse can result in its deformation making it unreliable or unusable. This action could be performed by a person who is often called an intruder.

The process of breaking into a system involves a series of stages that begin with target identification, followed by reconnaissance that provides as much information about the target as possible. Once sufficient information is gathered about the target and vulnerabilities are mapped, the next step is to gain access to the system and finally the actual use of system resources. The software and hardware used for intrusion detection has the ability to safely analyze the collected data and derive useful results to take appropriate protection measures, which is more intelligent than other network security tools [1-4]. This paper will introduce the concept of "detection" of misuses and specific user behaviors and will recommend the development of intrusion detection systems.

Material and Methods

Detection is the process of gathering information about the target system, details of its operation, and weak points. Hackers rarely attack an organization's network before they have gathered enough information about the target network. They collect information about the type of information used on that network, where it is stored,

how it is stored, and the weak point of access to that information. They perform detection by scanning the system for vulnerabilities [5].

Vulnerability assessment is an automated process in which a scanning program sends network traffic to all computers or selected computers on the network and waits for traffic to return that will indicate whether those computers have known vulnerabilities. These vulnerabilities may include: vulnerabilities in operating systems, application software and protocols.

In addition to scanning the network for information that will eventually enable intruders to illegally access an organization's network, intruders can also access an organization's network by disguising himself as a legitimate user. They can do this in a number of ways ranging from obtaining special administrative privileges to low-privilege user on system accounts. The intruder could also gain remote access privileges [6].

Denial-of-service (DoS) attacks are where an intruder tries to crash a service (or machine), overload network connections, overload the CPU, or fill up (block) the hard drive. The risks of system intrusion are numerous, including the loss of personal data that may be stored on a computer. More problematic is the way digital information is lost which is not the same as losing physical data. In the case of physical data loss, if it is stolen, then someone has it, so you can take precautions. For example, you can report to the police and call your credit card issuer. Physical loss is not the same as digital loss because in digital loss you may never know your data is lost. Hackers can break into your system and copy your data and you'll never know. Therefore, we emphasize that the damage from the loss of personal digital data can be much bigger [7, 8].

Intrusion detection system (IDS) is a system used to detect unauthorized intrusions into computer systems and networks. Intrusion detection mechanisms can be put into three models: anomaly-based detection, signature-based detection and hybrid detection. Malfunction detection is different from anomaly detection where we label each intrusive activity as an anomaly, assumes that each intrusive activity is represented by a unique pattern or signature so that small variations of the same activity produce a new signature and hence he can be discovered. Malfunction detection systems are commonly known as signature systems. Malfunction pattern analysis is performed better by expert systems, pattern-based reasoning, or neural networks.
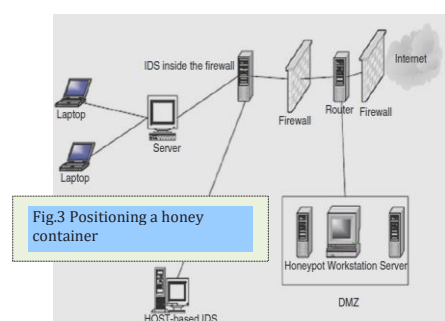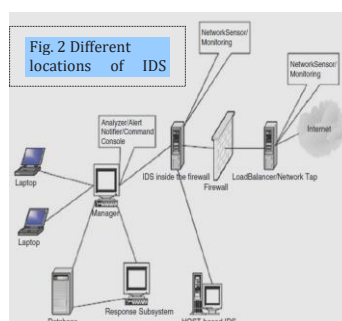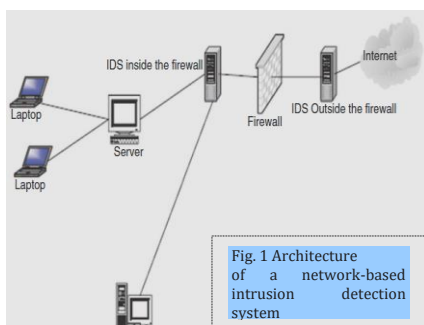
Two main problems arising from this concept:

• The system cannot detect unknown attacks with unmapped and unarchived signatures.

• The system cannot predict new attacks and therefore will respond after an attack has occurred. This means that the system will never detect a new attack [9-11].

Identification of intrusions into the system is supposed to identify three categories of users: legitimate users, legitimate users performing unauthorized activities and of course intruders who have illegally obtained the required identification and authentication.

Results and Discussions

Types of intrusion detection systems. Figure 1 Architecture of a network-based intrusion detection system. Intrusion detection systems are also classified based on their monitoring scope. Those that monitor a wide area are known as network-based intrusion detection and those that have a limited scope are known as host-based detections. Network-based intrusion detection systems (NIDS) have the entire network as their monitoring scope. They monitor network traffic to detect intrusions. They are responsible for detecting anomalies, inappropriate or other data that may be considered unauthorized. Only when the traffic matches an acceptable pattern is it allowed to proceed regardless of what the packet contains. A NIDS also captures and inspects every packet that is destined for the network, regardless of whether it is allowed or not. If the packet signature based on the packet content is not among the acceptable signatures, then an alert is generated [12-14].

Fig. 1 Architecture of a network-based intrusion detection system

Fig. 2 Different locations of IDS

Fig.3 Positioning a honey container

The network-based intrusion detection architecture consists of several parts that must work together to produce an alarm. However, it is normal practice to deploy IDS Sensors in the following areas:

• Inside the DMZ.

• Between the firewall and the Internet.

• Behind the front-end network firewall.
• Within the network.

Host-based intrusion detection systems (HIDS) have shown that the problem of misuse of organizational information is not limited to "bad" outsiders, and to address this problem, security experts have turned to inspecting systems within an organizational network. This local inspection of systems is called Host Based Intrusion Detection Systems (HIDS).

The Hybrid Intrusion Detection System envisages the deployment of NIDS and HIDS where each patrol of its own area of the network to verify unwanted and illegal network traffic. Both bring network security to their strengths and weaknesses that best complement and add to network security. Having both components provide better flexibility in their deployment options. Although NIDS and HIDS and their hybrids are the most widely used tools in network intrusion detection, there are others that are less used but more targeted and therefore more specialized.

a. System integrity verifiers (SIVs) monitor critical files in a system, such as the file system, to find out if an intruder has changed them. Figure 2 shows the different places where ID sensors can be placed.

b. Log File Monitors (LFMs) first create a record of log files generated by network services.
A honeypot is a system designed to look like something an intruder could hack. They are built for many purposes, but the main one is to deceive attackers and learn about their tools and methods [15, 16]. Figure 3 shows the positioning of a honey pot. Response to system intrusion. A good intrusion detection system alarm should produce an appropriate response. The type of response is related to the type of attack. Some attacks require no response, others require a preliminary response. The Incident Response Team (IRT) is a primary and centralized group of dedicated people charged with the responsibility of being the first team of contact whenever an incident occurs. An IRT should have the following responsibilities:

• Keeping up to date with the latest threats and incidents. • Being the main point of contact for incident reporting. • Notifying others whenever an incident occurs. • Assessing the damage and impact of each incident. • Finding how to avoid exploiting the same vulnerability. • Eliminating the effects (Healing) from the incident.
There is a particularly difficult challenge facing organizations trying to deploy IDS on their networks. Network-based IDS sensors should be placed in areas where they can "see" network traffic packets [17,18]. Among the things to consider, in addition to the IDS, in setting up a good IDS for the company's network, the following measures should be taken:
• In updating the Operating Systems. • Improving services in web servers, e-mail and databases. • In updating Firewalls.
• In the Network Management Platform.

Conclusion

In the process of computer network security, the research and design of the intrusion detection system is very important. A good intrusion detection system can effectively compensate for the shortcomings of the firewall, can provide a reliable guarantee for the security of the computer network, and is the most effective protection technology in modern network security measures.

All network-based intrusion detection systems and tools can provide probes in addition to port and host scans. As monitoring tools, they provide information on:

• Hundreds of thousands of network connections. • Attempts at external penetration. • Internal scans. • Misuse of confidential data models. • Unencrypted remote logins or web sessions. • Observed unusual or potentially troublesome network traffic.

References

1. Chand, N., Mishra, P., Krishna, C. R., Pilli, E. S., & Govil, M. C. (2016, April). A comparative analysis of SVM and its stacking with other classification algorithm for intrusion detection. In *2016 International Conference on Advances in Computing, Communication, & Automation (ICACCA)(Spring)* (pp. 1-6). IEEE.
2. Kizza, J. M., Kizza, W., & Wheeler. (2013). Guide to computer network security.
3. Saheed, Y. K., Abiodun, A. I., Misra, S., Holone, M. K., & Colomo-Palacios, R. (2022). A machine learning-based intrusion detection for detecting internet of things network attacks. *Alexandria Engineering Journal*, *61*(12), 9395-9409.

4. SANS Institute, "The History and Evolution of Intrusion Detection." [Online]. Available: https://www.sans.org/reading-room/whitepapers/detection/history-evolution-intrusion-detection-344. [Accessed: 20-Feb-2016].
5. Sharma, R. K., & Pippal, R. S. (2020, September). Malicious Attack and Intrusion Prevention in IoT Network Using Blockchain Based Security Analysis. In *2020 12th International Conference on Computational Intelligence and Communication Networks (CICN)* (pp. 380-385). IEEE.
6. Mitchell, R., & Chen, I. R. (2014). A survey of intrusion detection techniques for cyber-physical systems. *ACM Computing Surveys (CSUR)*, *46*(4), 1-29.
7. Kumar, R., Kumar, P., Tripathi, R., Gupta, G. P., Garg, S., & Hassan, M. M. (2022). A distributed intrusion detection system to detect DDoS attacks in blockchain-enabled IoT network. *Journal of Parallel and Distributed Computing*, *164*, 55-68.
8. Mishra, N., & Pandya, S. (2021). Internet of things applications, security challenges, attacks, intrusion detection, and future visions: A systematic review. *IEEE Access*, *9*, 59353-59377.
9. Liu, Y. S., Lai, Y. K., Wang, Z. H., & Yan, H. B. (2019). A new learning approach to malware classification using discriminative feature extraction. *IEEE Access*, *7*, 13015-13023.
10. Masduki, B. W., Ramli, K., Saputra, F. A., & Sugiarto, D. (2015, August). Study on implementation of machine learning methods combination for improving attacks detection accuracy on Intrusion Detection System (IDS). In *2015 International Conference on Quality in Research (QiR)* (pp. 56-64). IEEE.
11. Basati, A., & Faghih, M. M. (2022). PDAE: Efficient network intrusion detection in IoT using parallel deep auto-encoders. *Information Sciences*, *598*, 57-74.
12. McHugh, J. (2000). Testing intrusion detection systems: a critique of the 1998 and 1999 darpa intrusion detection system evaluations as performed by lincoln laboratory. *ACM Transactions on Information and System Security (TISSEC)*, *3*(4), 262-294.
13. Al-Taleb, N., & Saqib, N. A. (2020, September). Attacks Detection and Prevention Systems for IoT Networks: A Survey. In *2020 International Conference on Computing and Information Technology (ICCIT-1441)* (pp. 1-5). IEEE.
14. http://www.combofix.org/what-it-is-network-intrusion-detection-system.php
15. Axelsson, S. (2000). Intrusion detection systems: A survey and taxonomy.
16. Liao, H. J., Lin, C. H. R., Lin, Y. C., & Tung, K. Y. (2013). Intrusion detection system: A comprehensive review. *Journal of Network and Computer Applications*, *36*(1), 16-24.
17. https://cyber-defense.sans.org/resources/papers/gsec/host-vs-network-based-intrusion-detection-systems-102574.
18. Soniya, S. S., & Vigila, S. M. C. (2016, March). Intrusion detection system: Classification and techniques. In *2016 International Conference on Circuit, Power and Computing Technologies (ICCPCT)* (pp. 1-7). IEEE.

Advanced Engineering Days

aed.mersin.edu.tr

Improvement of e-education systems in Albania

Alfons Harizaj*[1] , Olgerta Idrizi [2]

[1]Canadian Institute of Technology, Faculty of Engineering, Albania, alfons.harizaj@cit.edu.al
[2] Mediterranean University of Albania, Faculty of Economic Science, Albania, idriziolgerta@gmail.com

Abstract

The isolation due to the pandemic caused by the Coronavirus, along with the panic and economic crisis around the globe, has prompted a very important discussion on distance education. Although hypotheses centered on the idea that the world will not be the same after the pandemic crisis will take a long time to study, for now it is clear that education, at all levels, has changed dramatically. The Ministry of Education, Sport and Youth (MoESY) of Albania created the Academi.al platform in the period of COVID-19. This digital platform was enriched with the official curriculum of pre-university education, 3-18 years old, to enable students to learn online in the conditions of the pandemic crisis in education. Its use facilitated the continuation of the teaching and learning process in conditions quite different from what was done before. On the other hand, this process together with the pandemic situation brought to attention a series of problems and challenges for the future. The great change that occurred in education in this period is requiring the continued use and improvement of the e-education system. we will avoid some necessary directions for the renewal of these systems in Albania.

Introduction

The pandemic found many countries and educational institutions unprepared. Its effect has been different depending on some factors related to economic development and investments in technology.

In the case of Albania, distance learning in pandemic situation was a complete innovation. Distance learning through different platforms was the only possibility for students to be in contact with teachers and in step with learning process. They do not have a ready platform with all the online learning services to follow the process.

Academi.al platform started to be built from this moment and continued to improve. Distance learning has influenced teachers to change the use of methods, which in classical teaching they have practiced very little or not at all, therefore it is reasonable that teachers feel challenged.

The education system has flaws even in the classical form, therefore online systems and services in education must be improved to serve the future. The e – education in Albania has shown promising results, and it has the potential to play a significant role in improving access to education in the country. This experience proved that the institutions that manage education must prepare strategies and invest in distance education to face similar crises in the future.

Material and data

Through distance education, where students and teachers are brought together by technology, student-teacher communication happens in real time, the teacher explains, shares direct information, offers tasks, waits for answers, all these are indicators that virtual learning is feasible and can life as a form of learning with particular benefit especially in emergency conditions.

With its beginnings, Academi.al was not a fully completed and certified platform. She continued to improve the services, but the number of requests increased very quickly and the time was not enough for her to guarantee the quality of the service.

The platform needed immediate funding, which for various reasons, some of which were mentioned above, was not received in time by the Ministry of Education. The continuation of the operation and improvement of the platform services was made possible by UNICEF - Albania. According to the data, the number of its users reached the following statistics [1]:

- 410,000 registered users: for the first time in Albania an e-learning platform was adopted at national level
- 16,000 free video lessons created together with State radio TV
- 3,000 video lessons adjusted for students with disabilities
- Children with no access to the internet for the first time could download lessons for offline use via the mobile app

Some results of distance education in Albania

Distance education in Albania has been gaining popularity in recent years, especially in response to the COVID-19 pandemic. The Online Learning Survey (Ascap-MoYES, March 2020) reported that about 86.4% of students agree and strongly agree to receive lessons through online communication and 90.2% of parents agree and strongly agree that they are part of online communication groups with teachers. The report said that online learning in home conditions has made teachers follow more online training platforms developing their professional capacities in this field [2].

Many students have reported that they are satisfied with the quality of education they receive through distance learning, and they appreciate the flexibility it offers. According to Western Balkans Regular Economic 2020 Report [3] almost a third of Albanian students do not own a computer. Providing an education budget that is adequate to ensure minimum conditions to deal with additional post-COVID-19 costs will be critical to ensure that students catch up and further inequalities are prevented.

It is important to reduce the difference between urban and rural inequities. The achievement gap between the poorest and richest students, (PISA 2018) will increase further since students from poorer backgrounds are less likely to benefit from remote learning modes [4]. In addition to improving online platforms, it is equally important to improve the current situation of equipment available to students and teachers.

Learning Management System (LMS) is a strategic solution for planning, creation, delivery, management and maintenance of all learning courses or events within an education setup. A good LMS provides a dynamic environment for creating interaction between learners and instructors [5].

The Albanian government has been supporting distance education through various initiatives, such as the establishment of the "National Platform for Open Education Resources," which provides free access to educational materials. Many educators in Albania lack the necessary training and experience to deliver education effectively through distance learning. There is a need for more training and professional development opportunities for teachers to improve their digital skills and pedagogy.

Conclusions and Recommendations

In the case of Albania, distance learning was a complete innovation, also due to the fact that such forms of teaching were not legally foreseen. It should be built a legal framework to enable the process in the present and the future. Internet connectivity.

One of the major challenges of distance education in Albania is the availability and quality of internet connectivity. Many rural areas lack proper internet infrastructure, which makes it difficult for students and teachers to access online resources and participate in virtual classes.

Teacher training: Many educators in Albania lack the necessary training and experience to deliver education effectively through distance learning. There is a need for more training and professional development opportunities for teachers to improve their digital skills and pedagogy.

Access to technology: Not all students have access to the necessary technology (e.g., computers, tablets, smartphones) to participate in online classes, which creates disparities in access to education.

Quality assurance: There is a need to ensure that the quality of education delivered through distance learning is of the same quality as traditional face-to-face education. There needs to be a framework for quality assurance that can evaluate the effectiveness of distance education and ensure that it meets the same standards as traditional education.

Student engagement: Maintaining student engagement and motivation in an online learning environment can be challenging. Educators need to develop strategies and techniques to keep students engaged, motivated, and on track.

Assessment: It can be challenging to assess students' learning effectively in a distance learning environment. There is a need to develop assessment methods that are appropriate for online learning and that can provide meaningful feedback to students.

Addressing these challenges will require a concerted effort from all stakeholders, including the government, educators, and the private sector. However, if these challenges are addressed, distance education has the potential to play a significant role in improving access to education in Albania.

References

1. https://albaniatech.org/akademi-al-digital-learning-platform/
2. https://www.ascap.edu.al/wp-content/uploads/2020/03/Sondazhi-i-m%C3%ABsimit-online.pdf
3. Western Balkans Regular Economic 2020 Report. https://openknowledge.worldbank.org/handle/10986/34644
4. Western Balkans Regular Economic Report No.17 | Spring 2020 Education.www.worldbank.org/eca/wbrer.
5. Viswanathan, N., Meacham, S., & Adedoyin, F. F. (2022). Enhancement of online education system by using a multi-agent approach. *Computers and Education: Artificial Intelligence*, *3*, 100057.

Assessing bio-diverse foods in dietary intake surveys-a case study considering random selected samples

Samanda Gjoni[1], Flavia Gjata[1], Florida Hajderaj[1], Emirjana Hasanaj[1], Klodjana Lamaj[1], Aurora Manaj[1]*, Manjola Sala[1], Megisa Sulenji[1], Nertila Mucollari[1], Spase Shumka[1]*

[1]Faculty of Biotechnology and Food, Agricultural University of Tirana, Tirana, Albania, aurora.manajj@gmail.com, sprespa@gmail.com

Keywords
Food diets
Food diversity
Consumption
Children
Woman
Poverty

Abstract
This survey is based on expressing diet diversity indicators such as the diet diversity score (DDS) or food variety score as a reflection for dietary quality and measure the diversity of unique food groups and food items consumed, respectively. During our approach the questionnaires conducted in the period of 2022 and 2023 the DDS for women was a count of the total number of food groups consumed from a list of 10: (i) grains, white roots and tubers, and plantains; (ii) pulses; (iii) nuts and seeds; (iv) dairy; (v) meat, poultry, and fish; (vi) eggs; (vii) dark-green leafy vegetables; (viii) other vitamin A-rich vegetables and fruits; (ix) other vegetables; and (x) other fruits. For children, a seven food-group classification was used, including the following: (i) grains, white roots and tubers, and plantains; (ii) legumes, nuts, and seeds; (iii) dairy; (iv) meat, poultry, and fish; (v) eggs; (vi) vitamin A-rich fruits and vegetables; and (vii) other fruits and vegetables. Following references, a 15-g minimum quantity consumed was considered as a cutoff for species inclusion in the DDS for women but not for children. The questionnaire considered 271 adult woman and 233 children. The Minimum Dietary Diversity (MDD) was used as a cutoff for higher nutrient adequacy and refers to a minimum of five and four food groups for women and children, respectively. The results shows that >50% of adult woman's have value of dietary species richness lower than 0.5, while in case of children's the average value was slightly higher (0.52).

Introduction

Following different approaches, a food system must be considered in the context of rapid population growth, urbanization, growing wealth, changing consumption patterns, and globalization as well as climate change and the depletion of natural resources [1]. The developments in food systems have yielded many positive results, especially over the past three decades in developing countries. These results include the expansion of off-farm employment opportunities as food industries have developed, and the widening of food choices beyond local staples, thus satisfying consumers' preferences in terms of taste, form and quality. The World Health Organization recently reported that malnutrition affects one in every three people worldwide, afflicting all age groups and populations, particularly in the developing world; malnutrition continues also to be a cause and a consequence of disease and disability in the children who survive [2, 3]. This is the largest number and proportion of malnourished people ever recorded in human history [4]. The food shortage and malnutrition problems are primarily related to rapid population growth in the world and to the declining per capita availability of land, water and energy resources [5].

This survey is based on expressing diet diversity indicators such as the diet diversity score (DDS) or food variety score as a reflection for dietary quality and measure the diversity of unique food groups and food items consumed, respectively.

The recent analyses [6] of dietary transition in developing countries, including Albania, in association with globalization have noted increases in the diversity of plants contributing to diets locally, along with a western type of diets transition in preference of energy-dense foods (i.e., animal products, plant oils, and sugars) over

cereals, pulses, and vegetables, and of particular major crop plants within these food categories over traditional crops [7]. This type of impact of such changes on overall crop diversity on a global scale has not been comprehensively documented, although recent changes in varietal and allelic level diversity of some crops have been investigated [6].

Materials and methods

The methodological approach is based on a questionnaires conducted in the period of 2022 and 2023 the DDS for women was a count of the total number of food groups consumed from a list of 10: (i) grains, white roots and tubers, and plantains; (ii) pulses; (iii) nuts and seeds; (iv) dairy; (v) meat, poultry, and fish; (vi) eggs; (vii) dark-green leafy vegetables; (viii) other vitamin A-rich vegetables and fruits; (ix) other vegetables; and (x) other fruits.

For children, a seven food-group classification was used, including the following: (i) grains, white roots and tubers, and plantains; (ii) legumes, nuts, and seeds; (iii) dairy; (iv) meat, poultry, and fish; (v) eggs; (vi) vitamin A-rich fruits and vegetables; and (vii) other fruits and vegetables. Following references, a 15-g minimum quantity consumed was considered as a cutoff for species inclusion in the DDS for women but not for children. The questionnaire considered 271 adult woman and 233 children. The Minimum Dietary Diversity (MDD) was used as a cutoff for higher nutrient adequacy and refers to a minimum of five and four food groups for women and children, respectively.

Due to the fact that the study assessed the level of food biodiversity in the diet, intake of breast milk was not considered in the calculation of biodiversity indicators, as recommended by [6]. The consumption of different parts of particular plant or animal species was counted once, with no minimum quantity. No minimum quantity consumed was applied to include a species in the biodiversity indicators.
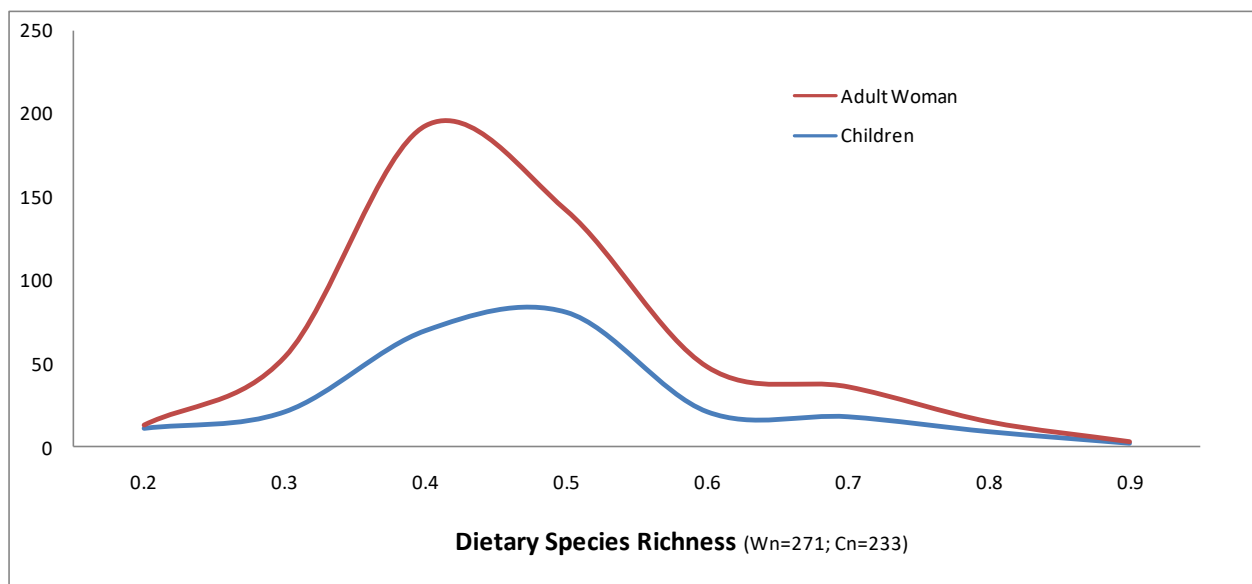

Figure 1. Dietary Species richness (Woman-n=271 and Children n=223)

Results and discussions

As presented at the introductory section, the current approach aimed to recommend a cross-cutting indicator that measures food biodiversity in human diets and helps guide interventions toward human and environmental health simultaneously. Similar approach has been performed by [6] where the applied three ecological biodiversity indicators to dietary intake data of women and children in seven lowland middle-income countries and evaluated how these indicators were associated with nutrient adequacy. Associations between food biodiversity, diet diversity, and nutrient adequacy as three complementary dimensions of diet quality were assessed. It is worth to mention that country (Albania) was facing serious changes within the last three decades, where large number of population was moving from upland to lowland regions, the western type food and diets were replacing the traditional one. Further on, within this article we assessed the use of a cutoff for minimal food biodiversity to identify diets with higher nutrient adequacy and compared it with the existing cutoff for minimum diet diversity. Following data presented in Figure 1 and Figure 2, the results of analyzed samples shows that >50% of adult woman's have value of dietary species richness lower than 0.5, while in case of children's the average value was slightly higher (0.52).
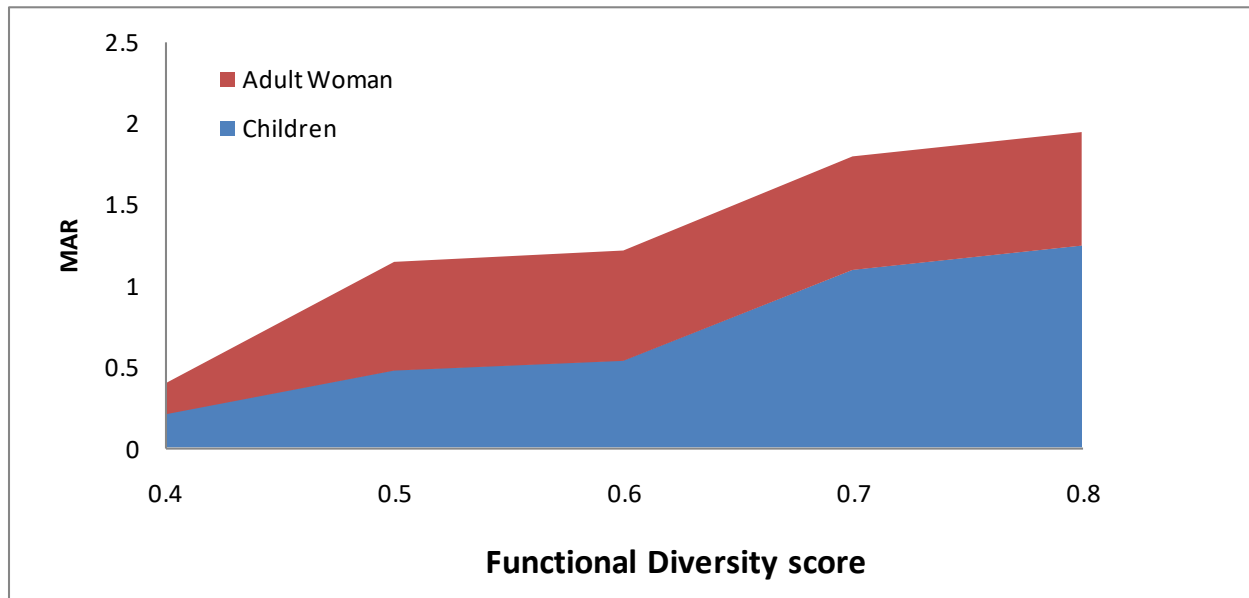
146

Figure 2. Functional Diversity score (Woman-n=271 and Children n=223)

Conclusion

Assessment of the contribution of species in the diet enables identifying species with the greatest potential to improve diets in different local contexts and provides additional imputes to assess the importance of food diversity in ensuring diet quality. The data can be further correlated with the health state of considered society groups. The present study provides evidence on the role of different foods commodities to both energy and micronutrient intakes in rural areas and also population coming from these regions. Identifying foods consumed at the species level adds information that supports both conservation and sustainable food system practices.

References

1. FAO, (2018). Sustainable food systems - Concept and framework. CA2079EN/1/10.18
2. World Health Organization. (1996). Micronutrient malnutrition – half of the world's population affected. World Health Organ 78, 1–4M.
3. World Health Organization (2000). Turning the Tide of Malnutrition: Responding to the challenge of the 21st Century. World Health Organization: Geneva.
4. Baroni, L., Cenci, L., Tettamanti, M., & Berati, M. (2007). Evaluating the environmental impact of various dietary patterns combined with different food production systems. *European journal of clinical nutrition*, *61*(2), 279-286.
5. Pimentel, D., & Pimentel, M. (2000). To improve nutrition for the world's population. *Science*, *288*(5473), 1966-1967.
6. Khoury, C. K., Bjorkman, A. D., Dempewolf, H., Ramirez-Villegas, J., Guarino, L., Jarvis, A., ... & Struik, P. C. (2014). Increasing homogeneity in global food supplies and the implications for food security. *Proceedings of the national Academy of Sciences*, *111*(11), 4001-4006.
7. Pingali, P. (2007). Westernization of Asian diets and the transformation of food systems: Implications for research and policy. *Food policy*, *32*(3), 281-298.

Advanced Engineering Days

aed.mersin.edu.tr

Practical QoS measurement and analyzes on a 5G non-standalone architecture

Olimpjon Shurdi*[1] , **Alban Rakipi** [1] , **Arjola Biti** [2]

[1]Polytechnic University of Tirana, Department of Electronics and Telecommunications, Albania, oshurdi@fti.edu.al, arakipi@fti.edu.al,
[2]Vodafone Albania, Albania, Arjola.biti@vodafone.com

Keywords
5G
Quality of Service (QoS)
Throughput
Jitter
Latency

Abstract
Fifth Generation (5G) networks are becoming the standard in the global telecommunications industry and are becoming a permanent part of everyday life. As mobile network operators have commenced to publicize the implementations of their 5G networks, measurements are not frequently used to demonstrate the actual aspects of these networks' capabilities. This article presents an actual 5G architecture based on the 5G Option 3x reference model, together with findings from Quality of Service (QoS) testing. The outcomes are compared to our actual hands-on measurements of the 4G network in addition to being compared to the expectations for the 5G network. Based on examination of the 5G testbed results, 5G performed much better than 4G in all fundamental QoS, including up- and downlink throughput, latency, packet error rate and jitter. Additionally, practical measurement results on this non-standalone 5G architecture demonstrate that latency and jitter are not greatly impacted by the load on the cell or the core network provided traffic preferences are set up correctly. The study of QoS and a first performance assessment of 5G, along with the identification of application-level performance concerns, are the paper's main conclusions. These results underline the necessity of validating and testing generic 5G services and applications through fair benchmarking approaches.

Introduction

The 5G is the newest mobile network being deployed worldwide. As it was stated 5G Network can provide high throughput, high reliability, low latency, increased capacity, availability and connectivity, and dynamic bandwidth allocation and in general better performance. In fact, it is expected that the 5G performance will span over the three extremes of bandwidth, latency, and capacity requirements, which enable enhanced Mobile Broadband (eMBB), Ultra Reliable and Low Latency Communication (URLLC), and massive Machine Type Communication (mMTC), respectively [1].

The 3rd Generation Partnership Project (3GPP) has regulated two primary 5G deployment modes in Release 15 (Rel-15), termed Non-Standalone (NSA) and Standalone (SA), to meet these requirements [2]. The main difference is that whereas 5G NSA uses the current 4G core network to handle the control plane, 5G SA uses its own 5G core and so operates independently of the 4G network (Figure 1). Both of these modes need a 5G New Radio (NR) Radio Access Network (RAN) made up of Next Generation Node Bs (gNBs), which are the 5G equivalent of 4G E-UTRAN Node Bs (eNBs).

The majority of Mobile Network Operators (MNOs) have chosen to use the NSA mode throughout the current stages of 5G implementation because it is an easier and less expensive option. However, 4G/5G co-dependence in the NSA presents a variety of setup, operational, and performance challenges that need for more research and analysis. Actual 5G networks claims include 20Gbps data throughput, 1ms latency, 1 million devices=km², and 10

times less energy usage (than 4G UE), although their combined effects on the network are not yet completely understood.

Analysis of the performance of an 5G network and service can also be done using a variety of techniques and technologies. Regardless of the fact that 5G networks can benefit from the same network and service validation systems now in use, considerable tool upgrades will be required for thorough validation and verification of 5G goals.

Recently, there has been significant research related to the 5G performance evaluation, however, these are not tested on live network, so it cannot be known which will fulfill the expectations. For examples, the authors in [3] had evaluated the performance of an NSA 5G architecture. They observed that if the traffic preferences are properly set, the load on the cell or the core network (CN) has no effect on latency and jitter. As well, the authors examined the performance of SA and NSA 5G new radio (NR) installations in terms of coverage, network capabilities, and deployment cost based on simulations in [4]. In more recent works, the effectiveness of NSA 5G networks has also been assessed; for examples, see [5] and [6].

In this paper, we present a testbed measurement study on 5G experimental mid-band NSA networks of Vodafone Albania. To the best of our knowledge, this work constitutes the first effort toward empirically studying deployment, coverage, and performance aspects of 5G NSA deployments in QoS terms, as well as providing insights with regard to future 5G version updates.

5G testbed proposed and design.

The testbed we employed is a defined architecture called "Option 3X," which stands for "migration path to Non-Standalone Next Generation Radio with LTE aided mode coupled to Evolved Packet Core" (Figure 1). The EPC is responsible for AAA functions, service mobility management, besides, it ensures connectivity with the IP network. Another key part of the 5G architecture is gNB, which is responsible for the radio attachment between UEs and the Core network's interfaces in case of 5G media. For the basic understanding, Figure 4 on [2] depicts the generic 5G architecture, where the main elements are also defined.
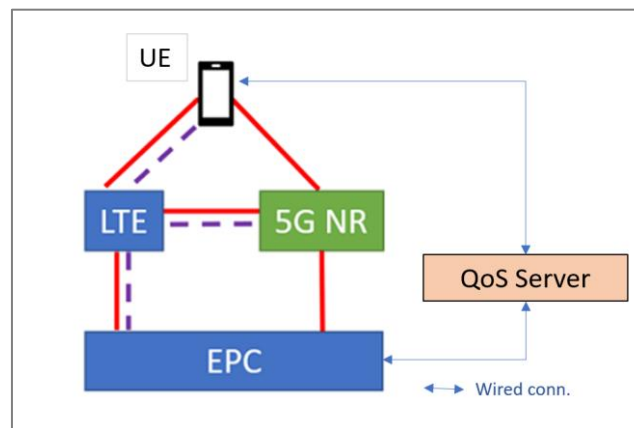

Figure.1 5G testbed NSA Option 3X

In our testbed, we use a dedicated server, where we have installed different tools like iPerf3, Speedtest by Ookla, SolarWinds. The 5G NR is simulated using Amarisoft Callbox Advanced, which is a self-contained 5G base station deployed in an indoor environment.

QoS parameters and Expectations

In the 5G networks, Quality of Service (QoS) model is based on the QoS Flows. Each QoS flow has a unique identifier called QoS Flow Identifier (QoI). There are always two types of bearer flows GBR (Guaranteed bit rate) QoS flows and NGBR(Non-Guaranteed bit rate) QoS flows. GBR bearers are used for real-time services such as rich voice and video services which occur in real-time. A GBR bearer has a minimum amount of bandwidth that is always reserved by the network. Non-GBR bearers do not have specific bandwidth allocation e.g., file downloads, email, internet access, etc.

There are different parameters to evaluate QoS in 5G networks, in this paper we will present some of the most important that end users and applications are affected.

Throughput: 5G throughput performance is one of the most important indicators of user experience. Increasing bandwidth, utilizing various coding techniques, and improving modulation all result in higher data transmission rates. Even 100 MHz of bandwidth can be employed in the downlink direction, and 1.5 Gbps is the maximum

theoretical capacity. Naturally, the quantity of receiver and transceiver antennas can also be used to tune the transmission rate.

Latency: One of the main promises of 5G is the dramatic reduction of latency from the levels experienced with 4G to approximately 1 ms. In particular, latency can be maintained at a low level even when the network is experiencing significant traffic loads.

Packet Error Rate (PER): It defines an upper bound for the rate of PDUs (e.g., IP packets) that have been processed by the sender of a link layer protocol (e.g., RLC in RAN of a 3GPP access) but that are not successfully delivered by the corresponding receiver to the upper layer (e.g., PDCP in RAN of a 3GPP access).

Maximum Packet Loss Rate: The Maximum Packet Loss Rate (UL, DL) indicates the maximum rate for lost packets of the QoS Flow that can be tolerated in the uplink and downlink direction.

Measurement and results

In our setup, the 5G network is operating with real live 4G network creating the perspective NSA network. Server is connected directly to EU and EPC, we are using several tools for timing synchronization and valuating the QoS mentions parameters. For better understanding these parameters are depicted in Figures 2-5.
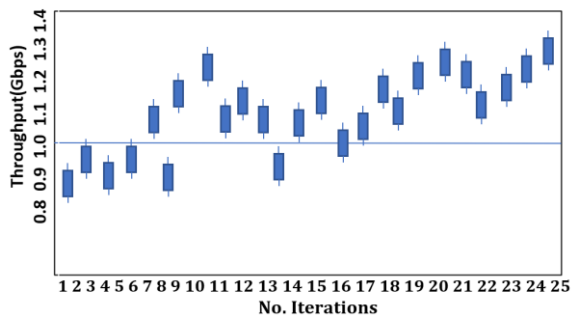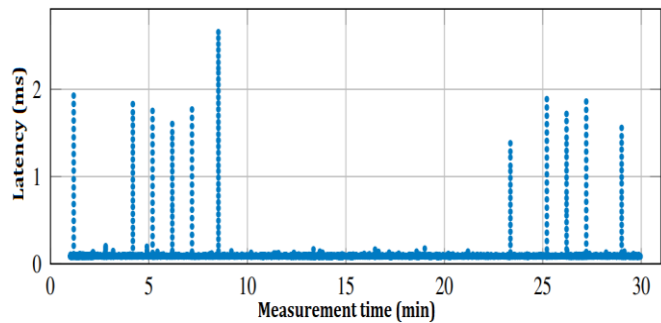

Figure 2. Throughput in 100MHz bandwidth

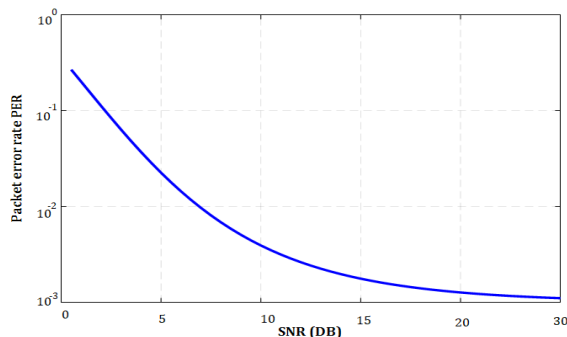**Figure 3.** Latency in 30 min with light traffic

Figure 4. Packet error rate PER vs SNR
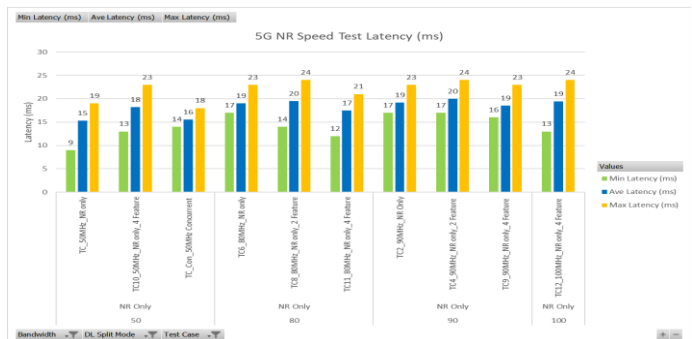
Figure 5. Latency vs bandwidth with heavy traffic

Conclusion

This paper aims to provide some comprehensive measurements and validating real-world 5G Quality of Service capabilities. As expected, 5G data latency is significantly lower than it is for 4G -although for heave traffic require further tune. Moreover, in the tested, real-world 5G network testbed, latency and jitter statistics do not dramatically rise with traffic load. On the throughput parameters it is observed that almost the theoretical limit is reached in the basic band of 100MHz. It is necessary to research more in cases of network loading with different types of traffic, as in these cases the tested data showed an increase of the latency.

References

1. ITU-R M.2083-0. IMT Vision-Framework and Overall Objectives of the Future Development of IMT for 2020 and Beyond; ITU: Geneva, Switzerland, 2015.
2. 3GPP (2018). Summary of Rel-15 Work Items, TR 21.915 version 0.5.0 Release 15. 3GPP, Version 15, 2018-12.
3. Soós, G., Ficzere, D., Varga, P., & Szalay, Z. (2020, April). Practical 5G KPI measurement results on a non-standalone architecture. In *Noms 2020-2020 IEEE/IFIP network operations and management symposium* (pp. 1-5). IEEE.

4. Liu, G., Huang, Y., Chen, Z., Liu, L., Wang, Q., & Li, N. (2020). 5G deployment: Standalone vs. non-standalone from the operator perspective. *IEEE Communications Magazine*, *58*(11), 83-89.

5. Heimann, K., Gorczak, P., Bektas, C., Girke, F., & Wietfeld, C. (2019, April). Software–defined end–to–end evaluation platform for quality of service in non–standalone 5G systems. In *2019 IEEE International Systems Conference (SysCon)* (pp. 1-8). IEEE.

6. Giordani, M., Polese, M., Roy, A., Castor, D., & Zorzi, M. (2019). Standalone and non-standalone beam management for 3GPP NR at mmWaves. *IEEE Communications Magazine*, *57*(4), 123-129.

Advanced Engineering Days

aed.mersin.edu.tr

IOT integration of electric vehicle charging infrastructure

Miranda Harizaj*1 , **Igli Bisha 1** , **Fatmir Basholli2**

1Polytechnic University of Tirana, Faculty of Electrical Engineering, Albania, miranda.harizaj@fie.edu.al, igli.bisha@fie.edu.al
2Albanian University, Department of Engineering, Tirana, Albania, fatmir.basholli@albanianuniversity.edu.al

Keywords
EV charger
EV ecosystem
IoT
Kempower
Smart charging

Abstract
All across the world, the electrification of road vehicles is growing quickly. With EV sales shooting up, there is a greater need to develop a robust charging infrastructure. More than just installing charging points, the bigger challenge lies in managing a large fleet of devices dispersed across geographic locations. There are challenges in developing the EV ecosystem, including infrastructure management, addressing customer experience, profitability, maintenance, monitoring, energy management, and ultimately, how to create a universal ecosystem that works for everyone. IoT technology is a promising player in bringing it all together. In this paper, through a specific case study, is pointed out the importance of IoT integration in the EV ecosystem, as one of the key management factors. By monitoring the charging network, it is possible to independently manage the power and its distribution and obtain real time reports on charging behavior and data on vehicle models. IoT usage enables CPOs to remotely monitor and manage operations and quickly resolve issues by presenting real-time insights into usage and device performance, including charger availability, fault monitoring, and troubleshooting – all of which help enormously when it comes to predictive maintenance and reducing downtime. In conclusion are identified the new benefits of IoT integration of the EV infrastructure.

Introduction

According to McKinsey, over 40% of the Internet of Thing's economic value will be contributed by operations optimization and account for $1.3 trillion by 2030. With EV sales shooting up, there is a greater need to develop a robust charging infrastructure. More than just installing charging points, the bigger challenge lies in managing a large fleet of devices dispersed across geographic locations. Unlike the non-networked gasoline fuel stations, the EV charging stations are connected devices and integrated with various third-party service providers such as energy suppliers, e-MSPs, and charge point operators [1-2]. The transition to electric mobility is a promising global strategy for decarbonizing the transport sector by hybrid energy system [3].

They use various protocols & connectivity options and back-end cloud infrastructure to ensure seamless charging operations such as payment processing, software updates, scheduling, predictive maintenance, and usage analytics. Besides all the factors favoring EV adoption, the key to success lies in the development of robust charging infrastructure [4]. The real challenge is not about installing a large number of charging stations, but the ability to remotely manage and smoothly operate dispersed devices. IoT has the potential to resolve the problems of the EV charging industry and enhance the overall adoption of EVs. The paper presents a network of electric chargers integrated in IoT [4-5], for managing the charging network and monitoring power and its distribution. It is also presented dynamic energy management, to utilize the maximum energy potential, where the whole process is achieved through special IOT communication protocols, as illustrated in Figure 1:
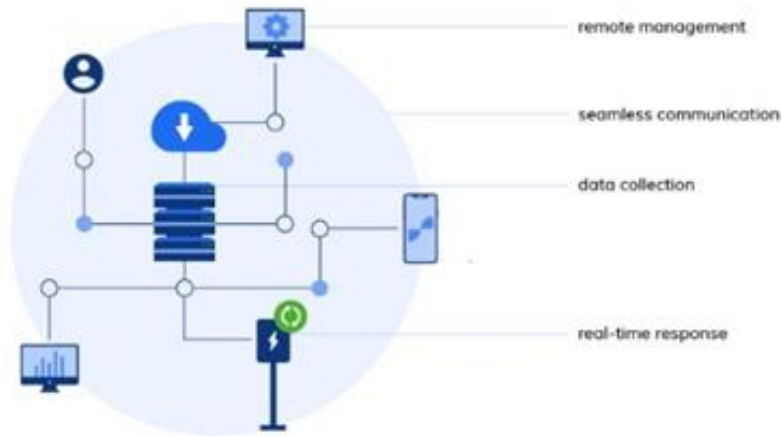
Figure 1. Implementation of IoT architecture

Electric vehicle charging station

An electric vehicle charging station connects an electric vehicle (EV) to a source of electricity to recharge electric cars, neighborhood electric vehicles and plug-in hybrids [1]. Some charging stations have advanced features such as smart metering, cellular capability and network connectivity, while others are more basic [2,4]. Charging stations are also called electric vehicle supply equipment (EVSE) and are provided in municipal parking locations by electric utility companies or at retail shopping centers by private companies.

These stations provide special connectors that conform to the variety of electric charging connector standards. There are three categories or types of charging: Trickle Charge, AC Charge and DC Charge. The slowest method of charging your EV at home, using a standard (three-prong) 220V plug.

IOT in ev charging

In simple terms, the IoT can be viewed as a convergence of OT (Operational Technology) and IT (Information Technology) [1]. While OT deals with the operations of physical properties such as devices, sensors, and connectivity, IT focuses on the digital transformation aspects. In the view of EV charging, IoT comprises three major elements charging equipment, mobile app, and charging management platform [2].

IoT in EV charging enables continuous monitoring and presenting data in form of reports & dashboards. It also helps in notifying users in the event of critical failures or important updates. Charge point operators can remotely troubleshoot devices without a physical visit. Network operators can enhance roaming services for their charging network as illustrated in Figure 2:
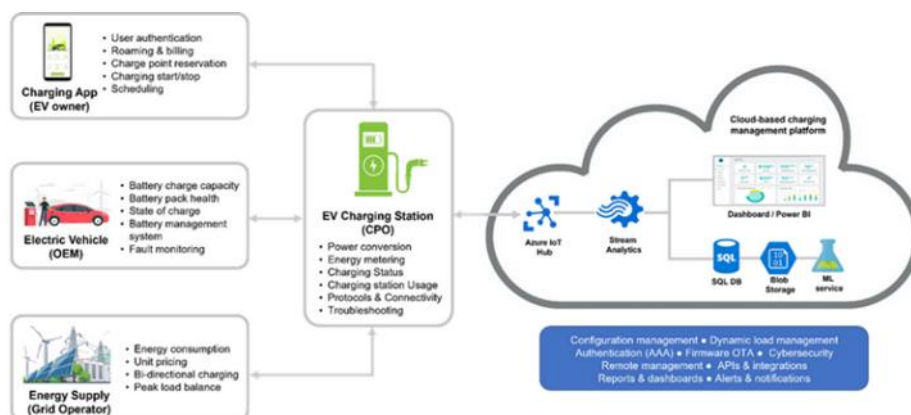
Figure Error! No text of specified style in document.**2.** Diagram of IoT in EV charging

IOT integration case study

The charging network system that is considered in this study consists of KemPower Satellite electric chargers, where each charger has Charging Power Unit (CPU) [6]. Each CPU cabinet provides up to 200 kW of charging power from four power modules into one or up to eight charging plugs on Satellite posts. Charging stations are geographically dispersed, making it challenging and expensive to manage 'onsite'. IoT enables CPOs to remotely monitor and manage operations and quickly resolve issues by presenting real-time insights into usage and device

performance, including charger availability, fault monitoring, and troubleshooting – all of which help enormously when it comes to predictive maintenance and reducing downtime.

Additionally, as charging station buildouts increase, data on existing deployments will help operators more accurately plan locations for new stations. Data can also be used to optimize charger utilization, identify areas for improvement, and track trends over time. In the Figure 3, the location of each charger is shown, which is continuously viewed in the system.
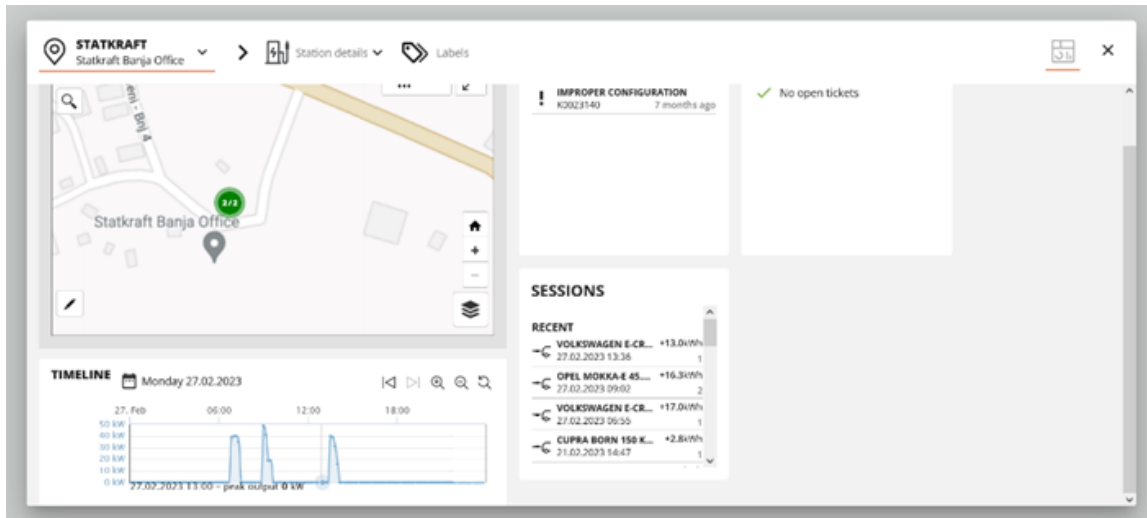
Figure 3. Geolocation of the charger

Each Charging Power Unit (CPU) consist of 1-12 power modules, with 2 independent power channels on each module and optional dynamic module that can route the power channels in any order to a maximum of eight charging outputs. To utilize full potential of each DC charger, dynamic power management is one of the key elements on Adaptive EV charging.

Compared to the traditional static charging, Adaptive EV charging can benefit from re- routing the power channels even during each charging session. It enables true flexibility to DC charging and improved OPEX as charging service power levels can also be adjusted to match with real-time energy price level as well as to eliminate possible power peaks in advance.

The Figure 4 shows in real time the power received by the cars, its distribution as well as the model of the car being charged. There are also errors in the system that may have occurred during charging.
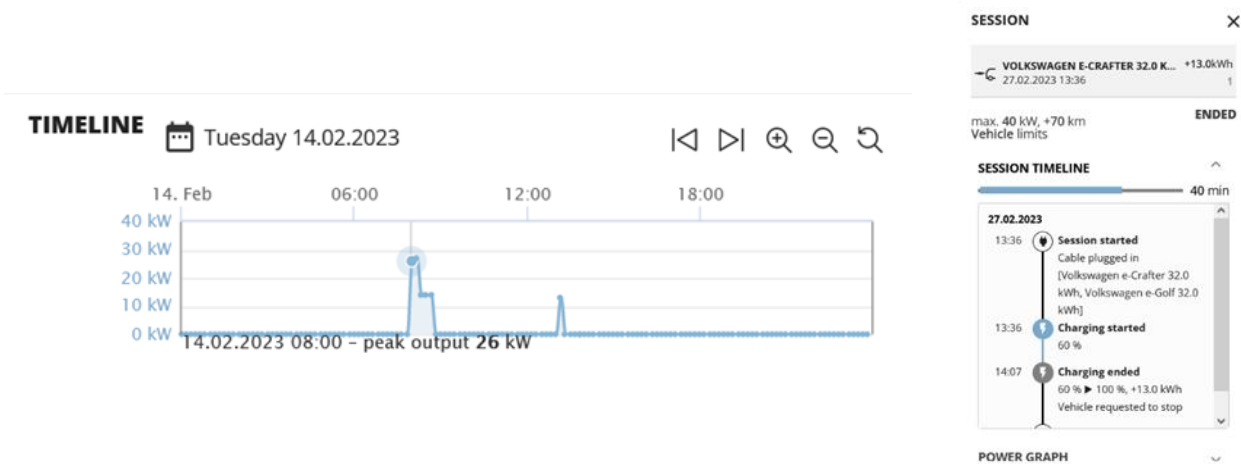
Figure 4. Data from the charging network in real time

In the democratic power management as illustrated in Figure 4, each charging output is granted with 25 or 50 kW from the beginning of each charging session, thus on an empty charging area, the first vehicle receives maximum power until next vehicle starts to charge. The starting power level is depending on the number of power modules versus number of charging outputs and their charging cable sizes.

Figure 5. A simplified example of democratic power management
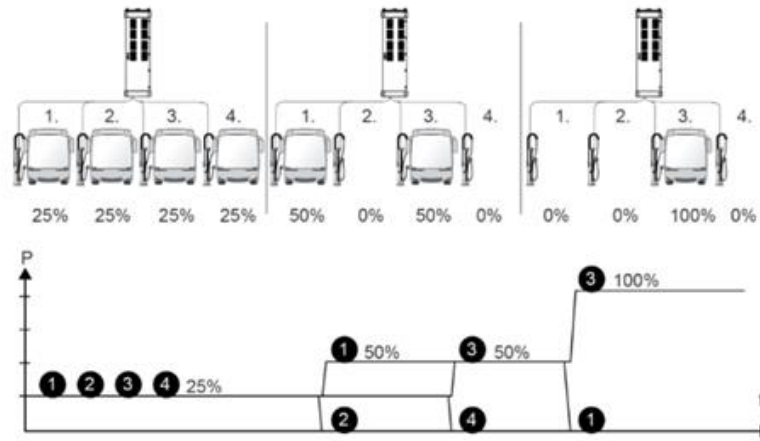
Results and conclusions

More than just remote monitoring, IoT is a fundamental block for developing next-gen applications such as smart charging and vehicle-to-grid. Not only for EV drivers, but IoT is also equally important and beneficial for everyone as it helps CPOs to prevent downtime, grid suppliers with energy management, and create a large roaming network for a seamless charging experience.

The case study of IoT integration of the KemPower chargers' network is presented and real-time data is obtained and analyzed . The main identified benefits:

- Improved Authentication

Before charging the EV, the users need to verify themselves with the help of smartphones or RFID tags for access. This high-end authentication ensures secure billing and transaction.

- EV Station Search

Finding an EV charging station in an unfamiliar area is hectic. With IoT, EV owners can easily find nearby stations by searching the application's location, checking availability, and reserving a slot in advance per the charging requirements.

- Smart Charging

With the help of IoT, the chargers can find the lowest rates available from the grid and start charging automatically. This facilitates the CPOs to manage the surge in energy demand and save costs.

- Remote Operation Management

IoT solutions have enabled the CPOs to take real-time device performance insight into account and quickly resolve the associated issues while remotely managing the other EV station operations.

References

1. Tesla Motors Launches Revolutionary Supercharger Enabling Convenient Long Distance Driving | Tesla Investor Relations*. ir.tesla.com.*
2. https://www.einfochips.com/blog/role-of-iot-in-fueling-ev-charging-future-growth/
3. Ma, Y. IoT Connectivity: What it Means for EV Charging Stations to Go Wireless. Plug and Play
4. https://www.conurets.com/how-is-iot-unlocking-the-future-growth-of-the-ev-charging-industry/
5. https://www.greenflux.com/spotlights/internet-of-things/
6. https://kempower.com/solution/kempower-chargeye-for-cpo/

Neural networks for bitcoin price forecasting

Katerina Zela*[1] , Lorena Saliaj[2]

[1]Mediterranean University of Albania, Department of Information Technology, Albania, katerina.male@umsh.edu.al
[2]Mediterranean University of Albania, Department of Business Informatics, Albania, lorenasaliaj@umsh.edu.al

Keywords
Bitcoin
Time series forecasting
ANN
ARIMA

Abstract
This paper concerns the problem of daily Bitcoin price prediction, aiming to find the best predictive model among the linear and nonlinear forecasting models. Finding the most accurate forecasting model would help investors take important decisions about taking the next step when investing. We compare the forecasting performance of linear and nonlinear forecasting models using daily Bitcoin price data for the period between 31 December 2017 until 24 November 2021. We discuss various forecasting approaches, including an Autoregressive Integrated Moving Average (ARIMA) model, a Nonlinear Autoregressive Neural Network (NARNN) model, a TBATS model and Exponential Smoothing on the data collected from 31 December 2017 to 24 November 2021 and compared their accuracy using the data collected from 01 June 2021 to 09 June 2021, choosing the model with the lowest Mean Absolute Percentage Error (MAPE) value. The chosen model has been used for daily Bitcoin price forecasting for the next 30 days without any additional intervention. The forecasting model can be applied to other cryptocurrencies available on the global cryptocurrency market cap.

Introduction

Since its creation, Bitcoin turns out to be the most traded currency in the world and occupies a significant part of the cryptocurrency market. Its birth marked the launch of a new asset class and a major step forward in forms of centralized control. Unlike other currencies, Bitcoin does not have a central bank that regulates the distribution of the currency, but is based on two principles: a network of nodes, composed of computers and cryptography to make transactions valid and secure. The value of Bitcoin has gone from 0, in 2009, to 57,873 in November 2021. Price prediction can be very useful, as it can help the decision-making process regarding possible investments in purchasing the currency.

In this article, we have tested the accuracy of predictions obtained from the most proposed models in the literature, including linear and nonlinear prediction models. The aim of this paper is to identify the most suitable model for predicting future values, starting from its value reported every day since January 2018, through the use of four different prediction models in the Bitcoin price time series. and comparing the validity of these models to analyze its progress for the next 60 days.

Material and Method

In this article, we have considered the data published online on Coin Market Cap, the website that reflects the daily price performance of cryptocurrencies, for the period from December 31, 2017 to November 24, 2021, considering the time series of the closing price for the period December 31, 2017- November 24, 2021 (Figure 1), the price of the last 8 days for testing the validity of the model and the last 60 days for predicting the future price.

Forecasting was performed using the R software forecasting package, which provides methods and tools for univariate time series forecasting. We implemented an ARIMA model, a Nonlinear Autoregressive (NNAR) model, a TBATS model as well as a Linear Exponential Square and selected the best model among them, considering the mean percentage error (MAPE).

The forecasting models

Artificial neural networks are predictive models inspired by biological neural networks. They identify and model non-linear relationships between the dependent variable and its predictors. A set of neurons, grouped into input, hidden and output layers to form the artificial network, can perform a large number of complex tasks, quite efficiently. This makes ANNs a powerful tool, capable of learning from previous examples and improving its performance, giving them the ability to analyze new data based on previous results. Artificial neural networks are nonlinear models that transform a set of inputs into a set of output variables, through hidden layers of neurons.
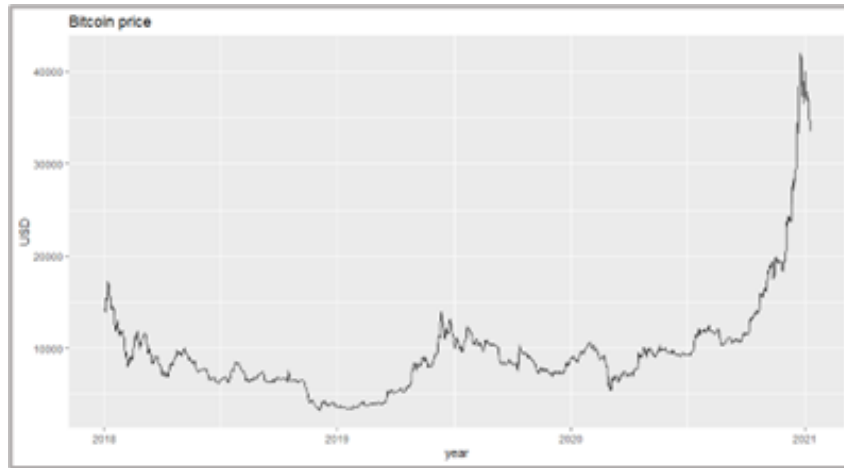

Figure 1. Bitcoin price in Dollars

In our work, the NAR network was developed using the *nnetar* function of the R software package "caret" to fit a neural network model to a time series [1] developed by Hyndman, O'Hara, and Wang. An NNAR (p,k), where p denotes the number of lags used as input and k the number of nodes in the hidden layer, can be described as an autoregressive process with nonlinear functions. We chose a (1-5-1) network, with 1 delay as input node and 5 hidden layer nodes. It has the form of a three-layer ANN, where neurons have a single connection with neurons of other layers [2]. The data set was divided into the training set (70%), the test set (15%), while the data of the last 8 days was used for testing the validity of the model.

The main objective of the ARIMA model is to predict future values through the stochastic mechanism of time series. Although this model is widely used for time series, it is not easy to choose the right order for its components, so we proceeded to determine the order automatically, by using the auto.arima function in the forecasting package of R, which gave us the best fitting ARIMA model as a result. This involves identifying the most appropriate lags for the AR and MA components and deciding whether the variable needs differentiation. The model that best fitted our time series was ARIMA (0,2,1). This model was used in this study to predict the price of Bitcoin currency for the next few days.

Results

The values of the validity indicators of the models, RMSE, MAE, MPE; MAPE, ME, and MASE are shown in Table 1. They were used to measure the performance of the models built for the Bitcoin price time series, taking into account the data used to train the models. Apart from the graph, where it can be clearly seen, the values in the following tables show that the NARNN model has given more accurate prediction results than the other linear models. Based on the MAPE values, NARNN improved the forecasting accuracy by 39% compared to the ARIMA model.

The NARNN model gives better results in almost all the indicators considered, with a significant difference from the indicators of other models. This model has improved the performance of predictions based on the ME indicator by 21% compared to the BATS indicator.

The selection of the best predictive model was based on the value of MAPE, since it is recommended to use this indicator as a comparative unit between predictive models for time series, considering as the most accurate model the one with the lowest value of MAPE. Based on the above, the NNAR model has the lowest value of MAPE (14.2%).

Table 1. Percentage and absolute error values

Model	ME	RMSE	MAE	MPE	MAPE	MASE
ARIMA	11.30	840.01	436.21	0.07	23.40	1.00
BATS	32.26	836.48	431.04	0.03	32.10	1.09
HOLT	11.96	842.12	435.83	0.73	33.48	1.09
NNAR	9.37	759.4	432.12	0.19	14.2	0.65

The above models were used to forecast Bitcoin price performance for the next 60 days (until January 25, 2022) and compared the data obtained from the forecast to the actual data for an 8-day period (November 17 - November 24). The values of MAPE for each model are presented in Table 2. From the results of the analysis, we can conclude that the results predicted by the model are similar to the real values of the time series. In particular, the NNAR model gave more accurate predictions, since the MAPE values for it were lower compared to the values of the other models.

Table 2. Percentage and absolute error values

Model	ARIMA	BATS	Holt's	NNAR
2021-11-17	4.61	4.45	4.57	3.45
2021-11-18	9.76	9.25	9.69	7.46
2021-11-19	9.86	9.00	9.75	6.57
2021-11-20	15.05	13.80	14.91	10.67
2021-11-21	12.71	11.13	12.53	7.56
2021-11-22	12.53	10.60	12.32	6.60
2021-11-23	14.31	12.00	14.06	7.54
2021-11-24	17.55	14.83	17.27	9.88

Discussion

For the construction of the NARNN model, the time series data were divided into two groups; model training set and test set. The training set was used to create the model, while the test set was used to evaluate the created model. The mesh structure was chosen based on the results in Zhang et al. [3], who showed that the optimal structure of neural networks contains 1 hidden layer. Since the layer with 5 hidden neurons performed better than those with 1, 2, 3, and 4 hidden neurons, we chose 5 hidden nodes for our model because it had a lower RMSE compared to other models. The neurons of the input layer were selected through the nnetar and accuracy functions. These functions resulted in a neural network with 28 input nodes, resulting in a model (1-5-1). Figure 2 presents the graphical output of Bitcoin price predictions made by the NARNN model for the next 60 days. The model manages to follow the trend of the time series well, thanks to the training and learning process, which enable the model to better understand the characteristics of the time series. Figure 3 shows the fit of the NARNN model to real time series data. All components are well represented and the difference between predicted and observed values tends to zero, thanks to the model's ability to identify non-linear relationships between observations. The ability to learn, to work with parallel and multiple inputs are some of the characteristics that make neural networks efficient in generating models suitable for time series forecasting [4].

Conclusion

In this article we have evaluated four different models for predicting the Bitcoin price time series. Our findings highlighted the difference between the accuracy of each model's performance. Using several models allows testing and comparing the accuracy of their predictions and leads to an optimal choice. For our time series, the NARNN model is preferred over other forecasting models. It was selected based on MAPE values, as it had the smallest value among all predictive models. In addition, the NARNN model improved forecast accuracy by 39% compared to the ARIMA model, according to MAPE.

The NARNN model gave better results in almost all the indicators considered, with a significant difference from the indicators of the other models. We selected the NARNN model as the best model based on the MAPE value, considering the model with the lowest MAPE value as the most accurate model. The NARNN model has the minimum MAPE value for the considered period (7.47%). He predicted a downward trend in the price of Bitcoin in the coming days. Forecasts are valid for a short period of time, because for the long term they can be influenced by other external factors, such as inflation, economic crisis, etc. The above models can equally be applied to the data of future periods, for predictions of the future price of Bitcoin, in order to improve the accuracy of the predictions. Predictions with a high degree of reliability about the future price of Bitcoin would be very important for speculators, investors and financial actors in general, to make future projections and prevent possible losses.

References

1. Batista, M. (2020). Estimation of the final size of the COVID-19 epidemic. Preprint. medRxiv.
2. Rodríguez Rivero, C., Pucheta, J., Laboret, S., Patiño, D. and Sauchelli, V. (2015) Forecasting Short Time Series with Missing Data by Means of Energy Associated to Series. Applied Mathematics, 6, 1611-1619, https://doi.org/10.4236/am.2015.6914
3. Zhang, P. G., Patuwo, E., Hu, M. (1998). Forecasting with artificial neural networks: The state of the art. International Journal of Forecasting, 14, 35-62, http://dx.doi.org/10.1016/S0169-2070(97)00044-7.
4. Tealab, A., Hefny, H., & Badr, A. (2017) Forecasting of nonlinear time series using ANN, Future Computing and Informatics Journal, 2, 39-47. https://doi.org/10.1016/j.fcij.2017.05.001

Functional substances in grape seed and seed processing research

Farmonov Jasur Boykharayevich[*1] , **Sobirova Mohichehra Shamsiddin qizi**[2] , **Kalonova Moxinur Muzaffar qizi**[3]

[1] University of Economics and pedagogy, Vice Rector for Research and Innovation, Karshi, Uzbekistan, farmonovjasur83@gmail.com
[2] Yangiyer branch of Tashkent Chemical-Texnological Instiute, Senior Lecturer, Yangiyer, Uzbekistan, mohichehrasobirova94@gmail.com
[3] Yangiyer branch of Tashkent Chemical-Texnological Instiute, student, Yangiyer, Uzbekistan, mohinurkalonov@gmail.com

Keywords
Grape seed
Khoraki grapes
Press-extraction methods
Vitamin
Oil contains

Abstract
The article provides information about the countries where grape seeds are most grown, about the healing substances contained in the seed oil kislots, vitamins, macro and microelements, as well as about their healing for various diseases. In addition, the article presents the results of research on the division of khoraki grapes into parts. Also listed are methods for producing oil from grape seeds.

Introduction

Grapes (Vitis vinifera) are planted on an area of about 7.5 million hectares around the world, being one of the most cultivated fruit crops in the world, where 78 million tons of products are grown per year. Fruits are consumed both fresh and as processed products, such as wine, juice, jam, grape seed extract, jelly, vinegar, dried grapes, and Grape Seed Oil [1]. The total production of grapes in the world is distributed between Europe (39%), Asia (34%) and America (18%), the main grape producing countries are China, Italy, USA, France, Spain and Turkey [2]. During the production of grape juice and wine, a large amount of grape skins, seeds and pulp comes out. Grape seeds account for about 20% - 26% of the waste that comes mainly from wineries.

Speaking at the Republican level, more than 60 thousand tons of grape products are processed by enterprises every year, 3 thousand tons of grape seeds are used fruitlessly per year from production processes. Grape seed oiliness is 9-24.5%, and when the production of Healing Grape oil, the results in sheep for human health can be achieved. According to the teachings of Abu Ali ibn Sina, one of the founders of oriental medicine, our great-grandfather, the oil of grape seeds contains the original treasure of nature, which is extremely useful for the human body. The main reason for the fact that it is a high-quality nutrient, a treatment – prophylactic and cosmetic product-it contains vitamins (E, A, B1, B2, B3, B6, B9, B12, C) macro-micro elements (potassium, calcium, sodium, iron and B.), an abundance of fatty acids, flavonoids, phytosterol, decomposing substances, phytoncides, chlorophyll and enzymes.

Grape seed oil is rich in melanin acid and Omega-6 (up to 70%). Therefore, this product moisturizes the skin, slows down the aging process.

When added with Omega-9 acid (25%), linolinic acid has the property of anti-inflammatory, raising immunity, improving lipid metabolism, meowing the work of the heart and blood vessels, improving the functioning of the nervous and endocrine systems, as well as cleansing the body from various harmful substances (toxins, slags, heavy metal salts, radionuclides). In addition, grape oil contains Omega-3 acids palmitin, stearin, palmitolein, arachine and linoleum, albeit in small quantities [3-4].

Extremely dangerous for the human body, it has a 20 times stronger effect on Aging before the deadline, vitamin C in the fight against free radicals that cause inflammation and Tumor Diseases. Resveratrol Meures estrogen levels, strengthens blood vessels and capillaries, improves blood and lymph circulation, cancer. Protects against Parkinson's and Alsheimer's diseases, preserves the activities of fat "farms in the same field. Due to the fact that it

retains the collagen substance in the skin, the skin retains its elasticity and tension for a long time. Resveratrol is a natural phytroalexine substance produced by the plant to protect against vomiting, bacteria and fungi [5-6].

Material and Method

The studies were carried out using the Central Asian family of grapes with an oil content of 16.10%. Chemical analysis of the initial, intermediate and final products is carried out according to known methods.

The oil content of seeds is understood as the content of crude fat and accompanying fat-like substances, which, together with fat, are in the ether extract from the seeds under study.

Results

During the study, khoraki grapes were cut into parts and studied. The mechanical composition of grape heads is of great importance in the production of wine. The quality of juice and wine is greatly influenced by the fruits of the hard parts of the grape (fruit stalks, skin, seed) (Figure 1).
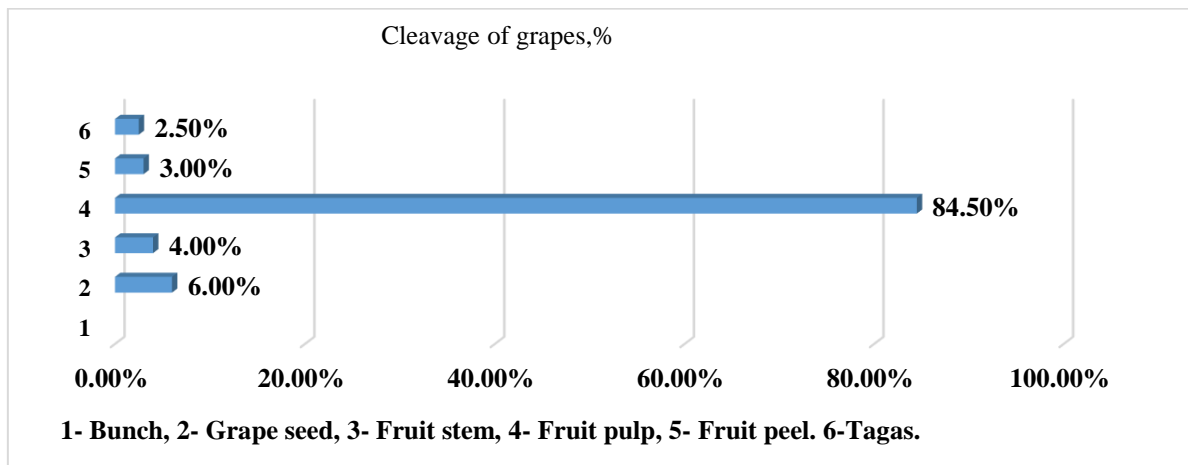

Figure 1. Cutting "Khorak" grapes into parts

When the "Khoraki" grapes were cut into parts, grape seed from the pulp was 6%, fruit stem was 4%, fruit flesh was 84.50%, fruit peel was 3.0%, tagas was 2.50%. These waste products have biological value and are rich in macro-and microelements, which can not only be used as raw materials in human feed, but also have the possibility of producing new types of food.

Based on the above, it will be necessary to pay great attention to the technological processes of oil production by processing Grape Grain. Because the preservation of biologically active substances contained in grape grains depends on the processing process.

We are told that osmosis oils are produced by pressing, for press-extraction methods. The pressing method also has the technology of oil extraction in one-step pressing, two-step pressing and cold pressing methods.

Methods of obtaining oil were analyzed, it can be said that such technological processes as mechanical impact on oil raw materials and thermal processing, and even short-term processing, lead to changes in the composition of raw materials, especially in the oil phase.

Research has shown that thermal treatment of "Yanchilma" in a convective way, accompanied by high-energy costs, especially high temperatures (100s and above), also leads to a deterioration in the quality of oil and "Kunjara" when exposed to it. If the oil is extracted by the extraction method, other substances in the oil seed will melt in the solvent effect and throw in the oil as well as additional electrical energy, the consumption of working kochi materials will be increased. By our side, it is proposed to obtain cold-pressed oil in recent years, Cold-pressed vegetable oils are more in demand due to their higher natural, safer and better nutritional value. In the cold pressing oil extraction method, no heat or chemicals are applied during or before the process. Therefore, the amount of useful phytochemicals in oil increases. By us, the technology of obtaining cold-pressed oil from Grape Seed is proposed in Figure 2 on the rock.

In Figure 2, the seed that comes to processing comes to bunker 1, which provides IT adjacent to the Shnek, from here through shnek 2 it falls to separator 3, in the separator the purified seed is collected to bunker 5, which provides it through noriya 4, from where through shnek 6 the milling equipment comes to 7 it is milled there and through filtr press is given to 14 where the oil is filtered and the oil bag comes to 15. Through the control Regiment 16, a small enterprise is managed. In this method, it is recommended to produce flour from the resulting kunjara, after separating the oil from the grape seed.
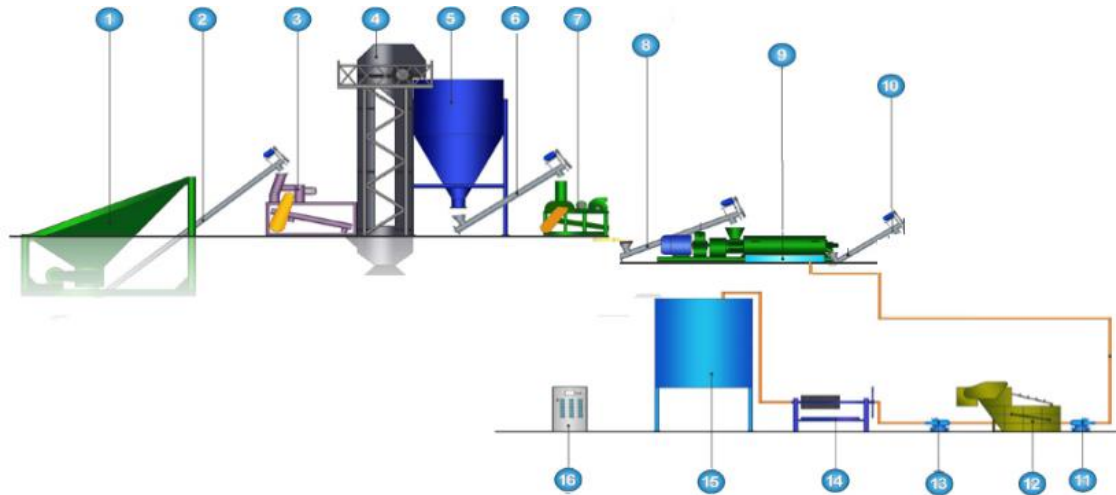
Figure 2. Seed production

Conclusion

The studies carried out showed that when the Khoraki grapes were cut into portions, the grape seed from gujum was 6 %, the fruit stem was 4 %, the fruit flesh was 84.50 %, the fruit post was 3.0 %, the tagas was 2.50%. Also, the technology of obtaining oil by cold pressing has been developed. In our further research work, we set ourselves the goal of developing optimal parameters for obtaining oil from grape seed in a cold way, as well as obtaining flour from kunjara, which comes out after the oil is obtained.

References

1. FAO and HIV (2016). Table and dried grapes. FAO-HIV Focus 2016.
2. Fiari, L. (2007). Graph seed oil supercritical extraction kinetic and solubility data: Critical approach and modeling. The Journal of Supercritical Fluids, 43, 4354.
3. HIV statistical report on World vitiviniculture. HIV, International Organisation of Vine and Wine, Intergovernmental Organisation. Pardo, J. E., et hand. (2009). Characterization of graph seed oil from different graph variations (Vitis vinifera). European Journal of Lipid Science and Technology, 111, 188-193.
4. Harutyunyan, N. S., Kornena, E. P., Yanova, L. I., & Pishchepromizdat, M. (1998). Technology of fat processing. 452, 102.
5. Loseva, N. V., Tarasov, V. E., & Pelipenko, T. V. (2011). Technological research of secondary resources of winemaking for the purpose of their application as part of cosmetics. New technologies. Issue 3. – Maykop: Publishing House of the Moscow State Technical University, 59-63.
6. Alalaf, S., Atkins, D., Barrett, D. J., Blaunt, M., & lacing, N. A. (2002). Etnicheskie razlichiya V soderjanii I melanina V fotoeksponirovannoy i Koje cheloveka fotozatshitnoy sostave click. Issledovanie pigmentnix kletok, 112-118.

BattSim-GDC Simulator: How much battery your green datacenter needs?

Enida Sheme[*1] **Igli Tafa**[1], **Fatmir Basholli**[*1]

[1]Polytechnic University of Tirana, Department of Computer Engineering, Albania, esheme@fti.edu.al, itafa@fti.edu.al
[1]Albanian University, Department of Engineering, Tirana, Albania, fatmir.basholli@albanianuniversity.edu.al

Keywords
Green Datacenter
Simulator
Energy storage device
Battery size
Solar panels

Abstract
Green datacenters topic has been highly researched in the last decade. Main sources of clean energy currently used to feed datacenters are solar, wind and geothermal. Their intermittence poses a challenge in the research field of green datacenters. Thus, the need of an energy storage device becomes present, to store the overproduced energy, while using it when there is not enough clean energy production. In this paper, we pose the question: "How much battery is appropriate for the needs of a given datacenter, while trading-off the cost of the battery and the overproduction of clean energy"? For this, we analyze, design, and implement a simulator called BattSim-GDC, to simulate different scenarios to find the best combination between clean energy quantity and battery size, aiming the lowest waste of renewable (clean) energy production. For this study, the input energy taken in consideration is solar. The results, obtained after the simulator's implementation, show that BattSim-GDC simulator is a necessary tool to be taken in account from administrators, when projecting a green datacenter.

Introduction

The revolution of big data has brought a need for hyperscale datacenters, which consume immense amount of energy and produce Megatons of carbon dioxide per year, based on a study of 2020 [1]. Researchers and administrators of datacenters are constantly aiming to achieve higher energy efficiency levels, to reach their environmental, social, and governance (ESG) goals [2-3].

Thus, datacenters operating in solar, wind and/or geothermal energy, are facing challenges regarding their intermittent nature. Certain periods of time, clean energy production is more than is needed and viceversa, the need is higher than the production of clean energy. At this point, being able to calculate the appropriate amount of energy storage device, e. g. battery, to balance the production with the need, becomes a requirement.

In this paper, we address this research question: How much battery is appropriate for the needs of a given datacenter, while trading-off the cost of the battery and the overproduction of clean energy? To answer this question, we have analyzed, designed, and implemented a simulator, called BattSim-GDC. The renewable energy we refer to is solar. The energy consumption refers to a datacenter of 100 servers, performing a synthetic workload for a full year. The total input values for the energy consumption are 8760, referring to number of hours in a year.

The remainder of this paper is organized as follows. Next section describes related work on the subject of simulators for green datacenters. Furthermore, we illustrate the process of analysis, design, and implementation of the simulator. In the end, we conclude the paper with conclusions and discussions on future work.

Material and Method

Many simulators address the issue of resource sharing in datacenters. CloudSim [4] is one of the most popular simulators used to test different algorithms on virtual physical resources. Nevertheless, in this section we will focus on a list of publications on simulators tackling the sustainability and/or greenness of a datacenter.

Authors at [5-6] present the implementation of a workload scheduling algorithm in CloudSim, aiming to maximize the renewable energy utilization, minimize the energy used from the grid and optimize battery usage.

Philharmonic [7-8], an energy aware cloud controller simulator for geographically-distributed clouds, controls the cloud's resource allocation dynamically to both consolidate resources and adapt to volatile geotemporal inputs.

ReRack [9] is an extensible simulation infrastructure that can be used to evaluate the energy cost of a data center using renewable energy sources, composed of a simulation and an optimization component. It requires a model that can simulate both the data center power usage and the location-dependent variability of the power generation source (solar and wind).

Authors at [10] present Sim2Win, a data center simulation framework that can replay any set of different power management strategies in the face of any set of markets for power flexibility.

As a part of a research project named BlueTool, the authors at [11] present Green Data Center Simulator (GDCSim), an iterative green data center design framework, for the design and development of energy-efficient data centers.

Sustainable datacenter simulator [12] represents an excel-based tool designed to help DC operators assess 16 different sustainability metrics. Five important categories of these sustainability metrics are energy efficiency, greenness, performance and productivity, air management, and storage metrics.

Different to the mentioned simulators, our simulator BattSim-GDC focuses on trading-off the battery size with the total area of solar panels needed by a green datacenter, aiming the highest efficiency between clean energy production and consumption.

The simulator design

The simulator aims to analyze and predict the amount of available energy in the battery over specific moments in a chosen time-period. We base the design on the concept of the battery as a finite state machine with 4 possible states at any time t: Full, Discharging, Charging or Empty. Therefore, there are 16 possible state transition combinations, as shown in "Figure 1". Practically, all these combinations are feasible except for the Full - Empty and Empty - Full transitions which are generally limited by the charge/discharge rate of the battery during a certain period of time. Possible triggers from one state to the other depend on the amount of available solar energy in a moment of time t, referred to as RE(t) (Renewable Energy) and the datacenter energy needs in that moment t, referred to as consum(t). Other affecting factors are the value of the stored energy in the battery, E(t), and the maximum energy capacity of the battery named Efull.
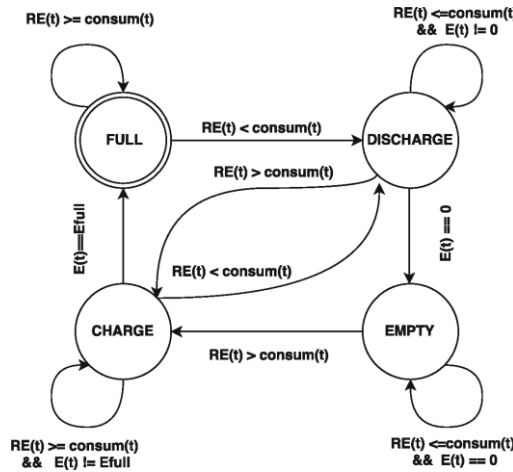
Fig. 1. Battery states over time represented as a finite state machine.

The simulator implementation and results

The pseudocode for developing the simulator is given below as a set of 8 steps, at "Fig. 2". BS (0) refers to the initial Battery State assigned to Full, assuming the battery is fully charged when the simulation begins running. Each of the 16 'current - next' state combinations are assigned a combination number (named combinationNr), which calculates the energy (E(t)) the battery will have on every t. The loop repeats 8760 times, corresponding to the renewable energy and consumption input data (every hour of the year).

Algorithm 1. Simulator tasks
$BS(0) \leftarrow FULL$, $t \leftarrow 1$
repeat
  Define $BS(t) = f[BS(t-1), RE(t), consum(t)]$
  Define $combinationNr = f[BS(t-1), BS(t)]$
  Calculate $E(t) = f[E(t-1), combinationNr]$
until $t \leq 8760$
$greenCoverage = $ annual $[RE(t) - over(t)]/$annual $[consum(t)]$
Print $charge(t), discharge(t), overproduction(t), grid(t), greenCoverage$

Figure 2. The pseudocode for developing the simulator

We have run the simulation tool by changing the input of battery size in different scenarios, varying from 0 to 1 kWh, 10 kWh, 100 kWh, 1MWh and 10MWh. We input the number of m² solar panels, the percentage of renewable energy we want to operate our datacenter with (a number from 0 to 1), referring as green coverage. We input also the consum(t), an Excel input file, representing the energy consumption of 100 servers over a synthetic workload in a year. The result after each simulation shows the level of overproduced energy, which is wasted. A datacenter operator would require this value to be zero. By empirical experiments, we found the best values between the required green coverage and battery size, aiming zero wasted renewable energy.

Conclusions and Discussion

The renewable energy sources are a promising means of energy supply for current datacenters. Nevertheless, they can be in excess or less than needed because of their variability, bringing the need of batteries as energy storage devices. In this paper, we investigate the impact of battery size in green coverage and green energy loss.

We built a battery simulator to provide the amount of available battery energy every time t in a chosen time period. Also, it provides the necessary information to calculate the most efficient amount of battery capacity in order to maximize the utilization of clean energy. This is a valuable tool to help datacenter operators decide on the best combination of solar panels quantity and battery size, that fits their strategies on operating datacenters with green energy.

Furthermore, we plan to propose an improvement of this simulator, by using genetic algorithms to find the optimal combination between solar panels and battery size over a given green datacenter.

References

1. Guerra, M. (2022). Big owners of hyperscale datacenters like Google and Microsoft are putting in place greener and smarter power solutions to achieve their energy efficiency goals. Oct 14, 2022. Accessed on https://www.batterytechonline.com/stationary-storage/battery-energy-storage-solutions-boosting-greener-data-centers.
2. Kiehne, D. (2019). Environmental, social and corporate governance (ESG) -also an innovation driver? InTraCoM GmbH. June 2019.
3. Childers, S. (2023). The IRA's Energy Storage Credits Take Data Centers into the Future. Jan 27, 2023. Accessed on https://www.datacenterknowledge.com/industry-perspectives/ira-s-energy-storage-credits-take-data-centers-future.
4. Calheiros, R. N., Ranjan, R., De Rose, A. F. C., & Buyya, R. (2009) CloudSim: A Novel Framework for Modeling and Simulation of Cloud Computing Infrastructures and Services.
5. Sheme, E., Stolf. P., Da Costa, G., Pierson, J. M., & Frasheri, N. (2016). Efficient Energy sources scheduling in green powered datacenters: A CloudSim Implementation. Proceedings of the Third International Workshop on Sustainable Ultrascale Computing Systems (NESUS 2016) Sofia, Bulgaria, October, 6-7, 2016.
6. Sheme, E. & Frasheri, N. (2016). Implementing Workload Postponing In Cloudsim to Maximize Renewable Energy Utilization. Int. Journal of Engineering Research and Applications. ISSN: 2248-9622, Vol. 6, Issue 8, (Part - 3) August 2016, 23-28.
7. D. Lucanin, A geo-distributed cloud simulator. URL https://philharmonic.github.io/
8. Lucanin, D., Jrad, F., Brandic, I., and Streit, A. (2014) "Energy-aware cloud management through progressive SLA specification," in 11th International Conference on Economics of Grids, Clouds, Systems, and Services (GECON). Springer, 2014, pp. 83–98.
9. Brown, M., & Renau, J. (2011) ReRack: Power Simulation for Data Centers with Renewable Energy Generation. ACM SIGMETRICS Performance Evaluation Review. 39. 77. 10.1145/2160803.2160865.
10. Klingert, S., Wilken, N. & Becker, C. (2020). Sim2Win: How simulation can help data centers to benefit from controlling their power profile. Energy Efficiency 13, 1007–1029 (2020). https://doi.org/10.1007/s12053-020-09873-5
11. Gupta, Sandeep K. S., Banerjee, A., Abbasi, Z., Varsamopoulos, G., Jonas, M., Ferguson, J., Gilbert, R. R., and Mukherjee, T. (2014). GDCSim: A simulator for green data center design and analysis. ACM Transactions on Modeling and Computer Simulation. Volume 24, Issue 1, Article No.: 3, pp 1–27, https://doi.org/10.1145/2553083
12. Omar E. (2019). Data Center Simulator for Sustainable Data Centers. Master Thesis. Institute of Architecture of Application Systems, University of Stuttgart. October 2019.

The trend of use of ICT among households and individuals in Albania

Berina Metanj*1

1Mediterrenian University, Department of Computer Science, Albania, blerina.metanj@umsh.edu.al

Keywords
ICT
internet
Albania

Abstract
The use of computer and Internet has reached unpresented figures. The aim of this article is to analyze the use of Internet and its trends among the population of Albania. The data are used from a secondary data analysis through administrative data source from national statistics of Albania and Eurostat. The aim is to better comprehend the profile of ICT users, such as age and gender, who is more familiar with the use of ICT and how Albania is placed in comparison with other countries in the region. Such analysis is important and useful in an area where ICT is becoming a substantial part of everyone in our everyday life.

Introduction

Everyone nowadays talk about digitalization and technology and how it has revolutionize our life. However, it is crucial to have some basic indicators in order to better understand the situation and how this technology have touch everyone. ICT statistics can help to better understand how digital technologies are transforming our world. On this basis Eurostat, since 2012 have conducted a standard survey about the use of Information and Computer Technology among Member States. Since 2018 Albania has implemented this study and as a potential candidate country has to fulfil some criteria's, among the standardization of statistics.

On this framework, this paper aims not only to understand how Internet is penetrating the Albanian society, but even to further comprehend how Albania stands in relation to the region countries, specifically Western Balkan Countries.

Material and Method

This study is based on a secondary data collection using data official data sources. The data used in the analysis come from the survey on the use of Information and Communication Technologies (ICT) in households and by individuals implemented by INSTAT annually since 2018 [1]. The Survey on Information and Communication Technologies Usage in Households and by Individuals is a statistical survey conducted in households. The eligible population to participate in such survey are resident population residing in Albania from 16 - 74 years old. Such study is implemented in line with international European recommendations and serves as one of the inputs for calculating the indicators on ICT's usage and communication technologies used by households and individuals.

The data will be compared with other countries using data from Eurostat. The same survey has begun implemented in the Member Staties since 2002 aiming at collecting and disseminating harmonized and comparable information on the use of ICT in households and by individuals.

Analysis of the trend of ICT use in Albania compared with other countries in the region of Western Balkan

This session aims to analyze the ICT indicators in Albania comparing them with the Western Balkan Region, Turkey and Eu average region.

According to the official data source, the vast majority of Albanian households have access to Internet. This percentage has steadily increased since 2018. In relative terms Albania is placed in a high position to other regions of the Western Balkan Region, holding the first place in the region when it comes to the percentage of households with access to Internet.

Table 1. Households with access to Internet (in %)

	2018	**2019**	**2020**	**2021**
Albania	82.79	85.45	87.15	90.87
Türkiye	82.49	87.91	89.86	91.95
Bosnia and Herzegovina	69.15	72.03	72.84	75.49
Serbia	72.54	79.01	80.76	81.42
Montenegro	69.39	72.37	78.13	77.82
North Macedonia	78.21	80.38	78.52	83.12
Kosovo*[1]	93.20	93.19	96.36	No data
European Union - 27 countries (from 2020)	84.91	87.53	89.36	90.21

"Source": Eurostat

About 4 percentage of Albanian households declare that they do not access Internet due to high costs of this service. Even if the vast majority of Albanian families do have access to Internet, Albania is second in the region of not accessing Internet due to costs, after Montenegro, 8% of households.
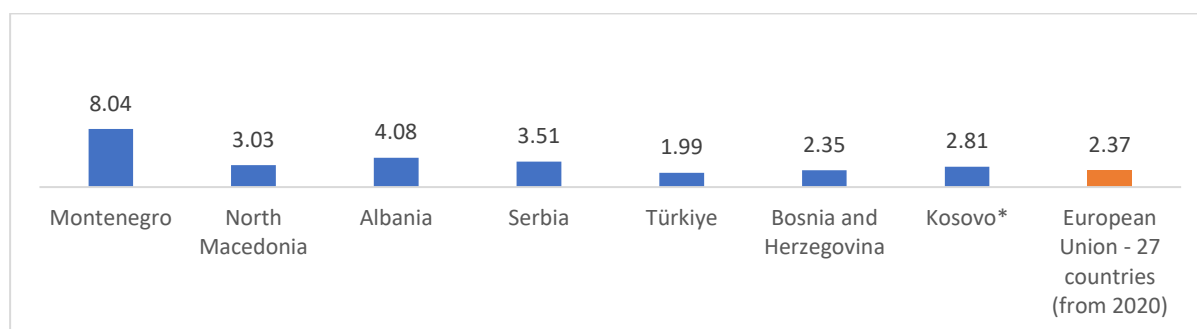
Figure 1. Household without access to Internet because of high costs (in%)

Even if data show that more nine out of ten Albania households have access to the Internet, still its access using a desktop computer is very low in the country compared to other regions in the Western Balkan and the EU average (Table 2). This implies that Internet in the country is being access mainly through mobile phones rather than using a desktop computer. There are no official recent data in Albania in order to comprehend how many households do have a PC. The latest data come from the Census of Population and Households in 2021, where 22% of households declared to have a computer in their homes. This shows that still the access to personal computer in Albania is very low compared to other regions in the country.

Table 2. Individuals used the internet on a desktop computer (in %)

	2018	2021
Albania	18.18	14.08
Türkiye	16.42	11.89
Bosnia and Herzegovina	37.85	36.19
Serbia	43.87	39.28
Montenegro	30.95	33.31
North Macedonia	36.60	28.51
Kosovo	18.38	No data
European Union - 27 countries (from 2020)	41.24	33.92

"Source": INSTAT

---

[1] *Under United Nations Security Council Resolution 1244/99

This hypothesis is confirmed by the ICT survey where the data show that in Albania Internet is mainly accessed by Mobile phones rather than by other devices. However, the use of Laptops using Internet has the major increase during the period 2018-20202 respectively

Profile of ICT users in Albania

ICT survey shows that the use of Internet has steadily increased among women and men. During the period 2018-2022 the percentage of men who access internet at least one time during the year, has been higher compare to women. However, this gap has decreased over years, and in 2022 the difference is only about 2-point percentage among men and women who access Internet.

The main users of Internet remain the youngest population, respectively the age group 16-24 years. Over the last five years they have remained the highest proportion of internet users in the country.

Even if the use among the youngest population is the highest, the growth rate between the last five years has been among the oldest population where the Internet users have almost double in this period.

Table 4. Growth rate of ICT users, 2018-2022 period

Year	*16-24*	*25-34*	*35-44*	*45-54*	*55-64*	*65-74*
Growth rate, Index 2018 base year	5%	9%	32%	66%	77%	96%

"Source": Author calculations

Conclusion

About nine out of then household in Albania have access to Internet. This places the country in the first place in Western Balkan region for this indicator. However, the access to Internet using personal computer is very low with only 14% of households using computer to access the Internet. Financial reasons for not using the Internet are among 4% of households. The main use of accessing internet in the country are through mobile phones. Men use the Internet more than women. However, the increase of the proportion of women using Internet have been higher compared to men. The youngest population use more Internet compared to other age groups. However, the proportion of internet users among older age groups, more than 65 years old, have almost doubled during the last five years. The data show that even if at the beginning the Internet was more a domain of men and of youngest population, still women and other age group are recuperating making Internet accessible and usable from everyone in the country.

References

1. INSTAT, Survey on Information and Communication Technologies (ICT) usage in Households and by Individuals in 2022.

Advanced Engineering Days

aed.mersin.edu.tr

On the formulation of the Cauchy problem for matrix factorizations of the Helmholtz equation

Davron Aslonqulovich Juraev*1 , **Mahir Jalal oglu Jalalov 2** , **Vagif Rza oglu Ibrahimov 3**

1University of Economy and Pedagogy, Department of Scientific Research, Innovation and Training of Scientific and Pedagogical Staff, Uzbekistan, juraevdavron12@gmail.com
2Azerbaijan Academy of Labor and Social Relations, Department of International Relations, Azerbaijan, mahircalalov@mail.ru
3Azerbaijan National Academy of Sciences, Institute of Control Systems, Azerbaijan, ibvag47@mail.ru

Keywords
Integral formula
Matrix factorization
Helmholtz equation
Bounded domain
Cauchy problem

Abstract
In this paper, we are talking about the formulation of the Cauchy problem for matrix factorizations of the Helmholtz equation in two-dimensional and three-dimensional bounded domains. Preliminary information and formulation of the Cauchy problem are given.

Introduction

It is known that the Cauchy problem for elliptic equations is incorrect: the solution to the problem is unique, but unstable. The Cauchy problem for matrix factorizations of the Helmholtz equation, like many Cauchy problems for finding regular solutions of elliptic equations, in the general case is unstable with respect to uniformly small changes in the initial data. Thus, these tasks are incorrectly posed [1].

In unstable problems, the image of the operator is not closed, therefore, the solvability condition cannot be written in terms of continuous linear functionals. So, in the Cauchy problem for elliptic equations with data on a part of the boundary of a domain, the solution is usually unique, the problem is solvable for an everywhere dense data set, but this set is not closed. Consequently, the theory of solvability of such problems is much more difficult and deeper than the theory of solvability of the Fredholm equations. The first results in this direction appeared only in the mid-1980s in the works of L.A. Aizenberg [2], A.M. Kytmanov and N.N. Tarkhanov [6]. For special domains, the problem of continuing limited analytic functions in the case when data is specified only on a part of the boundary was considered by T. Karleman [7]. The research of T. Karleman was continued by G.M. Goluzin and V.I. Krylov. The use of the classical Green formula for constructing a regularized solution of the Cauchy problem for the Laplace equation was proposed by academician M.M. Lavrent'ev in his famous monograph [4]. Using the ideas of M. M. Lavrent'ev [3-4], Sh. Yarmukhamedov constructed in explicit form a regularized solution of the Cauchy problem for the Laplace equation (see for instance [5]) In work [6], an integral formula was proved for systems of equations of elliptic type of the first order with constant coefficients in a bounded domain.

The construction of the Carleman matrix for elliptic systems was carried out by Sh. Yarmukhamedov, N.N. Tarkhanov, A.A. Shlapunov, I.E. Niyozov and others. In papers [8-9] The questions of exact and approximate solutions of the ill-posed Cauchy problem for various factorizations of the Helmholtz equations are studied. Such problems arise in mathematical physics and in various fields of natural science (for example, in electro-geological exploration, in cardiology, in electrodynamics, etc.)

Basic information and formulation of the Cauchy problem

Let R^2 be a two-dimensional real Euclidean space, $x = (x_1, x_2) \in R^2$, $y = (y_1, y_2) \in R^2$.

$G \in \mathbb{R}^2$ is a bounded simply connected domain with a piecewise smooth boundary consisting of the plane $T : y_2 = 0$ and some smooth curve S lying in the half-space $y_2 > 0$, i.e. $\partial G = S \bigcup T$.

We introduce the following notation:

$$r = |y - x|, \ \alpha = |y - x|, \ w = i\sqrt{u^2 + \alpha^2} + y_2, \ u \geq 0, \ \partial_x = \left(\partial_{x_1}, \partial_{x_2} \right)^T, \ \partial_x = \xi^T,$$

$$\xi^T = \left(\xi_1 \ \xi_2 \right)^T - \text{-transposed vektor } \xi, \ U(x) = (U_1(x), ..., U_n(x))^T, \ u^0 = (1, ..., 1) \in \mathbb{R}^n,$$

$$n = 2^m, \ m = 2, \ E(z) = \begin{Vmatrix} z_1 ... 0 \\ .... \\ 0 ... z_n \end{Vmatrix} \text{ - diagonal matrix, } z = (z_1, ..., z_n) \in \mathbb{R}^n$$

Let $D(\xi^T)$, $(n \times n)$ - be a matrix with elements consisting of a set of linear functions with constant coefficients of the complex plane for which the condition is satisfied:

$$D^*(\xi^T) D(\xi^T) = E((|\xi|^2 + \lambda^2) u^0) \tag{1}$$

where $D^*(\xi^T)$ - Hermitian conjugate matrix to $D(\xi^T)$, $|\xi|^2 = \sum_{j=1}^{2} \xi_j^2$, $\lambda -$ real number.

Consider in the domain G a system of partial differential equations of the first order with constant coefficients of the form

$$D\left(\partial_x \right) U(x) = 0, \tag{2}$$

where $D\left(\partial_x \right)$ is the matrix of differential operators of the first order.

We denote by $A(G)$ the class of vector functions in the domain G continuous on $\bar{G} = G \bigcup \partial G$ and satisfying system (2).

The Cauchy problem 1. Suppose $U(y) \in A(G)$ and

$$U(y)\big|_S = f(y), \ y \in S. \tag{3}$$

Here, $f(y)$ a given continuous vector-function on S.

It is required to restore the vector function $U(y)$ in the domain G, based on it's values $f(y)$ on S.

Example 1. Let given a system of first-order partial differential equations of the form

$$\begin{cases} \partial_{x_1} U_1 - \partial_{x_2} U_2 + iU_4 = 0, \\ \partial_{x_2} U_1 + \partial_{x_1} U_2 + iU_3 = 0, \\ -\partial_{x_1} U_3 + \partial_{x_1} U_4 - iU_2 = 0, \\ \partial_{x_2} U_3 + \partial_{x_1} U_4 + iU_1 = 0. \end{cases}$$

Assuming $\partial_{x_1} \rightarrow \xi_1, \partial_{x_2} \rightarrow \xi_2$, we compose the following matrices:

$$D(\xi^T) = \begin{pmatrix} \xi_1 & \xi_2 & 0 & i \\ -\xi_2 & \xi_1 & -i & 0 \\ 0 & i & -\xi_1 & \xi_2 \\ i & 0 & \xi_2 & \xi_1 \end{pmatrix}, \ D^*(\xi^T) = \begin{pmatrix} \xi_1 & -\xi_2 & 0 & -i \\ \xi_2 & \xi_1 & -i & 0 \\ 0 & i & -\xi_1 & \xi_2 \\ -i & 0 & \xi_2 & \xi_1 \end{pmatrix}.$$

Relationship (1) is easily verified.

Let $\mathbb{R}^3$ be the three-dimensional real Euclidean space, $x = (x_1, x_2, x_3) \in \mathbb{R}^3$, $y = (y_1, y_2, y_3) \in \mathbb{R}^3$, $x' = (x_1, x_2) \in \mathbb{R}^2$, $y' = (y_1, y_2) \in \mathbb{R}^2$.

$G \subset \mathbb{R}^3$ be a bounded simply-connected domain with piecewise smooth boundary consisting of the plane T: $y_3 = 0$ and of a smooth surface S lying in the half-space $y_3 > 0$, that i.s., $\partial G = S \bigcup T$.

We introduce the following notation:

$$r = |y - x|, \ \alpha = |y' - x'|, \ w = i\sqrt{u^2 + \alpha^2} + y_3, u \geq 0, \ \partial_x = \left(\partial_{x_1}, \partial_{x_2}, \partial_{x_3} \right)^T, \ \partial_x \rightarrow \xi^T,$$

$$\xi^T = \left(\xi_1 \; \xi_2 \; \xi_3 \right)^T - \text{transposed vector } \xi, \; U(x) = (U_1(x),...,U_n(x))^T, \; u^0 = (1,...,1) \in R^n,$$

$$n = 2^m, \; m = 3, \; E(z) = \left\| \begin{matrix} z_1...0 \\ ...... \\ 0...z_n \end{matrix} \right\| - \text{diagonal matrix, } z = (z_1,...,z_n) \in R^n.$$

Let $D(x^T)$ the $(n \times n)$ – the matrix with elements consisting of a set of linear functions with constant coefficients of the complex plane for which the following condition is satisfied:

$$D^*(\xi^T)D(\xi^T) = E((|\xi|^2 + \lambda^2)u^0), \tag{4}$$

where $D^*(x^T)$ is the Hermitian conjugate matrix $D(x^T)$, $|\xi|^2 = \sum_j^3 \xi_j^2$, λ – real number

Consider in the region G a system of differential equations in partial derivatives of the first order

$$D(\partial_x)U(x) = 0, \tag{5}$$

where $D(\partial_x)$ is the matrix of differential operators of the first order.

We denote by $A(G)$ the class of vector functions in the domain G continuous on $\overline{G} = G \cup \partial G$ and satisfying system (5).

The Cauchy problem 2. Suppose $U(y) \in A(G)$ and

$$U(y)|_S = f(y), \; y \in S. \tag{6}$$

Here, $f(y)$ a given continuous vector-function on S.

It is required to restore the vector function $U(y)$ in the domain G, based on it's values $f(y)$ on S.

Example 2. Let a system of first-order partial differential equations of the form

$$\begin{cases} \partial_{x_1}U_1 + \partial_{x_2}U_4 + \partial_{x_3}U_6 + iU_8 = 0, \\ \partial_{x_1}U_2 + \partial_{x_2}U_3 + \partial_{x_3}U_5 + iU_7 = 0, \\ \partial_{x_2}U_2 - \partial_{x_1}U_3 + \partial_{x_3}U_8 + iU_6 = 0, \\ -\partial_{x_2}U_1 + \partial_{x_1}U_4 + \partial_{x_3}U_7 + iU_5 = 0, \\ \partial_{x_3}U_2 + \partial_{x_1}U_5 + \partial_{x_2}U_8 + iU_4 = 0, \\ \partial_{x_3}U_1 - \partial_{x_1}U_6 + \partial_{x_2}U_7 + iU_3 = 0, \\ \partial_{x_3}U_4 - \partial_{x_2}U_6 + \partial_{x_3}U_7 + iU_2 = 0, \\ \partial_{x_3}U_3 + \partial_{x_2}U_5 + \partial_{x_1}U_8 + iU_1 = 0. \end{cases}$$

Assuming $\partial_{x_1} \to \xi_1$, $\partial_{x_2} \to \xi_2$ and $\partial_{x_3} \to \xi_3$, we obtain the matrices

$$D(\xi^T) = \begin{pmatrix} \xi_1 & 0 & 0 & \xi_2 & 0 & \xi_3 & 0 & i \\ 0 & \xi_1 & \xi_2 & 0 & \xi_3 & 0 & i & 0 \\ 0 & \xi_2 & -\xi_1 & 0 & 0 & i & 0 & \xi_3 \\ -\xi_2 & 0 & 0 & \xi_1 & i & 0 & \xi_3 & 0 \\ 0 & \xi_3 & 0 & i & \xi_1 & 0 & 0 & \xi_2 \\ \xi_3 & 0 & i & 0 & 0 & -\xi_1 & \xi_2 & 0 \\ 0 & i & 0 & \xi_3 & 0 & -\xi_2 & \xi_1 & 0 \\ i & 0 & \xi_3 & 0 & \xi_2 & 0 & 0 & \xi_1 \end{pmatrix}, \; D^*(\xi^T) = \begin{pmatrix} \xi_1 & 0 & 0 & -\xi_2 & 0 & \xi_3 & 0 & -i \\ 0 & \xi_1 & \xi_2 & 0 & \xi_3 & 0 & -i & 0 \\ 0 & \xi_2 & -\xi_1 & 0 & 0 & -i & 0 & \xi_3 \\ \xi_2 & 0 & 0 & \xi_1 & -i & 0 & \xi_3 & 0 \\ 0 & \xi_3 & 0 & -i & \xi_1 & 0 & 0 & \xi_2 \\ \xi_3 & 0 & -i & 0 & 0 & -\xi_1 & -\xi_2 & 0 \\ 0 & -i & 0 & \xi_3 & 0 & \xi_2 & \xi_1 & 0 \\ -i & 0 & \xi_3 & 0 & \xi_2 & 0 & 0 & \xi_1 \end{pmatrix}$$

Relation (4) is easily verified.

Conclusion

In this paper, we present the basic concepts and formulation of the Cauchy problem for matrix factorizations of the Helmholtz equation. To prove the conditions for the matrix factorization of the Helmholtz equation to be satisfied, the corresponding examples are given. On the basis of these examples, approximate solutions of the Cauchy problem for matrix factorizations of the Helmholtz equation are found (see, for instance [8-9]).

References

1. Hadamard, J. (1978). The Cauchy problem for linear partial differential equations of hyperbolic type. Nauka, Moscow.
2. Aizenberg, L. A. (1990). Carleman's formulas in complex analysis. Nauka, Novosibirsk. The Cauchy problem for linear partial differential equations of hyperbolic type. Nauka, Novosibirsk.
3. Lavrent'ev, M. M. (1957). On the Cauchy problem for second-order linear elliptic equations. *Reports of the USSR Academy of Sciences. 112*(2), 195-197.
4. Lavrent'ev, M.M. (1962). On some ill-posed problems of mathematical physics. Nauka, Novosibirsk.
5. Yarmukhamedov, Sh. (1997). On the extension of the solution of the Helmholtz equation. *Reports of the Russian Academy of Sciences*, 357(3), 320-323.
6. Tarkhanov, N. N. (1995). The Cauchy problem for solutions of elliptic equations. V. 7, Akad. Verl., Berlin.
7. Carleman T. (1926). Les fonctions quasi analytiques. Gautier-Villars et Cie., Paris.
8. Juraev, D.A., & Noeiaghdam, S. (2021). Regularization of the ill-posed Cauchy problem for matrix factorizations of the Helmholtz equation on the plane. *Axioms*,*10*(2), 1-14.
9. Juraev D.A. (2021). Solution of the ill-posed Cauchy problem for matrix factorizations of the Helmholtz equation on the plane. *Global and Stochastic Analysis*, *8*(3), 1-17.

Hospital capacity management through simulation

Farzaneh Sarbandi Farahani[*1]

[1]*Islamic Azad University, Central Tehran Branch, Iran, farzaneh.farahani86@gmail.com*

Keywords
Hospital
Resource management
Simulation
Patient Surge

Abstract
This paper investigates different strategies that hospital managers can implement to use their resources more efficient. the resources in the hospital can be human resources, equipment and spaces that can be shared during extraordinary situations that hospitals have a surge in their arrivals for example earthquakes and pandemics. These different strategies are Internal Resource management, Patient transfer management between hospitals, Resource transfer between hospital and Temporary improvement of hospital resources. Required framework with simulation is provided. Then different outcomes are introduced which are Unmet demand, utility of the resources, served patients and queue length. Lastly expected outcome and the reasons for these expectations are described. These results provide insights for the managers who want to plan for improvement of their hospitals serving more patients.

Introduction

Hospitals are institutions that provide services to save people's lives, where different resources work together to provide the best service to patients. Therefore, proper planning and optimal use of hospital resources for providing services with the best stage of service has been the focus of planners and researchers. This planning becomes more important when the hospital is out of normal conditions. There are many examples of these special conditions. For example, Ghayoomi et.al showed that resource management plays a more important role during pandemics such as Covid-19, when people need to use hospitals more [1]. To the extent that some hospitals change all their resources to treat this group of special patients. Resource management can go beyond this and become inter-hospital resource management. Ghayoomi et.al showed sample of resource management in the situation that the hospital needs to investigate more resources for the management of the hospital when faced with a cyber-attack [2]. This article aims to investigate one of the most important methods of managing hospital resources in emergency situations, which is simulation.

Material and Method

There are many ways to manage hospital resources in non-normal situations. Some of the researchers have made these plans using deterministic methods [3]. These methods are usually complex mathematical models whose complexity has made them less practical. On the other hands, hospital simulation has been favored by researchers like Shahverdi et.al [4] due to the great flexibility it provides for problem analysis. To manage hospital resources, it is necessary to simulate each hospital separately. Then, according to the scope and type of the problem, they apply the existing solutions to improve the hospital's performance on the basic hospital and compare the results of using the scenarios [4]. Shahverdi et al illustrated that these kinds of simulation are implemented in estimating regional hospital capacity by simulating the hospitals in a region [5]. Figure 1 shows the regional map of the hospitals in Istanbul and the individual hospital.

A summary of these solutions is presented as:

Internal Resource management: in this scenario the resources (human resources, spaces and equipment) in the units that can be used in other units can be assigned to them but not wise versa (for example ICU Dr can serve isolation room patients but not wise versa) [6]. This is implemented in the simulation by pooling the resources and running the model. In fact, it is some kind of relaxation in the constraints of the problem. When we let them to be assigned from a bigger pool of resources, the feasibility region increases and the optimal solution can be improved (Figure 2a).

Patient transfer management between hospitals: In this kind of management, the patients are transferred to a hospital having Idle resources and doing so the unmet demand is reduced [7]. In this strategy, a central planner sends the patients than can't be visited in a hospital to other hospitals. for example, in case of a cyber attack the patients can be transferred to other hospitals until recovery of the hospital (Figure 2c).

Resource transfer between hospital: In this strategy, the resources between hospitals are shared. For example, ICU nurses can work on other hospital with more patient arrival (Figure 2b).
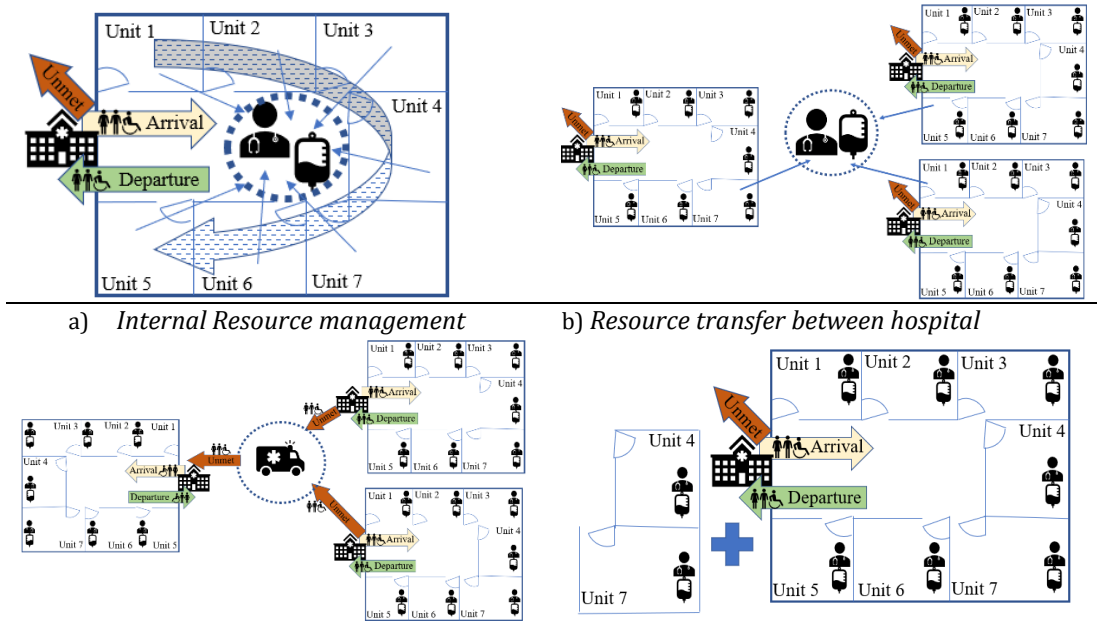
Temporary improvement of hospital resources: There are a lot of examples in which the hospital needed to add extra and temporary units in tents or by repurposing space like parking to increase their capacity for serving patients and by hiring new human resources (Figure 2d).
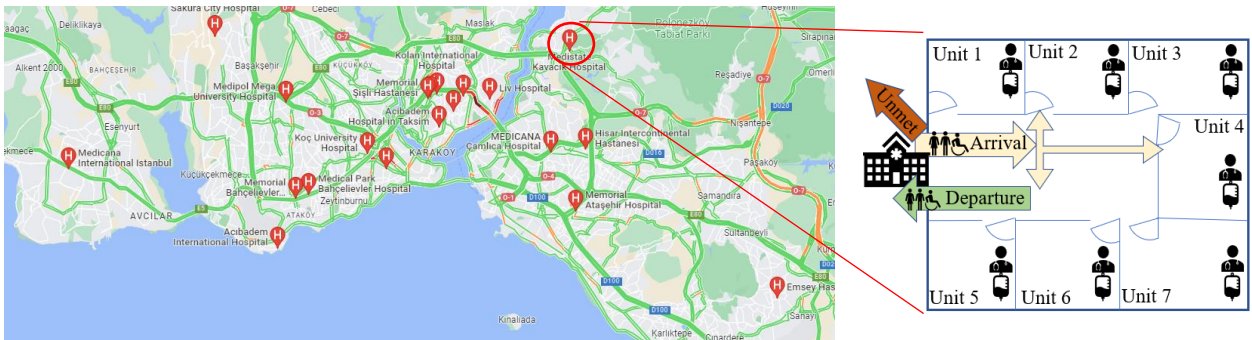
| a): Hospitals in Istanbul | b): Individual hospital |

Figure 1. Regional map of hospitals in Istanbul and the system of one of the hospitals

a)   *Internal Resource management*

b) *Resource transfer between hospital*

c) Patient transfer management between hospitals

d) Temporary improvement of hospital resources

Figure 2. Different strategies for managing hospital capacity efficiently during disasters

Experimental run design

In order to test different strategies a hospital can be simulated separately. The assumptions for the resources, flows and service times can be adopted from existing literature. Each of these four mentioned strategies can be tested with high surge of patients and can be compared to base hospitals without any policy. In order to simulate internal resource management a pool of resource with relevant units are defined in each hospital and is assigned to units with higher demands to remove the bottlenecks. That's while in the resource transfer between hospitals, these pools are bigger and the share of the resources are between hospitals and not the specific hospitals. in the temporary improvement of hospital resources, extra resources are added to each hospital to see how much resources are needed for the hospital to handle this surge of the patients. It can be used to provide an upper bound estimate for the required resources to make serve all the patients. Then by considering these bound hospital managers can provide plans to improve their performance during these extraordinary circumstances. In the patient transfer between hospital policy, a central triage sends unmet demand from busy hospitals to the Idle ones to use their resources.

Results

Different measures can show the performance of each strategy which is presented below that is summarized in Table1:

Unmet demand: the patients that can't be seen in the hospital due to unavailability of services or the patients who leave hospital because of long queue time are called unmet demand [8]. during the surge, expect to see a lot of unmet demand in the base case and those four strategies will reduce the unmet demands [9].

Utility of resources: Resource management during extraordinary conditions means that the Idle resources are used in the units and services that we need them [10]. Therefore, by implementing these strategies we can see increase in the utility of idle units and maybe a reduction in the utility of the busy units. notice that we cannot force our resources to work out of their capacity and doing so we can consider these regulations for human resources.

Queue length: In the surges the patients wait more on the queues and therefore longer queue length in the base scenario without improvement is seen [11]. But by implementing these strategies, in fact the ability of units for serving the patients are increased and therefore the queue length is reduced.

Served patients: managing resources lowers the unmet demand by providing service for the patients in the queues and the patients who leave the hospital in the base hospital. therefore, served patients are improved. We expect to have the most served patients in the Temporary improvement of hospital resources because it increases the capacity of the hospitals until they can see the all the patients. In fact, it provides an estimate for required resources to serve these patients.

Table 1. Expected outcomes by implemented strategies

Unmet demand	Utility of resources	Queue length	Served patients
Reduce	Increase in the Idle units and remaining constant or reduce in busy units	Reduce	Increase

Conclusion

Hospitals are one of the most important elements of society for treatment of the patients. When disaster happens, hospitals are needed more to serve the surge of the patients. Recent Covid-19 is an example of the situation in which many hospitals totally changed their resource role to handle these patients. During the surges the resources got more valuable to be able to save more lives. This study aims to briefly describe different solutions to handle this surge and provides a simulation framework to handle it within a hospital or in a region with multiple hospitals through simulation. Simulation of complex disasters is a well-known tool for analyzing them. For example, Ghayoomi and Partohaghighi [12] used this tool for investigating lake drought prevention using a DRL-based method combined with simulation [12].

The future works will try to simulate the hospital and test these different strategies with some scenarios to test the efficiency of the results and provide insights with numerical examples.

References

1. Ghayoomi, H., Miller-Hooks, E., Tariverdi, M., Shortle, J., & Kirsch, T. D. (2022). Maximizing hospital capacity to serve pandemic patient surge in hot spots via queueing theory and microsimulation. IISE Transactions on Healthcare Systems Engineering, 0(0), 1–19. https://doi.org/10.1080/24725579.2022.2149936

2. Ghayoomi, H., Laskey, K., Miller-Hooks, E., Hooks, C., & Tariverdi, M. (2021). Assessing Resilience of Hospitals to Cyberattack. Digital Health, 7, 20–25. https://doi.org/10.1177/20552076211059366

3. Abir, M., Nelson, C., Chan, E. W., Al-Ibrahim, H., Cutter, C., Patel, K. V., & Bogart, A. (2020). RAND Critical Care Surge Response Tool: An Excel-Based Model for Helping Hospitals Respond to the COVID-19 Crisis. Santa Monica, CA: RAND Corporation. https://doi.org/10.7249/TLA164-1

4. Shahverdi, B., Miller-Hooks, E., Tariverdi, M., Ghayoomi, H., Prentiss, D., & Kirsch, T. D. (2022). Models for Assessing Strategies for Improving Hospital Capacity for Handling Patients during a Pandemic. Disaster Medicine and Public Health Preparedness, 3(2), 1–26. https://doi.org/10.1017/dmp.2022.12

5. Shahverdi, B., Ghayoomi, H., Miller-Hooks, E., Tariverdi, M., & Kirsch, T. D. (2022). Regional Maximum Hospital Capacity Estimation for COVID-19 Pandemic Patient Care in Surge Through Simulation. 2022 Winter Simulation Conference (WSC), 508–520. https://doi.org/10.1109/WSC57314.2022.10015328

6. AHA. (2020). Hospitals and Health Systems Face Unprecedented Financial Pressures Due to COVID-19 (No. 11). American Hospital Association (AHA). Retrieved from American Hospital Association (AHA) website: https://www.aha.org/guidesreports/2020-05-05-hospitals-and-health-systems-face-unprecedented-financial-pressures-due

7. CDC. (2020, February 11). Key Considerations for Transferring Patients to Relief Healthcare Facilities when Responding to Community Transmission of COVID-19 in the United States. Retrieved November 15, 2021, from Centers for Disease Control and Prevention website: https://www.cdc.gov/coronavirus/2019-ncov/hcp/relief-healthcare-facilities.html

8. Mianroodi, M., Guillaume Altmeyer, and Siham Touchal. "Experimental and numerical FEM-based determinations of forming limit diagrams of St14 mild steel based on Marciniak-Kuczynski model." Journal of Mechanical Engineering and Sciences 13.4 (2019): 5818-5831.

9. Moghanizadeh, Abbas, Fakhreddin Ashrafizadeh, & Maziyar Bazmara. (2022). Development the flexible magnetic abrasive finishing process by transmitting the magnetic fields." The International Journal of Advanced Manufacturing Technology 119.3, 2115-2125.

10. Touchal-Mguil, S., Mianroodi, M., Altmeyer, G., & Ahzi, S. (2016, July). Prediction of forming limit diagrams using the Phi-model and the Marciniak Kuczynski Model. In *Research Trends in Mechanical Engineering 2016 Conference Proceedings, First International Conference and Workshop on Mechanical Engineering Research 11-13 July 2016*.

11. Moghanizadeh, Abbas, Fakhreddin Ashrafizadeh, and Maziyar Bazmara. "Development the flexible magnetic abrasive finishing process by transmitting the magnetic fields." The International Journal of Advanced Manufacturing Technology 119.3 (2022): 2115-2125.

12. Ghayoomi, H., & Partohaghighi, M. (2023). Investigating lake drought prevention using a DRL-based method. Engineering Applications, 2(1), 49–59.

Steady state error and equivalent noise bandwidth analysis of the null-seeker architecture for GPS receivers

Alban Rakipi*1 , Olimpjon Shurdi 1 , Aleksander Biberaj 1

1Polytechnic University of Tirana, Department of Electronics and Telecommunications, Albania, arakipi@fti.edu.al, oshurdi@fti.edu.al, abiberaj@fti.edu.al

Keywords
Null-seeker
GPS
Tracking
Noise bandwidth
Receiver

Abstract
In this paper is studied the architecture of closed-loop synchronizers. For a GNSS (Global Navigation Satellite System) receiver, the fine estimation of the code delay and Doppler frequency is generally performed by two concatenated null-seekers, the PLL (Phase Lock Loop), and the DLL (Delay Lock Loop). The null-seeker is implemented, tested and analyzed in a software receiver. The noise equivalent bandwidth, integration time and different incoming signal structures are considered for testing and performance evaluation. Different tests have been performed by changing the input signal from a step unit function to a ramp signal and finally to a parabolic shaped signal. The noise-free steady state value of estimation error is evaluated. The type of loop filter defines the tracking capability of the loop. The estimation error must quickly reach zero for a certain input model and any initial error, in the absence of noise.

Introduction

Synchronizing with the visible satellite signals is an important function of any GNSS receiver [1]. A receiver must first produce a local signal that matches the incoming signal from the satellite before it can give measurements to compute a position, velocity, and timing (PVT) solution. This is done in two stages, namely acquisition and tracking [2]. The objective of the acquisition stage is to find coarse estimates of the Doppler shift and timing offset [3]. An extremely crucial component is the carrier tracking loop, which is utilized to synchronize the local carrier with the incoming signals. Commonly used in the carrier tracking loop, the phase lock loop (PLL) is incredibly fragile, especially in difficult environments [2].

The tracking bandwidth and integration time play an important role on accuracy and dynamic stress tolerance. To reduce the noise and improve accuracy, the tracking bandwidth should be narrow and the integration time long [3]. As a result of the oscillator noise and dynamics on the carrier tracking loop, the bandwidth cannot be reduced arbitrarily. Otherwise, it will cause the phenomena of lock-lose [4]. Due to the complicated environment in the tracking system, accurate models and noise statistics are difficult to be known [2]. For a high sensitivity receiver, no matter whether in acquisition or tracking, the key problem is to extend the coherent time [4]. In [5] the focus is on the process of carrier phase tracking in a scalar PLL. The authors in [6] propose an accurate receiver clock drift estimation method to increase prediction effective time.

In this work is implemented, tested and analyzed a digital synchronization loop architecture in a software receiver. The noise equivalent bandwidth, integration time and different incoming signal structures are considered for testing and performance evaluation.

Material and Method

The architecture of a closed-loop synchronizer, namely the null-seeker is given in Figure 1 [7]. The input signal $y[k, \xi]$ is combined with a locally generated reference signal $x_{ref} = (k, \hat{\xi}[k])$ which has typically the same basic structure as the input signal, apart from the presence of noise and other nuisances. It is characterized by the estimated parameter computed during the previous iteration $\hat{\xi}[k]$. The discrimination function is able to transform $z[k, \xi]$ into a different metric (error signal). $e_\xi[k, \xi]$ value depends on and is proportional to the estimation error $e_\xi[k, \xi] \propto \xi - \hat{\xi}[k]$. A fundamental property is that one of its zeros corresponds to the searched value of the parameter to be estimated. The key operation of a null seeker is to find a zero of its discrimination function (iteratively). The discrimination function S(.) in (1) can be nonlinear, but it is convenient to study the overall system in its linearity region therefore: $e_\xi[k, \xi] \approx \beta \cdot (\xi - \hat{\xi}[k])$ where β is the slope of the S-curve in $\xi - \hat{\xi}[k] = 0$.

$$e_\xi[k, \xi] = S(\xi - \hat{\xi}[k]) \tag{1}$$

The Low-pass loop filter smoothens the error signal to reduce the contribution of the noise $w[k]$ and it still preserves the reactivity of the loop to the dynamics of the parameter to be estimated. The new estimated parameter is extracted from the filtered error signal.

$$\hat{\xi}[k + 1] = \hat{\xi}[k] + e_\xi[k] \tag{2}$$

The updating rule in (2) followed by the "Delay" block, represents an IIR digital filter, with input $e_\xi[k]$ and output $\hat{\xi}[k]$ and its transfer function is $z\hat{\xi}(z) = \hat{\xi}(z) + e_\xi(z)$. Transfer function from $e_\xi(k)$ to $\hat{\xi}(k)$ can be written in the form:

$$D(z) = \frac{\hat{\xi}(z)}{e_\xi(z)} = \frac{1}{z - 1} = \frac{z^{-1}}{1 - z^{-1}} \tag{3}$$

As the received signal is noisy, then the error signal contains an additive noise component $e_\xi[k, \xi] = \beta \delta_\xi[k] + \eta[k]$ where $\delta_\xi[k] = \xi - \hat{\xi}[k]$ is the instantaneous error and $\eta[k]$ is a discrete-time random process, white and Gaussian. It is independent from $\delta_\xi[k]$ and "circulates" within the loop coupled with $\delta_\xi[k]$.
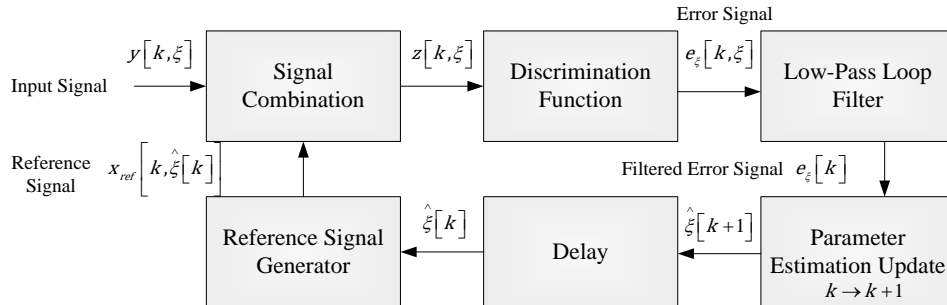

Figure 1. Null-seeker architecture

Simulation and Results

To test the behavior of the null-seeker we have implemented at the software level using Matlab the block diagram in Fig 1. Different tests have been performed by changing the input signal from a step unit function to a ramp signal and finally to a parabolic shaped signal. The other two variable parameters of the simulations are respectively the order of the filter and the product of the equivalent noise bandwidth with the integration time. The steady-state estimation error is evaluated and plotted in Figure 2 to 5.

One can observe from Fig. 3 and Fig. 4 that an increase of one order of magnitude of the loop noise equivalent bandwidth (from BeqTs = 0.0005 to BeqTs = 0.005) decreases k (from 4601 to 456), and the estimation error decreases with the same order of magnitude (from 50 to 5). So, the integration time is decreased by an order of magnitude. Another important remark that can be derived is that in order to minimize the steady-state error, the noise equivalent bandwidth should be increased. In Fig. 5 can be easily observed that the estimation error $\delta_\xi[k]$ is unlimited because of the unlimited characteristic of the quadratic input.
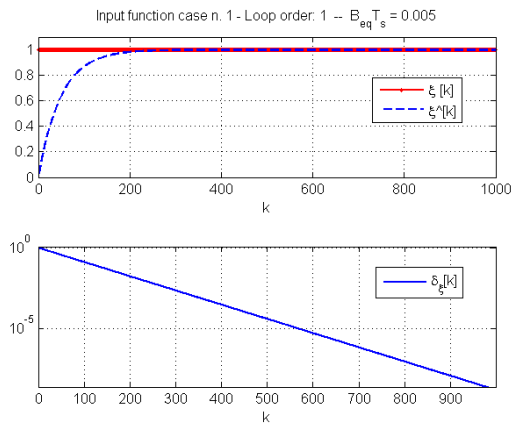
Figure 2. Plot of the estimation error $\delta_\xi[k]$ in the logarithmic scale, for step input
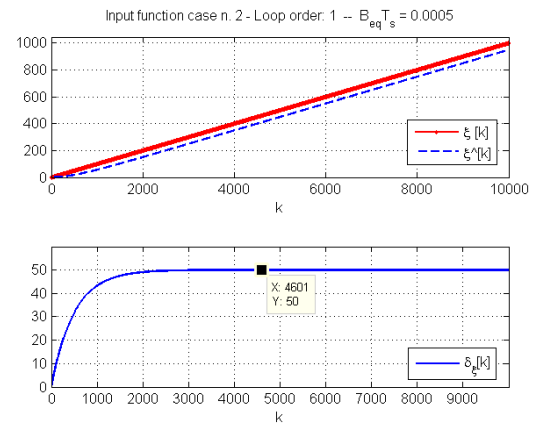

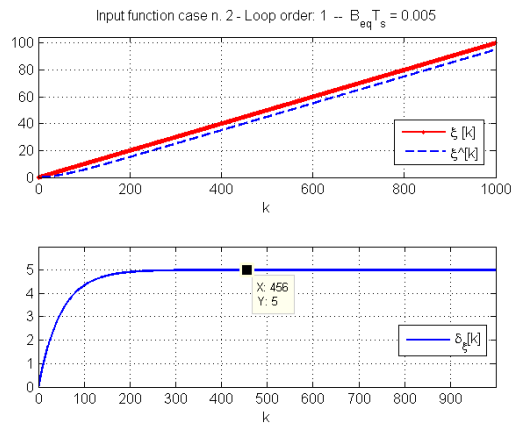**Figure 3.** Plot of the steady state error $\delta_\xi[k]$ for a ramp input

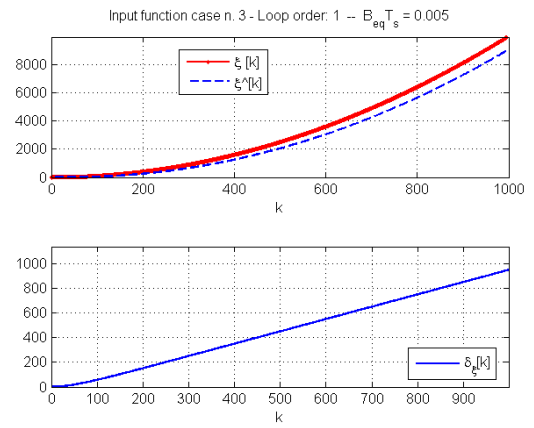**Figure 4.** Plot of the steady state error $\delta_\xi[k]$ for a ramp input and different $B_{eq}T_s$

Figure 5. Plot of the steady state error $\delta_\xi[k]$ for a parabolic input

Conclusion

In this article, the architecture of digital synchronizers for GPS receivers was studied. To evaluate the performance of the null-seeker, numerous simulation tests were performed. Three types of input signals were applied: step, ramp and parabolic. From the results we concluded that a higher noise equivalent bandwidth reduces the steady-state error, but this also reduces the integration time.

References

1. Roncagliolo, P. A., García, J. G., & Muravchik, C. H. (2012). Optimized carrier tracking loop design for real-time high-dynamics GNSS receivers. International Journal of Navigation and Observation. Retrieved from https://doi.org/10.1155/2012/651039
2. Cheng, Y., & Chang, Q. (2020). A carrier tracking loop using adaptive strong tracking kalman filter in GNSS receivers. IEEE Communications Letters. Retrieved from https://doi.org/10.1109/LCOMM.2020.3018742
3. Clare, A., Lin, T., & Lachapelle, G. (2017). Effect of GNSS receiver carrier phase tracking loops on earthquake monitoring performance. Advances in Space Research. Retrieved from https://doi.org/10.1016/j.asr.2016.07.002
4. Cheng, L., Dai, Y., Guo, W., & Zheng, J. (2021). Structure and performance analysis of signal acquisition and doppler tracking in LEO augmented GNSS receiver. Sensors (Switzerland). Retrieved from https://doi.org/10.3390/s21020525
5. Curran, J. T. (2015). Enhancing Weak-Signal Carrier Phase Tracking in GNSS Receivers. International Journal of Navigation and Observation. Retrieved from https://doi.org/10.1155/2015/295029
6. Li, Z., Zhang, T., Qi, F., Tang, H., & Niu, X. (2019). Carrier phase prediction method for GNSS precise positioning in challenging environment. Advances in Space Research. Retrieved from https://doi.org/10.1016/j.asr.2018.12.015
7. Won, J. H., & Pany, T. (2017). Signal Processing. In Springer Handbooks. Retrieved from https://doi.org/10.1007/978-3-319-42928-1_14

Advanced Engineering Days

aed.mersin.edu.tr

Fundamental solution for the Helmholtz equation in the plane

Davron Aslonqulovich Juraev*1

1University of Economy and Pedagogy, Department of Scientific Research, Innovation and Training of Scientific and Pedagogical Staff, Uzbekistan, juraevdavron12@gmail.com

Keywords
Integral formula
Matrix factorization
Helmholtz equation
Bounded domain
Cauchy problem

Abstract
This paper deals with the construction of a family of fundamental solutions of the Helmholtz equation, parameterized by an entire function with certain properties. The lemma for the Helmholtz equation on a two-dimensional bounded domain is proved.

Introduction

It is known that the Helmholtz equation in different spaces has a fundamentally different solution. In the future, using the construction of constructing a fundamental solution, we will construct an approximate solution for the Helmholtz equation. The fundamental solution for the Laplace equation was constructed by Sh. Yarmukhamedov [1]. The fundamental solution for the matrix factorization of the Laplace equation was proved in [2]. Using the construction of work [1], as well as work [2], we prove the validity of the fundamental solution for the Helmholtz equation in the plane case.

For the matrix factorization of the Helmholtz equation, the validity of fundamental solutions in various spaces was considered by the author [3-9].

Basic information and formulation of the Cauchy problem

This section deals with the construction of a family of fundamental solutions of the Helmholtz equation, parameterized by an entire function with certain properties.

Let R^2 be a two-dimensional real Euclidean space,

$$x = (x_1, x_2) \in R^2,\ y = (y_1, y_2) \in R^2,\ \alpha = |y_1 - x_1|,\ r = |y - x|.$$

$G \subset R^2$ is a bounded simply connected region whose boundary consists of a smooth curve $S = \partial G,\ \overline{G} = S \bigcup G$. We consider the Helmholtz equation

$$\Delta U(y) + \lambda^2 U(y) = 0, \tag{1}$$

where $\lambda > 0$, $\Delta -$ is the Laplace operator.

We denote by $K(w)$ is an entire function taking real values for real w ($w = u + iv; u, v -$ real numbers) and satisfying the following conditions:

$$K(u) \neq 0,\ \sup_{v \geq 1} \left| v^p K^{(p)}(w) \right| = \mathrm{M}(u, p) < \infty,\ -\infty < u < \infty,\ p = 0, 1, 2. \tag{2}$$

We define a function $\Phi(y, x)$ when $y \neq x$ by the following equality:

$$\Phi(y, x) = -\frac{1}{2\pi K(x_2)} \int_0^\infty \mathrm{Im} \frac{K(w)}{w - x_2} \frac{u I_0(\lambda u)}{\sqrt{u^2 + \alpha^2}} du,\ w = i\sqrt{u^2 + \alpha^2} + y_2, \tag{3}$$

where $I_0(\lambda u)$ – is the Bessel function of the first kind of zero order.

Lemma. *The function* $\Phi(y,x)$ *can be represented as*

$$\Phi(y,x) = -\frac{i}{4} H_0^{(1)}(\lambda r) + g(y,x). \tag{4}$$

Here $-\frac{i}{4} H_0^{(1)}(\lambda r)$ – is the fundamental solution of the Helmholtz equation in P^2, defined through the Hankel function of the first kind, $g(y,x)$ – is the regular solution of the Helmholtz equation with respect to the variable y, including the point $y = x$.

We note that the proof of the lemma remains valid if, in (3), for $K(w)$ we take an analytic function that is regular in some domain and takes real values for real w, satisfying condition (2).

Proof. For convenience, we introduce the notation

$$f(w) = \frac{K(w)}{w - x_2}, \quad w = i\sqrt{u^2 + \alpha^2} + y_2, \quad \varphi(y,x) = \int_0^\infty f(w) \frac{u I_0(\lambda u)}{\sqrt{u^2 + \alpha^2}} du. \tag{5}$$

In these notation

$$\Phi(y,x) = \frac{1}{2\pi K(x_2)} \operatorname{Im} \varphi(y,x). \tag{6}$$

Our goal is to prove that the function $\varphi(y,x)$ is a solution of equation (1) with respect to the variable y at $\alpha > 0$.

This will follow that the function $\Phi(y,x)$ is a solution of equation (1) with respect to y at $\alpha > 0$.

Taking into account conditions (2), from formula (5), by differentiation we obtain

$$\frac{\partial \varphi(y,x)}{\partial y_1} = \int_0^\infty \frac{\alpha u i f'(w)}{u^2 + \alpha^2} I_0(\lambda u) du - \int_0^\infty \frac{\alpha u f(w)}{\left(u^2 + \alpha^2\right)^{3/2}} I_0(\lambda u) du, \quad y_1 > x_1. \tag{7}$$

The first integral is integrable by parts

$$\int_0^\infty \frac{\alpha u i f'(w)}{u^2 + \alpha^2} I_0(\lambda u) du = \int_0^\infty \frac{\alpha I_0(\lambda u)}{\sqrt{u^2 + \alpha^2}} du =$$

$$= -f(w) + \int_0^\infty \frac{\alpha u I_0(\lambda u)}{\left(u^2 + \alpha^2\right)^{3/2}} f(w) du - \lambda \int_0^\infty \frac{\alpha I_0'(\lambda u)}{\sqrt{u^2 + \alpha^2}} f(w) du.$$

Substituting these expressions in (7), we obtain

$$\frac{\partial \varphi(y,x)}{\partial y_1} = -f(w) - \lambda \int_0^\infty \frac{\alpha I_0'(\lambda u)}{\sqrt{u^2 + \alpha^2}} f(w) du, \quad y_1 > x_1. \tag{8}$$

In the same way, we get

$$\frac{\partial \varphi(y,x)}{\partial y_1} = f(w) - \lambda \int_0^\infty \frac{\alpha I_0'(\lambda u)}{\sqrt{u^2 + \alpha^2}} f(w) du, \quad y_1 < x_1. \tag{9}$$

Taking into account (8) and (9), we have

$$\frac{\partial \varphi^2(y,x)}{\partial y_1^2} = -i f(w) - \lambda \int_0^\infty \frac{I_0'(\lambda u)}{\sqrt{u^2 + \alpha^2}} f(w) du +$$

$$+ \int_0^\infty \frac{\alpha^2 I_0'(\lambda u)}{\left(u^2 + \alpha^2\right)^{3/2}} f(w) du - \lambda \int_0^\infty \frac{i\alpha^2 I_0'(\lambda u)}{\sqrt{u^2 + \alpha^2}} f'(w) du, \quad y_1 \neq x_1,$$

or

$$\frac{\partial \varphi^2(y,x)}{\partial y_1^2} = -i f'(w) - \lambda \int_0^\infty \frac{u^2 I_0'(\lambda u)}{\left(u^2 + \alpha^2\right)^{3/2}} f(w) du - \int_0^\infty \frac{i\alpha^2 I_0'(\lambda u)}{\sqrt{u^2 + \alpha^2}} f'(w) du. \tag{10}$$

Now we will calculate the partial derivatives of the function $\varphi(y,x)$ with respect to y_2 at $y_1 \neq x_1$.

$$\frac{\varphi(y,x)}{\partial y_2} = \int_0^\infty \frac{f'(w)\,u\,I_0(\lambda u)}{\sqrt{u^2 + \alpha^2}} f(w)du, \quad y_1 \neq x_1.$$

Integrating in parts, we obtain

$$\frac{\partial \varphi(y,x)}{\partial y_2} = f(w) + i\lambda \int_0^\infty I_0'(\lambda u) f(w)du, \quad y_1 \neq x_1. \tag{11}$$

From here

$$\frac{\partial^2 \varphi(y,x)}{\partial y_2^2} = if'(w) + i\lambda \int_0^\infty I_0'(\lambda u) f'(w)\,du, \quad y_1 \neq x_1. \tag{12}$$

Taking into account (10), (12) and (1), we have

$$\Delta\varphi(y,x) + \lambda^2\varphi(y,x) = -\lambda\int_0^\infty \frac{u^2 I_0'(\lambda u)}{\left(u^2 + \alpha^2\right)^{3/2}} f(w)du +$$

$$+ i\lambda\int_0^\infty \frac{u^2 f'(w) I_0'(\lambda u)}{u^2 + \alpha^2}du + \lambda^2\int_0^\infty \frac{f(w) I_0'(\lambda u)u}{\sqrt{u^2 + \alpha^2}}du, \quad y_1 \neq x_1.$$

Integrating the second integral in parts, we obtain

$$\Delta\varphi(y,x) + \lambda^2\varphi(y,x) = -\lambda\int_0^\infty \frac{f(w)}{\sqrt{u^2 + \alpha^2}}\left[\lambda u I_0''(\lambda u) + I_0'(\lambda u) + \lambda u I_0(\lambda u)\right]du.$$

Since, the integrand

$$\lambda u I_0''(\lambda u) + I_0'(\lambda u) + \lambda u I_0(\lambda u) = 0$$

is the zero order Bessel equation and $I_0(\lambda u)$ is its solution, then

$$\Delta\varphi(y,x) + \lambda^2\varphi(y,x) = 0, \quad y_1 \neq x_1.$$

It follows from this equality that $\Phi(y,x)$ is a solution of equation (1) with respect to y on the line $y_1 \neq x_1$. For this it is enough to show its differentiability as $y_1 = x_1$ (then, according to the well-known property of solving an elliptic equation, it continues on the line $y_1 = x_1$ as a solution).

Similarly, take the partial derivative of the function $\Phi(y,x)$ with respect to y_2, and we can completely prove the lemma. But due to the limitation of the number of pages, we will give a complete proof of the lemma in the future in other papers.

The lemma proved.

Conclusion

In this work, on the basis of previous research works, we proved the validity of the fundamental solutions of the Helmholtz equation. The construction of a fundamental solution allows, in the future, to find in an explicit form a regularized solution for the Helmholtz equation.

References

1. Yarmukhamedov, Sh. (1997). On the extension of the solution of the Helmholtz equation. *Reports of the Russian Academy of Sciences*, 357(3), 320-323.
2. Tarkhanov, N. N. (1995). The Cauchy problem for solutions of elliptic equations. V. 7, Akad. Verl., Berlin.
3. Juraev, D. A. (2014). The construction of the fundamental solution of the Helmholtz equation. *Reports of the Academy of Sciences of the Republic of Uzbekistan*, (4), 14-17.
4. Juraev, D. A., & Noeiaghdam, S. (2021). Regularization of the ill-posed Cauchy problem for matrix factorizations of the Helmholtz equation on the plane. *Axioms*, *10*(2), 1-14.

5. Juraev, D. A. (2021). Solution of the ill-posed Cauchy problem for matrix factorizations of the Helmholtz equation on the plane. *Global and Stochastic Analysis*, *8*(3), 1-17.
6. Juraev, D. A., & Gasimov, Y. S. (2022). Regularization of the ill-posed Cauchy problem for matrix factorizations of the Helmholtz equation on the plane. *Azerbaijan Journal of Mathematics*, 12(1), 142-161.
7. Juraev, D. A., & Noeiaghdam, S. (2022). Modern Problems of Mathematical Physics and Their Applications. *Axioms*, 11(2), 1-6.
8. Juraev, D. A., & Noeiaghdam, S. (2022). Modern Problems of Mathematical Physics and Their Applications. Axioms, MDPI. Switzerland. 1-352.
9. Juraev, D. A. (2022). On the solution of the Cauchy problem for matrix factorizations of the Helmholtz equation in a multidimensional spatial domain. *Global and Stochastic Analysis*, 9(2), 1-17.

Advanced Engineering Days

aed.mersin.edu.tr

Speed control of three phase induction motor using Field Oriented Control technique

Darjon Dhamo*1 , **Denis Panxhi** 1 , **Aida Spahiu** 1 , **Jonadri Bundo** 1

¹Polytechnic University of Tirana, Automation Department, Albania, darjon.dhamo@gmail.com; denis_panxhi@yahoo.com; aspahiu@upt.al; jonadribundo@gmail.com

Keywords

Induction motors
Field Oriented Control
SVPWM
Speed control
Vector control

Abstract

Induction motors are very common in industrial applications like pumps, blowers, compressors, fans, air-conditioning systems and others. The main reason for this popularity in the industry is because they are very simple, require minimum maintenance and manufacturing costs are low. This paper is aimed to give a contribution in speed control of a 250 W three phase induction motor in an application which requires a high performance of electric drive. The Field Oriented Control (FOC) technique is implemented in order to have the required performance. This algorithm has some advantages compared to scalar control such as improved dynamics, full torque control from zero to nominal speed, decoupled control of flux and torque, higher efficiency and others. This study is done in the Simulink/MATLAB environment where the model of speed control of 250 W three phase induction motor is created. Firstly, the fifth order model of the motor is built in a stationary frame. Secondly, the Field Oriented Control technique is implemented when are found also PI regulators coefficients. In the end, Space Vector Pulse Width Modulation (SVPWM) technique was built. This is the final step of FOC to determine the pulse width modulation signal for the inverter switches in order to generate the desired three phase voltage to the motor. Numerical simulations which are presented graphically at the end of this paper shows the advantages of using FOC.

Introduction

Before 1971, induction motors were run at constant speed. This speed was determined by number of pole pairs and frequency. The difficulty of controlling the speed of an induction motor consists in the nonlinearity relationship between the motor current and electromagnetic torque provided by the motor. This nonlinearity does not exist in the DC motor and therefore controlling the speed of the DC motor is a simple task. But, the reason why industrialists were not satisfied with this solution was because there are some disadvantages of DC motors compared to induction motors in terms of maintenance and costs [1-2].

Many studies are made in terms of speed control of induction motors because they can work for a long time without maintenance, they are robust and inexpensive. This type of motor does not need a supply current from outside the motor to create a magnetic field like a DC motor does. After much effort, F. Blasche in 1971 presented the first paper on Field Oriented Control (FOC) technique for speed control of an induction motor. Since that year, the technique was completely developed and nowadays Field Oriented Control technique is implemented for speed control of induction motors in applications which require high performance of electric drives [3-6].

The idea of FOC is to express the machine space vector model in the rotating dq reference frame which has a direct axis aligned with the flux-linkage vector [7]. In this paper the d axis is aligned with the rotor flux-linkage vector because it gives best results and a complete separation of the torque and flux control. This is the same as the DC motor.

Knowing that Simulink/MATLAB is powerful environment for simulating dynamics system, there is built the fifth order model of three phase induction motor and is implemented FOC technique. To determine the state switches of the inverter is used SVPWM technique to offer 15 % increase in the DC link voltage utilization and low output harmonic distortions compared with sinusoidal PWM.

Material and Method

The mathematical model of the induction motor which is built in Simulink is expressed on stator reference frame. The stator voltage is expressed:

$$U_{s\alpha} = R_s i_{s\alpha} + \frac{d\psi_{s\alpha}}{dt} \tag{1}$$

$$U_{s\beta} = R_s i_{s\beta} + \frac{d\psi_{s\beta}}{dt} \tag{2}$$

where:

$$\psi_{s\alpha} = L_s i_{s\alpha} + L_m i_{r\alpha} \tag{3}$$

$$\psi_{s\beta} = L_s i_{s\beta} + L_m i_{r\beta} \tag{4}$$

The rotor voltage is expressed:

$$U_{r\alpha} = 0 = R_r i_{r\alpha} + \frac{d\psi_{r\alpha}}{dt} + \omega_r \psi_{r\beta} \tag{5}$$

$$U_{r\beta} = 0 = R_r i_{r\beta} + \frac{d\psi_{r\beta}}{dt} - \omega_r \psi_{r\alpha} \tag{6}$$

where:

$$\psi_{r\alpha} = L_r i_{r\alpha} + L_m i_{s\alpha} \tag{7}$$

$$\psi_{r\beta} = L_r i_{r\beta} + L_m i_{s\beta} \tag{8}$$

The electromagnetic torque is:

$$T = \frac{3}{2} p \frac{L_m}{L_r} (\psi_{s\alpha} i_{s\beta} - \psi_{s\beta} i_{s\alpha}) \tag{9}$$

The fundamental equation of dynamics is:

$$\frac{d\omega_r}{dt} = \frac{p}{J} (T - T_{load} - \frac{B}{p} \omega_r) \tag{10}$$

Were, $U_{s\alpha}, U_{s\beta}, U_{r\alpha}, U_{r\beta}$ - stator and rotor voltages expressed on stator reference frame, $i_{s\alpha}, i_{s\beta}, i_{r\alpha}, i_{r\beta}$ - stator and rotor currents expressed on stator reference frame, $\psi_{s\alpha}, \psi_{s\beta}, \psi_{r\alpha}, \psi_{r\beta}$ - stator and rotor fluxes expressed on stator reference frame, T - electromagnetic toque, T_{load} - load torque, ω_r - angular speed of rotor.

The parameters of induction motor are listed in Table 1.

Table 1. Parameters of induction motor

Parameters	Symbol	Value	Unit
Nominal power	P_n	250	W
Nominal stator voltage	V_n	230	V
Nominal frequency	f_n	50	Hz
Nominal current	I_n	0.9	A
Number of pole pairs	p	2	
Stator resistance	R_s	25.223	Ω
Rotor resistance	R_r	23.004	Ω
Stator inductance	L_s	0.534	H
Rotor inductance	L_r	0.534	H
Magnetizing inductance	L_m	0.487	H
Moment of inertia	J	0.000303	kgm^2
Viscous friction	*B*	0.000359	Nms

The FOC implemented in Simulink has the stator current of the q axis decoupled into the torque producing and the stator current of the d axis is decoupled into the rotor flux-producing:

$$\psi_{rd} = L_m i_{sd} \tag{11}$$

$$T = \frac{3}{2} p \frac{L_m}{L_r} \psi_{rd} i_{sq} \tag{12}$$

Figure 1 shows the complete model of speed control of induction motor using the FOC technique created in the Simulink/MATLAB environment.
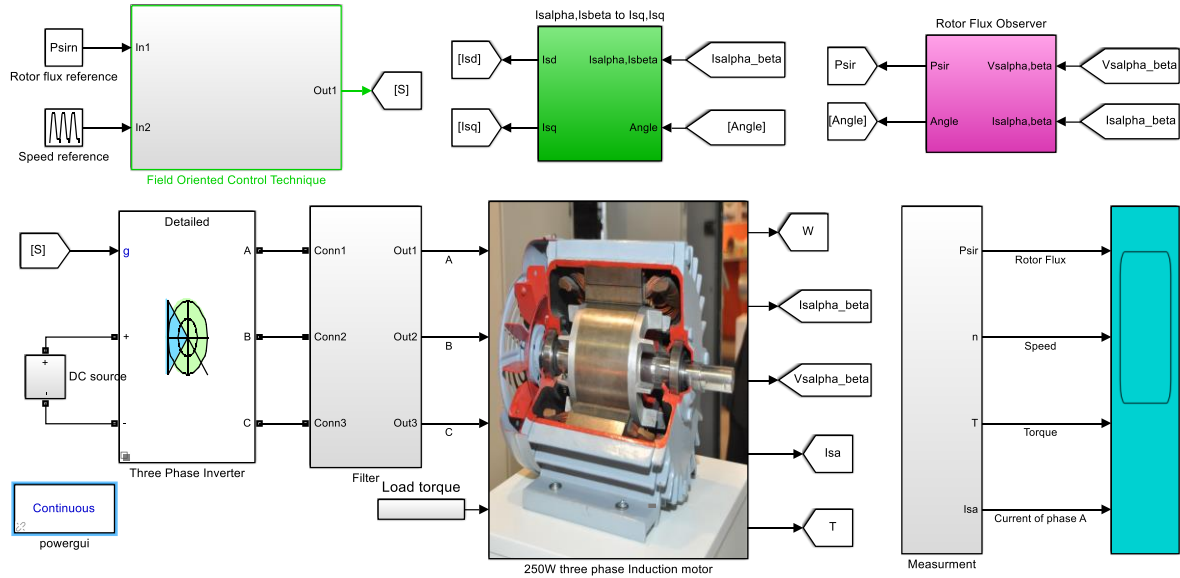

Figure 1. Speed control model of three phase induction motor using FOC technique

Results

The simulation of speed control is carried out using Simulink/MATLAB software.
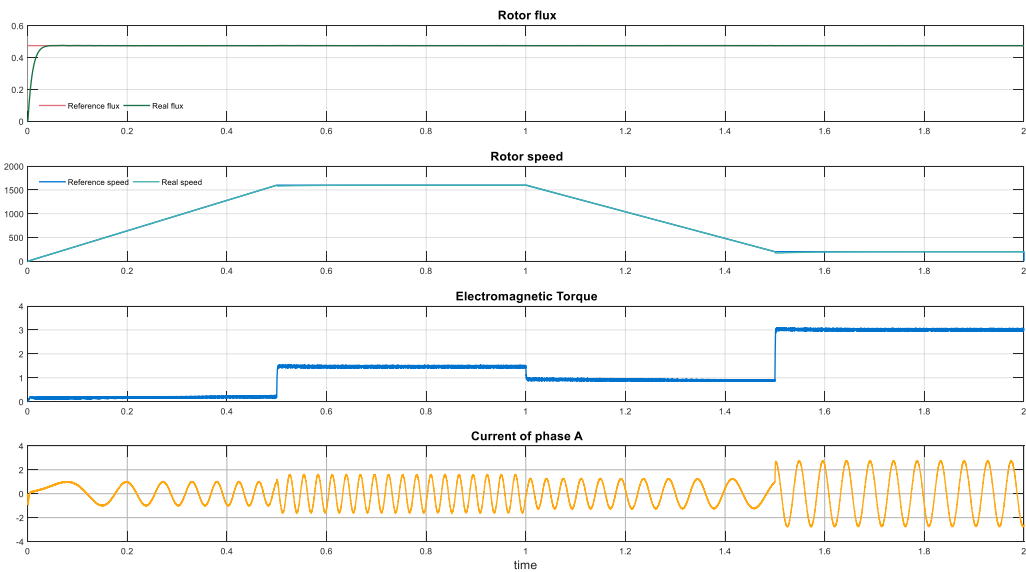

Figure 2. Results of speed control of 250W induction motor using Field Oriented Control technique

The values on Table 2 are the input of the model which is simulated and the result are shown in Figure 2.

Table 2. Reference speed and load torque applied on the motor

Time (s)	Reference speed (rpm)	Load torque (Nm)
0	0	0
0.5	1600	1.4
1	1600	1
1.5	200	3
2	200	3

Discussion

The simulation result shows that the reference value of the rotor flux matches the real value of the flux from time 0.0324 seconds until the end of the simulation. During this time, even though the reference speed and load torque have changed, the flux has remained the same as the reference value. The PI regulator coefficients inserted for rotor flux control are $k_P = 5.23$ and $k_I = 110.87$.

The reference value of the rotor speed is the same as the real speed throughout the simulation, except the cases when the induction motor has been in a transient process because of reference value and load torque have been changed. There is a little difference between the reference speed and the real speed in the transient process thanks to the use of FOC technique. This technique made it possible to change the q-axis current of the stator where the d-axis current has remained the same. With this situation, the flux remains constant and the electromagnetic moment changes quickly to reach the steady state operation. The PI regulator coefficients inserted for speed control are $k_P = 0.56$ and $k_I = 8.7$.

Electromagnetic torque and stator current are characterized by low values of ripples because of voltage signal that feeds the motor, which is not a pure sinusoid but contains high-order harmonics. Placing the filter in the model has smoothed out some of the harmonics but has not completely neutralized them.

Conclusion

In this paper the Field Oriented Control technique for speed control of 250 W three phase induction motor was implemented. The speed control model was created in Simulink/MATLAB when the numerical result was obtained.

Table 3. Quality indicators of speed response

Time (s)	Overshoot (%)	Undershoot (%)	Setting time (s)
0.5	0	1.06	0.07
1	0.18	0	0.04
1.5	0	15	0.15

Based on numerical result and quality indicators in Table 3, it comes to the conclusion that Field Oriented Control technique allows induction motor to operate smoothly over the full speed range. Another benefit of this technique is that it can deliver fast acceleration and deceleration of the induction motor, giving more accurate control.

References

1. Hashemnia, N., & Asaei, B. (2008, September). Comparative study of using different electric motors in the electric vehicles. In 2008 *18th International Conference on Electrical Machines* (pp. 1-5). IEEE.
2. De Santiago, J., Bernhoff, H., Ekergård, B., Eriksson, S., Ferhatovic, S., Waters, R., & Leijon, M. (2011). Electrical motor drivelines in commercial all-electric vehicles: A review. *IEEE Transactions on vehicular technology*, *61*(2), 475-484.
3. Haq, H., Imran, M. H., Okumus, H. I., & Habibullah, M. (2015). Speed control of induction motor using FOC method. *Int. J. Eng. Res. Appl*, *5*, 154-158.
4. Yousef, A. Y., & Abdelmaksoud, S. M. (2015). Review on field oriented control of induction motor. *Int. J. Res. Emerg. Sci. Technol.(IJREST)*, *2*, 5-16.
5. BT, V. G. (2017). Comparison between direct and indirect field oriented control of induction motor. *Int. J. Eng. Trends Technol*, *43*(6), 364-369.
6. Li, W., Xu, Z., & Zhang, Y. (2019, May). Induction motor control system based on FOC algorithm. In *2019 IEEE 8th Joint International Information Technology and Artificial Intelligence Conference (ITAIC)* (pp. 1544-1548). IEEE.
7. Dhamo, L., & Spahiu, A. (2013). Simulation based analysis of two different control strategies for PMSM. International Journal of Engineering Trends and Technology, 4(4), 596-602.

Application of the ratio of satellite image channels for mineral mapping using the example of Kokpatas-Okjetpes from the direction of the trend (Bukantau Mountains)

Goipov Akrom[*1] , **Khaydarova Arofat** [2] , **Jurabekov Navruzbek** [2]

[1] Institute of Mineral Resources
[2] University of Geological Sciences navruzbek.jurabekov@bk.ru

Keywords
ASTER
Bukantau
Kokpatas-Okjetpes trend
Gold deposits
Mineralized zone

Abstract
Research using remote survey materials contributes to the improvement of existing and the creation of new research methods, the further study of the geological structure of large regions, and the identification of factors responsible for the localization of minerals. At the same time, the structural patterns of mineralization localization in individual areas are revealed, the connections of cosmo-geological objects with the distribution of minerals are studied. The object of research in this work is the perspective area of Derbez - the western flank of the Kokpatas deposit, Kokpatas-Okjetpes trend.

Introduction

The method of using the results of decoding satellite images and the images themselves is an integral part of geological research.

Cosmo-geological work on the object of research was carried out on the basis of digital space materials Landsat TM, Quick Bird, Aster, Radar using modern software products ENVI, ERDAS, ArcGIS. The use of mathematical and statistical apparatus embedded in software tools, in combination with the materials of geological, geophysical, geochemical, and other studies increases the objectivity of the results obtained.

Processing of digital materials of space surveys was carried out on the basis of methods of processing satellite images: CC (Color composition), PCA, Sobel, Kirsha, etc.

The results of processing by these methods made it possible to map all the structural units represented on the geological map on the studied area, as well as to record new and suspected discontinuous faults, fracture zones, ring structures, etc. Also, these methods made it possible to clarify the boundaries of structurally deciphered complexes.

Digital processing of satellite images of Landsat-7,8 ASTER and Quick Bird was carried out in 3 ways. MinComp, Kirsch, Sobel. As a result of the work, a variant of processed satellite images was prepared at a scale of 1:25000 per study area.

Determination of the main factors of localization of gold ore and other manifestations of minerals is a necessary condition for improving the efficiency of forecasting and prospecting.

To date, the identification of localization factors of gold deposits is based primarily on empirical data, on the search for patterns of deposit placement relative to the elements of the geological structure of the regions. Therefore, one of the main conditions for the successful identification of factors of localization of deposits is the study of the geological structure and history of geological development of territories with the determination of the place and time of formation of ore concentrations.

The range of varieties of geological and structural positions of mineralization is not so large: zones of crushing, fracturing, scarring zones, contacts of heterogeneous rocks, zones of hydrothermally altered rocks, and shale. As can be seen from this, the role of the fault recedes into the background, and the physical state of the fault zones, and contacts of dissimilar rocks come to the fore (Figure 1).

Among the geological and industrial types of deposits, the following are distinguished: gold-sulfide (Kokpatas), gold-quartz (Altyntau), gold-silver (Okjetpes), gold-sulfide-quartz (Bulutkan, Barkhannoe), tungsten scarn-skarnoid with superimposed gold (Southbay).
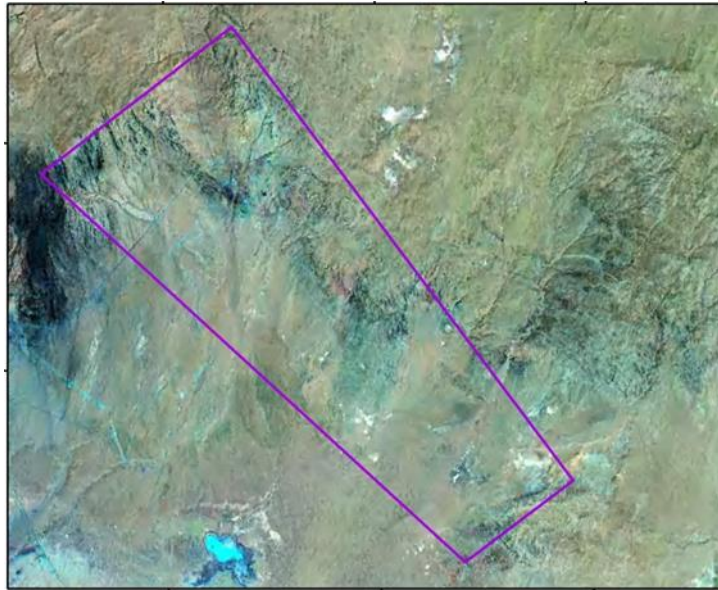

Figure1. Satellite image of the studied territory (Landsat-7)

Material and Method

When mineral deposits are formed and endogenous mineralization is placed in them, it occurs not only under the influence of certain geological factors, but also under the influence of physical fields of the areas of mineralization, under the influence of geodynamic conditions and tectonic deformation of rocks.

Geophysical methods in forecasting and prospecting for deposits solve problems, the results of which give indirect signs of the presence or absence of hidden mineralization. Despite this, the results of magnetometry and gravimetry were used in this taxonomy in order to identify promising areas on a regional scale during prospecting, which, according to their geophysical parameters, correspond to the geophysical data of the areas of known deposits and ore occurrences.

Search signs are understood as factors indicating the presence or possibility of finding a particular mineral deposit in a certain place [1-10].

One of the main structures of the south of Bukantau, the authors consider the zone of the Kokpatas fault (structural-formation subzone) with a width of about 10-13 km, including the Okjetpes, Kokpatas, and Boztau mountains. The Kokpatas subzone south of Bukantau is divided into two large blocks – western and eastern. According to modern concepts, the Kokpatas subzone is an Okjetpes–Kokpatas antiform, i.e., a folded structure of the first order. The division of Southern Bukantau into western and eastern blocks is not justified (Figure 2).
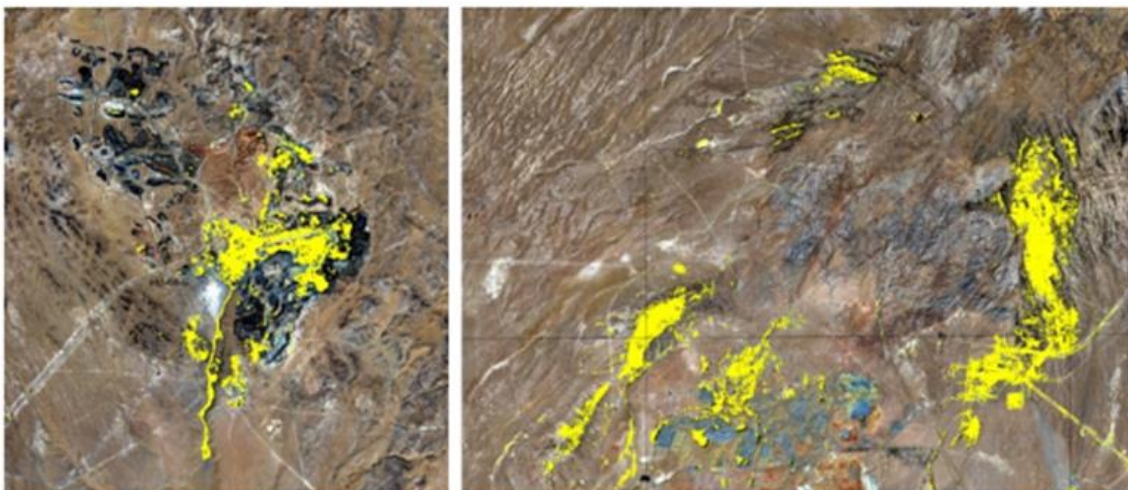

Figure 2. Manifestation of the iron index (yellow light). A – contour of the Kokpatas quarry; B – south-western flank of the Altyntau intrusive

Results

In 1993 and 1996. V.S. Korsakov, S.Ya. Lapidus conducted the GGK of the Altyntau mountains and the Kokpatas ore field. In 1999 M.U. Umarkhodzhaev, and G.A. Yusupov the assessment of the conditions for the placement of gold mineralization in the deposits of the Kokpatas formation (Central and Eastern Bukantau) has been completed. In 1964, the Bukantau party (N.I. Oransky, G.N. Korobeynikov) in the area of the Kokpatas ore field performed a ground-based magnetic survey at a scale of 1:25000 over a network of 250*50m, and in 1965, gravimetric survey at a scale of 1:50,000 was carried out by a gravimetric batch of DGFE (I.F Gaydamaka, Yu.S. Shmanenko) over a network of 1000 * 250m. This information report used these materials.

Based on the results of gravimetric work, maps of gravity anomalies in the Buge reduction at the density of the intermediate layer with σ p.s. 0.23 and 0.267 c/u, with corrections for relief and loss deposits on a geological basis, a map of local gravity anomalies was compiled.

Based on the obtained gravimagnetic data, a diagram of the elements of deep tectonics and magmatism of the Kokpatas ore region was drawn up, areas of development of hidden granitoid intrusions were identified, three systems of tectonic disturbances of deep laying-northwestern, northeastern and sub-latitudinal strike were identified, and areas of distribution of ultrabasic rocks-serpentinite rod-shaped bodies were identified.

Conclusion

The results of processing materials of remote sensing of the Earth using the ratio of channels of satellite images obtained from the ASTER satellite are presented. Mineral changes were mapped on the territory of the Bukantau-Kokpatas-Okjetpes trend: indices of iron, kaolinite, and quartz. The interrelation of mineral metasomatic changes with zones of ore mineralization, ore occurrences, and deposits, as well as with fault zones that control metasomatic mineral changes has been established. Structural, magmatic, and lithological factors of mineralization are substantiated.

References

1. Golovanov, I. M., Gidroingeo, T. (2001). Ore deposits of Uzbekistan, 660 p.
2. Mirkamalov, R. H., & Golovanov, I. M. (2010). Atlas of models of ore deposits of Uzbekistan, 100 p.
3. Crosta, A. P., De Souza Filho, C. R., Azevedo, F., & Brodie, C. (2003). Targeting key alteration minerals in epithermal deposits in Patagonia, Argentina, using ASTER imagery and principal component analysis. *International journal of Remote sensing*, *24*(21), 4233-4240.
4. Pour, A. B., & Hashim, M. (2012). The application of ASTER remote sensing data to porphyry copper and epithermal gold deposits. *Ore geology reviews*, *44*, 1-9.
5. Zhang, X., Pazner, M., & Duke, N. (2007). Lithologic and mineral information extraction for gold exploration using ASTER data in the south Chocolate Mountains (California). *ISPRS Journal of Photogrammetry and Remote Sensing*, *62*(4), 271-282.
6. Rowan, L. C., Hook, S. J., Abrams, M. J., & Mars, J. C. (2003). Mapping hydrothermally altered rocks at Cuprite, Nevada, using the Advanced Spaceborne Thermal Emission and Reflection Radiometer (ASTER), a new satellite-imaging system. *Economic Geology*, *98*(5), 1019-1027.
7. Yamaguchi, Y., & Naito, C. (2003). Spectral indices for lithologic discrimination and mapping by using the ASTER SWIR bands. *International Journal of Remote Sensing*, *24*(22), 4311-4323.
8. Mars, J. C., & Rowan, L. C. (2006). Regional mapping of phyllic-and argillic-altered rocks in the Zagros magmatic arc, Iran, using Advanced Spaceborne Thermal Emission and Reflection Radiometer (ASTER) data and logical operator algorithms. *Geosphere*, *2*(3), 161-186.
9. Tangirov, A. I., Urunov, B. N., & Karshiev, A. B. (2015). Types of deposits and features of the manifestation of gold mineralization in the mountains of Bukantau. Gorny Vestnik of Uzbekistan, 1, 52-59.
10. Oransky, N. I. (1984). The position of the Boztau-Okzhetpes graben in the regional structures of the Kyzylkum. Uzbek geol. Journal, 4, 73-75.

Advanced Engineering Days

aed.mersin.edu.tr

Remote piloting UAS in extreme environments with challanging climatic conditions - An overview of modern UAS capabilities in the field of volcanology, geosciences, atmospheric chemistry and interplanetary exploration

Ian Godfrey[*1] , **José Pablo Sibaja Brenes** [1] , **Emanuel Montealegre Viales** [1]

1Atmospheric Chemistry Laboratory, Universidad Nacional, Costa Rica Igodfrey@mail.usf.edu, jose.sibaja.brenes@una.cr, emanuel.montealegre.viales@est.una.ac.cr

Keywords
Drone
Volcanic Climate
Atmosphere
Turbulence
Geology

Abstract
Unmanned Aerial Systems have recently had advanced payloads configured by engineers for various atmospheric sampling experiments and have been proven a successful and innovative technology. Climatic stability in volcanic regions can change in less than one minute. And with that comes relative humidity fluctuations, 80% change in visibility conditions, wind speed change, wind direction change, enhancing wind gusts. It's the data collection on how UAS operate in these conditions that will eventually assist the development of UAS with the ability to conduct complex photogrammetry and atmospheric sampling flight missions of the Moon and Mars. For this reason, we created a short article on our findings on using UAS in some of the most extreme and complicated atmospheric environments.

Introduction

Monitoring volcanic degassing is an essential aspect of a complete surveillance program for volcano observatories. Advancements in UAS have assisted in the ability to take better gas readings via UAS which has significantly reduced risk for scientists' studding the volcanoes. The team of remote pilots with the Atmospheric Chemistry Laboratory of Universidad Nacional LAQAT-UNA has successfully operated drones in the Irazú, Poás Turrialba and Arenal active craters in Costa Rica. The foundation of UAS in volcanic degassing began with a drone survey of a volcano was conducted in 2016 and 2017; Researchers from Universidad Nacional collaborated on an international undertaking where advanced remote pilots flew drones at both the Turrialba Volcano in Costa Rica and the Masaya Volcano in Nicaragua. The flight mission objectives were to measure the degassing deriving from the active craters. At the time these two volcanoes were the largest time integrated source of CO_2 in all of Central America. During the 2016-2017 period when the research project was conducted both volcanic systems were actively degassing and showing increased signs of a potential eruption. Researchers and remote pilots managing this project noted that; Remote pilots operating in high altitude volcanic environments especially active systems had to be particularly concerned with the hardware because the devices are often subject to harsh field conditions [1].

Methods

Operating UAS in volcanic environments are much more complicated than altitudes of 0'4000 feet Above Ground Level (AGL). In UAS research conducted at the summit of the Irazú Volcano National Park in Costa Rica

researchers started outlining what the exact challenges were for using UAS in high altitude tropical, volcanic environments. The Risk/Reward ratio for flying a drone was very significant. The ratio consists of weighing the value of the drone itself (not including the Remote Control batteries in the case) against the value of the data which can be obtained during that particular flight. It was concluded that remote pilots flying drones in volcanic regions should carry extra Micro SD cards in their drone case because valuable data may be obtained and the pilot may want to continue with more flight missions. By changing the Micro SD card, the data from the previous flight is guaranteed to be returning to the lab for processing. Sometimes valuable photos used to generate 3-D Digital Surface Model have been collected and the remaining flight missions are non-essential, in these situations it's important that the remote pilot remember to switch the Micro SD cards in-between flights.

Figure 1 – Main Active Crater of the Irazú Volcano National Park Costa Rica via UAS January 2020

When flying in volcanic craters there is not just the altitude in meters Above Ground Level or AGL like in the Part 107 remote pilot listening test. When piloting remote aircraft in volcanic terrain one must also consider the atmosphere below, just as importantly if not more significant is the reduction in altitude (Below Ground Level) BGL. A critical point of preflight planning as flying into an active crater is not already complicated enough but one must consider the Return to Home RTH flight will most likely require more battery energy than the flight path used to enter the volcanic crater because the drone needs to lift itself higher to get out of the crater. The same concept applies when launching from a volcanic summit and surveying the flanks or slopes of a volcano; the drone flight altitude will be lower than the altitude of the home point. In these high altitude volcanoes in Costa Rica random periodic rain showers pass by sometimes quite quickly perhaps 10 minutes from start to finish for example. Remote pilots will need to wait for their next window of opportunity and then weight the flight risk/reward ratio. These frequent rain showers can last from 10 minutes to over a full day.

Degassing fumaroles, steep slopes, and unconventional hidden factors all play a role in the environment a volcanic remote pilot must operate in. There can be visibility complication due to water vapor and volcanic degassing. Visibility issues can impact the drone itself and the display on the RC, and they can directly impact the remote pilot at the home point. For example, if a cloud passes and visibility is reduced by 70% at the home point than observing the drone via line of sight will be severely impacted. Tropical sunlight reflecting off the RC screen can all be challenging in volcanic environments so hat and sunglasses are quite essential. Usually there are people visiting or others studying these volcanoes and therefore it's highly recommended never to fly directly over any people, vehicle's or valuable infrastructure such as National Park housing or equipment and especially telecommunications towers. Telecommunications towers are frequently located at volcanic peaks due to their strategically high location being ideal for broadcasting networks. These broadcast towers also contribute to interference between the drone and the RC. Flying with an insurance policy is always important for risk reduction.

Figure 2 – Main Active Crater of the Irazú Volcano National Park Costa Rica via UAS 2022

Figure 3 – Main Active Crater of the Irazú Volcano National Park Costa Rica vie UAS January 2020

In the above image LAQAT-UNA researchers were trying to find a waterfall that drains to the main crater. At the end, we found the path of the water, but there wasn't water. That is the place where the water could fall. We used the drone to see the terrain and if there were problems with the way to go down to the crater. The conditions were good on this day, not much wind and good visibility. The drone was flying from the SW side of the crater and flew down the main lookout site of the park. They wanted to know if there were more places where the water could drain to the crater and used a UAS to make these observations at the Irazú Volcano National Park. One of the most complex remote flight climate conditions on Earth. The altitude above 10,000 feet has a different atmospheric make up with less 0_2 the air is thinner and operation of a remote aircraft becomes more complicated. Certain UAS have altitude ceilings which have significant improved over the past several years. Due to a reduction in air density in high altitudes flying a drone above 3,000 meters is significantly more complicated. How the drone hovers and uses batters is different, flight inclination is different and therefore the remote pilot must operate the UAS differently as well. Temperature in these volcanic regions are significantly reduced relative to the tropical lowlands of Costa Rica, and therefore remote pilots must also consider the temperature of the air during the drone flight and how that will affect the equipment.

Results

Between the lower air density due to altitude and reduced temperatures actual flight time will be reduced and this must be taken into consideration. Research with UAS pilots has shown pilots can expect a 10% reduction in battery preference every 2,000 meters. Remote flight operations will become extremely complicated at 4,000 meters and above, most drones will require proper modifications and specialized parts for these altitudes. There is greater wind turbulence inside craters, next to cliff faces and in valley's. If there is a Thunderstorm it's an almost certainly to cancel the flight mission and postpone for a better day. If there are lightning strikes it's an outright stand down. Lighting will destroy the connection capabilities of the RC and drone and will cause a complete disconnect [2]. The most unpredictable and hazardous feature of a volcano is the lava dome. Degassing fumaroles, updrafts, ambient temperature change and potential eruption with explosive molten material and volcanic bombs all add to the complexity of the atmospheric environment in which the remote pilot must operate the UAS [3]. During the course of an eruption volcanoes change levels of degassing and the species of emissions fluctuate. There may be various amounts of lava extruding from the volcano and during the eruption period the level of activity varies. This fluctuation results in ever changing geo morphology which can be mapped and tracked by UAS photogrammetry flight missions. UAS can also take measurements of volcanic plumes and industrial pollutants. One of the best volcanic plume samples taken by drone was published by Earth, Planets and Space scientific journal which focused on the Mt. Ontake eruption in Japan 2014 [4].

Engineers with many research institutions, universities and private companies are designing strategies for UAS to assist with future challenges [5]. The Indian Institute of Technology in Roorkee conducted the UASG2021 conference specifically outlining how drones can be used to assist the United Nations with they're Sustainable Development Goals [6]. UAS have gained particular attention in the fields of geochemistry, atmospheric chemistry and interplanetary exploration. In 2018-2019 Chilean researchers used UAS to monitor carbon degassing at the Volcán Villarrica in Chile. Volcanic degassing is an essential aspect to monitor because it offers insight into the magmatic and hydrothermal systems below the degassing crater or fumarole. The article outlined plume transport & dispersion which was successfully documented by UAS in a very intense and extreme atmospheric environment. The authors published their work in Advancing Earth and Space Science 2019 [7]. The American Association for the Advancements of Science has particular interest in advanced engineering of micro sensor technology to optimize GIS applications via UAS, but also for interplanetary scientific mapping missions of the surface of the Moon and Mars. This team emphasized the importance of using UAS to monitor volcanic degassing to better understand Earth's Carbon Cycle. By deploying UAS with multi-GAS sensing technology, thermal IR sensors and other specially configured hardware, we can collectively advance mankind's ability to measure Global Volatile Fluxes from transport emissions, industrial manufacturing associated with economical productivity and degassing volcanoes around the world [8].

Conclusion

Volcanic environments are one of the most extreme climates on Earth, especially inside of active degassing craters. Today drones have become an important tool in different types of scientific and engineering jobs. The reason of it, is because they can facilitate the work, besides they can prevent injuries form repetitive and heavy works and can help us understand, explore, and study different subjects such as atmospheric science, or planetary exploration. Despite the different applications that drones have, there will be great focus on biological, physical, and chemical sampling in different fields such as enviromental science and interplanetary exploration.

Researchers with LAQAT-UNA retrieved water samples from the hyperacidic extremely hot crater lake named Laguna Caliente of the Poás Volcano National Park. José Pablo Sibaja Brenes of Universidad Nacional Costa Rica has been using an advances fleet of UAS for volcanic sampling of both water from the hyperacidic

crater lake and they have completed air quality measurements around the degassing fumaroles with drones using electrochemical gas sensors as UAS payloads specially configured for volcanic emissions. The most difficult flight was in Poás volcano, 2022. When José Pablo was trying to collect the water from the hyperacid lake, there was a lot of evaporation.Visability droped to zero and he couldn't see anything. He continued descending the drone about 3 meters of the water, because there was a problem with the rope, the bottle and the batteries. At the end, the he had to return the drone to the look out launch site of the volcano and check the rope and change the batteries. After a few adjustments he did the measurement with the new batteries and successfully droped the bottle on the rope 30 meters down for a sampling the hyperacidic water.

Figure 4 – Laguna Caliente Active Crater of the Poás Volcano National Park via UAS February 2022

Figure 5 & 6 – Laguna Caliente Active Crater of the Poás Volcano National Park via UAS February 2022

Other applications of drones can be visualized in geoscience, especially in surface mapping. Applications of Unmanned Aerial Vehcles in Geosceince suggest that UAVs are commonly used by geoscientist for making maps of Earth's surface by photogrammetric methods. Beside of it, he also suggests that drones help geoscientist in underground survey and underwater survey by using an UAV-borne ground penetrating radar and an UAV's equipped with the light detection and ranging sensor specifically. He also implies that miniaturization of geophysical instrument has opened new opportunities in this kind of analysis. This can be verified by the efforts of NASA scientist. The reason of it, is because in 2020 mission they land a rover and a miniaturized helicopter, Perseverance and Ingenuity specifically [9].

In the case of Ingenuity, NASA planned to demonstrate the first controlled flight in another world were the physical conditions are different from Earth, and after three successful flights, he proved its technology demonstration. After that Ingenuity completed 41 flights, with a flight time of ~67.7 minutes and a distance flown of 8.191 meters. For the case of Perseverance rover, NASA planned to explore and study past life sings in

the Jezero crater by identifying and collecting compelling rock core and soil samples. For these, NASA engineers and scientist attach to the rover different types of instruments to the rover such as the Mastcam-Z for imaging, the mMars Environmental Dynamics Analyzer (MEDA) for temperature, wind speed & direction, pressure, relative humidity and dust sampling for analysis of size a shape of the particulate matter PM (10).

The rover was also carrying equipment for the Mars Oxygen ISRU Experiment (MOXIE) designed for producing oxygen from atmospheric carbon dioxide, Planetaru Instrument for X-ray Lithochemistry (PIXL) for elemental composition of Martian surface by an X-ray fluorescence spectrometer, Radar Imager for Mars' Subsrface Experiment (RIMFAX) for centimeter-scale resolution of geological structure, Scanning Habitable Environments with Raman & Luminescence for Organics and Chemicals (SHERLOC). The rover had equipment specially engineered for experiments in Mars mineralogy and detection of organic compounds by UV Raman spectrometer. Therefore, it can be concluded that drones are an helpful tool in our daily basis and can help us reach fields that the human being can explore in this moment such as upper atmosphere or interplanetary research [9].

References

1. Stix, J., de Moor, J. M., Rüdiger, J., Alan, A., Corrales, E., D'Arcy, F., ... & Liotta, M. (2018). Using drones and miniaturized instrumentation to study degassing at Turrialba and Masaya volcanoes, Central America. *Journal of Geophysical Research: Solid Earth*, *123*(8), 6501-6520.
2. Godfrey, I., Brenes, J. P. S., Cruz, M. M., & Meghraoui, K. (2022). Evolution of the Main Crater, Irazú Volcano National Park, Costa Rica–Consumer Drones in professional research. *Advanced UAV*, *2*(2), 65-85.
3. Zorn, E. U., Walter, T. R., Johnson, J. B., & Mania, R. (2020). UAS-based tracking of the Santiaguito Lava Dome, Guatemala. *Scientific Reports*, *10*(1), 1-13.
4. Mori, T., Hashimoto, T., Terada, A., Yoshimoto, M., Kazahaya, R., Shinohara, H., & Tanaka, R. (2016). Volcanic plume measurements using a UAV for the 2014 Mt. Ontake eruption. *Earth, Planets and Space*, *68*, 1-18.
5. James, M. R., Carr, B., D'Arcy, F., Diefenbach, A., Dietterich, H., Fornaciai, A., ... & Zorn, E. (2020). Volcanological applications of unoccupied aircraft systems (UAS): Developments, strategies, and future challenges. *Volcanica*, *3*(1), 67-114.
6. Liu, E. J., Wood, K., Mason, E., Edmonds, M., Aiuppa, A., Giudice, G., ... & Bucarey, C. (2019). Dynamics of outgassing and plume transport revealed by proximal unmanned aerial system (UAS) measurements at Volcán Villarrica, Chile. *Geochemistry, Geophysics, Geosystems*, *20*(2), 730-750.
87 Liu, E. J., Aiuppa, A., Alan, A., Arellano, S., Bitetto, M., Bobrowski, N., ... & Wood, K. (2020). Aerial strategies advance volcanic gas measurements at inaccessible, strongly degassing volcanoes. *Science Advances*, *6*(44), eabb9103.
8. Niedzielski, T. (2018). Applications of unmanned aerial vehicles in geosciences: introduction. *Pure and Applied Geophysics*, *175*, 3141-3144.
9. Snyder, C. W. (1997). National Aeronautics and Space Administration (NASA) NASA.

Research of ore-controlling factors and significant sign of mineralization of Kokpatas and Cenral Bukantau Regions (Uzbekistan)

Goipov Akrom *1 , **Jurabekov Navruzbek** 2 , **Khaydarova Arofat** 2

1 Institute of Mineral Resources
2 University of Geological Sciences navruzbek.jurabekov@bk.ru

Keywords
Ore-control
Mineral
Complex
Manifestation
Formation
Magmatism

Abstract
The mineral components method is based on a color composition of 3 indices: the clay rocks index, the iron-containing minerals index, and the iron oxide index. In the resulting image, the red color corresponds to clay rocks, the green color corresponds to iron–containing minerals, and the blue color corresponds to rocks with iron oxide. Each image processing software includes numerous processing methods, some of which are used by geologists in their research. The main methods of image processing for obtaining geological information include PCA, ITS, CC color composition in standard and natural colors, some filtration methods, and others. The geological informativeness of the results obtained by these methods is noted in the works of domestic and foreign researchers.

Introduction

In addition to the above-mentioned image processing methods, there are methods based on linear combinations of channels of a single image. The results obtained by these methods are called indexes or new channels. Indexes are the result of the mathematical combination of digital values of different source channels of the same image.

All indexes are based on absorbing and reflecting properties. They are related to the chemical composition of the studied surface. From a geological point of view, these indices determine the difference between different types of rocks (Figure 1).
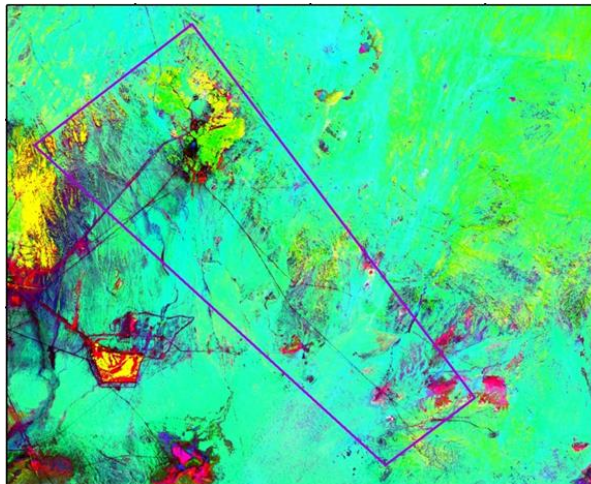

Figure 1. The result of processing by the mineral composition method

Material and Method

Determination of the main factors of localization of gold ore and other manifestations of minerals is a necessary condition for improving the efficiency of forecasting and prospecting.

The gold deposits and manifestations of Bukantau belong to four formations: gold-sulfide veined-interspersed ores, gold-sulfide-quartz, gold-silver, and gold-scarn. The deposits of the gold (sulfide)-quartz formation can be divided into two sub-formations: a) low-sulfide vein-veined zones and stockwork and b) low-sulfide veins, linear vein zones, and breccias.

It should be noted that the isolated gold ore formations cannot be considered as genetically separate groups, since they do not differ either in the source of the metal, in connection with magmatism, or in the time of formation, i.e., different stages. Their formational appearance is determined by the degree of development of certain mineral associations and depends, first of all, on the nature of the host environment and spatial relationships with the massifs of granitoid rocks, as well as the composition of the latter.

The established main factors of localization of ore fields are common to the entire folded system.

Along with this, the roles of some of them may be different in each tectonic segment. As well as for each formation type of gold deposit, the selected factors have a slightly different meaning.

The main factors of mineralization are Structural; igneous; lithological.

In the Pre-Mesozoic basement between the Kokpatas and Okjetpes mountains, deposits of the Kokpatas and Tubabergen formations, Devonian-carboniferous carbonate formations, granitoid massifs, ore-bearing faults have been identified. Promising sites have been identified for setting up deep searches for gold, silver, and tungsten. The gold content in core samples reaches 0.15-0.3 c/u, however, in most samples, it does not exceed tenths of c/u.

The results of the interpretation of gravimetric data used made it possible to clarify the structure of the Bokalin intrusive massif, to draw up a diagram of discontinuous tectonics and a diagram of the block structure of the central part of the Bukantau mountains. Four systems of hidden deep foundation faults were identified - latitudinal, meridional, north-eastern, and north-western. In the complex analysis of geological and geophysical materials, six blocks have been identified, each of which is characterized by its magmatic, tectonic, lithological, and geochemical factors. To study the deep tectonic structure and magmatism, the information in (Figure 2) was attracted.
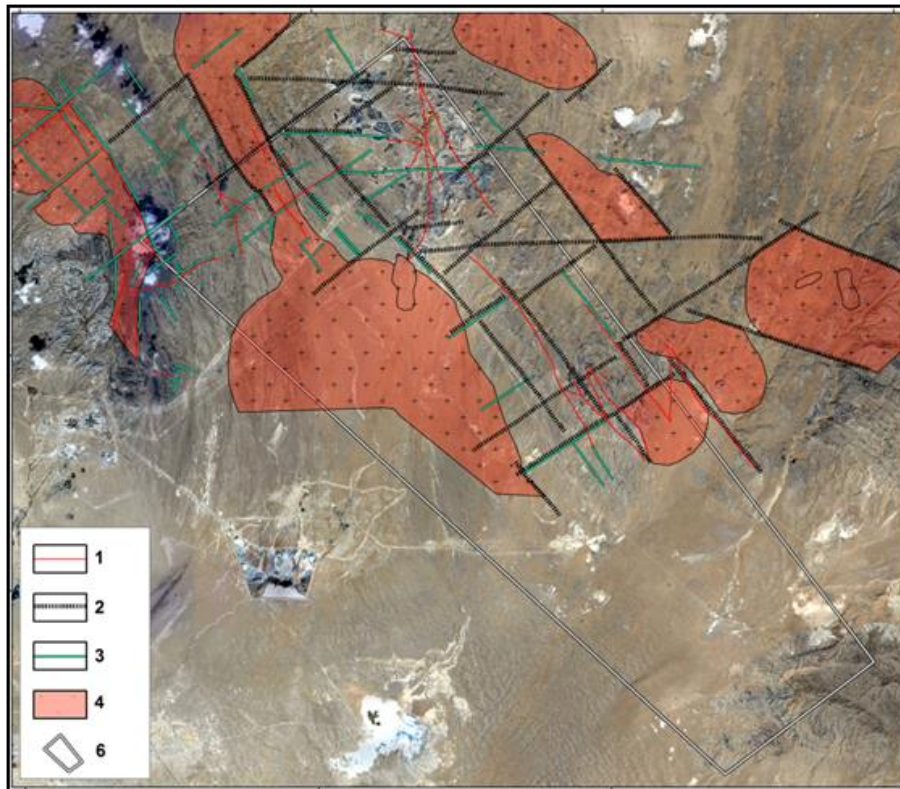

Figure 2. Deep tectonics and magmatism of the Kokpatas ore region according to gravity and magnetic exploration data

Results

Compiled using materials by [1] Symbols: 1-tectonic disturbance according to geological data; 2-Tectonic disturbance established according to gravity survey data; 3-tectonic disturbance established according to magnetic survey data; 4-counter area of work of the Kokpatas-Okjetpes trend.

The above-mentioned intrusive boundaries must be taken into account when conducting prospecting operations, in which the main factor of mineralization is the magmatic factor.

The structure of the surface of the Karashakho formation has been studied and a structural map has been constructed along the sole of volcanogenic formations. On the map of the isodynamic of the field, the zonal magnetic maxima of the field, mainly of the submeridional and north-western strike, are confined to the development of hyperbaric bodies within their limits. On Derbez-Boztau Square, a map of the anomalies of the Bug Δg has been compiled, on which the northeastern end of the Kokpatas granitoid is characterized by an intense gravitational minimum in the southwestern part of Derbez Square. The spatial relationship of gold mineralization with elements of geophysical fields is determined. Areas of local negative anomalies have been identified that have a close connection with all known gold ore objects. The regions of the local positive components of the field Δg are associated with a local increase in the power of the productive thickness. The regions of local negative anomalies of the gravity field associated with tectonically weakened zones of increased fracturing, to which all known objects of gold mineralization gravitate, are determined. Numerous magnetic anomalies have been identified mapping the area of contact-metasomatic transformations of the Kokpatas intrusive and the ultrabasic body, including the Karashakho anomaly. The work carried out made it possible to predict endogenous gold mineralization using the pattern recognition technique, to identify a number of promising sites for setting up prospecting for gold, as well as for the search for tungsten mineralization of the scarn type and sites promising for the localization of nickel associated with ultrabasic.

Kokpatas monzodiorite-granodiorite complex C₃k

It was isolated by [1]. It is represented by the reference array of the same name, located in Southern Bukantau. It breaks through the deposits of the Kokpatas formation, cornified in a narrow (up to 100 m) exocontact zone of the intrusive. It is discordant in relation to the host rocks.

The Kokpatas massif is exposed on the surface by only 3 sq.km, but its total area, almost completely covered by the Mesocainozoic cover, is about 350 sq.km.

The structure of the bulk of dike rocks varies from microgranite to felsic, often complicated by blastomylonite; the composition is close to the rocks of the main phases. The accessories of the complex are apatite, sphene, orthite, monazite, and zircon. An unstable type of alkalinity, moderate total ferruginousness is characteristic.

In high–carbon content – rubidium, strontium, chromium, thorium in moderate – fluorine, zirconium, in low - barium.

Central Bukantau diorite-lamprophyre dike complex (Ps)

The complex includes dikes of medium composition, common only in the area of the South-Bukantau zone, which arose at the final stage of Permian intrusive magmatism. These dykes belong to the Kokpatas intrusive complex of the middle carboniferous [2-4].

The study of the Kokpatas ore field revealed a wide distribution of dikes of diorites and lamprophyres here. The areas of their maximum accumulation are located outside the Kokpatassky intrusive. In the intrusive body itself, such dikes are rare, while in other intrusive arrays, which are accompanied by their own dike series, the greatest condensation of dikes is observed precisely within the arrays themselves.

The dikes of the complex form the Kokpatas dike belt, elongated in the sub-latitudinal direction by almost 60 km with an average width of 10-15 km). The area of th [1] Kokpatas ore field is characterized by the greatest saturation of dikes. The size of individual dikes is 0.4-5m power, the length is from several tens to the first hundreds of meters.

Spatially and in time, gold mineralization is close to the formation of the described dyke complex.

Conclusion

In this study, the object of research is the perspective area of Derbez - the western flank of the Kokpatas deposit, Kokpatas-Okjetpes trend.

Studies were carried out using remote survey materials that contribute to the improvement of existing and the creation of new research methods, the study of the geological structure of large regions, to the identification of factors responsible for the localization of minerals. At the same time, structural patterns of mineralization localization in individual areas were revealed, and the connections of cosmo-geological objects with the distribution of minerals were studied.

References

1. Akhmedov, N. A., Paramonov, Yu. I. (2008). Kyzylkum gold ore province of the Southern Tien Shan and potential opportunities for expanding the mineral resource base of Uzbekistan. Mining Bulletin of Uzbekistan – Navoi, 2(33), 9-16.
2. Goipov, A. B., Turapov, M. K., Akhmedov Sh. I. (2020). Application of the ratio of channels of satellite images for mapping minerals on the example of Kokpatas-Okjetpes from the direction of the Trend (Bukantau Mountains). Gorny Vestnik of Uzbekistan. – Navoi, 3(82), 35-37.
3. Korobeynikov, A. F. (2012). Forecasting and prospecting for mineral deposits textbook for universities; Tomsk Polytechnic University. -2nd ed., corrected and supplemented Tomsk: Tomsk Polytechnic University Publishing House, 255s.
4. Pirnazarov, M. M. (2017). Gold of Uzbekistan: Ore-formation types, predictive-prospecting models and complexes. Tashkent SI "IMR",248
5. Gidroingeo, (2001). Ore deposits of Uzbekistan. Tashkent, 661 p.

Prospects of the mafic-ultramafic belt of the Nuratau Mountains for platinoids (Uzbekistan)

Jurabekov Navruzbek [*1] , **Khaydarova Arofat** [1] , **Kholikov Azimjon** [2]

[1] University of Geological Sciences navruzbek.jurabekov@bk.ru
[2] Institute of Mineral Resources

Keywords

Northern Nuratau
Platinoids
Mafia-ultramafic
Belt
Gabbroids

Abstract

Mafic-ultramafic belts, tracing zones of deep faults, and suture zones have been discovered in Uzbekistan. Within their limits, in the mountains of Sultanuvais, Bukantau, Tamdytau, Nurata, and Chakylkalyan, studies have been conducted for the detection of platinum group metals (PGM). The article discusses the prospects of the mafic-ultramafic belt (intrusive massif) of the Nuratau mountains for platinoids. It is located on Yuzhno-Gissarsky and Kuldzhuktau-Zirabulak-Karatyubinsky and includes intrusions of the Kyzylturuk ore poly, etc. The host rocks are represented by metamorphosed Devonian formations (siliceous shales, siltstones, sandstones). The Zarafshan-Turkestan mafic-ultramafic belt (MUB) is a core belt in the Southern Tien Shan, which is traced intermittently for a distance of about 1000 km. From the north, it borders the Turkestan-Alai MUB, in the South Kuldzhuktau-Zirabulak-Karatyubinsky MUB (along the South Auminzatau and Zarafshan deep fault). The belt covers the Malguzar Mountains, the western end of the Turkestan ridge, most of the North Nuratinsky ridge, the South Nuratinsky Ridge, and the Kyzylkum hills: Sangruntau (southern part), Aristantau, Tamdytau (northern half), Auminzatau and Beltau. In the eastern direction, it can be traced to Tajikistan and Kyrgyzstan, in the western direction it stretches up to the Ural-Tien Shan transverse fault. After which it is planned to move to the Mugodzhar and Ural-Tobolsk zones, which form a single Mugodzhar-Alai zone of the Ural-Tien Shan belt.

Introduction

Zarafshan-Turkestan is essentially "gabbroid", it is also characterized by the widespread development of Precambrian and Early Paleozoic formations, enclosing manifestations of the main magma in the form of effusions and hypabyssal intrusions, which are part of the Malguzar gabbro-diorite-diabase complex. It is composed of diabase, gabbro-diabase, micro gabbro, gabbro-diorites, and their corresponding porphyrites, diorite lamprophyres (causalities), diorites, diorite porphyrites (including quartz) and granitoid [1-7].

Gabbro-diorites and diabases are found in Western Sultan-Uwais (Zengebobo, Sheikhjeyli squares), Auminzatau (Zahkuduk, Dzhetymtau exits), Northern Nuratau (Baipurushli, Yukari-Sarai sections, etc.). But they are especially widely developed in the Malguzar Mountains, Karakchatau, Northern Nuratau, on the northern slopes of Southern Nuratau, the elevations of Auminzatau, Gobduntau, Marjanbulak and the northern slopes of the Turkestan ridge, where they form two bands of the sub-latitudinal strike. The North-Malguzar strip, which can be traced for 180 km, stands out most clearly. With a width of 10-12 km in inflation.

The complex is developed on the northern slopes of Northern Nuratau, where serpentinite melange forms at the base of the Majerum tectonic cover in the Ukhum-September and Yatak-Arvatyn synforms, clearly distinguished by a high positive magnetic field. As a rule, the rocks of the complex are tectonically "underlain" by the Asmansai volcano plutonic Association and are overlain by pyrazine shales of the Majerum formation, being rockless formations.

The complex is represented by serpentinites, gabbro, pyroxenites, plagiogranites and related metasomatic formations: rodingites and albitites. Serpentinites of the area are apoperidotite (apogartsburgite) by the nature of the initial rocks, apodunite is less common. By the nature of the minerals, serpentinites are represented by chrysotile-antigorite (± lizardite), antigorite-chrysotile, and chrysotile, and less often lizardite differences. Serpentinites have the following composition: serpentine - up to 92% (antigorite up to 21%, chrysotile up to 48%, bastite up to 22%) magnetite - 1.5%, chrome spinelides - 0.5-1%, carbonates up to 2.2%.

The rocks of the complex are associated with manifestations of chromium, nickel (often with increased platinum contents), and asbestos, but due to their small size and low contents, they are not of practical importance.

Granitoids of the complex are widely distributed in Northern and Southern Nuratau. They composed most of the Temirkabuk intrusive (170 sq.km.), Ustuksky (120 sq.km.), September (25 sq.km.), Akchobsky (23 sq.km.), Koytashsky (47 sq.km.), Aktau (190 sq. km.), Yangaklyk (20 sq.km.), Halbashinsky and Sartakchinsky intrusive arrays and most of the intrusive arrays are not exposed by erosion but fixed by gravitational minima.

In the southeast, the Ukhum-September synform is cut off by the Majerum surge and completely wedged at the kish. Balaban. Along this fault, the rocks of the upper plate of the Majerum formation are brought into contact with the sand-shale Kansai formation of the upper Riphean.

In the northern wing, the plate deposits connect with the main field of sand-shale deposits developed in the foothills of the North Nuratinsky ridge and lie in the cores of antiform folds.

Shales serve as cement for the "pellets" of sandstones of rounded, sometimes fusiform shape, ranging in size from 5-10 to 30-40cm (commensurate with the thickness of the layers), lenticular bodies (sometimes clear blocks) of limestones, dolomites, siliceous rocks, albitophyres ranging in size from the first tens of cm to 3-5m. Sometimes these rocks compose rather long (up to 600m) formation-like bodies with a capacity of up to 60m.
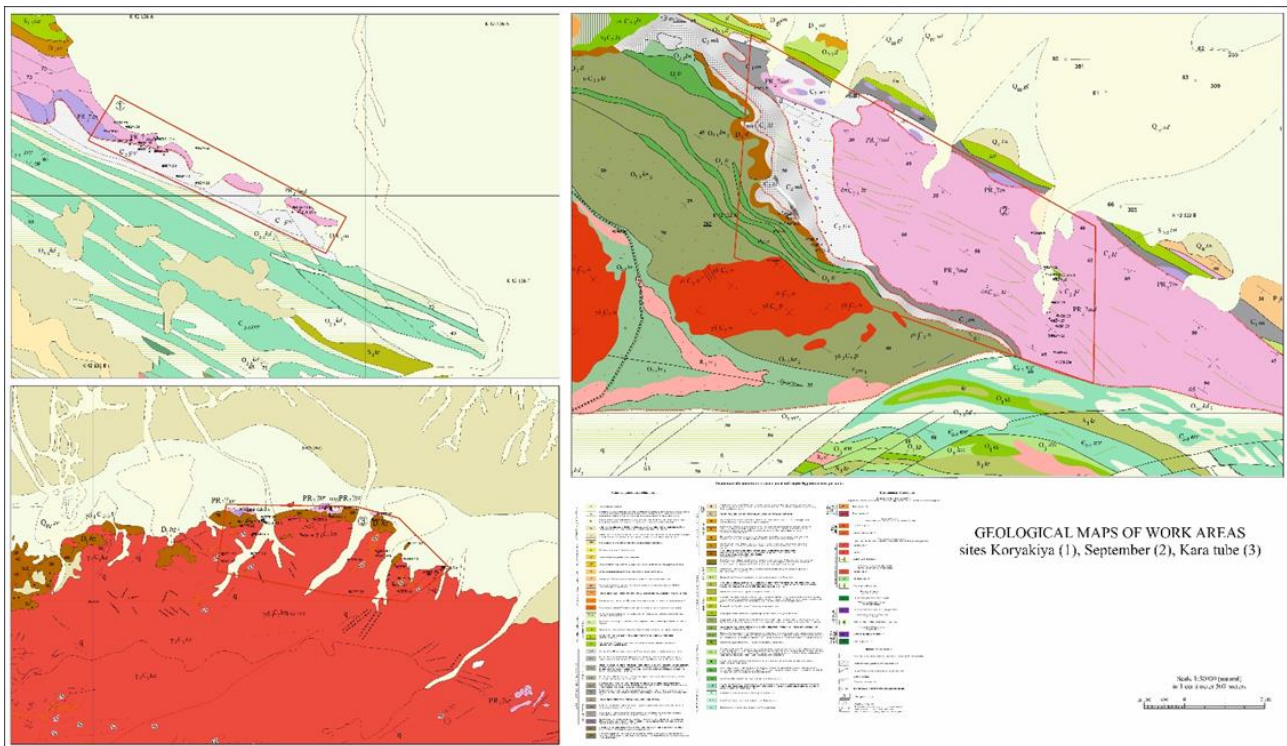

Figure 1. Geological map of the study area

Material and Method

The research methodology is based on the results of collection, examination and analysis of previously performed correction work.

After the analysis to clarify promising positions, field-verification work was carried out.

The actual fieldwork consisted of the following:

- cosmophotogeological works (field interpretation);
- geological linking routes;
- examination of ore occurrences and anomalies;
- points of detailed geological observations;
- structural and lithological sections;
- mineralogical sections;
- thematic specialized works

- construction of geological sections, analysis of ore-controlling factors with an assessment of their information weights (additional study of geological factors, assessment of information weights of factors, signs), comparative analysis with reference units, allocation of forecast positions (assessment of the prospects of favorable geochemical and geological-structural positions, allocation of forecast-promising cosmo structural, geochemical and geological-structural positions).

Results

A promising section of the Nuratau mountains, statistical calculations by spectral analysis-(spillage). Reduced average content for many elements, including traditional satellites of gold - As, Ag (18 and 0.6 cu/e, respectively). And also, the low maximum value–As-200 cu/e (0.02%), raises the question of the possibility of its use as an indicator of gold mineralization. Accordingly, concentrations of most chemical elements were obtained for the Nuratau mountains (concentrations Sb-81.3; Au-42.2; Ta-22.2; W-22; Sn-10; Ag-8.8; As-7.2; Cr-6.8; Pb-4.4; Ni-4.1; Bi-3.8; Cd–3.1; Zn-2; Co-1,9; V-1,9; Mn-1,4; Mo–1,3; Ga-1,2; Ge-1,1). Normalized according to A.P. Vinogradov.

To compare the concentrations on the site of the Nuratau mountains, the concentrations for the regional background were taken with the concentrate according to A.P. Vinogradov (granite-metamorphic shell), y/E. Accordingly, concentrations of most chemical elements were obtained according to the regional background, (concentrations of Ag-79,1; W – 24,6; Nb-17,6; Ge -14,1; As–10,2; Mn – 9,2; Mo-8,4; Cu -5,8; Co– 5,2; V–3,4; Ti-3,3; Li-3,1; Pb-3.

To compare the concentrations for the Nuratau mountains section, the concentrations for the regional background with the concentrate according to A.P. Vinogradov (granite-metamorphic shell), y/e were taken. Accordingly, concentrations of most chemical elements were obtained by regional background, (concentrations of Ru-62,3; Pt-33; Pd-23,3; Os-5,7; W-3,2; Te-1,9; Ir-1,9; Sb-1,9; As-1,7; Rh-1,4; Se-1,3; Cr-1,3; Ag-1,2; Au-1,2; Re-1,1; Y-1,1; Zn-1,1; Mg-1,1; Mo-1,1; Na-1,1; P-1; Ti-1; V-1; B-1; Sc-1; In-1; Co-1; Mn-1; Ca-0,9; Fe-0,9; Ni-0,7; Cu-0,6).

The most significant correlations - 43 samples with a critical value of the correlation coefficient for 5% of the significance level of Pk-0.303) are noted with Ti, Sc, Mo, Cr, P, Y, Ca, Fe, V, Co, Mn, In, Mg, Zn, Te, Na, Sb, Pd, Re, As, Ru, Os, Pd, Rh, Ag, W, Cu, Pt, Au, Ni.

Conclusion

40 samples were taken from the named sites analyzed by mass spectrometric analysis (GP "CL"). First of all, we note the geological position of the testing site – this is the eastern, rather steep slope of the ridge, representing the wing of the North Nurata anticline, which compose metamorphosed outcrops of terrigenous-carbonate deposits of the ancient Zhenvachisai formation (EO_1zv), and the wings compose metamorphosed -carbonate–shale formations of the Majerum formation (Omd), and further north, metavolcanic and subvolcanic of the Shavaz formation. A winding and intermittent, but sustained power strip (300-400m) can be traced along the slope of the rocks from the main to the ultrabasic composition: gabbro, peridotites, pyroxenites, dunites. This band with a length of >10 km is a structural position favorable for the localization of platinoids. But in this case, nickel was more significantly manifested: out of 40 analyzed samples, it showed contents from 0.12 to 0.33% in 25 (63%), and the rest were elevated.

Of the platinoids, palladium showed up better: in 17 samples out of 40 (43.5%) it has a content of 0.1 c/u up to 0.46 c/u, platinum is much weaker – 8 times (20%) and with a content from 0.1 to 0.19 c/u.

The positions of the North Nuratinsky Mountains on platinoids are significantly weaker than the previous ones described, and therefore we did not evaluate their potential. But it should be noted that they can attract the attention of the industry for joint mining with nickel, which undoubtedly needs to be further explored.

References

1.Abdullaev, L. A., Baev, G. A., Sedelnikov, L. V. (2019). Assessment of the metallogenic potential of Southern and Western Uzbekistan with the allocation of promising areas for complex mineralization. Tashkent (SI "IMR").
2.http://resources.krc.karelia.ru/library/doc/collections/sovremennye_problemy_i.pdf
3.https://cyberleninka.ru/article/n/mineraly-platinovyh-metallov-i-novye-dannye-o-glavnyh-mineralah-rud-fedorovo-panskogo-massiva
4.http://www.spsl.nsc.ru/FullText/konfe/%D0%A3%D0%BB%D1%8C%D1%82%D1%80%D0%B0%D0%BC%D0%B0%D1%84%D0%9C%D0%B0%D1%84%D0%B8%D1%82VI.pdf

5.Kholikov, A. B. (2014). Platinum bearing of Sultanuvais mountains // Materials of the International Scientific and Technical Committee / Integration of science and practice as a mechanism for effective development of the geological industry of the Republic of Uzbekistan. Tashkent, 2014, 328-331.
6.Kholikov, A. B. (2014). Mafit-ultramafic formations of the Western Tien Shan and their platinum bearing // Materials of the international STC / Integration of science and practice as a mechanism for effective development of the geological industry of the Republic of Uzbekistan. Tashkent, 332-337.
7.Babajanov, A. A. (2013). Platinum-bearing scarn-rare-metal deposits of Western Uzbekistan. Tashkent.

Geobotanical and comparative data on vegetation in selected areas of central Albania, Elbasan region

Selma Myslihaka[1]

[1] *Faculty of Natural Sciences, University "A. Xhuvani", Elbasan, Albania,* selma.myslihaka@yahoo.com

Keywords
Conservation
Vegetation
Floristic element
Biological forms
Habitats

Abstract
At the current circumstances phytocenosis – agroecosystems and geobotanical approaches has been more difficult to avoid the transformation associated with the growth of global anthropogenic pressure. Concurrently, anthropogenic factors affect all parts of ecosystems, causing changes in the living component of nature. The study of the real state of ecosystems, their changes and stability under the load of anthropogenic factors is impossible without a comprehensive, in-depth study of them. In this contribution are presented vegetation data of the region of Elbasan, central Albania following comparative features from the systematic spectrum, biological forms and floristic element. It is worth to mention that survey area and associated vegetation is of particular interest due to its location and influences by the multifaceted Mediterranean-Atlantic climate with the continental one which enables this region to have rich biodiversity values and particular floristic composition. This survey is dedicated the region of Elbasan and covers three areas: Byshek, Xibraka-Shkumbini Valley and Elbasan. Based on geographical location and field expeditions there are identified and compared well-developed plant species, which are spontaneously growing, as well as plants that are rare and grow in limited areas in different climates and microclimates. Following the identified plant lists, systematic spectra and the percentage occupied by each family are constructed. The floristic diversity of this region is of scientific, economic and medical importance as the collection of plants provides a significant amount of raw materials for export, the pharmaceutical and chemical industries, making a valuable contribution to the country. Compliance with the requirements of environmental management, environmental protection and optimization of management of landscapes is becoming one of the main conditions for increasing ecosystems and associated species and habitats conservation.

Introduction

The city of Elbasan is characterized by 35 species of plants. The vegetation is mainly rich in Mediterranean deciduous shrubs [1] such as: Erica arborea L., Myrtus communis L., Arbutus unedo L., Juniperus oxycedrus L., Rosa canina L., Olea europea L. Also present are the plant associations of the families Leguminosae, Graminaceae, Labiatae etc.. Shelcan is a village in the Municipality of Shushica in the district of Elbasan in Albania. This village is located in the north of the city of Elbasan. Dominated by plants of the families: Rosaceae, Poaceae, Asteraceae, Fabaceae. The Shkumbin River originates in the Valamara Mountain [2]. Given the consistency of the relief and climatic conditions is characterized by 90 species. Plants of the families Rosaceae, Poaceae, Labiatae, Fabaceae, Urticaceae, etc. predominate. Letan is a village in Bradashesh Commune in Elbasan District. It lies southwest of Elbasan. Dominated by plants of the families: Leguminosae, Poaceae, Rosaceae, Plataginaceae.

Materials and methods

The study was conducted working according to a methodology divided into three phases: (i) Preparatory phase (preparatory work); (ii) Fieldwork phase (outdoor data collection); (iii) Laboratory work phase (data processing in the laboratory) [3, 4].

This study was divided into several stages: (i) Conducting field surveys; (ii) Estimation of quantity and coverage of species and (iii) Determination of species found in the territory taken for analysis.
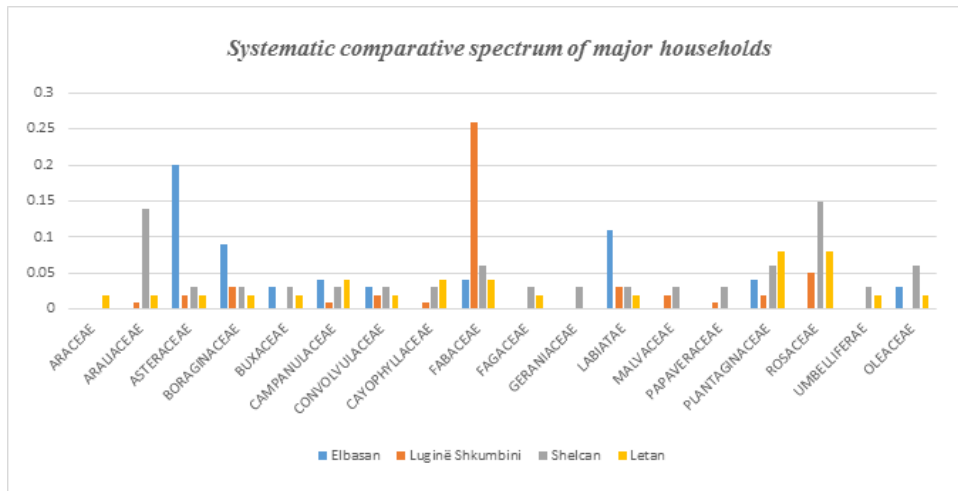

Figure 1. Comparative graph of systematic spectra

Results and discussions

Our study relied on the main habitat of forest flora and Mediterranean shrubs in these four vegetation areas. This habitat represents a variety of species in the floristic composition [5, 6]. The physiognomy of the Mediterranean forest is almost approximately the same throughout the territory. Other elements are Mediterranean and sub-Mediterranean shrubs such as Paliurus aculeatus, thana (*Cornus mass*), blackberry (*Rubus ulmifolius*) and a number of lianas such as: hard mulberry (*Smilax aspera)*, Heartburn (*Hedera helix*), larch (*Vitis silvestris*). The flora of forest herbaceous plants is the same, rare (Naqellari P. 2000) and most of its species belong to the ecological species xeroph. In addition to the phanerogamic flora, we also have low cryptogamous vegetation such as: lichen (*Lichene*) on trunks and stones; briophytes (*Briophyta*) in soil, hardwoods or rocks, hardwoods or stones; ferns (*Pteridophyta*); mushrooms (*Mycophyta*) etc.

Referring to the data of the comparative Figure 1, we notice that the vegetation is similar and that most of the families of these three areas are presented in approximate values.

Floristic flora spectra by areas under study.

In the region of Elbasan the dominant floristic elements are: Euro-Mediterranean, Central-European, Paleotempered, Eurasian.
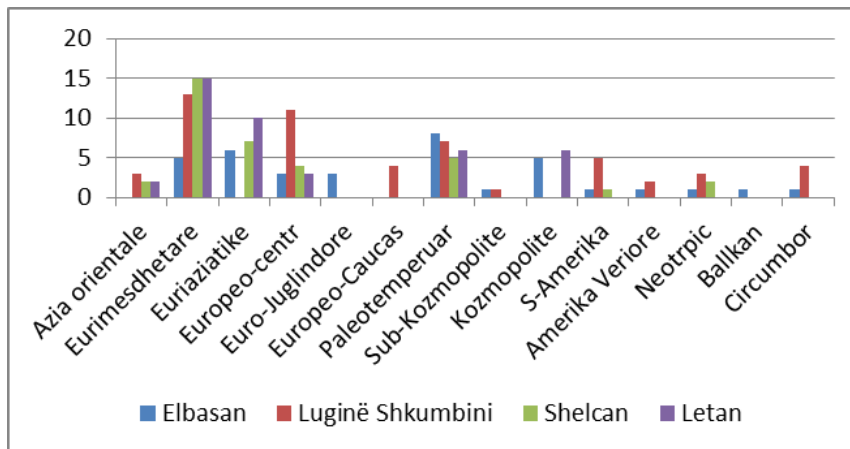

Figure 2. Comparative graph of floristic spectrum

Based on the graphic data of the comparative floristic spectrum (Figure 2) we find that the vegetation is similar to the Mediterranean character, while according to the comparative Figure 3, the biological forms of the vegetation of these areas are generally similar mainly of the Hemicryptophyte type.
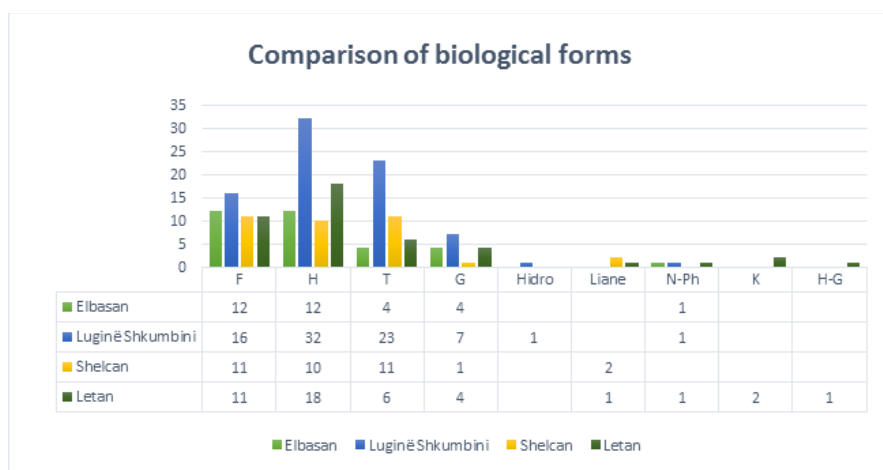

Comparison of biological forms

	F	H	T	G	Hidro	Liane	N-Ph	K	H-G
Elbasan	12	12	4	4			1		
Luginë Shkumbini	16	32	23	7	1		1		
Shelcan	11	10	11	1		2			
Letan	11	18	6	4		1	1	2	1

Figure 3. Comparative graph of biological forms

Formation *Carpinus orientalis: T*his formation lies at an altitude of 300-700 meters above sea level and is widespread in Shelcan. These plants have encountered alkaloids in this association: *Helleborus odorus* Waldstet Kit., *Achillea millefolium* L., etc.

Table 1. Spectrum of life forms: H=75 %; Th=5, 5 %; Ch=7,1%; G=2,4%

No.	Life forms	The scientific name of the plant	**Associations:** Carpinus Orientalis-Fraxinus ornus
22	Th	*Capsella bursa-pastoris* (L.) Med.	1.1 I
23	G	*Colchicum autumnale* L.	1.1 I
24	H	*Aristolochia clematitis* L.	1.1 I
25	H	*Viola odorata* L.	1.1 I
27	Ch	*Cichorim intybus* L.	1.1 I
28	H	*Convolvulus arvensis* L.	1.1 I

Conclusion

At the end of this study we reached some conclusions. We are practically familiar with the growing habitat of these plants and depending on the distribution according to the average relief height of 422m above sea level.

During the study it was observed that: The vegetation belonged mainly to the plant floor of the Mediterranean forest and shrub area; The most common families are: Fabaceae, Poaceae, Asteraceae dhe Labiatae; In terms of floristic element, the following species dominate: Euro-Mediterranean, Euro-Central, Euro-Southeast and Eurasian; The most common biological forms are: Hemicryptophytes, Phanerophytes, Therophytes and aquatic.

References

1. Mersinllari, M., & Naqellari, P. (2006). The practice of botany and the methodology of plant determination (Phanerogams). Tirana, 167
2. Kabo, M. (1998). Physical Geography of Albania, AAS, 2, 675
3. Xhulaj, M. (2005). Guide to teaching practices in botany. Tirana.
4. Annonymous, (2000). Flora of Albania, vol.1, 2, 3, 4. Tirana.,
5. Demiri, M. (1983). Excursionist flora of Albania. Tirana, 420.
6. Naqellari, P. (2000). Biodiversity, rare and endemic plants in the region. Together for a cleaner environment. Elbasan, Proceedings, 34-41

.